The investigation of a hydrophobic matrix for oral controlled drug delivery systems

Chigwanda, Tapuwa Rosemary Jabulani

Award date:
1995

Awarding institution:
University of Bath

THE INVESTIGATION OF A HYDROPHOBIC MATRIX FOR ORAL CONTROLLED DRUG DELIVERY SYSTEMS

Submitted by

Tapuwa Rosemary Jabulani Chigwanda, B Pharm, for the degree of Doctor of Philosophy of the University of Bath

1995

This research was carried out within the School of Pharmacy and Pharmacology, University of Bath, under the supervision of Professor J. N. Staniforth and Professor D. J. G. Davies.

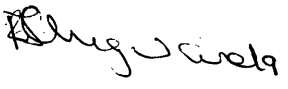

ProQuest LLC
789 East Eisenhower Parkway
P.O. Box 1346
Ann Arbor, MI 48106-1346

ACKNOWLEDGEMENTS

I would like to thank Professor John Staniforth for his supervision of this work. It could not have been attempted and completed without his guidance, understanding and encouragement, for which I am most grateful. I would like to express my sincere gratitude as well to my co-supervisor, Professor Davies for his help and advice.

My sincere thanks go to Mr Richard Sadler for ordering equipment and materials. I would like to thank Dr Linda Reeves and Dr Paul Heng for their assistance with some of the equipment, and in particular Dr Heng for the fruitful discussions we had. I would also like to thank Mr Rodney Murray for constantly repairing the dissolution equipment and Mr Geoff Venn and his staff in the workshop, for technical assistance. Sincere thanks also go to Mr H. R. Perrot in the Centre for Electron Optical Studies for assisting with the scanning electron microscopy studies. I would like to thank Mr Alan McLean for assisting in obtaining some of the materials. Many thanks go to Ms S. M. Hancock, Mrs M. W. Hughes-Jones and Mrs S. B. Johnson, for their kind words and encouragement. Many thanks also go to J. Peart and C. Challinor for their morale boost. I would like to thank Mrs Jennifer Boardley for correcting part of the thesis and many thanks to my brothers and sisters for their spiritual support.

Last but not least, many thanks to my husband Christopher and our daughter Kudzai for their patience, presence, comfort, reassurance, love and loyalty without which I would have never ventured this far.

This work was carried out with the aid of a scholarship partly from the British Council and the University of Zimbabwe.

To Nhamo

SUMMARY

The principal aim of this study was to improve the physico-mechanical properties of hydrogenated vegetable oil (HVO) tablets and to alter their predominantly square-root of time release characteristics, so as to produce a per-oral controlled release delivery system capable of being targeted to the proximal colon.

In the introduction to the experimental study, the physics of tablet compaction, tablet strength, friction and lubrication, effects of particle size effect on tablet strength and oral controlled drug delivery are discussed. The experimental work is divided into two parts: firstly a study dealing with the characterisation and optimisation of the physico-mechanical performance of processed HVO tablets. The second part of the study deals with the modification of the mechanism of drug release from processed HVO tablets.

Physico-mechanical properties were improved by processing HVO with polymeric binders as well as a low melting point fatty acid, stearic acid, which acted as an "auxiliary" binder. Tablet tooling adhesion of processed HVO was reduced by the addition of anti-adherents. The mechanism of drug release from processed HVO tablets was modified by the incorporation of a low melting point material, Myverol. Myverol is mainly glyceryl monostearate.

The type and concentration of binder were found to affect tensile strength of tablets produced from processed HVO. The minimum compaction force required

to achieve maximum tensile strength and release - sustaining characteristics was approximately 9 kN. However, formulations containing Myverol had compaction force independent release - sustaining characteristics as from 3 kN. Large particles were found to produce tablets with significantly better tensile strength and release-sustaining characteristics than small particles.

Myverol was found to alter the mechanism of drug release from processed HVO tablets: from Higuchi model - type kinetics to Fickian diffusion - relaxation model - type kinetics. It was considered that such a controlled release system of the latter type could be targeted to the proximal colon which:- (a) has increased residence time, (b) is responsive to drug absorption enhancing agents and (c) has decreased enzymatic activity. An increase in drug release rate with time would compensate for the reduced epithelial absorption and the gradual increase in the consolidation of faecal matter in this region.

LIST OF CONTENTS

SECTION	PAGE	TITLE
Chapter 1	**12**	**Introduction**
1.1	12	The physics of tablet compaction
1.1.1	15	Mechanisms of bond formation in tablets
1.2	20	Tablet strength
1.2.1	20	Binders and tablet strength
1.2.2	22	Tablet strength evaluation
1.3	27	Friction and lubrication
1.3.1	31	Tablets and lubricants
1.3.2	34	Evaluation of lubrication properties
1.3.2.1	34	True lubricant activity
1.3.2.2	35	Glidant activity
1.3.2.3	35	Anti-adherent activity
1.4	38	The effects of particle size on tablet strength
1.5	42	Controlled release drug delivery
1.5.1	45	Oral controlled release drug delivery
1.5.1.1	45	The oesophagus
1.5.1.2	46	The stomach
1.5.1.3	47	The small intestines
1.5.1.4	48	The colon
1.5.1.4.1	51	Colonic drug delivery
1.5.1.5	55	Types of materials used for oral controlled release systems
1.5.1.5.1	55	Hydrophilic systems

1.5.1.5.2 59 Hydrophobic systems

1.5.1.6 66 Diffusion in polymers

1.5.1.6.1 68 Drug release in matrix type delivery systems such as HVOs

1.5.1.6.2 72 Diffusion coupled with relaxation

Chapter 2 77 **Materials and Methods**

2.1 77 Aims and objectives

2.2 81 Materials

2.3 91 Methods

2.3.1 91 Preparation of the composite excipients

2.3.1.1 91 Composite excipients containing less than or equal to three ingredients

2.3.1.2 92 Composite excipients containing more than three ingredients

2.3.1.2.1 93 Composite excipients containing either Avicel, Starch or Junlon

2.3.1.2.2 93 Composite excipients containing either hydrogenated rapeseed oil, Myverol or Myverol and Eudragit

2.3.1.3 94 Preparation of Myverol - based water - free composite excipients

2.3.2 100 Preparation of an active composite excipient containing propranolol hydrochloride

2.3.3 101 Size fractionation and reconstitution of composite excipients and active composite excipient

2.3.4 104 Drug and composite excipient dry mixing

2.3.5 105 Differential scanning calorimetry (DSC)

2.3.6 106 Anti-adherent addition

2.3.7 107 Tableting

2.3.7.1 107 Equipment and preparation of the tablets

2.3.7.2 108 Data acquisition and manipulation

2.3.7.3 112 Evaluation of adhesion to tablet tooling

2.3.8 113 Tablet tensile strength measurement

2.3.9 116 Determination of wavelengths of maximum absorption and Beer-Lambert plots for aqueous solutions of propranolol hydrochloride and theophylline

2.3.10 122 Preparation of buffer solutions

2.3.10.1 122 Buffer pH ≈ 6.8:- Imidazole/Hydrochloric acid

2.3.10.2 123 Buffer pH 7.0:- Imidazole/Hydrochloric acid

2.3.10.3 123 Buffer pH ≈ 1.4:- KCl/HCl (Clark & Lubs Buffer)

2.3.11 123 Determination of Beer-Lambert plots for propranolol hydrochloride in buffer solutions

2.3.12 128 Measurement of release characteristics of tablets made from the various formulations using an automated dissolution technique

2.3.13 129 Scanning electron photomicrography of tablet surfaces

131 **RESULTS AND DISCUSSION**

Chapter 3 131 **Investigation of the optimisation of physico-mechanical performance characteristics of processed HVO**

3.1 131 Objectives

3.2 132 Characterisation of materials

3.3 138 Characterisation of particles of composite excipient 3

3.4 143 Drug release mechanism of processed HVO matrices

3.5 147 Enhancement of tensile strength of processed HVO compacts

3.5.1 148 Effect of binder concentration on tablet tensile strength and release - sustaining characteristics

3.5.2 156 Effect of type of binder on tablet tensile strength and release - sustaining characteristics

3.5.3 159 Effect of type of matrix on tablet tensile strength and controlled release efficiency

3.5.4 161 Optimisation of tensile strength and release-sustaining characteristics of processed HVO compacts

3.5.4.1 161 Effect of particle size on tablet tensile strength and release-sustaining characteristics

3.5.4.2 169 Effect of compaction force on tablet tensile strength and release-sustaining characteristics

3.5.5 175 Scanning electron photomicrography of tablet surfaces

3.6 186 Reduction of adhesion of processed HVO to tablet tooling

Chapter 4 192 **Modification of the mechanism of drug release from processed HVO matrices**

4.1 192 Objectives

4.2 193 Enhancement of drug release from processed HVO matrices

4.3 198 Alteration of mechanism of drug release from processed HVO matrices

4.3.1 199 Effect of biological enzymes on propranolol hydrochloride

release from processed HVO matrices

4.3.2 201 Propranolol hydrochloride release from tablets made from Myverol-based water-free composite excipient formulations

4.3.3 207 Determination of optimum Myverol concentration

4.3.4 209 Drug release properties of tablets made from composite excipient 25 formulation (30 % Myverol)

4.3.5 220 Optimisation of the constant release rate or "second burst" release

4.3.6 228 Analysis of mechanism of propranolol hydrochloride release from tablets made from composite excipient 29 formulation, in distilled water

Chapter 5 233 **Conclusions**

References 236

Appendix 1 I **Tables**

I Table A1:- The effect of compaction force on tensile strength

VI Table A2:- The effect of particle size on tensile strength

XI Table A3:- The effect of binder (PVP K-30) concentration on tensile strength

XXI Table A4:- The effect of binder (PVP K-30) concentration on release - sustaining characteristics

XXII Table A5:- The effect of particle size on release - sustaining

characteristics

XXII Table A6:- The effect of compaction force on release - sustaining characteristics

XXIII Table A7:- The effect of particle size on release - sustaining characteristics

XXIII Table A8:- The effect of compaction force on release- sustaining characteristics

XXIV Table A9:- First order kinetics: $\log_{10}(100\ \% - Q) = kt$

XXVIII Table A10:- Higuchi mechanism kinetics: $Q = kt^{1/2}$

XXXIV Table A11:- Zero order kinetics: $Q = kt$

XXXVI Table A12:- Diffusion - Relaxation kinetics: $Q = k_1t^{0.46} + k_2t^{0.92}$

XXXVIII Table A13:- Linear regression calibration data

Appendix 2 XL Basic programmes

XL Basic programme for tableting

XLIII Basic programme for dissolution

CHAPTER 1

INTRODUCTION

1.1 THE PHYSICS OF TABLET COMPACTION

Compaction is an irreversible change in the dimensions of a solid material as a result of the application of pressure. [1] Compression is a reversible or an irreversible dimensional change in a solid material under pressure. The former process results in an intact compact, while the latter does not necessarily produce a compact.

Pharmaceutical powders or granules are compacted between the upper and lower punches of a tablet machine and an intact compact is ejected from the die. The stages which occur during tablet compaction include:- transitional repacking or particle rearrangement, deformation at points of contact, fragmentation and/or deformation (plastic and elastic), bonding, decompression and ejection. [2, 3] These stages are depicted in figure 1.1.

At low applied loads the granules/powder consolidates to higher densities. This depends on the type of material and the particle size. However, energy expended during this stage, is of minor consideration in the whole process of tablet compaction. [3] As the compaction load increases further, granule/powder deformation via the areas of true contact occurs. The stress is relieved by either fragmentation or deformation (plastic or elastic). This depends on the

Figure 1.1:- Stages in Tablet Compaction[3]

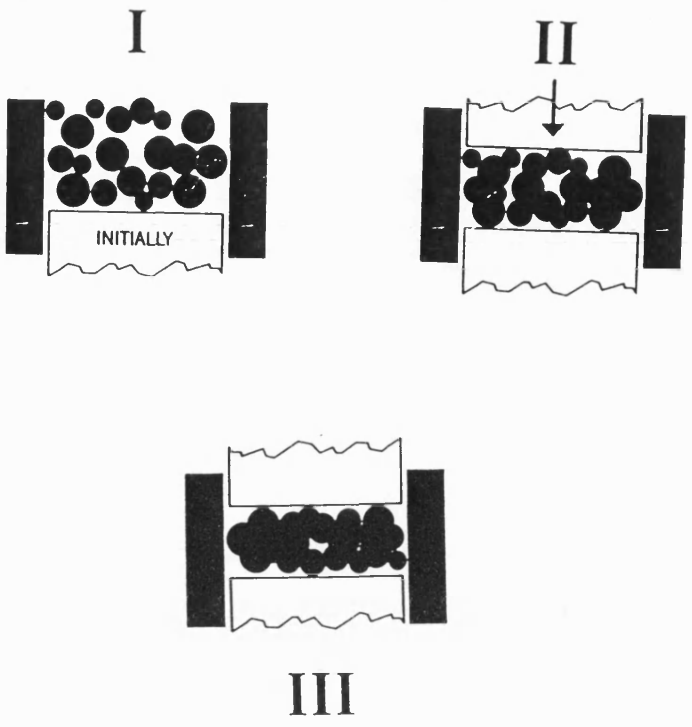

Key:- I - Initial loose particle packing

II - Rearrangement of particles at low pressure

III - Particle derfomation at high pressure

IV - Tablet axial relaxation

rate of application of the load, the magnitude of the load, duration of the locally induced stress, physical properties of the material(s) and temperature. [3, 4] Usually two or more of the above changes occur either simultaneously or consecutively. [5]

Materials such as sodium chloride and microcrystalline cellulose are among the ones which mainly undergo plastic deformation. [6, 7] Materials that mainly fragment include crystalline lactose, sucrose and Emcompress. [7, 8] Compact strength in plastically deforming materials is believed to be the result of surface flow or slippage of one surface over another. This results in a contact area capable of increasing both the number of bonds and their strength. In fragmenting (brittle) materials, compact strength is due to an increase in contact area. Plastically deforming materials generally produce stronger compacts than brittle materials at given applied loads. Low temperatures and fast loading during compaction generally facilitate consolidation by fragmentation. [9, 10]

For metals and most crystalline materials, after the initial elastic deformation, the materials undergo plastic deformation. Finally, if the stress is high enough, the materials show brittle behaviour and fragment. However, most pharmaceutical materials are organic compounds and exhibit different consolidation properties from the above simple model. The main difference is that many pharmaceuticals seem to undergo particle fragmentation during the initial loading. [3, 8]

Several methods have been used to determine the volume - reduction mechanisms both qualitatively and quantitatively. These include:- scanning electron microscopy; work measurements from force - displacement curves; axial to radial tensile strength ratio (isotropy ratio); measurement of surface area changes and measurement of porosity changes during compaction. [8]

1.1.1 Mechanisms of Bond Formation in Tablets

Bond formation releases energy (exothermic process). Several mechanisms of bonding in the process of compaction have been postulated. Three theories put forward are the mechanical theory, the intermolecular theory and the liquid surface theory. [2]

The mechanical theory proposes that, under pressure, the individual particles undergo elastic, plastic or brittle deformation and the edges of the particles intermesh, forming a mechanical bond. However, this mechanism is not a major one in tablet bonding. It is probably important in press-coating and is thought to be responsible for holding the different layers together.

The intermolecular theory proposes that molecules at the surface of solids have surface free energy. This energy enables the molecules to interact with other surface molecules on other particles, in true contact. This implies that absolutely clean surfaces are a requirement for the interaction of these intermolecular forces. Intermolecular forces are thought to constitute the majority of bonding forces in pharmaceutical materials. [8]

Intermolecular forces include van der Waals' forces, electrostatic forces, and hydrogen bonding. It is believed that the most prevalent type of force in materials, including tablets, are the van der Waals' forces (75-100 % of the total forces). [8] Van der Waals' forces operate in vacuum, air and liquid environments up to distances of approximately 10 - 100 nm from molecular surfaces. They owe their origin to fluctuating electrical moments/dipoles produced by the movement of electrons in their atomic orbits. These dipoles are able to induce a corresponding and opposite dipole in an adjacent atom thus leading to a net attraction. Van der Waals' forces act between all atoms regardless of polarity or electrical charge.

Electrostatic forces occur due to a separation of charges. They usually arise during mixing and compaction.

Hydrogen bonding takes place when the negative pole of a strong dipole approaches another dipole, positively charged, which consists of a hydrogen atom. Hydrogen bonding is predominately an electrostatic interaction and can occur intramolecularly and intermolecularly. It is an important mechanism of bonding in materials such as microcrystalline cellulose (MCC), starch and lactose. [8, 11] These materials have hydroxyl groups, -OH, which are responsible for the hydrogen bonding.

Solid bridges are due to either covalent or ionic bonds and hence do not fall into the category of intermolecular bonds. The main differences between solid

bridges and intermolecular bonds are the strength of the bonds formed, the bond length at equilibrium and the attracting distances. [8] Hydrogen bonds have bond strengths ranging from 10-30 $kJmol^{-1}$, equilibrium distances of 0.3-0.4 nm and attracting distances ranging from 10 nm to 100 nm. Hydrogen bonds and van der Waals' forces have similar equilibrium and attracting distances. However, van der Waals' forces have bond strengths ranging from 5 to 40 $kJmol^{-1}$; by comparison solid bridges have bond strengths of 200-800 $kJmol^{-1}$, bond lengths of less than 0.3 nm and attracting distances of less than 1 nm. Electrostatic forces have the same attracting distances as the other two intermolecular forces (hydrogen bonds and van der Waals' forces). However, electrostatic forces are incapable of contributing to thermodynamically stable bonds between molecules or ions.

The liquid surface theory attributes bonding to the presence of a thin liquid film, which may be a result of fusion or solution although the bonds formed are usually solid bridges. [8] During compaction, an applied force is exerted upon the granules/powder, but locally the force is applied over a small area of true contact: therefore, high pressure exists at the areas of true contact. The local effect of the high pressure on the melting point and solubility of a material is important to bonding.

The relationship of pressure and melting point is expressed by the Clapeyron equation below:- [2, 12]

$$\partial T/\partial P = T(V_l - V_s) / \Delta H \qquad \text{equation 1.1}$$

where $\partial T/\partial P$ is the change in melting point with pressure, T is the absolute temperature, ΔH is the molar latent heat of fusion, and V_l and V_s are the molar volumes of liquid melt and the solid, respectively. As latent heat of fusion is positive, this equation predicts that for a solid that expands on melting ($V_l > V_s$), the melting point is raised by an increase in pressure. For a solid that contracts on melting ($V_l < V_s$), the melting point is lowered by increasing the pressure. Except for a few substances, such as water, most solids expand on melting. Thus the Clapeyron equation indicates that during compaction, the rise in melting point with pressure for most substances would make it difficult for fusion to occur. This equation is derived from thermodynamically reversible processes with systems exposed to uniform pressure. However, the compaction of pharmaceutical tablets is non-reversible and the pressure is not uniformly distributed. For these reasons and the existence of frictional forces, which raise temperatures during compaction, the potential of melt/fusion bonding of particles in tablets cannot be discounted. This is more so in tablets made from materials such as hydrogenated vegetable oils (HVOs) which have relatively low melting points.

Skotnicky [2, 12] derived an equation relating heat of fusion, volumes of liquid and solid states, temperature and pressure applied to the liquid and solid phases. For an ideal system where there is exposure to uniform pressure the relation reduced to Clapeyron equation. However, if the pressure at the points of true contact is exerted only on the solid, and any liquid being subjected to constant atmospheric pressure, then the relation simplifies to the equation below:-

$$\partial T/\partial P_s = - V_s T / \Delta H \qquad \text{equation 1.2}$$

For such a system, the isolated pressure acting locally on the solid always lowers the melting point regardless of the expansion or contraction of the solid on melting. This is especially true for hydrophobic materials such as HVOs, fatty acids and waxes which have relatively low melting points.

The reasoning employed in the analysis of pressure effects on melting point could also be extended to changes in solubility of solids with pressure. The variation in solubility of a solid with uniform pressure has been expressed in the following equation:- [12]

$$(\partial \ln x / \partial P)_T = -(V_l - V_s) / RT \qquad \text{equation 1.3}$$

where x is the mole fraction of the solid in saturated solution, R is the gas law constant and the rest are as described above. This equation predicts that for a solid that expands on melting ($V_l > V_s$), an increase in pressure will decrease solubility with the converse true for a solid that contracts upon melting ($V_l < V_s$). However, consideration of pressure and stress at areas of true contact in tablet compaction, one could conclude that an increase in pressure results in an increase in solubility.

The liquid in which solution takes place is usually the film of moisture adsorbed on the particle surface. The strength of the inter-particulate bridge formed depends on the amount of material deposited and the rate of crystallisation. High crystallisation rates produce fine crystalline structures and strong bridges. The poor compactibility of most water insoluble compounds and

the relative ease of compaction of most water soluble compounds seem to support this compaction - solution phenomenon. [2]

1.2 TABLET STRENGTH

Tablets ought to possess sufficient strength and toughness to be able to withstand mechanical handling and transport. [13] In addition, the mechanical characteristics of matrix sustained release tablets should allow the compact to provide reproducible drug dissolution profiles. The strength of tablets is known to be influenced by a number of properties such as:- the physico-mechanical properties of the drug and excipients, which influence the main bond type formed and their number; type, amount and distribution of binder and how it is added; the characteristics of the tablet compaction process, including the applied compaction force and speed; particle size and distribution of powder/granulation; type, amount and blending time of lubricants; size and shape of finished tablets; temperature and rate of drying of granulation and final moisture in granulation and tablets. [13-20]

1.2.1 Binders and Tablet Strength

In order to improve tablet strength, a binder is usually added during granulation, sometimes in dry form, but usually in solution. Symecko and Rhodes [16] defined a binder as a substance that is included into a solid dosage formulation as a technical additive, to improve compactibility and flowability of powders or granules.

Of particular importance is the binder's compatibility with other tablet components, especially the drug. It should impart sufficient cohesion to powders or granules, to allow normal processing such as sizing, lubrication, compaction and packaging. Ideally, binders ought to possess low elastic modulus and undergo high plastic deformation. Binders increase the number of bonds, produce stronger bonds, produce a number of bonds that can withstand stress relaxation and elastic recovery of the particles and deform plastically during powder/granulation consolidation and decompaction. [16, 20] Besides this, binders also help in the formation of solid bridges in tablets when they crystallise and harden. [17] However, in HVO matrices the majority of the solid bridges are probably as a result of partial particle melting and localised fusion-welding. [17]

Generally, binders exert strong van der Waals' forces in the presence of small amounts of moisture. Most binders are not effective at zero percent moisture. Therefore when used in the dry state, they are less effective as they exhibit minimal surfaces for cohesive binding in this state. As indicated initially, they are usually added as solutions or suspensions. [15]

Binders have recently been classified in two ways namely:- (a) chemical origin (source) and (b) method of tablet manufacture. [16] Source is further divided into three groups namely:- (i) natural, (ii) semi-synthetic and (iii) synthetic. Method of tablet manufacture is divided into:- (i) wet granulation, (ii) slugging and (iii) direct compression. Binders of natural origin include acacia and gelatin. Semi-synthetic binders include celluloses (such as carboxymethylcellulose, ethyl

& methylcellulose) and pregelatinised starch. Some synthetic binders are polyvinylpyrrolidone (PVP) and the polymethacrylates. [16] However, binders such as acacia are now rarely used due to their tendency of having bacterial contaminants. Nevertheless, starch, another binder of natural origin, is still commonly used as a material which tends to produce soft but firm granules. PVP, a synthetic binder, continues to be extensively used as a binder in water, alcohol or blends of each solvent. [15] Binders which are more hydrophobic are potentially useful in combination with hydrogenated vegetable oils (HVOs) as they are likely to provide better release-sustaining characteristics.

1.2.2 Tablet Strength Evaluation

Various techniques and tests have been used to assess tablet strength, including: abrasion; bending; static indentation; cutting; erosion; scratch; rebound; ploughing and diametral crushing. [21, 22] The mechanical strength of tablets has been quantified by means such as:- crushing strength, axial tensile strength, radial tensile strength, hardness and work required to cause tablet failure. [8, 23]

A common method for evaluating the strength of tablets involves the measurement of the force required to break a tablet in a diametral compression test. This is often termed the crushing or peak force. Tablet failure maybe due to more than one type of force and a tablet may fail in more than one way. The ways in which a tablet may fail are depicted in figure 1.2 (a). When the tablet fails by mechanism 1, which is pure tensile fracture, the stress distribution within the tablet can be calculated as shown in figure 1.2 (b).

Figure 1.2:- Failure Patterns (a) During Diametral Loading of Tablets and Stress Distribution (b) in Pure Tensile Failure

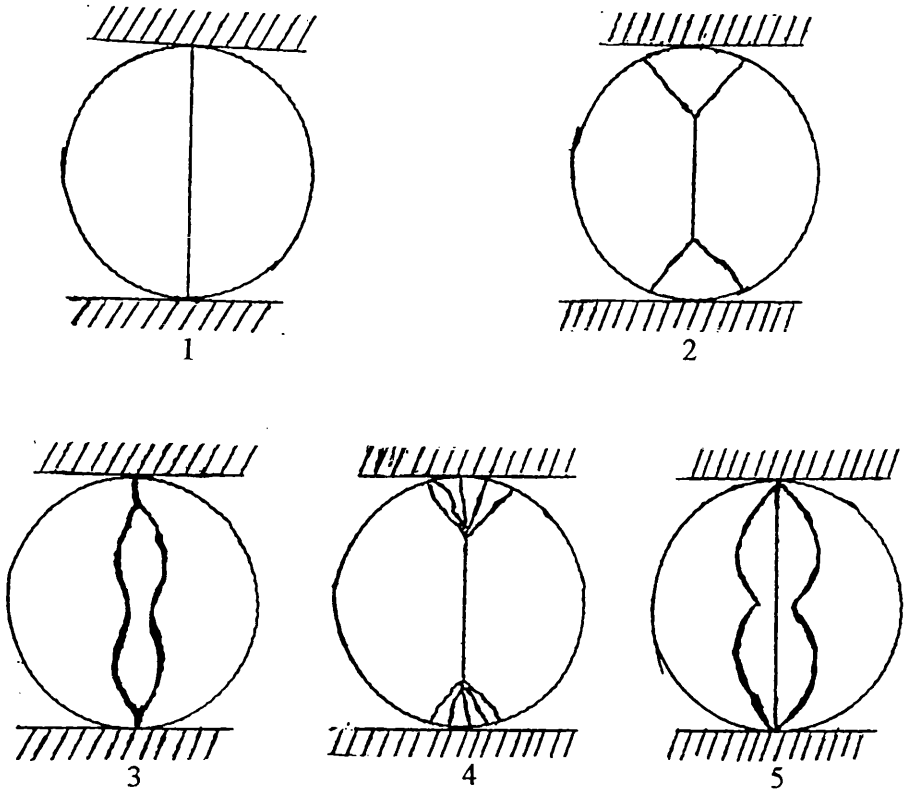

(a)

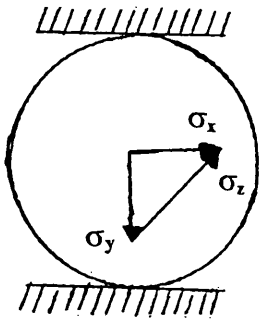

(b)

NB:- In (b) the applied load may be resolved into three components, σ_x, σ_y and σ_z

Where:- σ_x is the tensile stress applied normal to the loaded diameter

σ_y is the compressive stress

σ_z is the shear stress

Large tablets will have higher crushing forces than smaller ones. This is so because the crushing force does not take into consideration tablet dimensions. Therefore in order to compare strengths of tablets having different diameters and thickness, tablet radial tensile strength, T_s, is normally used. T_s can be calculated from the crushing force, F_c, as shown below:-

$$T_s = 2F_c / \pi dt \qquad \text{equation 1.4}$$

where T_s and F_c are as described above, d and t are the tablet diameter and thickness respectively. However, some authors [13, 23] claim that the radial tensile strength is sensitive to crack propagation variations, hence the determination of axial tensile strength, T_{sx}. [11] This can be calculated from the following equation:-

$$T_{sx} = 4F_p / \pi d^2 \qquad \text{equation 1.5}$$

where F_p is the force required to pull the tablet apart in the axial direction and d is as above. Axial tensile strength has been found to be of value in assessing capping and/or lamination tendencies of materials. [24] Besides this, T_{sx} is also used in combination with the radial tensile strength to calculate the isotropy ratio. This ratio has been used as a measure of particle fragmentation during compaction. [25, 26] Isotropy ratios close to unity generally indicate that the material consolidates mainly by particle fragmentation while low ratios are obtained when plastic deformation is the predominant mechanism. [26]

The radial tensile strength, T_s, is believed to reflect a kind of average strength value, while the axial tensile strength, T_{sx}, is related to the weakest part of a tablet. [26] Therefore the former is a better indicator of tablet strength than the

latter. The majority of pharmaceutical tablets are anisotropic and heterogeneous and properties such as density, porosity and strength vary in different directions. For an isotropic homogeneous body, radial and axial tensile strengths are equal.

Crushing force is often erroneously termed hardness (a surface property). Hardness is often defined as the resistance of a solid to local permanent deformation. It can be measured by static methods such as Brinell and Vickers hardness tests or by dynamic methods. [21-23] The static methods involve the formation of a permanent indentation on the surface of the material and hardness is determined by the load applied and the size of the indentation formed. [23] For example, the Brinell hardness tester measures directly the depth of penetration into a material such as a tablet face, by means of a displacement transducer. The results are independent of tablet geometry. [21, 22] For the Vickers hardness tester, instead of the use of a ball to penetrate the surface of the tablet, a pyramid is used. [21, 27] Generally, for ductile materials, there is a linear relationship between compact tensile strength and Vickers hardness. [22] Dynamic methods involve a pendulum which is allowed to strike from a known distance, or an indenter which is allowed to fall under gravity onto the surface of the material. Hardness is determined from the rebound height of the pendulum or volume of the resulting indentation. [23]

"Corrected" work of failure, CW_f, has sometimes been termed tablet "toughness". A material could be strong but not tough. For example, glass is

strong but is not tough as it shatters easily, while in contrast rubber is not strong but is very tough. During diametral compression testing, Rees and Rue [28] studied platen displacement as a means of assessing tablet deformation before failure. A displacement transducer recorded the relative movement of the platens until failure occurred. The load, F, was plotted against displacement, x. The area under the curve, calculated by integrating the load with respect to platen movement, represented the work done, W_f, on the tablet to cause its failure as shown below:-

$$W_f = \int_{F_o}^{F_{max}} F.dx \qquad \text{equation 1.6}$$

W_f has units of Joules. In order to correct for the size of a circular cylindrical compact, the work done, W_f, is divided by the cross-sectional area of failure to obtain the corrected work of failure, CW_f, which has units of Joules m^{-2}. Rees and Rue [28] then concluded that materials with similar tensile strength values may show markedly different work of failure values. This is due to variations in their resistance to deformation prior failure.

Generally, materials that consolidate mainly by plastic deformation during compaction, tend to show high work of failure values. This is probably due to a combination of high tensile strength values and large deformation before failure, during a diametral loading test. In contrast, materials consolidating mainly by fragmentation during compaction, tend to show low work of failure values.

1.3 Friction and Lubrication

The atomic or molecular processes that occur at the interface of two materials when they are brought into contact or moved with respect to one another is fundamental to many technological problems such as adhesion, friction, wear, lubrication and fracture. [29] Solid surfaces irrespective of method of formation, generally contain surface irregularities. When two surfaces are placed in contact, surface roughness causes contact to occur at discrete contact points. Deformation (plastic and elastic) occurs at these points depending on the applied stress, surface roughness and material properties. Usually, the total area of true contact under normal loads is a small fraction of the area that would be in contact if the surfaces were perfectly smooth. [29,30] If this area is minimal, then adhesion, friction and wear would be minimised.

Studies on the interaction between two surfaces when brought close together and between two surfaces in contact as they are separated have been studied. [29] Such interactions can be modified by the presence of an intervening medium such as a liquid or a material with a lower shear strength than the other two surfaces. The frictional properties of such systems have been studied by moving the surfaces laterally, hence providing insight into the molecular-scale operation of lubricants. Therefore friction force in terms of the tableting process can be defined as the force required to shear inter-granule/particle junctions formed at regions of real contact plus the force required to plough the surface of the softer material (tablet) by the asperities of the harder (die). However, the

relationship between friction and surface topography is not always simple and obvious.

If two surfaces are in true molecular contact when sliding begins, their friction will be high and their adhesion may be strong enough to tear them apart. However, if the surfaces are separated by one or more molecular layers of fluid lubricant and if this cushioning film remains in the liquid-like state during sliding, then the frictional force will be low and sliding will proceed smoothly. [29] For example, one layer of water molecules approximately 0.25 nm thick between two hydrophilic surfaces can be sufficient to reduce the interfacial friction force to very low values. On the other hand, if the surface-fluid interactions induce the liquid molecules to solidify, the molecular configuration during sliding is complicated. The film alternately melts and freezes during motion and the resulting friction is of the "stick-slip" type. Sticking will occur in the frozen state, giving rise to the static friction force and slipping will occur in the shear-induced molten state, giving rise to the kinetic friction force. [29] This stick-slip phenomenon is probably important in the compaction and ejection phases of tablets, especially those made from HVOs in combination with low melting point lubricants such as stearic acid [31] and HVO. [32] In these phases, powders/granules move over each other and the die wall and formed tablets slide along the die wall. Experiments have shown that in cases such as these the forces of friction and adhesion are closely related. [29]

During the sliding of two surfaces that contain boundary layers of "surfactant" molecules which might be either solid-like (eg magnesium stearate), amorphous-like or liquid-like (eg liquid paraffin), dynamic film structures can arise. Generally, solid-like films exhibit stick-slip motion, amorphous-like films exhibit high friction due to the molecular entanglements occurring between the two surfaces, and liquid-like films exhibit low viscous-like friction with smooth sliding. This is schematically shown in figure 1.3. [29] These dynamic states are dependent on temperature, pressure, applied load and relative velocity of the shearing surfaces. High sliding speeds make the film more solid-like whereas slower speeds make it behave more like a liquid.

In tableting, the attainment of low adhesion, low friction and low wear (surface damage) is a most desirable goal. By choosing the right lubricant and in some cases chemically grafting molecules such as surfactants, polymers, chromium nitride, zinc or iron dihydrogen phosphate to the tooling surfaces, controls and modifies the frictional properties. [29, 31, 33] In such cases, very small amounts of the lubricant are required. This reduces cost plus detrimental effects on the tablets.

Figure 1.3:- Schematic Illustrations of Different Types of Dynamic Thin - Film Structures that can Arise During Lubricated Sliding [29]

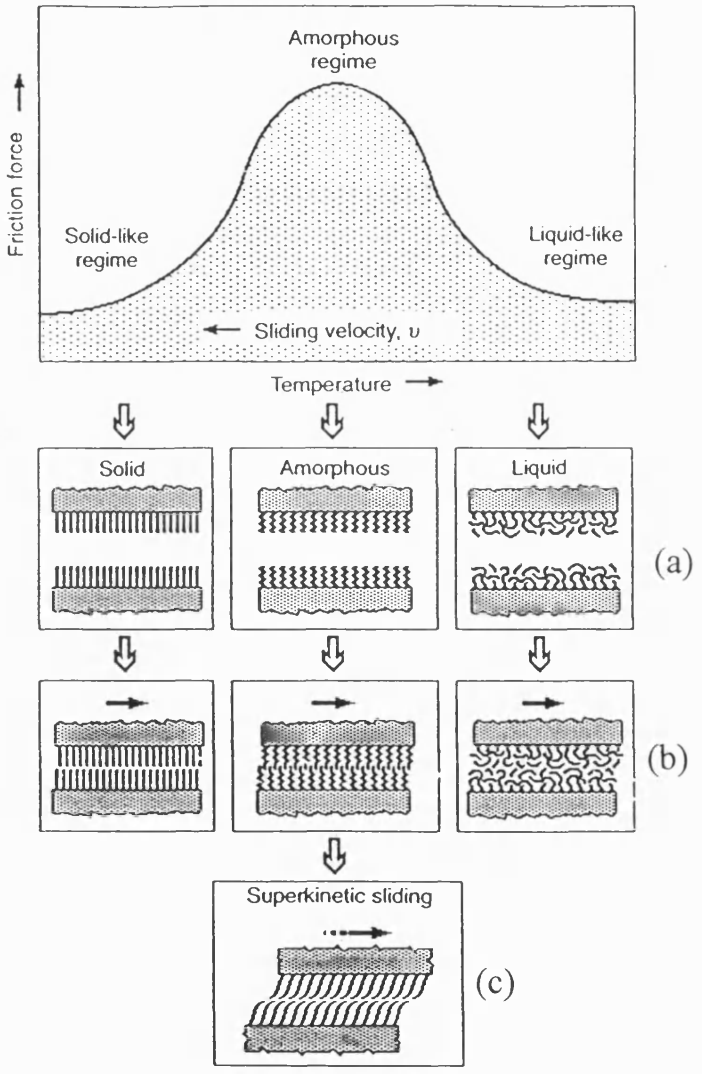

NB:-

(a) surfaces approach each other

(b) contact of surfaces

(c) model that results from amorphous materials

1.3.1 Tablets and Lubricants

Lubricants are most essential components of a tablet formulation. A tablet lubricant has three primary functions namely:- (a) reducing friction at the tablet-die wall interface especially during ejection (true lubricant activity), (b) facilitating the flow of powder or granulation from the hopper to the feed shoe/frame into the die (glidant activity), and (c) preventing adherence of formulation to the punches and die (anti-adherent activity). [15, 30, 34] Most lubricants exhibit at least one or more of the above functions.

Lubricants that exert their effect by separating surfaces by the formation of a finite and continuous liquid film on the punches, die and granulation, are called fluid lubricants. Some are liquids at room temperature such as liquid paraffin, [31] while others melt at compaction pressures and temperatures such as HVOs [32] and stearic acid. [31] Most lubricants consist of long chain fatty acids and the polar portions of which attach to the metal oxide film on the punch and die surfaces and are called boundary lubricants. These include the metallic stearates and sodium stearyl fumarate. [35]

Whether a lubricant is a boundary one or a liquid film one, there is an overall reduction of the coefficient of friction (ratio of friction force to the normal load). This will reduce the work required to compact the powder/granulation and more importantly, the reduction of the work done in tablet ejection. Coefficients of friction for fluid lubricants can be as low as 0.001 with negligible wear of surfaces, while with boundary lubricants, coefficients are

higher (0.15-0.5), and wearing occurs. Ideally, for effectiveness, boundary lubricants ought to have low shear strength and adhere readily and firmly to interacting surfaces. [15, 31] How boundary and fluid lubricants are thought to behave or align themselves on granular and die surfaces is depicted in figure 1.4. In tablets prepared by wet granulation, lubricants are added only after granulation has been dried prior to compaction. In direct compression, they are added when all the other excipients have been added.

Particle size and shape are very important to lubricant distribution and effectiveness, with mixing time and type of mixer having an effect as well. However, blending time and conditions are not so critical with stearic acid as they are with its salts. The salts are incompatible with acid drugs such as aspirin, while stearic acid is incompatible with alkaline drugs such as sodium saccharin and sodium phenobarbital. [15] HVOs' blending conditions are less critical but still important. [32] Water soluble lubricants are usually used in effervescent tablets and other water soluble tablets and examples include polyethylene glycol 6000, sodium benzoate, sodium lauryl sulphate and dl leucine. [15]

Although lubricants play a very important role in tableting, they also have detrimental effects on tablets. These include:- (a) significant decrease in tablet tensile strength, (b) decrease in work of failure, (c) increase in disintegration times and (d) decrease in dissolution rate especially with magnesium stearate. [5, 31, 32] The mechanism of decrease in tensile strength is thought to be due to

Figure 1.4:- Schematic Illustration of How Different Lubricants Act [31]

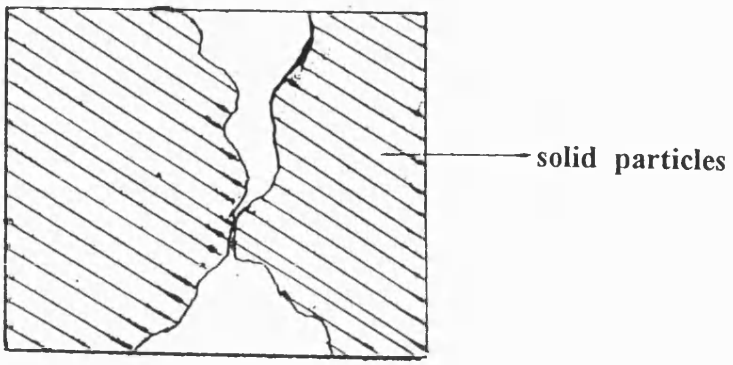

(a) Frictional interparticle contact

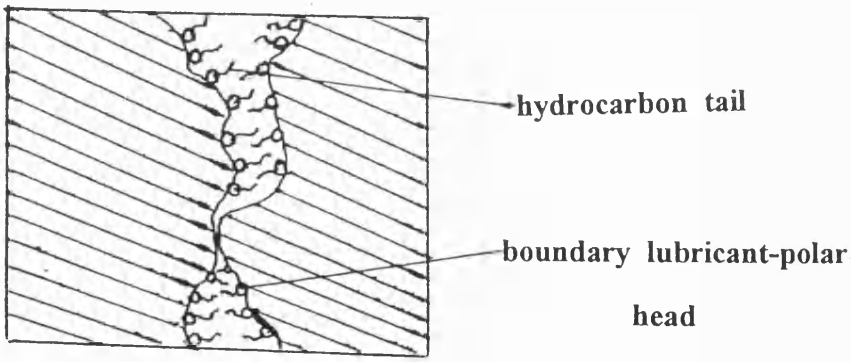

(b) Boundary film lubrication

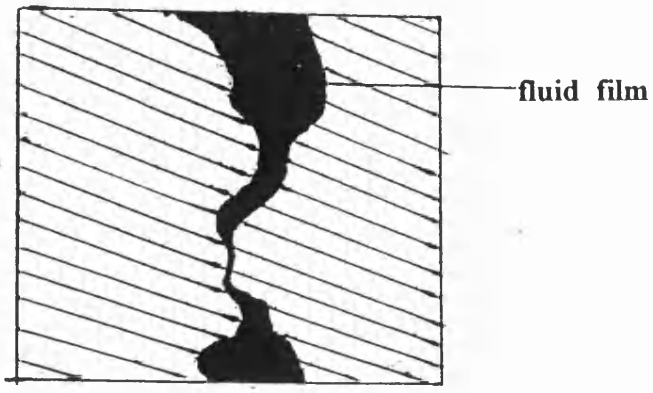

(c) Liquid film lubrication

finer lubricant particles coating the larger excipient and drug particles and interrupting inter-particle bonding. Particles that show ductile/plastic deformation seem to be affected to a greater extent than those that show brittle consolidation behaviour, due to the formation of new clean surfaces in the latter during compaction. [5]

1.3.2 Evaluation of Lubrication Properties

1.3.2.1 True Lubricant Activity

By the application of instrumentation technology to tableting equipment, true lubricant activity has been quantitatively evaluated by the measurement of parameters such as:- ejection force, R-value, residual force and force lost to the die wall. [30, 35-37]

The R-value is the ratio of the maximum lower punch force to the maximum upper punch force or the fraction of maximum force exerted by the upper punch transmitted to the lower punch. [38] Generally, for tablet machines with a stationary lower punch such as the Manesty E2 and F3, the R-values are less than 1. The closer the R-value to 1 the better the lubricant efficiency. There is a correlation between the force lost to the die wall and the ejection force.

Simultaneous measurement of compaction and lubrication forces (ejection and residual forces) has been always difficult, due to vastly different magnitudes of the forces. This has been overcome by measuring the residual area on the force - time curves which include both the static residual and dynamic ejection

event following compaction. [37] Actually, there are two schools of thought as to whether the static (residual) or dynamic (ejection) force is more appropriate for the evaluation of true lubricant activity. [36] The same authors then suggested that the former is more suitable for comparing the efficiency of different lubricants while the latter is more suitable for optimisation of lubricant concentrations.

1.3.2.2 Glidant Activity

Glidant activity has been evaluated by means such as hopper flow rate measurements, angle of repose measurements and analysis of tablet weight variation. [17, 30, 39] Angle of repose is best suited for particles ≥ 150 μm. [17] Values for angle of repose $\leq 30°$ generally indicate a free flowing material and values $\geq 40°$ suggest a poor flowing material. If a granulation/powder has good flow properties then tablet weight variation will be minimal.

1.3.2.3 Anti-adherent Activity

Anti-adherent activity continues to be evaluated mainly by tool inspection. [30] However, a number of quantitative evaluation of anti-adherent activity of lubricants have been carried out. [30, 34, 35]

A device designed to measure the "slipping force" between tablet surface and upper punch has been reported. [30] Tablets were compacted on a single punch instrumented machine with modified upper punch assembly and a split die. The upper punch was not retracted after compaction. The intact upper punch-tablet die assembly was transferred to a device which measured the force required to

rotate the upper punch while the tablet was held stationary in the die. A number of direct compression formulations were evaluated. The data showed that slipping force measurement could be used to predict the tendency of formulations to stick.

Using an instrumented strain gauge measuring arm of a rotary tablet machine, the "strippability" of tablets was quantified. [30] Three of the formulations tested contained polyethylene glycol (PEG) 4000 and lactose in various proportions as the basic materials and 0.5 % silica-type glidant. The fourth formulation contained only lactose granulation and 1 % magnesium stearate. Mixtures were compacted at different compaction forces. It was concluded that the stripping force of the tablets decreased with decreasing PEG 4000 concentration in the mixtures and increased with increasing compaction force or with running time with some mixtures. However, no details of the design or calibration of the measuring device were given.

Mitrevej and Augsburger [30] designed instrumentation to measure the adhesion of tablets to the lower punch face. A strain gauged cantilever beam affixed to the feed frame in front of the sweep-off blade detached the tablet from the lower punch face. The adhesion force was the total force measured by the beam less that due to the momentum of the tablet. A Stokes RB-2 press was used for the tableting. Generally, the higher the compaction force or the lower the magnesium stearate concentration, the higher the adhesion in three direct compression fillers (compressible sugar, microcrystalline cellulose, lactose). With

microcrystalline cellulose (MCC) and 0.1 % magnesium stearate, adhesion decreased with increased tablet thickness or decreased tablet diameter (constant thickness) at constant compaction force. Measurement of ejection forces simultaneously, revealed that differences in true lubricant efficiency did not necessarily reflect differences in adhesion. Therefore anti-adherent activity can not be inferred from true lubricant activity.

Studies which have been done to compare lubricated and unlubricated MCC suggest two opposing effects on tablet adhesion:- (a) enhancement of adhesion due to increased reaction at the lower punch due to reduced die wall friction, and (b) reduction of adhesion due to the anti-adherent effect of the lubricant. [34] In the same study, these authors found out that at any given compaction force, adhesion of MCC tablets lubricated with magnesium stearate appeared to decrease with increases in blending time or intensity of blending. Over a three hour running time, adhesion force increased to peak values and then declined with both direct compression systems (MCC and lactose). However, ejection forces gradually decreased to apparently limiting values in all cases. Even though stearic acid appeared to be less efficient than magnesium stearate as a true lubricant and as an anti-adherent with the MCC blends, the converse was true with the hydrous lactose blends at 1 % lubricant concentration. From this study, these authors also concluded that differences in true lubricant efficiency do not necessarily reflect differences in anti-adhesion efficiency and in some systems, the general belief that anti-adhesion efficiency increases with lubricant concentration is not true, especially with lubricants such as stearic

acid. This is so because such lubricants partially melt at compaction forces and temperatures.

The tendency for picking or sticking to occur in tablets during compaction can also be obtained from residual force measurements.[35] Non-sticking formulations such as those that contain high proportions of MCC tend to yield high residual forces. This is due to reduced tendency of the tablets to be raised away from the lower punch when the upper punch lifts away from the compact. Formulations that tend to stick or pick, such as those containing low melting point excipients such as HVOs, waxes, gums and stearic acid, tend to be slightly withdrawn from the lower punch when the upper punch lifts up following compaction. This reduces the residual force on the lower punch.

However, as indicated initially, evaluation of adhesion tendencies of a formulation is still primarily done by tool inspection as this is cheap, reliable, easy to perform and convenient.

1.4 The Effects of Particle Size on Tablet Strength

The physico-chemical and mechanical properties of pharmaceutical powders/granules have a profound effect on tablet strength. Physico-chemical properties include particle density, particle size, size distribution, particle shape and texture. Solid state properties include crystal hardness and hygroscopicity and mechanical properties include elasticity, plasticity and brittleness of the excipients and drugs.[23] Beside affecting the ultimate tablet strength, all these

properties determine how a formulation will behave during tableting and its ultimate performance as a drug delivery system.

Alderborn and Nyström [25] studied the effect of particle size on the mechanical strength of tablets made from acetylsalicylic acid BP, sodium citrate dihydrate, α lactose monohydrate, Sta-Rx 1500, sodium chloride, Emcompress and saccharose. This effect was strongly dependent on the properties of the materials. For Emcompress and saccharose which undergo extensive particle fragmentation during compaction, tablet strength was almost independent of particle size. As for the first three materials (acetylsalicylic acid BP, sodium citrate dihydrate and α lactose monohydrate), which fragment to a lesser extent than Emcompress and saccharose, tablet strength decreased with an increase in particle size. This was attributed to the fact that smaller particles have a larger surface area for bonding than larger particles. For the mainly ductile materials, sodium chloride and Sta-Rx, tablet strength increased with an increase in particle size. For Sta-Rx this was thought to be due to the change in particle texture. Smaller particles were fairly smooth while the larger particles were rougher. As for sodium chloride it was thought that larger particles probably create stronger bonding forces than smaller ones with total contact area having minimal effect.

The effect of particle size on the consolidation of sodium chloride and lactose powder during compaction was also evaluated. [23] Particle size and size distribution were found to affect particle slippage and deformation and hence

consolidation. The ratio of particle size to diameter of die, affected the amount of void spaces during compaction. It was observed that contact points between particles and hence the number and total area of true contact depended on the particle size and particle size distribution as well as powder arrangement. There was a linear relationship between compaction force and crushing strength for all particle sizes of sodium chloride fractions except at high pressures. Increase in tablet strength was also observed with an increase in particle size and compaction force.

A study on the effect of particle size of crystalline and spray dried lactose on the density changes in tablets made from these materials, [23] revealed that relative volumes of compacts measured under pressure at low compaction speeds for smaller particles were less than those of larger particles, under the same conditions. However, the relationship was reversed at high compression speeds. The differences ceased to exist when measurements were done post-ejection. At low speeds, time dependent volume reduction mechanisms probably predominate, with smaller particles producing denser and smaller compacts than the larger ones, with the converse true at high speeds. Post compaction, the differences ceased to exist probably due to equal stress relaxation.

McKenna and McCafferty [40] studied the effect of particle size on the compaction mechanism and tensile strength of compacts of spray-dried lactose, Sta-Rx 1500 and Avicel PH101. Decrease in particle size of spray-dried lactose and Sta-Rx 1500 resulted in stronger compacts while Avicel PH101 compacts

were unaffected by changes in particle size. This was probably due to larger surface areas for bond formation in small particles than in large particles of lactose and Sta-Rx. Sta-Rx results in this case, were contrary to those obtained by Alderborn and Nyström. [25] The compaction mechanism was found to be independent of size fraction for all the 3 materials.

Particle size was found to have an effect on the compaction properties of sulfadimethoxine (SD) and sulfaphenazole (SP). [23] SD compacts were found to be more affected by changes in particle size than SP ones, although the latter compacts had higher tensile strengths than the former. SD compacts produced from larger particles had higher tensile strengths than those produced from smaller particles. This was attributed to more effective bonding between the larger particles of SD than between the smaller particles.

Katikaneni and co-workers [5] also studied the effect of particle size on the strength of ethylcellulose compacts. Smaller particles produced stronger tablets which they attributed to the theory that, smaller particles allow greater packing density and greater number of contact points for inter-particulate bonding. All the tablet strength-compaction force profiles at all particle sizes studied had curved shapes which indicated an approach to a limiting compact strength in relation to compaction force.

A study of the effect of original particle size and tablet porosity on the increase in tensile strength during storage of sodium chloride tablets in a dry

atmosphere was carried out by Eriksson and Alderborn. [41] Compacts were made from three particle size ranges, 425-500, 90-150 and 20-40 μm at a series of compaction forces. Tensile strength was determined immediately post-compaction and after storage for different time periods. For compacts formed from the two coarser particle sizes, tensile strength increased during storage with low compact porosity increasing the magnitude but decreasing the rate of compact strength increase. Compacts made from the smallest particle size range did not alter in strength during storage irrespective of applied load and porosity.

1.5 Controlled Release Drug Delivery

Modern science has always been in search of economical, efficient and safe means of providing for the health and well being of humankind. This has been done by the production of active agents that manipulate the biological environment around and within us. The majority of active agents/drugs (70 - 80 %) are taken per - orally, mainly as plain tablets, coated tablets or capsules, while the remainder are:- parenteral, rectal, ocular, intrauterine, intravaginal and dermal delivery systems. [42, 43]

The use of drugs is fraught with inefficiencies due to the inability to deliver these agents in the right amounts, at the right time and to the specific target. This usually result in the agents' loss, undesirable side effects and repeated dosage regimen so as to acquire and sustain the desired effect. Periodic dosage of drugs produce peaks and valleys in drug concentration in the blood, possibly between harmful and ineffective levels. The different drug

concentrations in blood produced by different dosage forms are shown in figure 1.5.

Attempts to alter the persistency and effectiveness of the active agents/drugs through modification of the reagents themselves has been made but it has always proved to be difficult, time consuming and expensive. More attention is now being focused on methods by which drugs are administered, giving rise to the field of "Controlled Release". This has been defined as the technique by which drugs are made available to a target site, at a rate and duration so as to produce a desired effect with minimum inconvenience to the patient. The objective is to maintain the desired concentration level. In some situations, it implies the delivery of drug more promptly for short periods (pulsed and circadian rhythm), [44] while at times prolongation of drug levels are necessary. In the latter case, terms such as "prolonged" or "sustained" release are employed. This designates only one aspect of controlled release, that is the production of protracted levels of drug. Controlled release implies predictable and reproducible release profiles, relatively independent of environment. This gives rise to a higher degree of control than achieved in sustained release formulations. [42] Generally, available sustained release preparations offer some degree of "controlled" release but the control is incomplete, with few systems releasing drug at zero-order rate.

Figure 1.5:- Typical Drug Levels in Blood versus Time Profiles for Various Modes of Delivery [92]

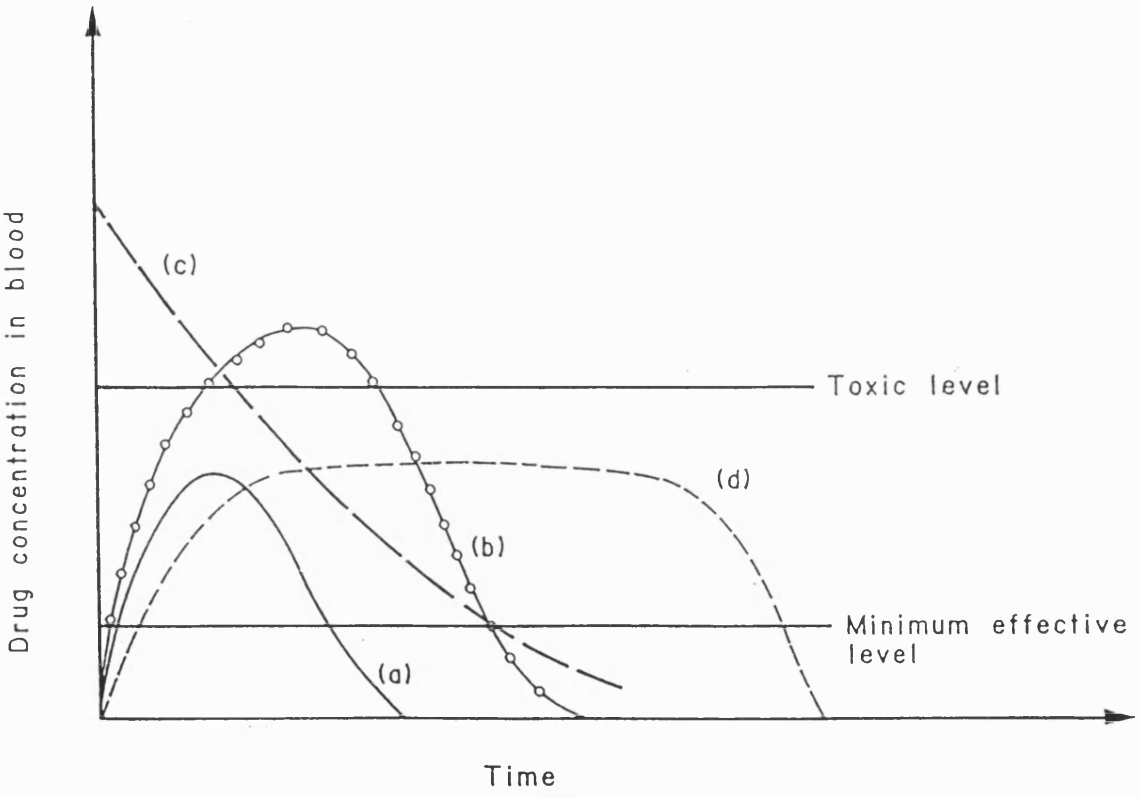

Key:- (a) standard oral dose

(b) oral overdose

(c) intravenous injection

(d) oral controlled release

1.5.1 Oral Controlled Release Drug Delivery

A discussion of oral controlled drug delivery would be incomplete without consideration of the gastrointestinal tract (GIT) and its advantages and disadvantages as a drug delivery route, since the majority of medicaments are taken per-orally. The GIT is divided into four major parts namely:- (a) oesophagus, (b) stomach, (c) small intestines and (d) large intestines/colon. All systematically acting drugs taken orally have to pass through epithelial cell layers to reach the target tissue or organ in order to elucidate the desired pharmacological effect. Different parts of the GIT have different cell types which produce different micro-environments, due to cellular secretions. All this pose a challenge for drugs targeted to these GIT regions for absorption. The period that a dosage form remains in each region depends on the local motility of that region. Total GIT transit time vary from 10-60 hours. [45]

1.5.1.1 The Oesophagus

Contact with the oesophagus is usually relatively short, (10-14 seconds), though in some pathological conditions such as achalasia, there can be prolongation of food bolus or dosage forms. In normal subjects, transit of heavy capsules is relatively faster than lighter capsules. [46] Retention of a formulation in the oesophagus can lead to delayed drug absorption. [47] Generally, liquids are cleared faster than solids in the oesophagus. Tablets or capsules taken in the supine position could stick on the oesophageal wall. [48-50] Factors that predispose a formulation to adhere are shape and size of dosage form, position of subject, volume of water taken with the dosage form, and surface characteristics of the

formulation. [48, 51]

1.5.1.2 The Stomach

The stomach temporarily stores food and slowly releases it into the duodenum. It is divided into the fundus, body, antrum and pylorus. Each has a different physiological function. The body has mucous cells which produce mucous, parietal (oxyntic) cells which secrete gastric acid and the intrinsic factor, chief (peptic) cells which secrete pepsinogen and G cells which secrete gastrin. Other enzymes secreted include gastric lipase, gastric amylase and gelatinase. In the fasted state, gastric pH of healthy people ranges from 1 to 2.5 and a meal can increase this to 3 - 5. [52]

Very little drug absorption occurs in the stomach, hence retention of drug here delays drug absorption in the small intestines. Gastric emptying is a major factor controlling the absorption of all the materials entering the body through the oral route. Gastric emptying, pH and motility are functions of variables such as diet, health, and medication. The behaviour of a dosage form in the stomach depends on the absence/presence of food. Liquids are generally emptied faster than solids. [53] Large monolithic units such as tablets and capsules, when given to fasted individuals, have variable gastric emptying times ranging from 5 minutes to 3 hours, as these rely on the inter-digestive migrating myoelectric complex (housekeeper waves) to effect emptying. [54-56] Some studies [57, 58] suggest a mean gastric emptying time of approximately 1 hour, in fasted individuals and this lies within the range quoted above. When

large monolithic units are given to healthy individuals after a light meal, gastric emptying is more predictable at around 2-3 hours. [59] Multi-particulate or pelleted systems empty from the stomach as a continuous series of small boluses. [60]

1.5.1.3 The Small Intestines

The small intestines are approximately 5 - 6 metres long and can be divided into three major regions, namely:- (a) duodenum (20 - 30 cm long); (b) jejunum (≅ 2.5 m long); and (c) ileum (≅ 3.5 m long). The main function of the small intestines is to mix food with enzymes so as to facilitate digestion and absorption over its large surface area enhanced by numerous villi and an ample blood supply. Unabsorbed material is propelled to the colon. The duodenum contains Brunner's glands which secrete an alkaline (bicarbonate) secretion to neutralise the gastric acid. The jejunum is thicker walled and more vascular than the duodenum, and has more villi than the ileum. The ileum has larger and more lymphatic follicles (Peyer's patches) than the other 2 regions. Intestinal cells found in all the three regions, secrete an intestinal juice called succus entericus, which has a pH of 7.5-8.0. The enzyme of importance in this juice is enteropeptidase which converts trypsinogen to trypsin.

The small intestines also receive the pancreatic juices (alkaline fluid plus enzymes) via the pancreatic duct, and the biliary secretions (bile acids, phospholipids, cholesterol and bilirubin) via the bile duct. Proximal jejunum pH lies within the range 5.0-6.5, rising slowly along the length to reach pH 6-7,

although values as high as 7-9 have occasionally been found. [61] Transit times through the small intestines range from 1-6 hours, [62-64] with a mean of 3±1 hours [56, 64] irrespective of fed or fasted state of subject and type of dosage form. It is generally agreed that the majority of drugs taken per-orally are absorbed in the small intestines.

1.5.1.4. The Colon

The large intestine/colon is responsible for the conservation of water and electrolytes, the formation of solid stool and storage until a convenient time for defecation. The colon extends from the ileo-caecal junction to the anus and is approximately 125 cm long *in vivo*. It comprises the caecum, ascending (proximal), transverse, descending (distal), sigmoid colon, rectum and anus as shown in figure 1.6. The caecum is the widest part, approximately 8.5 cm long and has a pH of 6.4 ± 0.4. The proximal colon is approximately 20 cm long and extends from the caecum to the hepatic flexure. The transverse colon is normally over 45 cm long and hangs loosely between the hepatic and splenic flexures. The distal colon extends downward from the splenic flexure and is approximately 30 cm long. The sigmoid colon is approximately 40 cm and joins to the rectum which is approximately 12 cm which in turn is connected to the approximately 3 cm long anal canal.

The mean pH in the colonic lumen is 6.4 ± 0.6 in the proximal colon, 6.6 ± 0.8 in the transverse colon, and 7.0 ± 0.7 in the distal colon. [65] Disease states such as cystic fibrosis, or diet may alter differences in pH between the proximal and

Figure 1.6:- Anatomy of the Colon [65]

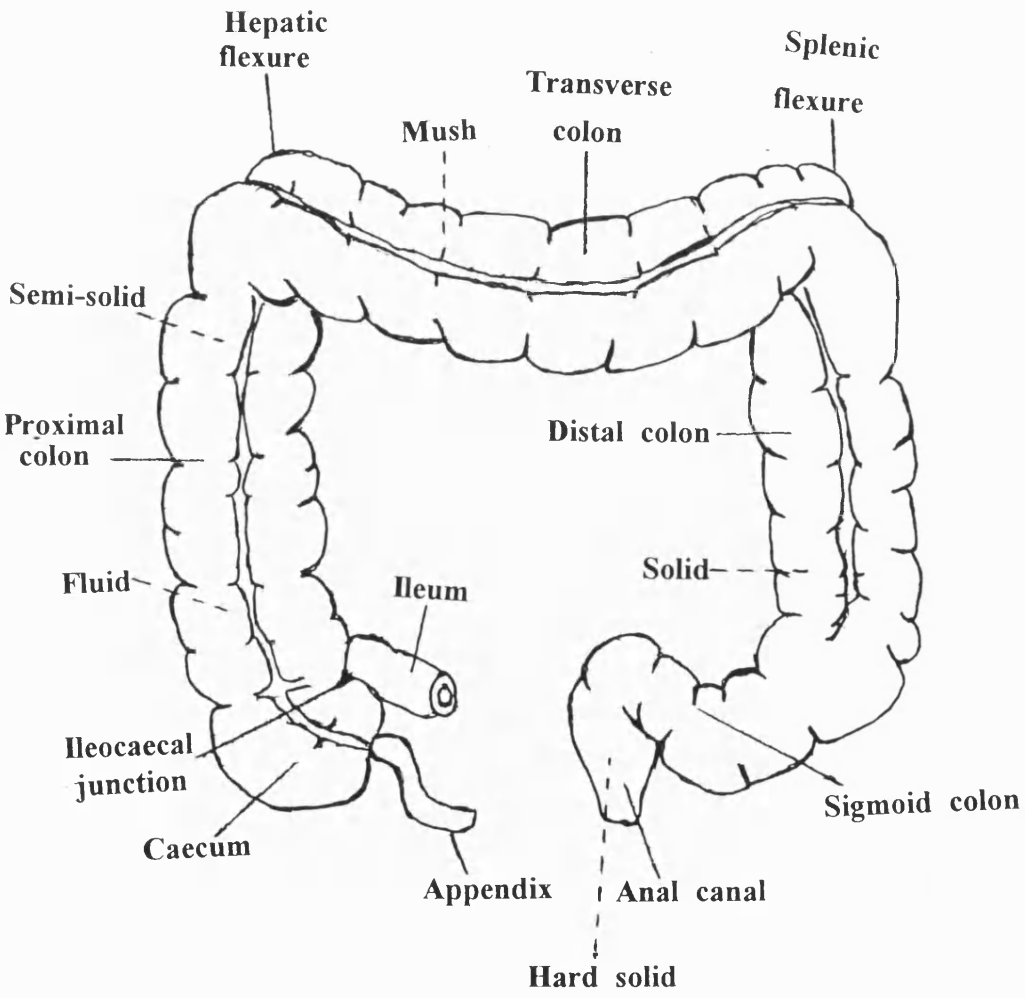

distal colon. Total colonic transit time ranges from 22-36 hours. [45, 62, 66] Transit time through the proximal colon (caecum to mid - transverse colon), distal colon (mid - transverse to sigmoid colon), and sigmoid colon is approximately 7-11 hours, 9-11 hours, and 12.5-18.5 hours respectively. [45, 62]

The colon contains up to 400 different microflora species. The most prevalent anaerobes are the *Bacteroides sp.* and *Bifido-bacterium*, while aerobes are enterococci and *Lactobacillus.* The major site of bacterial activity is the caecum where anaerobic bacteria ferment substrates in a liquid mixture. Bacteria make up to 30 % of faecal dry weight. Colonic bacteria possess exocellular enzymes (lipases) capable of hydrolysing fatty acid esters at the 1 & 3 positions of the triglyceride molecule. They also produce enzymes capable of metabolising long chain fatty acids such as oleic acid. Oleic acid is hydroxylated to hydroxystearic acid. Stilboestrol, morphine and indomethacin are excreted in bile as inactive sulphates or glucuronic acid conjugates. These conjugates are metabolised by bacterial enzymes in the colon, which release the active forms, hence prolonging their pharmacological activity via this enterohepatic loop. [65]

The colon has attracted interest as a site where drug molecules that are poorly absorbed from the small intestines may have an improved bioavailability and for local action of drugs such as aminosalicylates and corticosteroids for the treatment of ulcerative colitis. [56, 66] It is recognised as having a less hostile environment than the stomach and the small intestines, [66, 67] hence an ideal target site for protein and peptide absorption. [68-73] In addition, the colon has a

longer retention time and appears to be highly responsive to agents that improve the absorption of poorly absorbed drugs. [66] The colon has its drawbacks as a drug delivery site, which include:- (a) consolidation of faecal matter after the hepatic flexure which increases the viscosity of the luminal contents, hence drug entrapment, (b) reduced surface area, (c) low dissolution fluid volume, (d) reduced epithelium permeability to polar compounds and (e) the presence of bacterial enzymes and toxins. [65] However, it is believed that these concerns are easier to deal with than the exhaustive destruction of drugs within the stomach and small intestines due to acidity in the former and enzymes in the latter. [66]

1.5.1.4.1 Colonic Drug Delivery

Specific drug delivery to the colon is becoming increasingly important for the local treatment of conditions such as inflammatory bowel disease. [74] Such targeting can lead to improved efficacy and reduction in systemic side effects. Drugs can be delivered to the colon either orally or rectally. Rectal delivery, although it avoids many of the drawbacks of oral colonic delivery, it is recognised as less appealing. Rectal preparations often fail to reach even the transverse colon. [75] The spreading of an enema solution within the colon is highly variable even in healthy subjects. [75] Therefore attention will be focused on oral drug delivery to the colon.

Successful oral colonic drug delivery implies that the drug or drug delivery system reaches the proximal colon at a precise time, which minimises drug loss

due to acidity and enzymatic activities in the stomach and small intestines respectively or complex formation within the faeces in the distal colon. [66] Such a system could be realised by the utilisation of site specific chemical or physical signals such as enzyme concentrations or pH values. A time controlled drug delivery system could be manufactured, in which the drug release profile corresponds to transit times through certain parts of the GIT. A combination of time and signal dependent release mechanisms is even more desirable. For example, a controlled release dosage form can release drug after 5 hours, when the device can be assumed to have arrived in the colon. pH sensitive coatings such as the Eudragits can protect the drug until its arrival in the colon or microbial enzymes predominantly present in the colon, can be exploited in site-specific drug delivery to the colon. [76]

Rao and Ritschel [77] developed a per-oral system for the delivery of vasopressin, a polypeptide hormone, utilising a combination of pH-dependent and time-controlled release mechanisms. They used the polymers Eudragit® NE 30 D, Eudragit™ S100 and cellulose acetate phthalate to coat the delivery system. The system was designed to have a lag time of 6 hours, thereafter, vasopressin was released at a maximum rate between 6 and 7 hours which corresponds to colonic arrival time of 6.5 hours in the rat.

A significant drawback to practical colonic drug delivery is inter- and intra-patient variability in GI transit times, with much variability arising from gastric residence times. GIT transit times for males and females differ slightly, with

emotional stress altering this. [66] Neuroactive substances such as enkephalins, cholecystokinin, neurokinin A, and substance P affect colonic smooth muscles, hence colonic residence time. Fluctuations in colonic residence time could be overcome by the use of bioadhesives in the formulations. [66, 78]

Pro-drugs could be used to target drugs to the colon, such as the delivery of 5 - aminosalicylate (5-ASA) by the use of the pro-drug sulphasalazine. Sulphasalazine undergoes azo-reduction by colonic resident bacteria to give 5-ASA and sulphapyridine. Anthracene laxatives can be converted by colonic bacteria into active sennosides. [72]

Drug granules have been coated with polymeric materials such as methacrylates to improve colonic delivery. [79] Azo-polymeric systems whereby the drug has been covalently or non-covalently entrapped within the matrix have been used with the intention of utilising colonic bacteria and their enzymes to release the drug by breaking down the matrices. For example, Brondsted and Kopecek [76] synthesised novel hydrogels based on cross-linked azo dyes. The cross-links were degradable by microbial azo-reductases predominantly present in the colon, hence the gels appeared to be suitable for colon-specific drug delivery. The degree of degradability *in vitro* and *in vivo* was found to be related to the degree of swelling of the gels, structural and electronic factors. High faecal enzymatic degradation in high degrees of swelling in azo-polymers was also noted in some studies. [68] This was attributed to a high accessibility of the azo bonds by the bacterial azo-reductase. Van den Mooter *et al* [80] prepared

on-cross-linked azo polymers which were insoluble in simulated gastric and intestinal juices, for colon-specific drug delivery. Microbial degradation of these polymers was found to be dependent on the hydrophilicity of the azo polymer. [81]

Colonic microbial controlled drug delivery has also been attempted with varying degrees of success. [69, 71, 72, 74, 82] However, use of pro-drugs or bacterial degradable matrices, depending on colonic bacteria and their enzymes to do the conversion to the active drug form or to release the entrapped drug from the matrix , is fraught with problems. This is so because colonic bacterial population is a function of diet, health and some antibiotics. [65]

Polyacrylic polymers which release incorporated drug molecules when the pH rises above 7 have been proposed as a potential colonic delivery system. This was based on the assumption that there is a shift in pH from slightly acid to slightly basic at the ileocecal junction. However, studies suggest that the pH might actually decrease in the colon. [66] Macromolecular drugs such as peptides and proteins could have their absorption in the colon enhanced by the incorporation in the formulation of absorption enhancers such as citrates, non-steroidal anti-inflammatory drugs (NSAIDS), surfactants and phenothiazines. [66, 68]

Acute and chronic colonic pathological conditions can affect drug delivery to the colon. For example, acute diarrhoea and increased muscular activity can reduce colonic transit time and hence decrease drug absorption. In summary,

colonic drug delivery has attractive aspects such as:- (a) prolonged residence time of luminal contents, (b) reduced epithelial enzymatic activity, (c) increased tissue responsiveness to absorption enhancers and (d) natural absorptive characteristics.

1.5.1.5 Types of Materials Used for Oral Controlled Release Systems

The majority of per-oral controlled release systems are made from either hydrophobic inert or hydrophilic materials.

1.5.1.5.1 Hydrophilic Systems

Hydrophilic materials/polymers are widely used for oral controlled drug administration. [72, 83-88] On contact with the dissolution medium or body fluids, these devices swell by polymer hydration and chain relaxation, forming a gel layer coat around a dry central core, with the two domains well defined. [83] Usually, the swelling of these hydrogels, such as the cellulose ethers, is influenced by cross-linking, heat treatment, pH, temperature and polymer substitution type. [86] The hydrated surface layer forms a barrier to drug release and further fluid ingress and is a viscous pseudo-gel.

Usually, the amount of drug released from these matrices is linearly related to the exposed external surface of the swollen matrix, with drug release kinetics sometimes dependent on the swelling kinetics. It is believed that the formation of the gel layer can be critical to the success or failure of the dosage form as a sustaining release device. [83] Hydrogels can deliver drug at a predetermined

rate for a defined period of time. [84] Mechanistically, it is believed that there are two distinct synchronised processes, polymer swelling and its true dissolution, that result in hydrogels releasing drug via zero order. [85] This synchronised front behaviour was reported for several hydrophilic glassy polymers such as polyvinyl alcohol and sodium carboxymethylcellulose (Na CMC) and for hydrophobic glassy polymers such as polymethyl methacrylate. [85] A wide variety of different hydrogel materials have been described for use in controlled release. Some of these are synthetic while the majority are semi-synthetic and natural, such as cellulose ethers, modified starches and the alginates. [88] The anionic polysaccharidic materials, λ-carrageenan and xanthan gum are also hydrophilic hydrogels which hydrate even at low pH values such as those found in the stomach. [89]

Rajabi-Siahboomi and co-workers [83] studied the swelling of hydrating hydroxypropylmethyl cellulose (HPMC) by NMR spectroscopy. They found out that hydration at the edges of the compacts occurred to a greater extent than the centre tablet surfaces giving rise to a convex shaped hydrated layer. However, gel layer development occurred to the same extent in both axial and radial directions and was similar in all the HPMC types examined. The predominately axial swelling of all the HPMC types examined was a result of the growth of the hydrated surface gel layer and expansion of the ungelled tablet core.

Fernandez Degiorgi and co-workers [84] incorporated ampicillin into the hydrogel 2-hydroxyethyl methacrylate (HEMA) produced by radiation polymerisation from its monomers. *In-vitro* release of ampicillin from the hydrogel was carried out. The drug-hydrogel tablets and "bullets" were also administered to dogs at a dosage of 20 mg/kg body weight. Drug release from the insoluble HEMA hydrogel was proportional to the square root of time according to the Higuchi equation. Bioavailability of the tablets and bullets was 44.2 % and 84.3 % respectively. The hydrogel did not produce toxic effects on cellular cultures or test animals.

Pham and Lee [85] investigated the synchronised dynamic swelling and dissolution behaviour during drug release from HPMC matrices using fluorescein as a model drug. They designed a flow through cell in order to provide a well designed hydrodynamic condition. They found out that there was a continuous increase in transient gel layer thickness irrespective of polymer viscosity grade or drug loading. This, they attributed to the faster rate of swelling solvent penetration than that of polymer dissolution (polymer chain disentanglement). However, over a longer period of time there was a shrinkage of matrix diameter confirming that polymer dissolution does indeed occur in HPMC matrices. The rates of polymer swelling and dissolution as well as the corresponding rate of drug release increased with either high levels of drug loading or low viscosity grades of HPMC. However, the two researchers concluded that the effect of HPMC dissolution on drug release was insignificant

with release kinetics mostly regulated by a swelling-controlled diffusion process. This was most notable with high viscosity grades of HPMC.

Wan and co-workers [86] examined the kinetics of HPMC-propranolol matrices' swelling according to the coupled Case I (Fickian) - Case II (Relaxational) equation. Previously, Wan [90] had described the swelling of HPMC-ibuprofen matrices according to first order kinetics. However, the former matrices deviated significantly from this square root of time relationship. Taking a as the original thickness of the dry matrix and s as the thickness of the swollen matrix, the above workers normalised the increase in the matrix thickness as a percentage, δ, which was used as a swelling index where:-

$$\delta = (s-a) / a \times 100\ \% \qquad \text{equation 1.7}$$

They analysed the dynamic swelling of the matrix as a function of time, t, according to:-

$$\log \delta = n_s \log t + c_2 \qquad \text{equation 1.8}$$

where δ is as defined in the previous equation and n_s is the exponent describing Fickian or anomalous swelling mechanism and c_2 a constant. The swelling mechanism of HPMC-ibuprofen matrices in pH buffer solution was approximately Case I (Fickian) with n_s clustering around 0.5. For HPMC-propranolol matrices, the swelling mechanism in water became non-Fickian with increasing amounts of HPMC thus indicating the importance of Case II relaxational mechanism. In order to ascertain the importance of the two swelling mechanisms it was decided to consider that the swelling of the matrices depended on two processes:- liquid diffusion into the matrix and

polymer swelling due to the penetrant. Approximate contribution of the two mechanisms was carried out by fitting the data on the second order equation analogous to that proposed by Peppas and Sahlin, [91] for release from swellable matrices. This second order polynomial equation gave the best data fit.

1.5.1.5.2 Hydrophobic Systems

Hydrophobic, inert materials are usually used to prepare reservoir and monolithic oral controlled release devices. Like hydrophilic devices, they can be made from synthetic, semi-synthetic or natural origin materials. Oral controlled drug delivery systems made from hydrophobic inert materials do not generally interact with the dissolution medium or GIT fluids. This implies a predominantly diffusion-controlled mechanism of drug release from them. [92]

Reservoir devices consist of a drug core surrounded by a polymeric membrane such as ethylcellulose, with diffusion of the dissolved drug through the polymer as the rate limiting step. In monolithic/matrix devices the drug can either be dispersed as a separate phase or dissolved within the hydrophobic inert material. Release occurs via diffusion through the matrix or the environmental fluid may leach the drug out of the matrix. [92] In matrix devices, diffusion of the dissolved drug out of the matrix or diffusion of the drug through the polymer, is the rate limiting step. Due to the increase in the diffusional distance with time in such matrices, drug release rate is not constant in relation to time but rather release follows a square root of time dependency.

In order to produce hydrophobic inert oral controlled release tablets, opium alkaloids such as morphine salts were homogenised with a fatty acid or its salt and ethylene vinyl acetate copolymer and compressed into tablets. *In vitro* dissolution studies of these tablets produced release profiles over extended periods of time. [93] In the same paper hydrogenated oils and polymeric substances were used to formulate long acting tablets for water soluble drugs such as diltiazem. In this case, HPMC phthalate, a hydrogenated oil, lactose, hydroxypropyl cellulose and magnesium stearate were used to prepare the sustained release diltiazem hydrochloride tablets.

A once a day dose tablet formulation for diltiazem hydrochloride was prepared using hydrogenated castor oil and stearic acid as the hydrophobic release controlling fillers. The drug was mixed with lactose, hydrogenated castor oil and stearic acid and heated to 60° C then cooled and granulated with Na CMC. Tablets produced from these granules released more than 60 % of the drug within 5 hours during *in vitro* dissolution studies. [93]

Another sustained release hydrophobic oral system was made from glyceryl monostearate, sugar, MCC, PVP and magnesium stearate, with diltiazem hydrochloride as the drug. Its *in vitro* dissolution results gave release profiles of 96 % after 24 hours. [93] The release was further delayed by coating the tablets with water insoluble polymers such as ethylcellulose or enteric polymers such as cellulose acetate phthalate or both.

El-Shanawany [94] prepared a hydrophobic oral controlled release system from stearic acid and glyceryl monostearate, with nitrofurantoin as the drug. Granules were prepared by either fusion, solvent evaporation or melt granulation. The researcher also evaluated the effect of materials such as Aerosil, MCC and Emcompress on drug release of the matrix. Granules prepared by the fusion method had the best release - sustaining characteristics. Aerosil, MCC and Emcompress increased drug release rate with release following the Higuchi mechanism of release at low concentrations (0 and 5 %) and primarily following first order release kinetics at 10 % concentration. *In vivo* studies revealed that urinary excretion of nitrofurantoin from the test granules occurred over 2-8 hours post oral administration.

Bansal and co-workers [95] directly compressed a mixture of castor wax and hydrogenated vegetable oil (HVO), in an optimised ratio of 1:1, based on bulk density, particle size distribution and compression properties, to form inert wax matrix tablets. As drug they used chloramphenicol maleate. Increase in compaction force resulted in tablets with higher strengths up to approximately 80 N. Further increase in compaction force resulted in a decrease in strength with apparent capping. Drug release was independent of tablet strength, shape and paddle rotational speed. Release was proportional to the square root of time. These results are in agreement with those obtained by Lockwood [96] and Ramzan [97] from HVO compacts.

Juul Thomsen *et al* [98] prepared hydrophobic pellets by melt pelletisation using paracetamol, glyceryl monostearate and MCC wax. 90 % of the pellets were approximately 500-1 400 μm in size. *In vitro* dissolution studies resulted in drug release over prolonged periods of time.

Kaewvichit and Tucker [99] studied the release of the macromolecule, bovine serum albumin (BSA), from a hydrophobic fatty acid matrix, stearic acid. They analysed the results in terms of BSA particle size (factor A), stearic acid particle size (factor B), BSA loading (factor C), compaction force (factor D) and the various interactions of the four factors. Drug release studies were done over 64 hours in an isotonic phosphate buffer pH 7.4 at 37° C.

Factors A, B and C were found to affect drug release. However, factor D was found to have no effect on release and this agreed with the results obtained by Bansal *et al* [95] where they found out that compaction force had no significant effect on chloramphenicol maleate release from a hydrophobic matrix. Interactions AB, BC and ABC were found to highly affect drug release from the matrices. At low drug loading (5 %), surface release depended on BSA particle size with release increasing with an increase in the drug particle size. At high drug loading (20 %), release increased with an increase in stearic acid particle size. This was probably due to the formation of a complete inter-connected pore network which resulted in simpler pathways (low tortuosity) and greater porosity for diffusion while at lower loading the converse was true. When stearic acid particle size was small (63 -125 μm) and drug particle

large (250-500 μm) there was an overall increase in release.

Kaewvichit and Tucker [99] proposed that release of the macromolecule from the hydrophobic monolithic system occurred through an inter-connected tortuous pore network. This was created by solid drug particles initially present in the matrix and the void space between stearic acid particles. The pores were randomly distributed within the matrix. The void spaces were believed to vary according to particle size - dependent arrangements of stearic acid and BSA particles.

Pentoxifylline release from hydrophobic waxy materials (palmitic and behenic acids) was evaluated by Otsuka and Matsuda. [100] The matrix tablets were prepared via co-grinding of the drug-wax and tableting. The hydrophobic waxy tablets produced formed a monolithic controlled release system, except for tablets prepared from the unground mixture which disintegrated with time. Drug release was proportional to square root of time according to the Higuchi equation.

Ibuprofen release from spherical hydrophobic cetostearyl alcohol matrices was analysed according to four release mechanisms namely:- (a) first order mechanism (b) Higuchi mechanism (c) Baker and Lonsdale model and (d) Hixson and Crowell cube-root equation by simulation. [101]

First Order Model:- where drug activity within the matrix is expected to decrease exponentially, with rate of drug release proportional to residual activity.

$$\log_{10}(100\ \% - Q) = kt \qquad \text{equation 1.9}$$

where Q is the amount (%) of drug released at time t.

Higuchi Model:- is used to describe drug release irrespective of shape of device.

$$Q = kt^{1/2} \qquad \text{equation 1.10}$$

where Q and t are as above

Baker and Lonsdale Model:- where drug is dispersed within a spherical diffusion rate-limiting matrix.

$$3/2\ [1-(1-Q_f)^{2/3}] - Q_f = kt \qquad \text{equation 1.11}$$

where Q_f is the fraction of drug released at time t

Hixson and Crowell Equation:- describes release from systems which show dissolution-rate limitation and do not dramatically change in shape as release proceeds.

$$(1-Q_f)^{1/3} = 1-kt \qquad \text{equation 1.12}$$

where Q_f and t are as above

The cube root model and the first order model gave satisfactory fits to the data although both simulations produced extents of release higher than those predicted for the small particles (212±54 μm). For the large particles (862±334

μm) the simulated values were above the experimental ones especially at low drug release levels. The square root model and the Baker and Lonsdale models described the release data poorly. The experimental release data of tablets made from equal weight of small particles and large particles and the simulated data mirrored each other closely, particularly with the Hixson and Crowell cube root model. The researchers concluded that the particles probably behaved as contracting cubes in that as drug was released from the outer layers, the depleted layers provided relatively little diffusion resistance to drug release. This implied that although the particles were apparently intact at the end of the release process, they behaved as dissolving particles.

Pozzi *et al* [44] developed a per-oral controlled delivery system with a hydrophobic (canauba wax and white beeswax) and a surfactant (polyoxyethylene sorbitan monooleate) coat. They called it the "time clock" system. The hydrophobic-surfactant layer was applied as an aqueous dispersion to which a hydrosoluble polymer (HPMC) was added to improve adhesion to the core. Cores were made as follows:- lactose, samarium oxide and dye or lactose and salbutamol sulphate were manually granulated with an aqueous solution of PVP. Cores containing samarium oxide and the dye, E110, were used for scintigraphic evaluation and *in vitro* dissolution characterisation while those containing salbutamol sulphate were for pharmacokinetic evaluation. After drying and sieving of the granules, magnesium stearate and corn starch were added prior to compaction. The coat was applied post-compaction in a fluid bed.

The above system was able to release drug after a predetermined lag time which was independent of normal physiological conditions such as pH, digestive state of subject and the anatomical position at the time of release. At the end of the lag time, disaggregation of the core was both rapid and complete. Such a system could be ideal for colonic drug targeting. The lag time would be equivalent to gastric residence time plus small intestine transit time. The rapid drug release post lag period is desirable for GIT areas such as the proximal colon which have reduced epithelial drug absorption due to reasons mentioned in section 1.5.1.4.1.

The types, classifications, characteristics, advantages, disadvantages and ideal attributes of various oral controlled drug delivery systems available have been described extensively by Merkus, [42] Fan and Singh. [92]

1.5.1.6 Diffusion in Polymers

Diffusion can be defined as a process of mass transfer of individual molecules of a substance, brought about by random molecular motion. It is associated with a concentration gradient. Diffusion has always been analysed in terms of Fick's first and second laws. Fick's first law states that the amount, M, of a material flowing through a unit cross section, S, of a barrier in unit time, t, is known as the flux, J.

$$\Rightarrow J = dM / Sdt \qquad \text{equation 1.13}$$

The flux in turn is proportional to the concentration gradient, dC/dx.

$$\Rightarrow J = -DdC/dx \qquad \text{equation 1.14}$$

where D is the diffusion coefficient of the diffusant, C is the concentration of the diffusant and x is the distance of movement perpendicular to the surface of the barrier. The negative sign indicates that diffusion occurs from a region of higher concentration to a region of lower concentration. D does not necessarily remain constant as it may change at higher concentrations and is affected by factors such as temperature, pressure, solvent properties and chemical nature of the diffusant. In diffusion the natural assumption is that the driving force is the concentration gradient.

Fick's second law of diffusion examines the rate of change of diffusant concentration at a point in the system. The equation's emphasis is on the change in concentration with time at a definite location. The concentration of diffusant in the volume element changes with time, $\Delta C/\Delta t$, as flux or amount diffusing changes with distance, $\Delta J/\Delta x$, in the x direction. Hence, Fick's second law states that:- the change in concentration with time in a particular region is proportional to change in the concentration gradient at that point in the system.

$$\Rightarrow \partial C / \partial t = - \partial J / \partial x \qquad \text{equation 1.15}$$

Differentiation of equation 1.14 with respect to x results in:-

$$-\partial J / \partial x = D \partial^2 C / \partial x^2 \qquad \text{equation 1.16}$$

Substituting $\partial C / \partial t$ from equation 1.15 into equation 1.16 results in:-

$$\partial C / \partial t = D \partial^2 C / \partial x^2 \qquad \text{equation 1.17}$$

Equation 1.17 represents diffusion in the x direction only. In order to express concentration changes of diffusant in three dimensions, Fick's second law is written in the general form:-

$$\Rightarrow \partial C / \partial t = D (\partial^2 C / \partial x^2 + \partial^2 C / \partial y^2 + \partial^2 C / \partial z^2) \qquad \text{equation 1.18}$$

1.5.1.6.1 Drug Release in Matrix Type Delivery Systems Such as HVOs

Higuchi [102] offered the first model for release from these types of devices. In such devices the drug is homogeneously dispersed in the matrix as discrete crystals or solid particles. It is believed that drug molecules can elute out of the matrix only by dissolution in the environmental fluid and then diffusion through the polymer porous structure. The drug solids in the layers close to the surface of the device elute first, and when this is exhausted, the drug in the next layer then begins to be depleted. This is schematically illustrated in figure 1.7. As the drug is released the diffusional distance becomes increasingly longer.

From Fick's first law:-

$$dM / Sdt = dQ / dt = DC_s / h \qquad \text{equation 1.19}$$

where dQ / dt is the drug release rate per unit area of exposed surface of matrix. As the boundary between drug matrix and the drug depleted zone recedes with time, the thickness of the empty matrix, dh, through which the drug diffuses increases with time. h is the hydrodynamic/static diffusion layer, while C_s is the solubility or saturation concentration of the drug in the matrix and A is the total concentration (amount per unit volume), dissolved and undissolved, of the drug in the matrix. As the drug passes out of the matrix the drug boundary represented by the vertical dotted line moves to the left by a very small (infinitesimal) distance, dh. The infinitesimal amount, dQ, of drug released is approximately:-

Figure 1.7:- Drug Release from Matrix Dosage Form

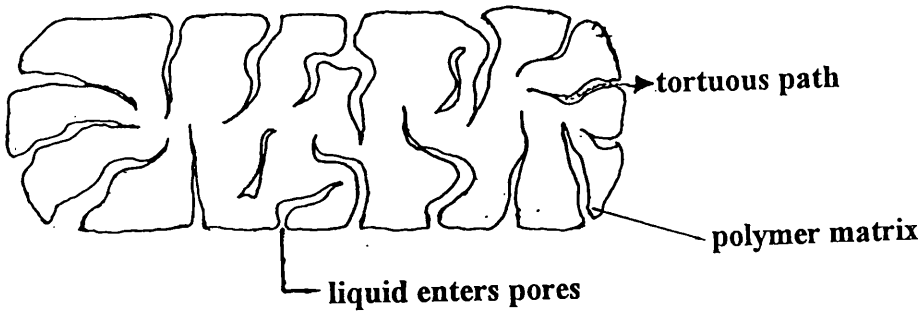

(a)

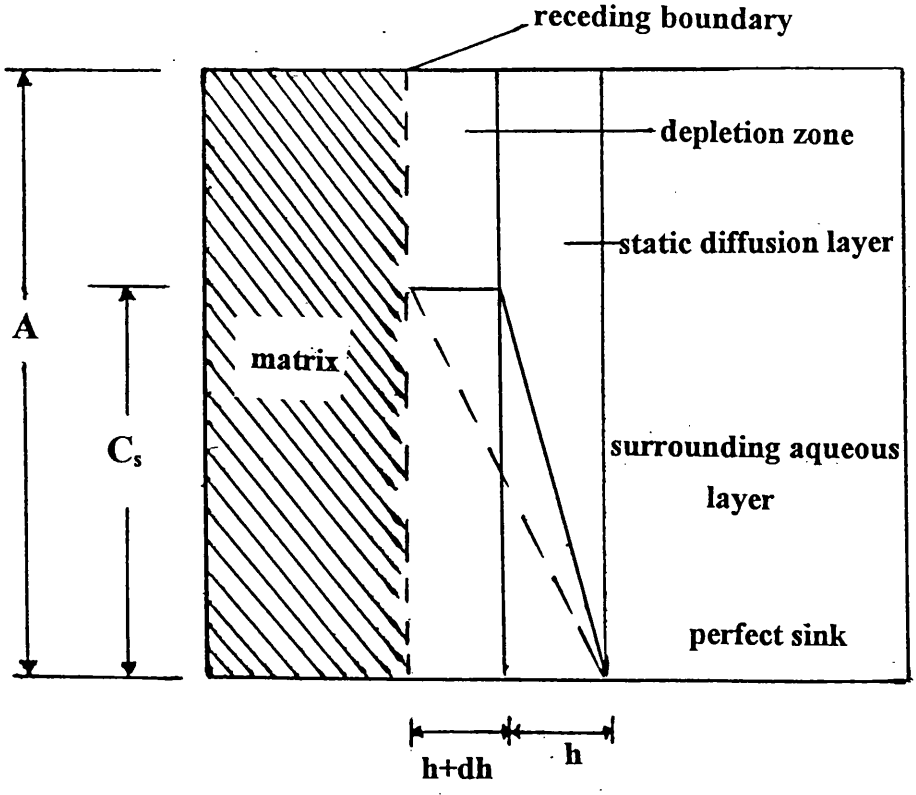

(b)

NB:- (a) Heterogeneous granular matrix after drug has been leached out

(b) Schematic illustration of matrix and receding boundary as drug diffuses from dosage form

$$dQ = Adh - 1/2C_s dh \qquad \text{equation 1.20}$$

dQ of equation 1.20 is substituted into equation 1.19:-

$$\Rightarrow (A - 1/2C_s)dh = DC_s dt / h \qquad \text{equation 1.21}$$

Integration of equation 1.21 results in:-

$$(2A - C_s) / 2DC_s \int h\, dh = \int dt \qquad \text{equation 1.22}$$

$$\Rightarrow t = \{(2A - C_s)h^2 / 4DC_s\} + C \qquad \text{equation 1.23}$$

The integration constant, C, can be evaluated at $t = 0$, when $h = 0$, giving:-

$$t = (2A - C_s)h^2 / 4DC_s \qquad \text{equation 1.24}$$

$$h = \{4DC_s t / (2A - C_s)\}^{1/2} \qquad \text{equation 1.25}$$

The amount of drug depleted per unit area of matrix, Q, at time t, is obtained by integrating equation 1.20 to yield:-

$$Q = hA - 1/2hC_s \qquad \text{equation 1.26}$$

Substituting equation 1.25 into 1.26 produces:-

$$Q = \{DC_s t / (2A - C_s)\}^{1/2} (2A - C_s) \qquad \text{equation 1.27}$$

$$\Rightarrow Q = \{D (2A - C_s)C_s t\}^{1/2} \qquad \text{equation 1.28}$$

Equation 1.28 is known as the Higuchi equation which can simply be written as:-

$$Q = kt^{1/2} \qquad \text{equation 1.10}$$

Drug release rate at time t is obtained by differentiating equation 1.28 with respect to t, to obtain:-

$$dQ/dt = 1/2\{D(2A - C_s)C_s / t\}^{1/2} \qquad \text{equation 1.29}$$

Generally, $A >> C_s$, and equation 1.28 reduces to:-

$$Q = (2ADC_s t)^{1/2} \qquad \text{equation 1.30}$$

Equation 1.29 becomes:-

$$dQ / dt = (ADC_s / 2t)^{1/2} \qquad \text{equation 1.31}$$

Drug release from a granular matrix involves simultaneous penetration of the surrounding medium, after surface wetting, dissolution of the drug and leaching out of the drug through the interstitial channels/pores. The volume and length of the opening in the matrix is accounted for by a diffusion equation, which is a second form of the Higuchi equation:-

$$Q = \{D\epsilon/\tau(2A - \epsilon C_s)C_s t\}^{1/2} \qquad \text{equation 1.32}$$

In which ϵ is the porosity of the matrix and τ is the tortuosity of the capillary system. Both terms are dimensionless. Porosity, ϵ, is the fraction of the matrix that exists as pores into which the eluting medium can penetrate. It is the total porosity after the matrix has been leached of drug. This is equal to the initial matrix porosity, ϵ_o, before leaching starts, and the porosity created by the extraction of the drug.

$$\Rightarrow \epsilon = \epsilon_o + A\,(1/\rho) \qquad \text{equation 1.33}$$

where ρ is the drug's specific density. Since the initial porosity, ϵ_o, of compressed tablets is very small relative to that created by dissolution and removal of the drug from the tablets, it can be estimated that:-

$$\epsilon \cong A / \rho \qquad \text{equation 1.34}$$

The tortuosity factor, τ, accounts for the increase in the pathlength of diffusion, due to the branching and bending of the pores, compared to the shortest "straight through" pores. Tortuosity tends to decrease drug release, while porosity tends to enhance drug release. Methods of obtaining factors such as tortuosity, porosity and diffusity have been described. [103] While equation

1.28 is suitable for release from homogeneous tablets that gradually erode and release drug into the medium, equation 1.32 applies to drug release mechanism whereby the eluting medium enters the matrix, dissolves the drug before it diffuses out leaving a shell of matrix with empty pores. Such is the case of hydrogenated vegetable oils matrices. [96, 97]

1.5.1.6.2 Diffusion coupled with Relaxation

Peppas and Sahlin [91] developed an equation coupling Fickian diffusion and relaxation contribution (Case-II) for drug release in controlled delivery systems. Case-II relaxation release is associated with stresses and state - transition in polymers. This equation was developed from a simple exponential expression shown below:-

$$Q = kt^n \qquad \text{equation 1.35}$$

where Q is the amount of drug released at time t, k is a kinetic constant and n is the diffusional exponent for drug release. This equation can be used to analyse the first 60 % of a release curve regardless of geometric shape of the delivery device. However, for a device releasing drug by both diffusion and relaxation, these two phenomena can be considered additive as shown below:-

$$Q = k_1t^m + k_2t^{2m} \qquad \text{equation 1.36}$$

where the first term on the right hand side is the Fickian contribution and the second term being the Case-II relaxation contribution. The coefficient m is the purely Fickian diffusion exponent for a device of any geometrical shape which exhibits controlled release. Regardless of geometry of device, the value of the

exponent for the Case-II relaxation mechanism is twice that of pure Fickian diffusion. The Fickian diffusion coefficient varies with the aspect ratio (diameter to height/thickness) of the device. For example, for a controlled release tablet of diameter 8 mm and thickness 2.8 mm, $m \approx 0.46$ and $2m \approx 0.92$ thus resulting in:-

$$Q = k_1 t^{0.46} + k_2 t^{0.92} \qquad \text{equation 1.37}$$

Equation 1.36 can be written as shown below:-

$$Q = k_1 t^m \{1 + (k_2/k_1) t^m\} \qquad \text{equation 1.38}$$

Therefore the fraction of drug release due to Fickian mechanism, F, is:-

$$F = 1/\{1 + (k_2/k_1) t^m\} \qquad \text{equation 1.39}$$

Solute release from any device, irrespective of geometry, can be evaluated in terms of Fickian and relaxation contribution as indicated by equations 1.36 and 1.37. m = n when relaxation mechanism is negligible. The diffusion-relaxation mechanism could be used in analysing drug release from some hydrophobic inert matrices such as HVO, which contain surfactants that facilitate erosion and/or relaxation of the matrices. In such cases drug releases often fail to follow pure Fickian diffusion.

Typical curves for zero order release mechanism **($Q = kt$)**, first order mechanism **($\log_{10}(100\ \% - Q) = kt$)**, and Higuchi release mechanism **($Q = kt^{1/2}$)** are shown in figures 1.8 -1.10.

Figure 1.8:- Typical Curve for Zero Order Drug Release (Q = kt)

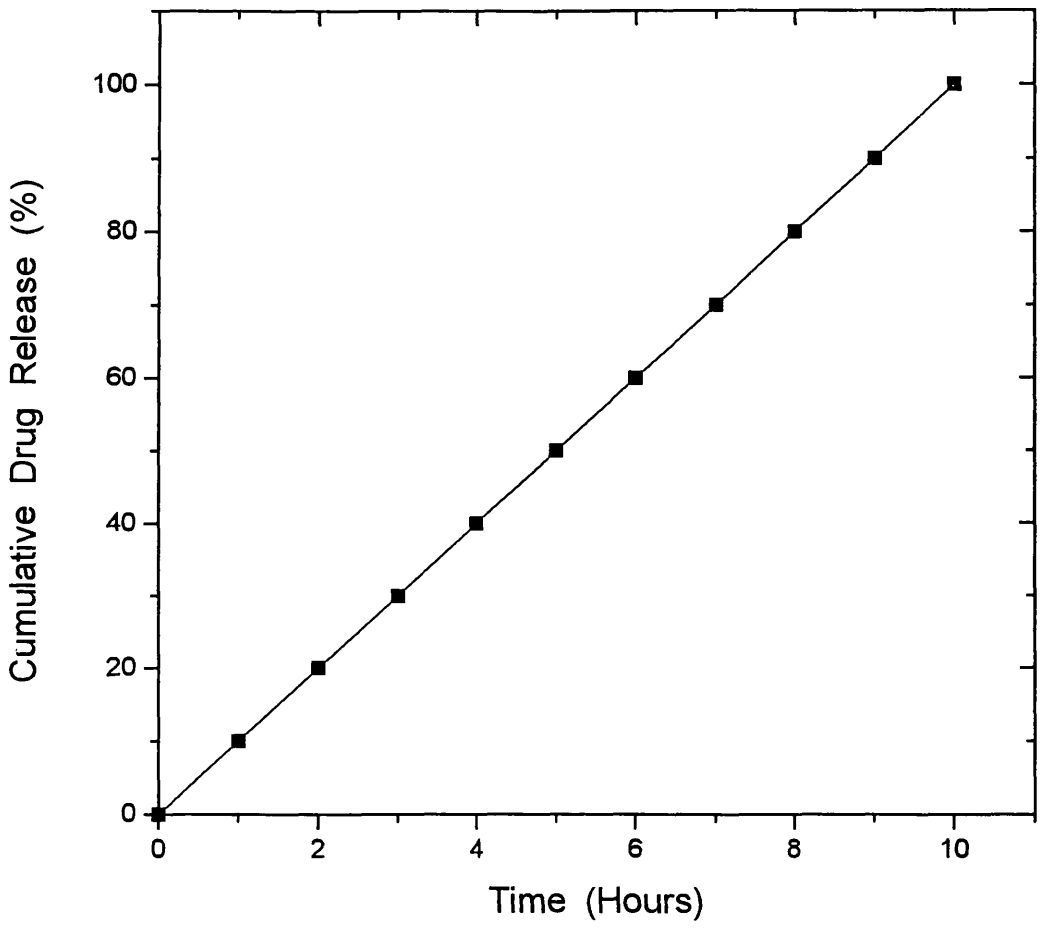

Figure 1.9:- Typical Curve for First Order Drug Release

($\log_{10}(100\ \% - Q) = kt$)

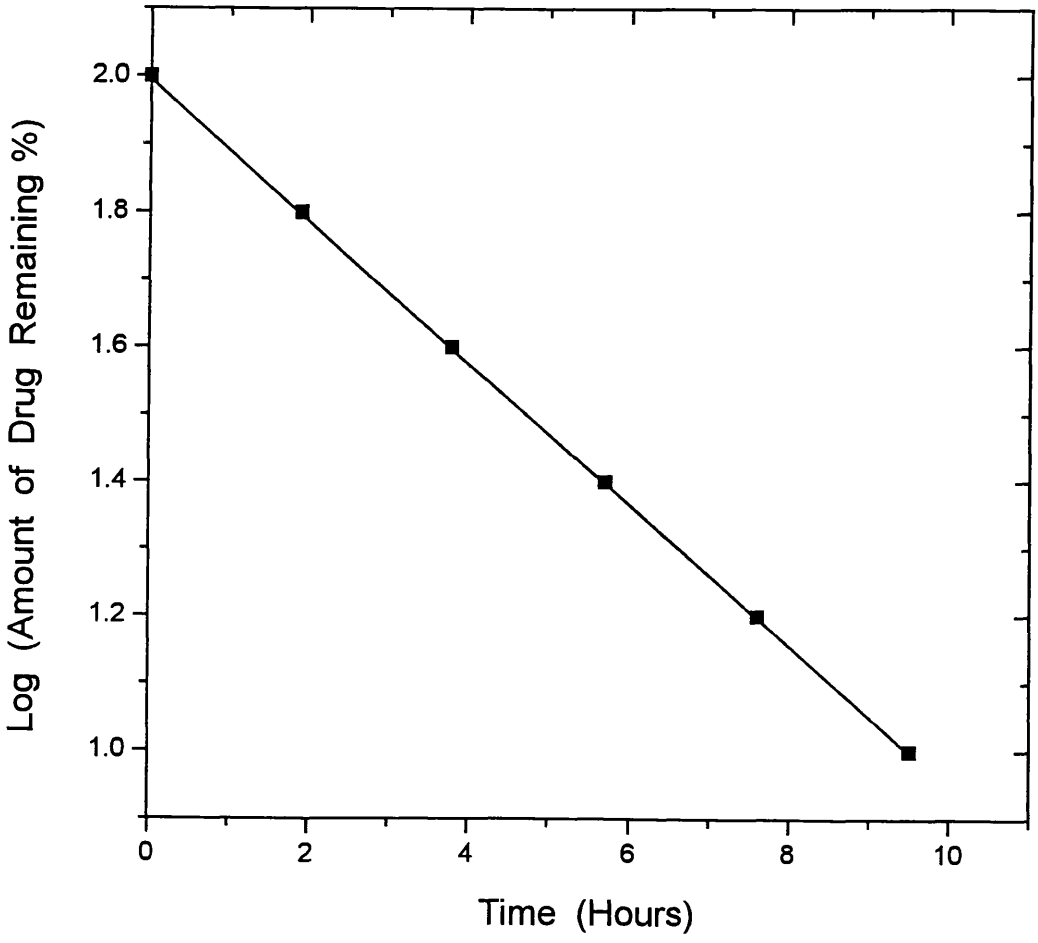

Figure 1.10:- Typical Curve for Square Root of Time (Higuchi)

Drug Release ($Q = kt^{1/2}$)

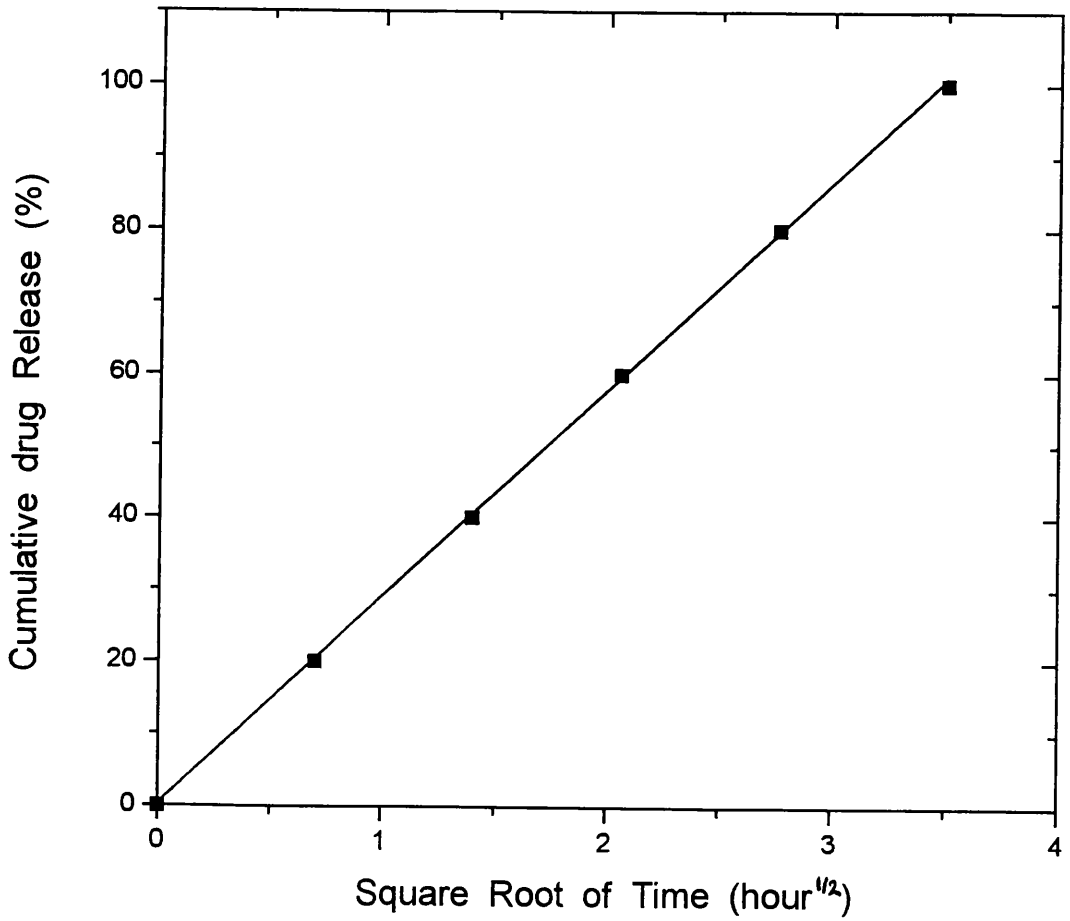

CHAPTER 2

MATERIALS AND METHODS

2.1 AIMS AND OBJECTIVES

Hydrogenated vegetable oils (HVO) matrices, like other controlled delivery systems, release drug predominantly by diffusion over long periods of time, without significant dimensional changes. [95-97] The drug release occurs through water filled tortuous pores within the matrices. Systems such as these, exhibit a gradual decrease in release rate with time, hence their non-linear concentration - time curves due to the longer distance that the drug in the deeper layers of the matrix has to travel to exit the matrix. Therefore such devices might actually deliver sub-therapeutic drug levels after extended periods of time. "Controlled" release partly implies reproducible drug delivery at a predetermined rate which may be constant. HVO matrices partly fulfil this aspect of controlled release.

For the maintenance of an optimum bioavailability over a prescribed period of treatment, the fraction of a drug dose released from a controlled release device and absorbed during a given time should be enough to compensate for the active drug species metabolised and/or excreted from the body during the same period. This is determined by the rate of drug release from the device. In most situations a constant rate of drug release (zero order) is presumed to be

optimal. For most oral controlled release devices, the ***rate of drug release*** and not the ***rate of drug absorption or removal*** is the rate limiting step. Altering the geometry of devices such as HVO matrices to achieve zero order release has been attempted by some researchers. [96, 104-106] The basic principle involved in these cases was to coat a matrix completely with a water impermeable polymer. A circular hole was made in the middle of the flat face of the hemispherical device. As drug was released, the section of the device depleted of drug continued hemispherical in shape, constantly increasing in radius, hence increasing the area of drug available for diffusion. This compensated for increase in diffusional distance, making drug release constant. Staniforth [107] invented a controlled release tablet with an impermeable membrane such as ethylcellulose, having an orifice, although the tablet was not necessarily hemispherical. Zero order release was achieved by altering the size of the orifice. However, the search for simpler methods of providing constant release rate still remains a challenge. Besides this, most designs of controlled delivery systems are a result of research work carried out in laboratories of commercial organisations, hence the majority are patented with their clinical data not readily available. [93]

For drugs that cause down-regulation at the site of action or those to which patients might develop a tolerance over a period of time, such as morphine sulphate and nitrates, [44] oral controlled release devices that are designed for them, ought to be pre-programmed to release the active agent at gradually increasing release rates with time, so as to compensate for the tolerance. In

some cases, a reduction of drug dosage also counteracts tolerance. When considering the proximal colon as a possible site for oral controlled release tablet targeting, an increasing release rate with time is desirable. This is so, because, as the formulation moves up the colon, the colonic contents gradually become viscous due to faecal consolidation. [66] More drug release per unit time will counteract this effect and probably maintain drug bioavailability.

A number of highly water soluble drugs such as diltiazem, captopril and morphine salts [93] are readily absorbed in the proximal colon. However, these hydrophilic drugs are more difficult to deliver orally in sustained or controlled release manner than lipophilic drugs. This is due to their relatively short plasma half-lives which ranges from 2 - 4.5 hours hence they require 3 -4 divided doses daily. Despite this, these hydrophilic drugs such as captopril, diltiazem hydrochloride and morphine sulphate are prescribed to chronically ill patients who require them for long periods in order to benefit therapeutically. Therefore sustained and controlled release systems for them, targeted to the appropriate site of the GIT such as the proximal colon, is desirable. Many attempts have been made to regulate highly water soluble drugs' release by the incorporation of hydrophobic inert fillers such as ethylcellulose, hydrogenated castor oil, stearic acid and glyceryl monostearate. [93] Besides such water soluble drugs, proteinaceous drugs such as vasopressin, are probably better absorbed in the colon than in the stomach and small intestines. The acid in the stomach

denatures the proteinaceous drugs, while the small intestines enzymatically degrade them. [66]

Besides exhibiting decreasing release rates with time, HVO compacts have a low compact strength. [96, 97] Due to the fact that HVOs probably partially melt and fuse to form compacts/matrices on compaction, the HVO adheres to the tablet tooling, impeding the tableting process. [96, 97]

Therefore the present study was aimed at:-

- Improving the tensile strength of HVO compacts.
- Reducing compact adherence to tablet tooling.
- Enhancing drug release of the HVO matrix.
- Using ***simple*** methods to alter the release mechanism of the HVO matrix to obtain:-
  - zero order release,
  - increasing release rate with time.

The overall aim was to formulate an oral controlled release system with adequate physico-mechanical properties capable of being targeted to the proximal colon.

2.2 MATERIALS

Sterotex K (hydrogenated castor/soybean oil), Batch number 333360, supplied by Aston Chemicals Ltd, England.

Sterotex K is a hydrogenated vegetable oil (HVO), consisting mainly of glyceryl-tris-12-hydroxystearate [108] and mixed esters of long chain fatty acids. Such long chain fatty acids include:- stearic acid, 12-hydroxystearic acid and palmitic acid. Small quantities of free fatty acids are expected in Sterotex K as well. In the study, Sterotex K was used as the basic release - sustaining hydrophobic matrix material. It has a melting range of 62-88° C. [108, 109] Its uses include:- (i) stiffening/hardening agent in some formulations, (ii) sustained release coating material, (iii) preparation of delayed release drug matrix and (iv) tablet lubricant. [108]

PVP K-30 (polyvinylpyrrolidone), Batch number 90916, supplied by Dykem Chemicals, England.

PVP K-30 has a relative molecular weight of approximately 40 kDa and a softening point of about 150° C. [110] In pharmaceutical technology, it has the following uses:- (i) tablet binder, (ii) carrier for drugs, (iii) dispersing agent, (iv) suspending or viscosity builder, (v) coating agent and (vi) tablet diluent. [110] It is soluble in water and is hygroscopic. It was used as a binder in the study.

PVP K-90, supplied by Dykem Chemicals, England.

The relative molecular weight of PVP K-90 is approximately 360 kDa. [110] It has pharmaceutical uses similar to those for PVP K-30. Due to its high molecular

weight, it produces higher viscosity solutions with water than PVP K-30 does. In the present study it was used as a binder as well.

Stearic acid (octadecanoic acid), Batch number 11H3414, supplied by Sigma Chemical Company, USA.

Stearic acid has been used as follows:- (i) tablet and/or capsule lubricant, (ii) enteric coating ingredient and (iii) emulsifying agent in ointments and creams. [112] It usually contains some palmitic acid. [111] Interestingly, stearic acid has been used as a hydrophobic binder in direct granulation. [109, 112] It has a relatively low melting point range (51-69° C), [109, 111] which makes it susceptible to softening/melting during compression. [34] This partial melt-fusion characteristics of stearic acid reinforces compact strength. Therefore in the present study, it was primarily used as an "auxiliary" binder to PVP. It was also used as an anti-adherent. Before use as an anti-adherent, it was passed through a 125 μm test sieve.

Propranolol hydrochloride, Batch number 3658, supplied by Industrie Chimiche Italiane.

Propranolol hydrochloride was one of the two drugs selected for the assessment of the release characteristics of the matrix because of its applicability to sustained release medication. It is a non-selective β-adrenoceptor antagonist: therefore it is used as:- (i) an anti-hypertensive, (ii) anti-anginal and (iii) anti-arrhythmic drug. Due to its non-selectivity, it is contra-indicated in patients suffering from bronchospasm and diabetes. [113] Propranolol hydrochloride

is readily soluble in water, with a maximum solubility of 5 % w/v. [114] It has a pK_a of approximately 9.5. [114] It is UV-assayable, with probably the naphthalene ring as the main chromophore. Propranolol hydrochloride has a maximum absorbance at approximately 290 nm. [114]

Theophylline, Batch number 102H0521, supplied by Sigma Chemical Company, USA; Batch number 5348833, supplied by Aldrich Chemical Company, England. Theophylline is used to relieve bronchospasm in asthma. [115] It is relatively cheap. Aldrich manufacturers stated that their sample was 99 % pure, while Sigma manufacturers stated that their sample was 90 % pure. Therefore the former was used in preparation of tablets for dissolution tests, while the latter was used in preparation of tablets for tensile strength evaluation. The Sigma sample was also used in the anti-adherent evaluations. Theophylline was selected because unlike propranolol hydrochloride, it is not so readily soluble in water. It has a maximum solubility of approximately 0.833%. [115] Like propranolol hydrochloride, theophylline is readily assayable by UV/visible spectrophotometry. It has a maximum absorbance at approximately 272 nm. [115]

Compritol 888 ATO (glyceryl tribehenate), Batch number 18641-57-1, supplied by Gattefosse, France.

In the study, Compritol was used as an alternative release sustaining matrix material to Sterotex K and as an anti-adherent. Before use as an anti-adherent, it was passed through a 125 μm test sieve. Unlike Sterotex K, which is chiefly a C_{18} fatty acid ester, glyceryl-tris-12-hydroxystearate, [108] Compritol is

mainly composed of a C_{22} fatty acid ester, glyceryl tribehenate. Compritol has a melting point range of 67-72° C. [109] It has the following uses:- (i) tablet lubricant [5] and (ii) hydrophobic binder in combination with glyceryl monostearate in direct granulation. [109] It is relatively new and has been reported to be less prone to tablet strength and dissolution problems. [5]

Luviskol Batch number 05-7199-05, supplied by BASF, Germany.

Luviskol is a copolymer of polyvinylpyrrolidone and polyvinyl acetate. It is a tablet binder which is heat labile. It was used for this purpose in the present study.

Polyplasdone XL-10, supplied by Gaf Chemicals, USA.

Polyplasdone is cross-linked polyvinylpyrrolidone. This material has sometimes been termed "super-disintegrant" due to its excellent disintegrating properties. It is effective at 2-5 % concentration and has been reported to be an effective binder-disintegrant in tablets made by wet granulation. [15] It also appears to be more effective than other agents in disintegrating water soluble tablets though it is not soluble in water itself. In the present study it was used as a binder. Since it is water insoluble, it was gradually dispersed in the water with the aid of heat, while stirring with a spatula.

Magnesium Stearate, Batch number 9595340E, supplied by BDH Chemicals, UK.

Magnesium stearate is a well known, currently and most commonly used tablet and capsule formulation lubricant. [5, 116] It is also used as a glidant and anti-

adherent. It exist in two pseudo-polymorphic forms namely, trihydrate acicular form and dihydrate lamellar form. [31] The latter form possesses greater lubricant activity than the former. In the study it was employed as an anti-adherent.

L - Leucine, Batch number 001FKCK, supplied by Forum Chemicals, Ltd, UK. Leucine is a white crystalline amino acid. It is one of a group of water soluble lubricants such as sodium benzoate, which find use in water soluble tablets such as lozenges. Leucine appears to be a better lubricant for ductile materials than for brittle ones. [31] Leucine sublimes at 145-148° C. [117] In the study, it was used as an anti-adherent. Before use, it was ground in a glass mortar using a glass pestle and then passed through a 125 μm test sieve.

Myverol 18 - 99, batch number D1832-1092, supplied by Eastman Chemical Company, USA.

Myverol consists mainly of distilled monoglycerides of stearic and palmitic acids, with smaller quantities of di- and triglycerides of the same acids. However, Myverol also contains very small amounts of water, propylene glycol, phosphoric acid, glycerol and citric acid. It is a non-dispersible non-ionic agent with a melting point range of 53-61° C. [109, 118] It has the following uses:- (i) non-ionic emulsifier, (ii) stabiliser, (iii) emollient, (iv) plasticiser (v) anti-tack agent in a variety of food, pharmaceutical and cosmetic products [118] and (vi) binder in direct granulation. [109] In the study, Myverol was used to alter the drug release mechanism of the Sterotex K matrix.

Some monoglycerides such as mono - olein have been known to form cubic phase structures in water at approximately 37° C. [119] These cubic phase structures release water soluble drugs in a sustained release fashion. Cubic liquid crystalline phases are common in surfactant and surfactant - like lipid systems at temperatures above the Krafft point. [120] They are transparent, viscous systems, with a wide range of stiffness. These systems are thermodynamically stable. Current proposals of cubic phase structures are:- (a) spherical aggregates (b) short rod like aggregates and (c) lamellar structures. [120] Structures in (a) and (b) could be either of the type "water-in-oil" or "oil-in-water" with units either closed or forming continuous networks.

Hydrogenated rapeseed oil, Batch number AVR 60, supplied by Anglia Oils Ltd, UK.

This is another HVO, primarily containing stearic acid mono-, di-, and triglycerides. [121, 122] Small quantities of palmitic acid glycerides, trace amounts of behenic acid glycerides and the respective free fatty acids are also found in hydrogenated rapeseed oil. [121, 122] Like Myverol, hydrogenated rapeseed oil is a semi-solid with a relatively low melting point. In the study, it was used as an alternative to Myverol.

Imidazole, Batch number 81327, supplied by Aldrich Chemical Company, England.

Imidazole is readily soluble in water. In the study, it was used in combination with hydrochloric acid to prepare biological buffer solutions used in the dissolution tests.

Hydrochloric acid (HCl), supplied by BDH Chemicals, England.

Hydrochloric acid was used in combination with either imidazole or potassium chloride (KCl) to prepare various biological buffer solutions used in the dissolution tests.

Potassium Chloride, Batch number 108551C294, supplied by Fisons, UK.

Potassium chloride, analytical grade, was used in combination with hydrochloric acid to prepare the biological buffer solutions used in the dissolution tests.

Aerosil® 200, Batch number 1084, supplied by Degussa, Germany.

Aerosil 200 is fumed silicon dioxide with a surface area of $200 \pm 25\ m^2/g$ and a particle size of approximately 12 nm. [123, 124] It has siloxan (Si-O-Si) [124] and silanol groups (Si-OH) [124, 125] on the surface of the particles. The latter are supposed to render it hydrophilic. Aerosils tend to form aggregates due to hydrogen bond formation via the silanol groups. [124] Aerosil 200, like all the other types of Aerosil, is used as follows:- (i) suspending agent, (ii) viscosity increasing agent, (iii) glidant, (iv) anti-caking agent, (v) flow conditioning agent and (vi) tablet disintegrant. [123-125] In the present study, Aerosil 200 was used as a carrier for Myverol, since the latter has a relatively low melting point and is very soft.

Aerosil® R 974, supplied by Degussa, Germany.

Unlike Aerosil 200, Aerosil R 974 is supposed to be a hydrophobic silica with Si - CH3 on the particulate surfaces. [125] These surfaces are chemically modified by treatment with organosilanes to change the hydrophilic nature to one which is predominantly hydrophobic. Aerosil R 974 has a mean particle size of 12 nm and a surface area of 170 ± 20 m^2/g. It is used as a (i) glidant and (ii) thickening agent. [125] In the present study, Aerosil R 974 was used as a carrier for Myverol.

Sipernat® D17, Batch number 8629, supplied by Degussa, Germany.

Sipernat D17 is precipitated silicon dioxide, having siloxane groups ($Si\text{-}O\text{-}CH_3$). [126] These groups are supposed to render it hydrophobic. Sipernat D17 is a free flowing powder. It has the following uses:- (i) anti-caking agent for powders sensitive to moisture and (ii) adsorbent and carrier in the feedstuffs industry. [126] In the present study it was used as a carrier for Myverol.

Sipernat® 22, supplied by Degussa, Germany.

Sipernat® 22 is spray dried silicon dioxide with a high absorptive capacity and an optimised particle size spectrum. Like Sipernat D17, Sipernat 22 is also used in the feedstuffs industry as a carrier for various solutions such as choline chloride solution. [126] It was also used as a carrier for Myverol.

Starch 1500, Batch number, 9046612C, supplied by BDH Chemicals Ltd, England.

Starch 1500 is partially hydrolysed relatively free flowing maize starch. Its uses are as follows:- (i) tablet binder, (ii) tablet disintegrant and (iii) filler in direct compression at times. [15] In the present study, it was incorporated into the HVO matrix formulation so as to function as a drug release enhancer.

Avicel PH 102, Batch number 5814, supplied by Honeywill and Stein Ltd, UK. Avicel PH 102 is partially agglomerated microcrystalline cellulose. It is derived from a special grade of purified alpha wood cellulose by partial acid hydrolysis. [15] It has an average particle size of 100 μm. [127] Avicel is a well known direct compression filler-binder-disintegrant. [15] It mainly deforms plastically on compaction. [15, 127] In the present study it had the same role as Starch 1500.

Eudragit S100, Batch number 05-80017, supplied by Röhm Pharma, Germany. Eudragit S is an anionic polymer synthesised from methacrylic acid and methacrylic acid methyl ester with an average molecular weight of approximately 135 kDa. [128] The ratio of the free carboxyl groups to the ester groups is approximately 1:2. It is insoluble in acids and pure water, rendering it an excellent enteric coat. It slowly dissolves in neutral to weakly alkaline solutions by forming salts with the alkalis. Eudragit S is soluble in solvents such as isopropyl alcohol, acetone and ethyl alcohol. Its uses include:- (i) enteric coat for capsules, tablets and pellets, (ii) protection of tablets and capsules against moisture, light and air, (iii) insulation of hygroscopic cores, (iv) isolation of porous cores and (v) controlled release coating film in combination

with Eudragit L. [128] In the present study, Eudragit S 100 was used to enhance zero order release mechanism of the tablets.

Junlon PW110, supplied by Honeywill & Stein Ltd, UK.

Junlon is a cross-linked polymer of acrylic acid known by the approved name carbomer. It is similar to Carbopol 934P. It has the following empirical formula:- $-(C_3H_4O_2)_x.\ (-C_3H_5\text{-Sucrose})_y-$. [129] Junlon is soluble in water and is very hygroscopic. It has the following uses:- (i) emulsifier (0.1-0.5 %), (ii) suspending agent (0.5-1.0 %), (iii) gelling agent (0.5-2.0 %), (iv) binder in sustained release formulations and (v) thickening agent in ointments and creams. [129] In the present study, Junlon was used as an alternative drug release enhancer to Avicel and Starch 1500.

Lipase and Esterase, both supplied by Sigma Chemical Company, USA.

Lipase and esterase are both enzymes. Lipase was supplied as a lyophilised powder containing 25 units of enzyme per mg solid. One unit was supposed to produce 1.0 μmole of glycerol from a triglyceride per minute at pH 7.0 and 37° C. Esterase was supplied as a crystalline suspension in ammonium sulphate (pH 8.5) with 100 units per mg protein. One unit was supposed to hydrolyse 1.0 μmole of o-nitrophenol butyrate to butyric acid and o-nitrophenol per minute at pH 7.5 and 25° C. In the study, both enzymes were used in an attempt to degrade the ester linkages of glyceryl-tris-12-hydroxystearate in Sterotex K so as to enhance drug release in relation to time.

2.3 METHODS

2.3.1 Preparation of Composite Excipients

The term "composite excipient" is used here to mean a single powder/granulation used as a tableting excipient, but containing more than one inert ingredient. The composite excipients (CEs) described here, all have use as matrix controlled release tablet components.

2.3.1.1 Composite Excipients Containing Less Than or Equal to Three Ingredients

In each case (unless otherwise stated), either HVO or Compritol was processed with a binder and stearic acid. The binders used were either PVP K-30, PVP K-90, Luviskol or Polyplasdone. PVP K-30 was used at concentrations ranging from 0 - 30 % w/w. The rest of the binders were used at one concentration, 7.5 % w/w. Stearic acid was also used at one concentration, 5 % w/w.

The binder was gradually dissolved (in the case of PVP) or dispersed (in the case of Luviskol and Polyplasdone) in water, with the aid of heat. The volume of water used in each case was equivalent to 20 % v/w of the total composite excipient (CE). A temperature of approximately 60° C was selected for the following reasons:- (a) it is within the melting point range of stearic acid (51-69° C), [109, 111] (b) it is below the melting point range of Sterotex K (62-88° C) [108, 109] (c) it is below the melting point range of Compritol (67-72° C) [109] and (d) not too hot for excess evaporation to occur.

Molten stearic acid was gradually added to the aqueous binder solution or dispersion while vigorously stirring with a spatula. This resulted in a warm stable colloidal dispersion. The dispersion was gradually added to either the HVO or Compritol in a high speed mixer granulator (Kenwood, Type FP600, Kenwood Ltd., UK). This was mixed at speed setting 5 (approximately 1000 rev min^{-1}) for approximately 1 minute and then for a further 1 minute at speed setting 8 (approximately 1450 rev min^{-1}). This type of food processor used, has been reported to be a good model high speed granulator. [97]

In the case of CE containing no stearic acid, the binder solution was used alone. For CE containing no binder, the molten stearic acid was added to the hot water with no other changes to the preparation protocol. All the CEs prepared were tray dried at 40° C in a convective oven (Baird and Tatlock Ltd., UK), overnight. The different dried CEs were subsequently passed through a 710 μm process sieve. They were then stored in tightly sealed plastic bags at room temperature and humidity, prior to use.

2.3.1.2 Composite Excipients Containing More Than Three Ingredients

In each case, HVO was processed with PVP K-30, stearic acid and one or more other ingredient(s), selected from:- Avicel, Starch 1500, Junlon PW110, Eudragit S100 and Myverol. In all cases, the ratio of HVO : PVP K-30 : stearic acid was kept at either **90 : 5 : 5** or **87.5 : 7.5 : 5**.

2.3.1.2.1 Composite Excipients Containing Either Avicel, Starch or Junlon

In all cases, either Avicel, Starch 1500 or Junlon was added at 5 % w/w of the total composite excipient (CE). The CEs were prepared as described in section 2.3.1.1 with the exception that the fourth component (either Avicel, Starch 1500 or Junlon) was mixed with the HVO powder in the mixer granulator at speed setting 5 for approximately 40 seconds, before addition of the granulating dispersion. The resulting wet CEs were treated as described above in section 2.3.1.1.

2.3.1.2.2 Composite Excipients Containing either Hydrogenated Rapeseed oil, Myverol or Myverol and Eudragit

In each case, HVO was processed with PVP K-30, Stearic acid and either hydrogenated rapeseed oil, Myverol or Myverol and Eudragit. In all cases, the amount of water used was equivalent to 20 % v/w of the total CE.

When hydrogenated rapeseed oil or Myverol was used as the fourth component, it was gradually melted at approximately 60° C and mixed with the molten stearic acid at the same temperature. The molten mass was then gradually added to the aqueous binder (PVP K-30) solution while stirring vigorously with a spatula. The resulting colloidal dispersion was slowly added to the HVO in the processor granulator. This was then processed as described in section 2.3.1.1.

When Myverol and Eudragit were incorporated as the fourth and fifth ingredients respectively, the former was treated as described above, while the latter was mixed with the dry HVO powder in the granulator. The two dry powders were mixed at speed setting 5 for approximately 40 seconds. The rest was done as described in section 2.3.1.1.

2.3.1.3 Preparation of Myverol - Based Water - Free Composite Excipients

Myverol was processed with either of the following silicas:- Aerosil 200, Sipernat D17 and Sipernat 22 in the ratio 60 : 40 respectively. When Myverol was processed with the silica Aerosil R 974, the ratio of the former to the latter was 60 : 32. Myverol was melted at approximately 60° C (melting point range is 53-61° C). [109, 118] The silica was then gradually incorporated into the molten Myverol while stirring with a spatula. As the Myverol adsorbed onto the silica, a free flowing CE was gradually formed. The resulting CEs were passed through a 710 μm process sieve and left at room temperature and humidity overnight. They were then stored as described in section 2.3.1.1.

Formulae of all CEs prepared are shown in tables 2.1 (a) - 2.1 (e).

Table 2.1 (a):- Formulae of Composite Excipients Containing Different PVP K-30 Concentrations **(NB:- all concentrations are in % w/w)**

Code	Sterotex K	PVP K-30	Stearic acid
CE1	95.00	0.00	5.00
CE2	92.00	3.00	5.00
CE3	90.00	5.00	5.00
CE4	89.00	6.00	5.00
CE5	87.50	7.50	5.00
CE6	85.00	10.00	5.00
CE7	80.00	15.00	5.00
CE8	75.00	20.00	5.00
CE9	70.00	25.00	5.00
CE10	65.00	30.00	5.00
CE11	92.50	7.50	0.00

Table 2.1 (b):- Formulae of Composite Excipients Containing Alternative Binders

(NB: all concentrations are in % w/w)

Ingredient	Code			
	CE12	**CE13**	**CE14**	**CE15**
PVP K-90	7.50	0.00	0.00	0.00
PVP K-30	0.00	0.00	0.00	7.50
Luviskol	0.00	7.50	0.00	0.00
Polyplasdone	0.00	0.00	7.50	0.00
Sterotex K	87.50	87.50	87.50	0.00
Stearic acid	5.00	5.00	5.00	5.00
Compritol	0.00	0.00	0.00	87.50

Table 2.1 (c):- Formulae of Composite Excipients Containing either Avicel, Starch or Junlon **(NB:- all concentrations are in % w/w)**

Ingredient	**Code**		
	CE16	**CE17**	**CE18**
Avicel	5.00	0.00	0.00
Starch	0.00	5.00	0.00
Junlon	0.00	0.00	5.00
Sterotex K	83.12	83.12	83.12
PVP K-30	7.13	7.13	7.13
Stearic acid	4.75	4.75	4.75

Table 2.1 (d):- Formulae of Myverol - Based Water - Free Granulated Composite Excipients **(NB:- all concentrations are in % w/w)**

Ingredient	**Code**			
	CE19	**CE20**	**CE21**	**CE22**
Aerosil® 200	40.00	0.00	0.00	0.00
Sipernat® D17	0.00	40.00	0.00	0.00
Sipernat® 22	0.00	0.00	40.00	0.00
Aerosil® R 974	0.00	0.00	0.00	34.78
Myverol	60.00	60.00	60.00	65.22

Table 2.1 (e):- Formulae of Composite Excipients Containing either Hydrogenated Rapeseed Oil, Myverol or Myverol and Eudragit

(NB:- all concentrations are in % w/w)

Code	Sterotex K	PVP K-30	Stearic acid	Myverol	Eudragit
CE23	78.75	6.75	4.50	10.00	0.00
CE24	70.00	6.00	4.00	20.00	0.00
CE25	61.25	5.25	3.50	30.00	0.00
CE26	52.50	4.50	3.00	40.00	0.00
CE27	45.00	2.50	2.50	30.00	20.00
CE28	36.00	2.00	2.00	30.00	30.00
CE29*	35.00	3.00	2.00	30.00	30.00
CE30#	61.25	5.25	3.50	30.00	0.00

Key:- CE = Composite Excipient

* PVP K-90 was used instead of PVP K-30

hydrogenated rapeseed oil was used instead Myverol

NB:- For all the composite excipients in tables 2.1 (a) - 2.1 (e), the drug, either **propranolol hydrochloride** or **theophylline** was added post-granulation and post - reconstitution (see also table 2.2, i.e. as a standardised direct compression system). In all cases, a drug content of ***40 mg per 150 mg*** tablet was used.

2.3.2 Preparation of an Active Composite Excipient Containing Propranolol Hydrochloride

In this case, the HVO : PVP K-30 : Stearic acid ratio was **87.5 : 7.5 : 5**. The Stearic acid was melted at approximately 60° C (melting point range = 51-69° C) [109, 111] and then slowly brought up to approximately 85° C. The HVO was melted at approximately 85° C (melting point range = 62-88° C). [108, 109] The two molten masses were then mixed thoroughly at approximately 85° C. The resulting molten mass was gradually cooled at room temperature while continually stirring with a spatula.

The powdered binder was gradually added to the thickening molten mass while stirring. As the molten mass continued to cool to a semi-solid (visual inspection) the drug, propranolol hydrochloride, was gradually incorporated while mixing. The ratio of propranolol hydrochloride to excipients was 40 : 110. Before the mass hardened completely, it was forced through a 710 μm process sieve. The resulting granulation was left at room temperature and humidity overnight. It was stored as described in section 2.3.1.1. This particular granulation produced an active composite excipient which was ready for direct compression into tablets without further processing was coded: ACE.

2.3.3 Size Fractionation and Reconstitution of Composite Excipients and Active Composite Excipient

Release-sustaining characteristics and tensile strength of compacts can be affected by variations in particle diameter distribution of granulations or powders. [88] Therefore in order to eliminate these effects, the various composite excipients (CEs) (unless otherwise stated) and active composite excipient (ACE) (see section 2.3.2) were fractionated and reconstituted. Also in order to evaluate the effect of particle diameter on release-sustaining characteristics and tensile strength of compacts, fractionation had to be done.

Fractionation was done by passing each CE or ACE through a series of test sieves (B. S. 410 / 1969, Endecotts Ltd, UK), which complied with international standards for nominal aperture size 710 μm, 500 μm, 355 μm, 250 μm, 180 μm, 125 μm, 90 μm, 63 μm and 45 μm. Approximately 50-60 g of each CE or ACE was fractionated at a time so as to avoid overloading the sieves. The stack of sieves, in order of decreasing aperture size from top to bottom with the sample on the top sieve, was vibrated on a sieve vibrator (Fritsch Analysette Vibrator, Type 03.502, Christison Ltd., UK).

Each sample was shaken until the end point was reached. This was determined according to the following procedure (B. S. 410/1976):- The whole sample was initially sieved for 5 minutes at amplitude 2. The weight of the material remaining on each sieve was recorded by subtracting the weight of the sieve from that of the sieve plus the CE or ACE. The sieves were then vibrated

repeatedly each time for 2 minutes at amplitude 2, until the weight of material passing through each sieve in 2 minutes was less than 0.2 % of the original test sample. A shaking period of 15 minutes at amplitude 2 was selected as a result of the preliminary tests. The sieve vibrator provided a three-dimensional controlled motion which produced a continuous movement of particles on the sieve screen.

The various fractions:- 710-500 μm, 500-355 μm, 355-250 μm, 250-180 μm, 180-125 μm, 125-90 μm, 90-63 μm, 63-45 μm and < 45 μm exclusively, were weighed individually on a balance after vibrational separation. The following size fractions:- 500-710 μm, 355-500 μm, 250-355 μm, 180-250 μm and < 180 μm from CE5 and CE24 (tables 2.1 (a) and 2.1 (e)) were each, dry blended with drug, propranolol hydrochloride (ratio = 110 : 40 respectively) and tableted.

The reconstituted particle size distributions of the various CEs and ACE used in tablet preparation are shown in table 2.2. Blend 1 (B1), was selected because most of the CEs prepared from stearic acid, PVP K-30 and HVO had approximately this particular particle diameter distribution. Blend 2 (B2), was selected after a series of experiments with B1. Blend 3 (B3), was not a reconstituted blend. In this case, the CEs were passed through a 710 μm test sieve only, before use.

The different fractions were reconstituted using geometric dilution. Mixing was carried out for 5 minutes on a clean A4 piece of paper, using a spatula. Care

Table 2.2:- Particle Size Distribution of Composite Excipients and Active Composite Excipient

Particle Size (μm)	Blend 1 **B1**	Blend 2 **B2**	Blend 3 **B3**
		Weight (% w/w)	
<710	--	--	100
500-710	25	50	N/D
355-500	35	25	N/D
250-355	25	15	N/D
180-250	10	7	N/D
<180	5	3	N/D

NB:- N/D = not determined

Therefore all the formulations were ***coded*** according to formula, particle size distribution and drug:- e.g. **CE1/B1/Prop** or **CE1/B1/Theo**

where:- CE1 is composite excipient 1 (see table 2.1 (a))

B1 is blend 1 particle size distribution (table 2.2)

Prop is propranolol hydrochloride

Theo is theophylline

was taken so as not to damage the granules. Approximately 40 g of blend of each CE or ACE was made at a time. The resulting reconstituted CEs or ACE were stored in sealed plastic bags at room temperature and humidity until further use.

2.3.4 Drug and Composite Excipient Dry Mixing

A drug dosage of 40 mg per 150 mg tablet was selected (drug : excipient ratio = 40 : 110). This particular dosage was chosen for the following reasons:- (a) so as to have a maximum absorbance value of less than 1 and this reduces the effects of stray light, which is particularly notable at absorbance values above 1 in most UV-visible spectrophotometers; and (b) it is one of the standard dosages of propranolol hydrochloride. A target tablet weight of 150 mg was selected partly due to:- (a) the punches size (8 mm) and (b) the maximum die depth. Also tablets with large diameters enhance tablet tooling adhesion. [30]

The drug (propranolol hydrochloride or theophylline), and CE were weighed separately on an analytical balance. They were then carefully mixed together geometrically for 5 minutes. Mixing was done on a clean A4 piece of paper. For each batch of tablets prepared for dissolution tests *or* tensile strength measurement, approximately 5 g of CE - drug mixture was made at a time. For evaluation of formulation adhesion to tablet tooling, approximately 150 g was made at a time.

2.3.5 Differential Scanning Calorimetry (DSC)

When two or more substances are mixed together and temperature is raised, as occurs in tableting, the possibility of chemical reaction(s) cannot be discounted. Chemical reactions in tablets are not desirable since they can have an effect on factors such as drug bioavailability, tablet strength and release sustaining - characteristics. Therefore in order to determine whether chemical reaction(s) between the excipients and propranolol hydrochloride were likely, differential scanning calorimetry (DSC) was carried out on samples of CE5/B1, CE5/B1/Prop (see tables 2.1 (a) and 2.2), propranolol hydrochloride, stearic acid, palmitic acid and propranolol hydrochloride - fatty acid mixtures. The ratio of propranolol hydrochloride to excipients in the samples was 40 : 110. The above fatty acids were selected because they are found in Sterotex K (see section 2.2). In the study, Sterotex K was the main basic release - sustaining characteristics matrix material. DSC is an easy and quick method for screening solid mixtures for likely chemical reactions. Usually, if a chemical reaction occurs between substances mixed together, on performing a DSC test, beside the transitions corresponding to the initial substances showing on the thermogram, transition(s) corresponding to the new product(s) is/are evident as well.

A differential scanning calorimeter (Type 910, Du Pont Instr. Wilmington, USA) connected to a computerised thermal analyser and a data acquisition unit (Type 9900, Du Pont Instr.) was used in the study. The instrument was

calibrated using Indium to obtain a cell constant of 1.1083 and a slope of -4.21. All experiments were run at a heating rate of 10° C per minute. An initial fast ramp was used to raise the temperature quickly to 30° C and then a constant heating rate of 10°C per minute was used up to 180° C under nitrogen atmosphere. Samples ranging from 1-5 mg were weighed into aluminium DSC pans on an analytical balance. The pans containing the samples were then sealed before the analysis. The heat of transition was automatically calculated by the analyser. At the end of each test the data was printed (see section 3.2 in chapter 3).

2.3.6 Anti-adherent Addition

Anti-adherents were added to CE11/B1/Theo (see tables 2.1 (a) and 2.2) formulation. CE11 was prepared as described in section 2.3.1.1. The ratio of theophylline to the CE was 40 : 110. The anti-adherents added, each at 1 % w/w and 5 % w/w concentrations, were magnesium stearate, stearic acid, Compritol and leucine.

The anti-adherent and CE11/B1/Theo were mixed geometrically on a clean white A4 paper. Total mixing time was 5 minutes. The resulting lubricated formulations were immediately evaluated for adhesion.

2.3.7 Tableting

2.3.7.1 Equipment and Preparation of the Tablets

An instrumented single punch Manesty E2 tablet machine equipped with 8 mm diameter flat faced punches was used to prepare the tablets used in tensile testing and dissolution. The fly-wheel of the machine was manually operated as the software could not process the collected data fast enough for power operation. It was found out that it was impossible to maintain exactly the same contact time for replicates of the same formulation at the same compaction force.

Formulation for each tablet was individually weighed on an analytical balance into small glass tubes to 0.1 mg. This was done for the achievement of the target tablet weight (150 mg) and constant compaction forces. Therefore each formulation sample for a tablet weighed 152.5 - 153.0 mg. Each sample was carefully tipped into the die and the fly-wheel manually turned in order to compact the formulation. Tablets were made at compaction forces ranging from 3 to 18 kN.

The first 5 tablets made at each compaction force for each formulation were rejected. For each formulation, 20 tablets were made for tensile testing, while 12 tablets were made for dissolution tests. All the tablets were stored in tightly sealed glass containers in desiccators containing saturated solutions of potassium acetate which produced a relative humidity of approximately 37 % at 20°C as measured by hygrometer and thermometer respectively. This relative

humidity was significantly higher than the literature value of 23 % at the same temperature. [130]

2.3.7.2 Data Acquisition and Manipulation

The upper punch signal was monitored by a pre-calibrated load cell (Type 9021, Kistler Instr. Ltd., UK). This load cell was calibrated by the manufacturers. The upper punch holder was modified so as to hold the load cell as well as the load distribution washer. This was arranged so that the top end of the upper punch pressed directly against the washer. The upper punch was loosely held in position by a retaining screw so as to allow movement and reduction in force lost to the screw during compaction. The conditioning amplifier (Type 5054A, Kistler Instr. Ltd., UK) converted the changes in capacitance into changes in voltage.

Force transmitted to the lower punch was monitored by two strain gauges (Welwyn Strain Measurement Ltd., UK) bonded to the lower punch holder. Signals from these strain gauges were passed through a conditioning amplifier (Type 2120, Welwyn Strain Measurement Ltd., UK) where changes in resistance were converted to changes in voltage. The pre-calibrated load cell was used to calibrate the strain gauges *in situ*. The punches were brought into contact and readings from both the load cell and strain gauges monitored and collected. It was realised that these results changed slightly with time, hence there was need for routine calibration of the strain gauges. The changes were time dependent rather than machine operation dependent. The strain gauges

were recalibrated whenever the readings altered significantly (e.g. when the recorded lower punch force was equal or greater than the upper punch force).

The analogue signals from the load cell and the strain gauges were both fed via an analogue-digital converter connected to a 1 MHz Bus of a microcomputer (Master series, British Broadcasting Co., UK). 500 digital values were obtained from each of the mentioned devices during one complete compaction cycle. These values were stored in the memory of the microcomputer and processed at the end of each run. The software provided the following parameters for each tablet produced:-

- peak upper punch force
- peak lower punch force
- time to peak force
- total compaction time
- peak upper punch to peak lower punch force ratio
- peak lower punch to peak upper punch force ratio

A typical set of calibration data for the strain gauges is shown in table 2.3 while the corresponding plot is shown in figure 2.1.

Table 2.3:- Calibration Data Corresponding to Electronic Digital Lower Punch Outputs at Given Applied Loads from the Upper Punch *In Situ*

Upper Punch Force (N)	Lower Punch (Digital Values)
2 584	6 704
4 499	9 344
5 682	10 848
6 933	12 464
8 191	14 240
9 449	16 048
10 707	17 872
11 904	19 568
13 018	21 152
14 017	22 576
14 899	23 856
15 719	24 960
16 464	25 856
17 736	27 424

Slope = 1.389

Intercept = 3001

Corr. Coefficient = 0.99984

Figure 2.1:- Calibration Plot for the Strain Gauges Corresponding to Data in Table 2.3

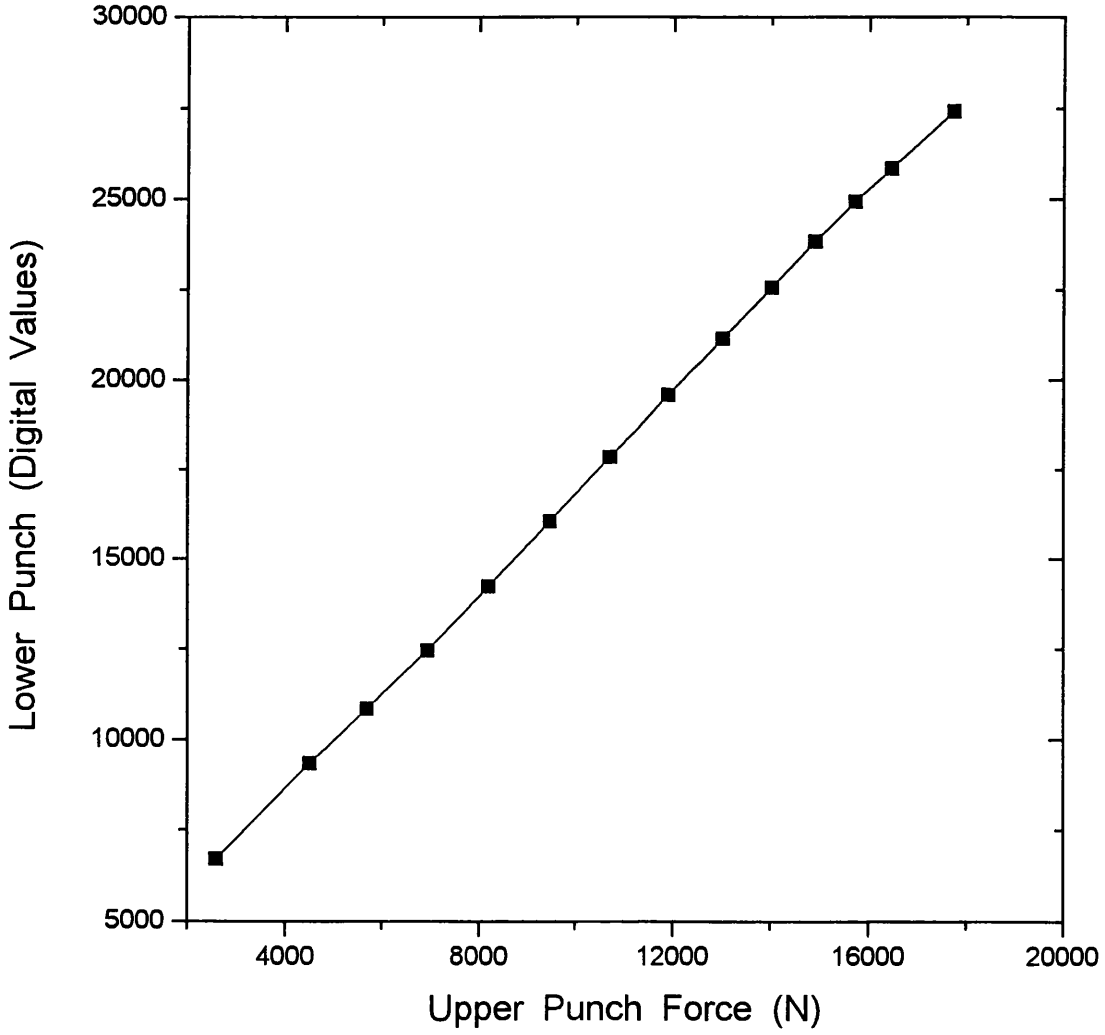

2.3.7.3 Evaluation of Adhesion to Tablet Tooling

A power operated single punch Manesty F3 tablet machine equipped with 8 mm diameter punches was used to evaluate the adhesion of lubricated and unlubricated CE11/B1/Theo (tables 2.1 (a) and 2.2) formulation to the upper punch face. CE11 was prepared as described in section 2.3.1.1. The anti-adherents used were magnesium stearate, stearic acid, Compritol, leucine and each was added at 1 % w/w and 5 % w/w concentrations to CE11/B1/Theo as described in section 2.3.6.

Before each run, the die and punch set were thoroughly cleaned with 95 % alcohol. The lower punch was set so that tablets of approximately 150 mg were made while the upper punch was fixed at its maximum position. Tablets were made at the minimum force required to produce the maximum crushing force (Schleuniger, type 2E, Germany) for each formulation. Once the die depth and compaction force had been set, the upper punch was carefully removed and thoroughly cleaned again using 95 % alcohol. It was then weighed on an analytical balance to 0.1 mg and secured back to the maximum position on the upper punch holder, with the aid of a retaining screw.

After every 40 cycles, the upper punch was carefully removed and weighed to 0.1 mg. For each formulation 1000 cycles were run except for one formulation containing 5 % stearic acid as anti-adherent, where only 240 cycles were run due to flowability problems. The weight of the upper punch was subtracted

from the series of data collected so as to obtain the actual quantity of formulation sticking on the face of the upper punch.

2.3.8 Tablet Tensile Strength Measurement

Tensile testing was done ***48 hours*** post-compaction. A tensile tester (Type T5000, JJ Lloyd Instr. Ltd., UK), capable of measuring force from 0.05 to 5000 N, fitted with a compression cage, was used to determine the diametral crushing force of the tablets. The tensile tester was calibrated annually by the manufacturers. The schematic representation of the compression cage used is shown in figure 2.2. The machine was operated in the compression mode. Before testing, tablet dimensions (diameter and thickness) were measured by means of a digital micrometer. Tablet weight was determined as well. 15 replicates were used for calculation of the mean values for each batch.

During the diametral loading test the force required to cause failure was monitored by a 100 N pre-calibrated load cell (JJ Lloyd Instr.) fitted to the centre of the moving cross-head and to the compression cage. Like the tensile tester, the load cell was calibrated by the manufacturers on a yearly basis. The tablet was placed on the bottom platen of the compression cage. As the two platens gradually moved towards each other during the test, the tablet was crushed in between them. The frictional force due to the movement of the platens was approximately ± 0.1 % of the lowest crushing force obtained. Therefore it was not taken into consideration. The cross-head speed was set at 1 mm/minute and the load cell sensitivity at x 1.

Figure 2.2:- Schematic Representation of the Compression Cage used in Evaluating the Crushing Force of the tablets

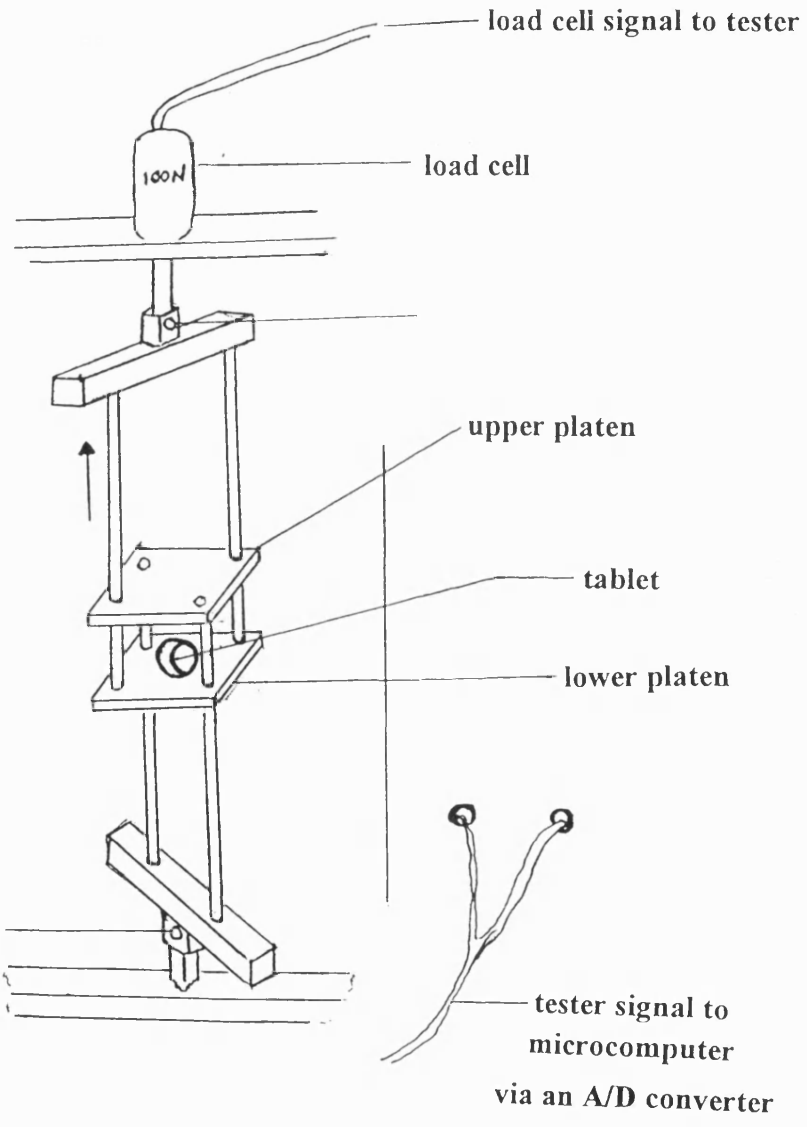

The displacement of the cross-head was measured by a self-contained transducer which had a precision of 0.1 mm. Tablet deformation before failure was in the range of 0.01 - 0.10 mm. This tensile tester used did not have an external extensometer such as a linear variable differential transformer, for accurate measurement of displacement or deformation. Consequently, although a work of failure was automatically calculated by the computer (Viglen Contender, Viglen Ltd., UK) interfaced with the tensile tester, this was not accurate and hence could not be used in the study.

The signal from the load cell was conditioned and amplified and then fed into a microcomputer (Viglen Contender) via an analogue digital converter. The values obtained were stored in the computer's memory and processed at the end of the experiment. The processed data was presented as stress versus strain curves by the microcomputer. From the maximum crushing force obtained, radial tablet tensile strength was calculated according to equation 1.4.

2.3.9 Determination of Wavelengths of Maximum Absorption and Beer-Lambert Plots for Aqueous Solutions of Propranolol Hydrochloride and Theophylline

A series of aqueous solutions of propranolol hydrochloride or theophylline in the range of 5-50 mg/litre were prepared. A scan of 30 nm on either side of the literature value for wavelength of maximum absorption, 290 nm [114] and 272 nm [115] respectively was performed using a double beam UV-visible spectrophotometer (Model CE594, Cecil Instruments, Cambridge, UK) and 1 cm pathlength quartz cuvettes. This procedure was carried out in order to determine the exact wavelength of maximum absorption of the two drugs on this particular instrument. The maximum absorbance for propranolol hydrochloride was at 289 nm, while that for theophylline was at 269 nm against a blank of distilled water.

For theophylline, the maximum concentration that gave a maximum absorbance just below 1 (0.989) was 20 mg/litre. This implied that the possible maximum theophylline content was 20 mg in an approximately 70 mg tablet of 8 mm diameter. Such a tablet was too thin for practical purposes. To allow the required amount of theophylline (40 mg per 150 mg tablet) to be incorporated and assayed it was decided to use a wavelength of 287 nm. Such an adjustment with theophylline has been done before with reliable results. [96] Therefore all the subsequent aqueous drug concentrations had their absorbances read at 289 nm for propranolol hydrochloride and at 287 nm for theophylline, against a blank of distilled water.

In order to establish whether any interference in the assays would be caused by any of the excipients which might dissolve from the tablets during the assays, the dissolution properties of blank tablets (tablets containing all the ingredients except the drug) were evaluated at the critical wavelength over 12 hours. Absorbance readings at all sample times were zero. This showed that the excipients used made a negligible contribution to the absorbances at the respective wavelengths selected. Therefore distilled de-aerated water was used as blank in all the dissolution tests.

The calibration data and plots for propranolol hydrochloride and theophylline in distilled water are shown in table 2.4, figure 2.3, table 2.5 and figure 2.4.

Table 2.4:- UV/Visible Spectrophotometric Calibration Data of Aqueous Solutions of Propranolol Hydrochloride λ_{max} = 289nm

Conc	Absorbance							
mg/l	1	2	3	4	5	6	Mean	sd
10	0.189	0.189	0.179	0.188	0.189	0.200	0.189	0.007
20	0.382	0.389	0.378	0.383	0.386	0.384	0.384	0.004
30	0.573	0.574	0.570	0.562	0.569	0.574	0.570	0.005
40	0.750	0.759	0.762	0.750	0.766	0.770	0.760	0.008
50	0.947	0.955	0.936	0.948	0.955	0.946	0.948	0.007

NB:- Conc = Concentration and sd = standard deviation.

Slope = 0.01894 ± 0.00013

Intercept = 0.00202 ± 0.00531

Corr. Coefficient = 0.99987 ± 0.00008

NB:- 1-6 are dissolution vessels

Figure 2.3:- Calibration Plot for Propranolol Hydrochloride in Distilled Water Corresponding to Data in Table 2.4

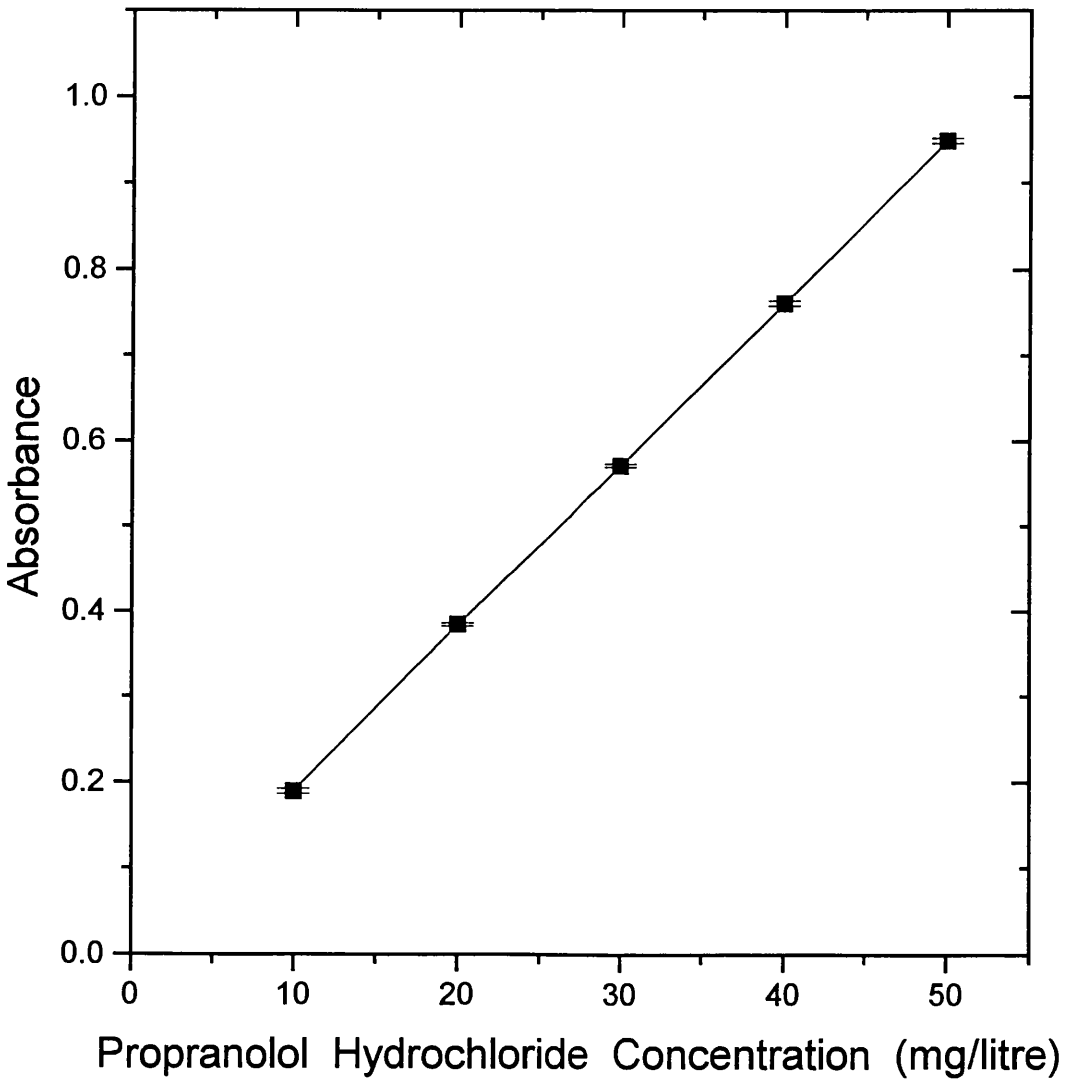

Table 2.5:- UV/Visible Spectrophotometric Calibration Data of Aqueous Solutions of Theophylline, $\lambda = 287$ nm

Conc mg/l	Absorbance 1	2	3	4	5	6	mean	sd
5	0.086	0.088	0.087	0.087	0.086	0.087	0.087	0.001
10	0.175	0.177	0.176	0.174	0.176	0.175	0.176	0.001
35	0.606	0.607	0.607	0.607	0.608	0.609	0.607	0.001
40	0.697	0.697	0.694	0.695	0.692	0.693	0.695	0.002
45	0.785	0.790	0.787	0.787	0.789	0.788	0.788	0.002
50	0.866	0.867	0.867	0.865	0.862	0.866	0.866	0.002

Slope = 0.01736 ± 0.00002

Intercept = 0.00091 ± 0.00065

Corr. Coefficient = 0.99995 ± 0.00003

Key:- Conc. = Concentration, sd = standard deviation

NB:- 1 - 6 are dissolution vessels

Figure 2.4:- Calibration Plot for Theophylline in Distilled Water Corresponding to Data in Table 2.5

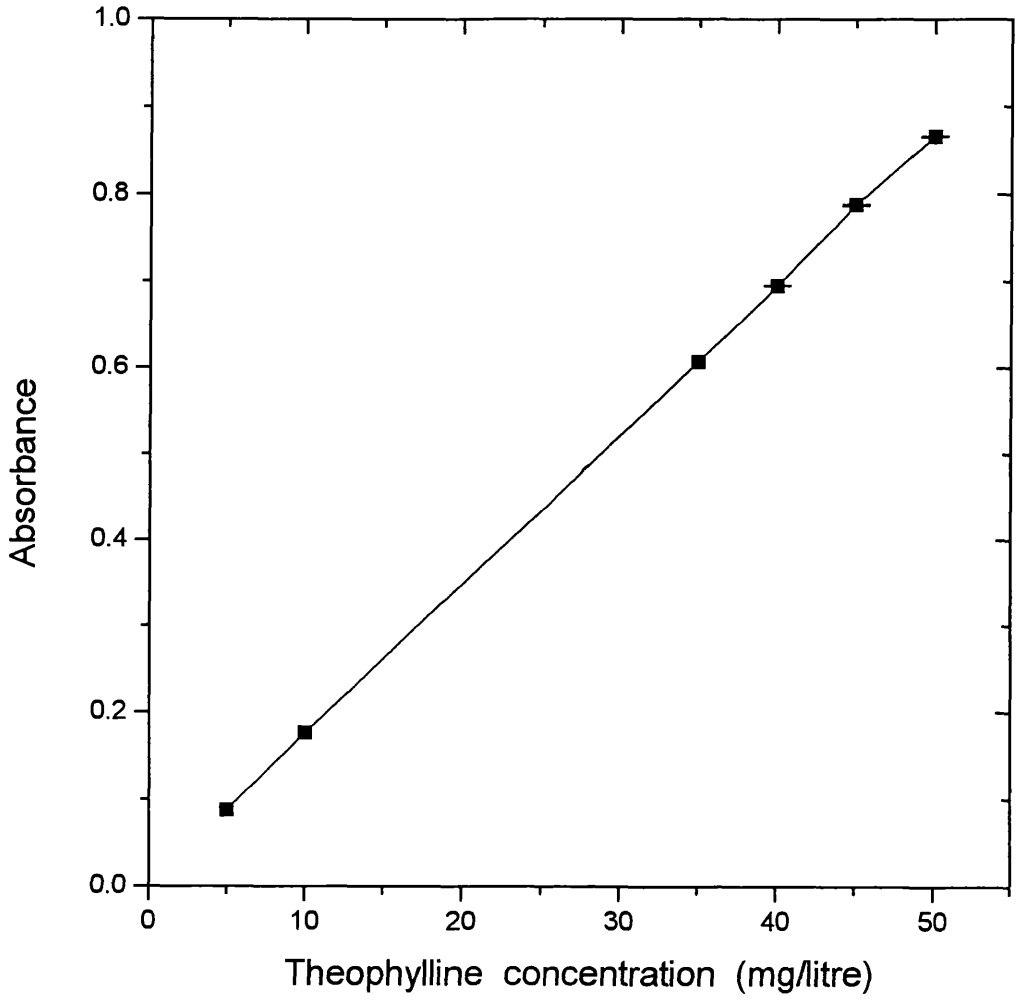

2.3.10 Preparation of Buffer Solutions

2.3.10.1 Buffer pH ≈ 6.8:- Imidazole / HCl [131]

25 ml 0.2 M Imidazole (13.62g/L) + 31.4 ml 0.1 M HCl made up to 100 ml.

Amount prepared = 8 Litres

∴ Amount of Imidazole in 8 litres of buffer:-

(8000/100)×(25×13.62/1000) = 27.24 g.

Moles of 0.1 M HCl in 100ml of buffer:-

(31.4/1000)×0.1 = 0.00314 moles.

∴ Moles of HCl in 8 litres of buffer:-

(8000/100)×0.00314 = 0.2512 moles.

∴ Volume of 1 M HCl required = 0.2512×1000 = 251.2 ml.

The imidazole was dissolved in distilled water with the aid of low heat (≈ 37° C) while stirring in a 10 litre flat-bottomed flask. The acid was added and the buffer made up to volume with distilled water and stirred. The buffer was then de-aerated by bubbling helium gas through the solution. The above formula is for pH 6.8 at 25 ° C, [131] yet the dissolution tests were carried out at 37 ± 0.5 ° C. Preliminary studies had shown that buffers prepared at 37 ± 0.5 ° were usually ± 0.2 of the literature value. However, the above buffer was supposed to be equivalent to small intestines pH which normally ranges from 6.5 to 7.0 in healthy subjects. [61] Therefore the above buffer was used as prepared without any adjustment. Also studies which have been performed indicate that HVO matrix release properties are not significantly affected by pH changes. [96, 97]

2.3.10.2 Buffer pH 7.0:- Imidazole / HCl [131]

25 ml 0.2 M Imidazole (13.62 g/L) + 25.4 ml 0.1 M HCl made up to 100 ml.

The calculations were done as in section 2.3.10.1.

⇒ 27.24 g Imidazole + 203.2 ml 1 M HCl made up to 8 litres.

This buffer solution was used with enzymes and hence had to be accurately prepared. In this case, preparation was done as in section 2.3.10.1 with buffer adjustment done by the addition of either a little base or acid.

2.3.10.3 Buffer pH ≈ 1.4:- KCl / HCl (Clark & Lubs Buffer) [131]

25 ml 0.2 M KCl (14.91 g/L) + 23.2 ml 0.2 M HCl made up to 100 ml.

Calculations were done as in section 2.3.10.1.

⇒ 29.82 g KCl + 371.2 ml 1 M HCl made up to 8 litres.

Preparation was as in section 2.3.10.1 with the buffer solution used as prepared without any adjustment. Gastric pH ranges from 1 to 2.5 in healthy fasted subjects.

2.3.11 Determination of Beer-Lambert Plots for Propranolol Hydrochloride in Buffers Solutions

This was done as in section 2.3.9, but instead of de-aerated distilled water, the respective de-aerated buffer solutions were used. All absorbances were read at wavelength (λ) 289 nm. In each case, the respective buffer solution was used as the blank instead of distilled water. The respective calibration data and calibration plots for propranolol hydrochloride in the buffer solutions are shown in table 2.6, figure 2.5, table 2.7 and figure 2.6.

Table 2.6:- UV/Visible Spectrophotometric Calibration Data of Propranolol Hydrochloride in Buffer Solution:- pH ≈ 6.8

λ = 289 nm

Drug Conc. (mg/l)	ABSORBANCE 1	2	mean	sd
5	0.094	0.093	0.094	0.001
10	0.184	0.185	0.185	0.001
20	0.378	0.374	0.376	0.003
30	0.568	0.564	0.566	0.003
40	0.752	0.739	0.746	0.009
50	0.938	0.933	0.936	0.004

Slope = 0.01872 ± 0.00013

Intercept = -0.00002 ± 0.00044

Corr. Coefficient = 0.99995 ± 0.00002

Key:- Drug Conc. = Drug Concentration, sd = standard deviation

NB:- 1 and 2 are replicates

Figure 2.5:- Calibration Plot for Propranolol Hydrochloride in Buffer Solution:- Imidazole/Hydrochloric acid pH ≈ 6.8, Corresponding to Data in Table 2.6

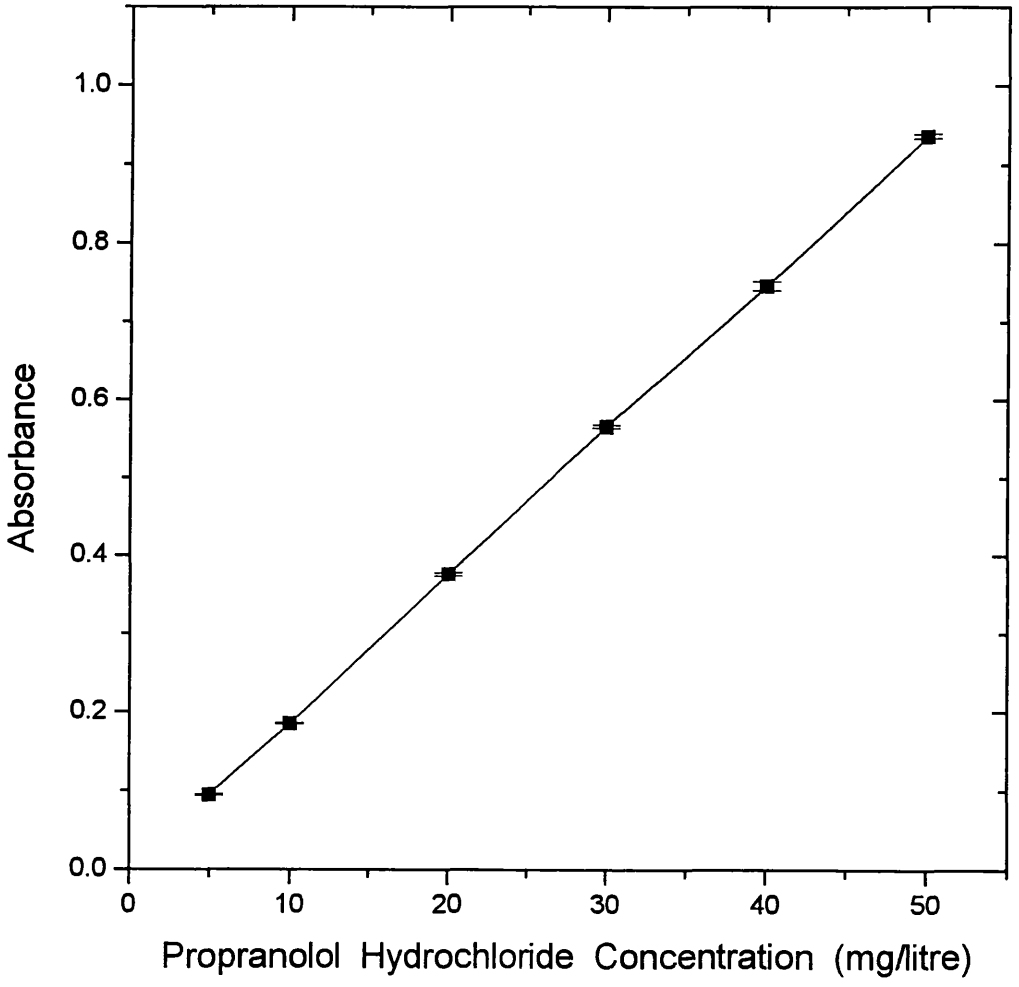

Table 2.7:- UV/Visible Spectrophotometric Calibration Data of Propranolol Hydrochloride in Buffer Solution:- pH ≈ 1.4

λ = 289 nm

Drug Conc.	ABSORBANCE			
(mg/l)	1	2	mean	sd
5	0.097	0.094	0.096	0.004
10	0.194	0.194	0.194	0.000
20	0.392	0.382	0.387	0.007
30	0.587	0.580	0.584	0.005
40	0.765	0.754	0.760	0.008
50	0.969	0.959	0.964	0.007

Slope = 0.01918 ± 0.00014

Intercept = 0.00178 ± 0.00116

Corr. Coefficient = 0.99986 ± 0.00003

Key:- Drug Conc. = Drug Concentration, sd = standard deviation

NB:- 1 and 2 are replicates

Figure 2.6:- Calibration Plot for Propranolol Hydrochloride in Buffer Solution:- Potassium Chloride/Hydrochloric acid pH ≈ 1.4, Corresponding to Data in Table 2.7

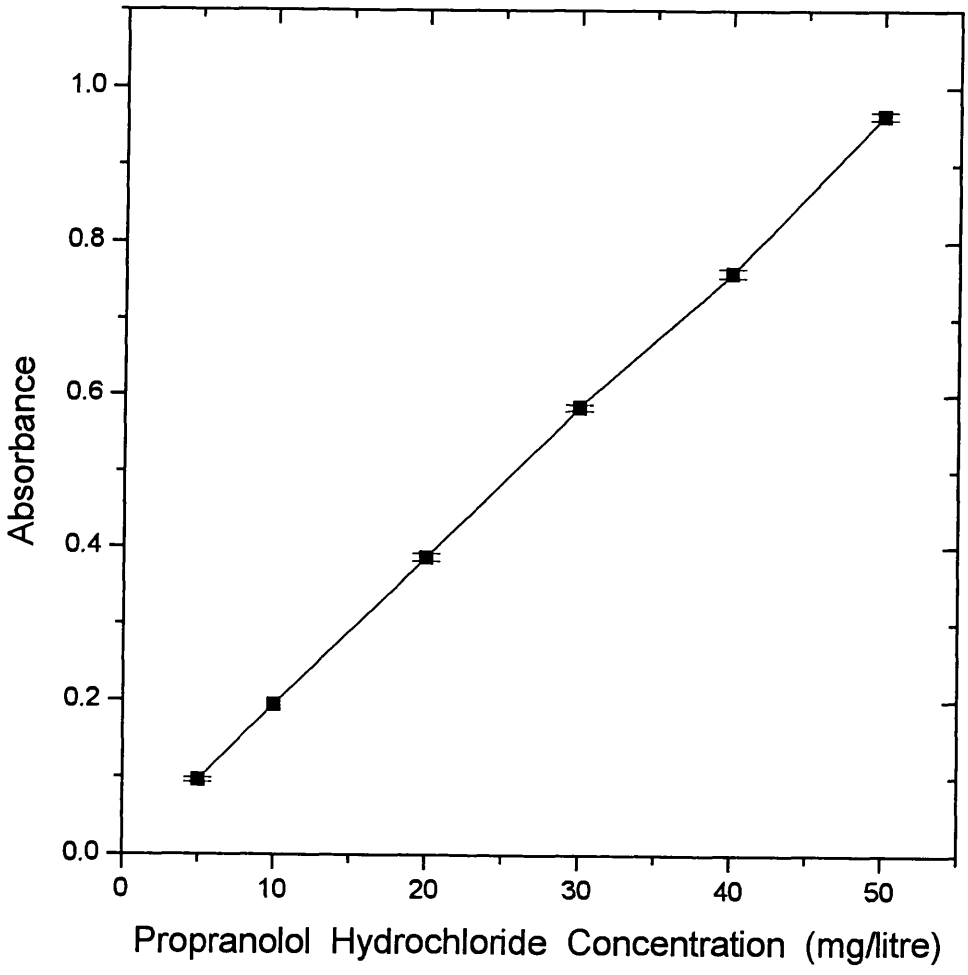

2.3.12 Measurement of Release Characteristics of Tablets Made from the Various Formulations using an Automated Dissolution Technique

Dissolution tests were done ***24 hours*** post-compaction. In all cases ***six*** tablets were assayed in one run. In order to automate the dissolution testing procedure, a cell controller with a motorised cell changer (Model CE830, Cecil Instr., UK) and 6 flow through quartz cuvettes of 1 cm pathlength (Cecil Instr.) were used with the UV-visible spectrophotometer (Model CE954, Cecil Instr.). Solutions were pumped out of the 6 dissolution vessels through the appropriate cuvettes in the cell changer via latex plastic tubing (Type TWR-350-110T, Fisons Scientific Equipments, UK) by use of a peristaltic pump (Model 502S, Watson Marlow, UK). Vinyl peristaltic tubes (Type 980-0279-000, Watson Marlow) were used at the pump head.

The water bath housing the dissolution vessels was fitted with a temperature controller (TE CAM TE7 Tempette) which maintained temperature at 37 ± 0.5 ° C. This, it did by automatically switching on and off the heating element. A stirrer (Model 6ST, G.B. Caleva Ltd., UK) dissipated the heated water around the bath. The dissolution vessels' paddles were set to rotate at 50 rev min^{-1}. Both the inlet and outlet tubes were inserted into the dissolution vessels to a depth of approximately a third of the depth of each dissolution vessel so that fluid was always removed and returned to the same point in each vessel. The outlet tubes were fitted with 60 μm filters (Type 091 501, G.B. Caleva Ltd.) to filter off any material above this size so as to avoid any interference with absorbance readings.

The solutions were pumped at 39 % maximum rate attainable by the pump in order to minimise turbulence in the dissolution vessels and to maximise pump and peristaltic tubing life. The cell changer was programmed to move each cell into the beam at the required time interval. The resulting absorbance reading was relayed to a microcomputer (BBC Model B, Acorn Computers, UK) which was interfaced with the spectrophotometer. A Basic programme was used to record the absorbance values and convert them to concentration values according to the data obtained from the calibration plots. Dissolution profiles were determined by calculating the cumulative percentage drug released with time and this data was printed and kept for subsequent analysis. The dissolution media was either de-aerated distilled water or de-aerated buffer solutions.

2.3.13 Scanning Electron Photomicrography of Tablet Surfaces

The outer flat faces of tablets made from CE5/B1/Prop and CE5/Prop (tables 2.1 (a) and 2.2) before and after dissolution testing, were examined using a scanning electron microscope (Model JSM T330, Japanese Electron Optics Ltd., Tokyo, Japan).

The samples were mounted on 10 mm diameter cylindrical aluminium stubs of approximate 20 mm length using colloidal graphite adhesive. A layer of gold was deposited onto the sample surface using a sputter coater (Model S150B, Edwards High Vacuum, Crawley, UK). Sputter coating was carried out for

5 minutes. The coated samples were then examined at various magnifications using an electron beam potential of 10 keV. A low electron voltage had to be used due to the susceptibility of the HVO matrix to melting (mp = 62-88° C).[108, 109]

RESULTS AND DISCUSSION

CHAPTER 3

INVESTIGATION OF THE OPTIMISATION OF PHYSICO-MECHANICAL PERFORMANCE CHARACTERISTICS OF PROCESSED HVO

3.1 OBJECTIVES

The main objectives in this part of the study were to optimise the tensile strength of HVO compacts and to reduce processed HVO formulations' adhesion to tablet tooling. In most cases the effect of formulation and process changes were studied in relation to release - sustaining characteristics.

All the tensile strength measurements and the dissolution tests were carried out as described in sections 2.3.8 and 2.3.12 respectively. All tablets, except those used in evaluation of adhesion to tablet tooling, were made as described in section 2.3.7.1. All the error bars on the figures are standard error of mean; values associated with means, quoted in the text and in the tables are standard deviations.

3.2 Characterisation of Materials

PVP, Luviskol and Polyplasdone formed stable colloidal dispersions with stearic acid in hot water. PVP K-30 and PVP K-90 dissolved in water, with PVP K-90 forming a more viscous solution than the former. Luviskol and Polyplasdone formed suspensions with the hot water. As the concentration of PVP K-30 increased, the colloidal dispersions formed with stearic acid gradually became viscous semi-solids. Myverol formed free flowing composite excipient (CE) powders/granulations with the various silicas used (Aerosil® 200, Sipernat® D17, Aerosil® R 974 and Sipernat® 22).

The differential scanning calorimetry (DSC) results are summarised in table 3.1 and figure 3.1. Table 3.1 shows the heat of fusion, ΔH, and the peak transition temperature, T_m, of the materials tested. The thermograms of some of the materials tested are shown in figure 3.1.

The thermogram of a propranolol hydrochloride sample showed a sharp endothermic transition at 165.13° C, with an onset of transition at 162.47° C (table 3.1 and figure 3.1). The heat of transition was 135.3 J/g. This experimental transition temperature corresponds to the literature melting range of propranolol hydrochloride which is 163-164° C. [132]

The thermogram of CE5/B1 (tables 2.1 (a) and 2.2), showed a broad endothermic transition with four distinct peaks at approximately 54.5° C, 60.0° C, 67.0° C and 77.0° C (figure 3.1). However, the average peak transition

Table 3.1:- Differential Scanning Calorimetry Results

Component		DSC Results			
1	2	1		2	
		T_m (° C)	ΔH (J/g)	T_m (° C)	ΔH (J/g)
Drug	--	165.13	135.3	--	--
Palmitic acid	--	63.25	205.1	--	--
Stearic acid	--	69.85	209.3	--	--
CE5/B1	--	59.48	147.9	--	--
Palmitic acid	Drug	≅ 63.27	137.4	147.80	35.02
Stearic acid	Drug	≅ 69.98	162.7	150.20	28.17
CE5/B1	Drug	59.21	100.3	155.87	29.61

NB Drug = Propranolol Hydrochloride

Key:- T_m = Peak transition temperature

ΔH = Heat of fusion

CE5/B1 see tables 2.1 (a) and 2.2

FIGURE 3.1:- Thermograms of Some of the Materials Tested

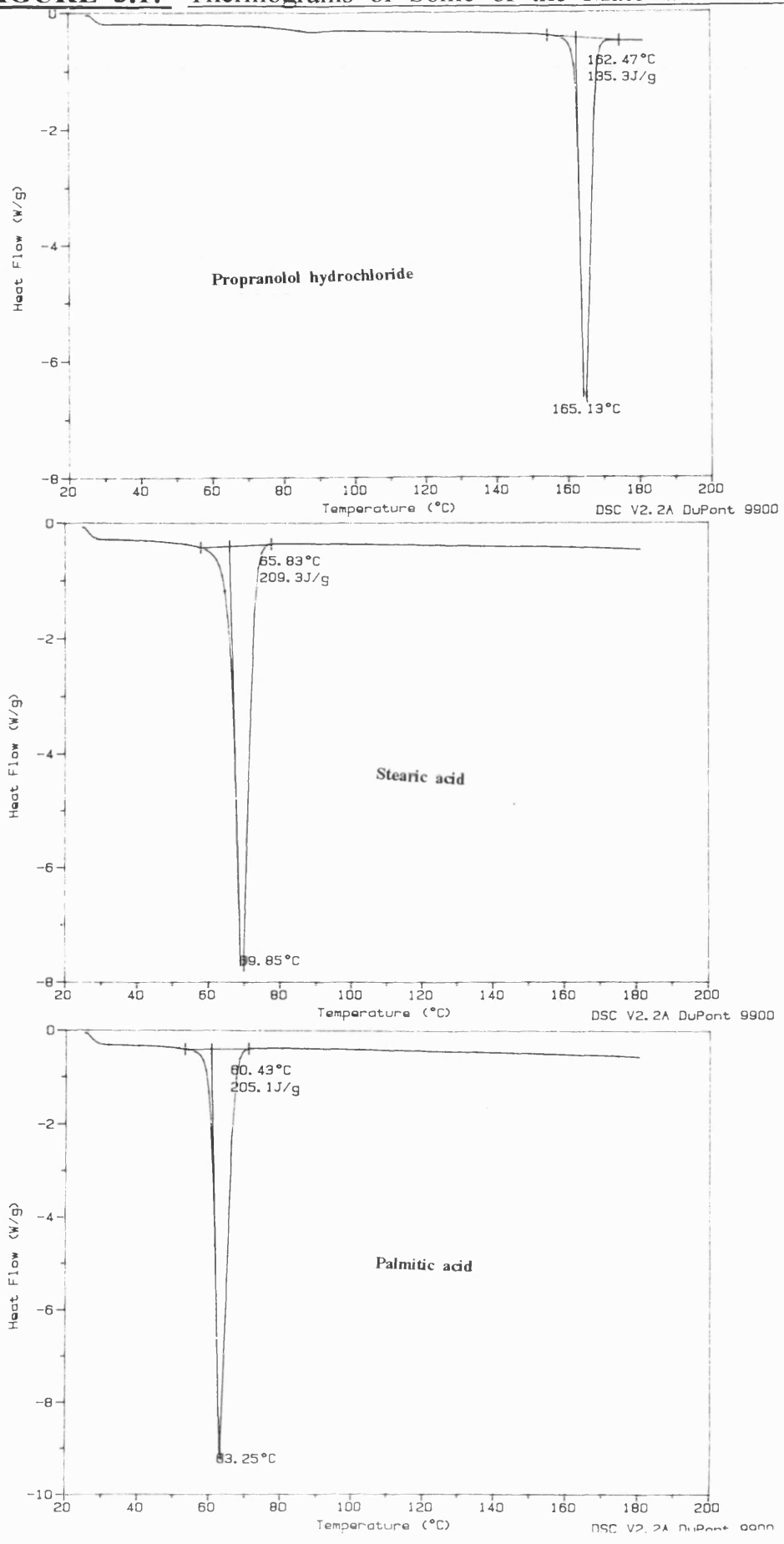

FIGURE 3.1:- Thermograms of Some of the Materials Tested

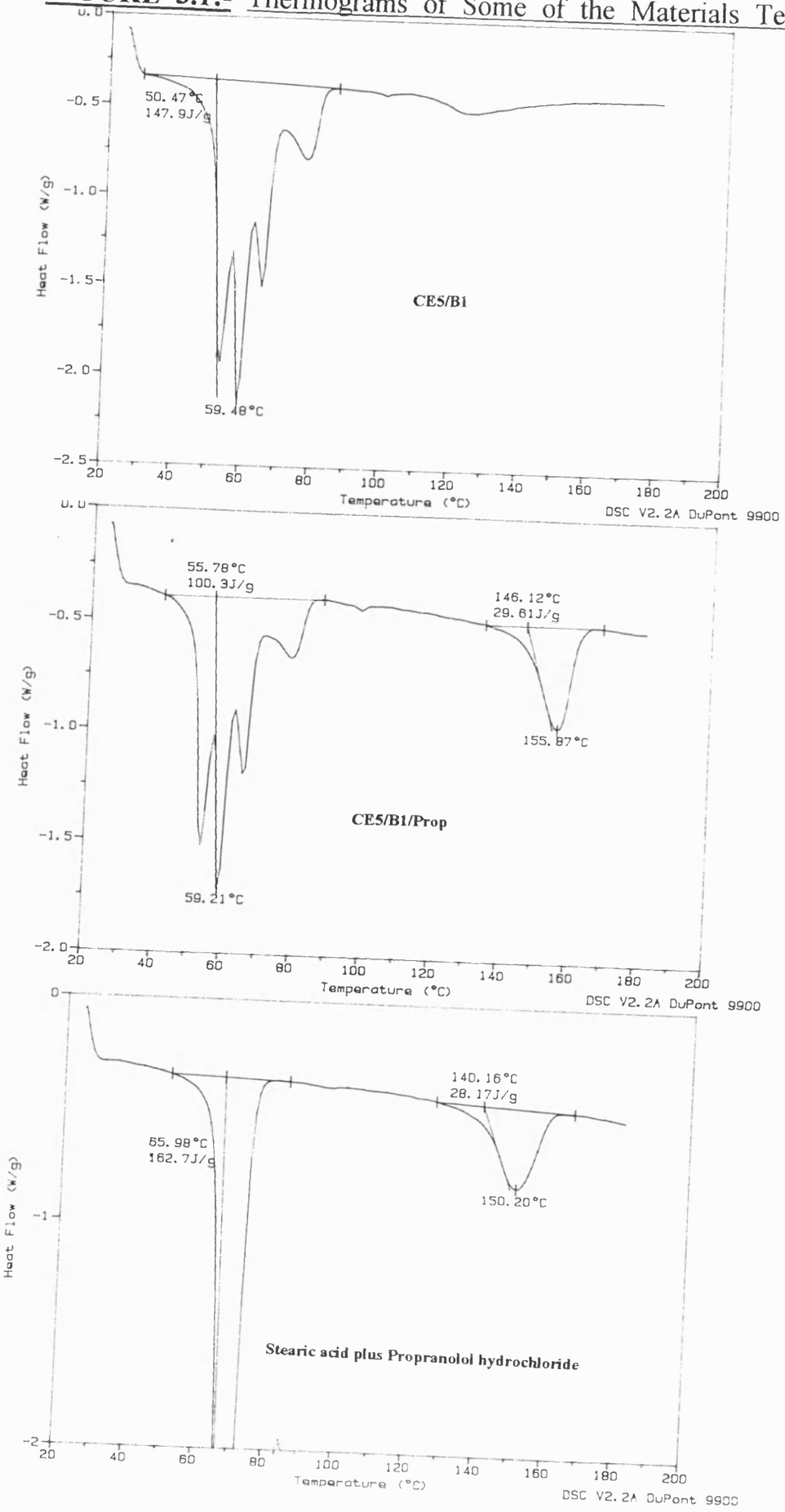

temperature was 59.48° C with an onset of transition at 50.47° C. The heat of transition was 147.9 J/g. This broad endothermic thermogram of CE5/B1 with its four peaks partly confirms the fact that HVO, Sterotex K, is composed of various fatty acid esters and their respective fatty acids. These fatty acids and their respective fatty acid esters probably have different melting points, with the majority having a melting point of approximately 60° C. Due to the fact that there were no exothermic peaks observed, which usually indicate degradation, [133] it was concluded that CE5/B1 was relatively stable. CE5 was prepared as described in section 2.3.1.1.

The two fatty acids analysed, palmitic acid and stearic acid, had sharp endothermic transitions at their expected melting point ranges. [134] None of the thermograms had any exothermic peaks indicating that the fatty acids had no degradation products.

All the respective thermograms of the fatty acids (palmitic acid and stearic acid) plus propranolol hydrochloride, with a drug to fatty acid ratio of 40 : 110, had sharp endothermic transitions at low temperature and distinctly small slightly broad endothermic transition at high temperature (see figure 3.1). The low temperature transition represented the respective fatty acid, while the high temperature endotherm was for propranolol hydrochloride. In both cases, the transition/melting temperature and the heat of fusion of propranolol hydrochloride were depressed by the fatty acids. This is common in mixtures of substances which have different melting points but do not react chemically. [133]

In the presence of low melting substances such as fatty acids, the energy, ΔH, required to convert (from solid to liquid), high melting substances such as propranolol hydrochloride, is lower than when it is pure. The temperature at which the transition of the "impure" propranolol hydrochloride occurs, T_m, is also depressed. This is due to a lowered degree of crystallinity of the propranolol hydrochloride in the presence of the low melting fatty acids. In contrast the transition temperatures of the fatty acids (palmitic acid and stearic acid), were not altered by the presence of the drug (table 3.1). This is to be expected since the mixtures contained almost 3 times as much fatty acid as propranolol hydrochloride (ratio = 110 : 40 respectively). Therefore the drug had minimal effect on the melting point of the fatty acids. However, the respective heats of fusion of the fatty acids were lowered by the presence of the propranolol hydrochloride (table 3.1).

The thermogram of CE5/B1/Prop (see tables 2.1 (a) and 2.2) had a distinct broad endothermic four peaked transition (T_m = 59.21° C) corresponding to CE5/B1 and a smaller endothermic transition at 155.87° C corresponding to propranolol hydrochloride (see figure 3.1). The depression of the melting point and heat of transition of propranolol hydrochloride was attributed to the reasons given above.

None of the DSC studies revealed exothermic transitions (indication of degradation), or notably inexplicable or unexpected endothermic peaks (general indication of the presence of a new compound as a result of a chemical

reaction). Therefore the DSC results were taken to indicate that CE5/B1 and the fatty acids (palmitic acid and stearic acid) had not chemically reacted with propranolol hydrochloride in the solid state during the period, post-mixing.

3.3 Characterisation of Particles of Composite Excipient 3

Particle size distribution of CE3 (table 2.1 (a)) was evaluated by the sieving technique as described in chapter 2, section 2.3.3. CE3 was prepared as described in section 2.3.1.1. Particle size distributions, whether unimodal or bimodal, can affect the final performance of a formulation. This factor, including the degree of kurtosis and skewness of the distribution, may be important in optimising mechanical properties, content uniformity and release-sustaining characteristics of a formulation. [88] The summary of the particle size distribution of CE3 is shown in table 3.2, figure 3.2 and figure 3.3.

From table 3.2:-

Volume mean diameter, $d_v = \sum wd/\sum w = 37\,365.3/99.8 =$ 374 μm.

Surface mean diameter, $d_s = \sum w/\sum(w/d) = 99.8/0.310723 =$ 321 μm.

Geometric mean diameter, $d_g = (x_1^{17.2} \times x_2^{30.0} \times \cdots\cdots \times x_8^{0.1})^{1/99.8} =$ 349.5 μm.

where x_1, x_2, ···· and x_8 are 605 μm, 427.5 μm ···· and 54 μm respectively.

The surface mean diameter is of practical significance as it is inversely proportional to the specific surface area of a powder or granulation sample. [17] The surface area of a powder or granulation is important in tablet bonding. Also the surface area of the granulation/powder may affect dissolution rate,

Table 3.2:- Particle diameter distribution of Composite Excipient 3 as Evaluated by Sieving Technique

Aperture (μm)	Aperture mean d (μm)	Retained (%) w	Cumulative Undersize Σw	wd	w/d
500-710	605	17.2	82.6	10 406	0.028430
355-500	427.5	30.0	52.6	12 825	0.071075
250-355	602.5	36.5	16.1	11 041.25	0.120661
180-250	215	12.1	4.0	2 601.5	0.056279
125-180	152.5	1.9	2.1	289.75	0.012459
90-125	107.5	1.4	0.7	150.5	0.013023
63-90	76.5	0.6	0.1	45.9	0.007843
45-63	54	0.1	0.0	5.4	0.001852
< 45	-	0	-	-	-
Totals (Σ)	1 940.5	99.8		37 365.3	0.310723

Key:-

w = % w/w frequency

Σw = cumulative % w/w undersize

Figure 3.2:- Cumulative Percent Undersize Curve for Composite Excipient 3 Particles as Measured by Sieving

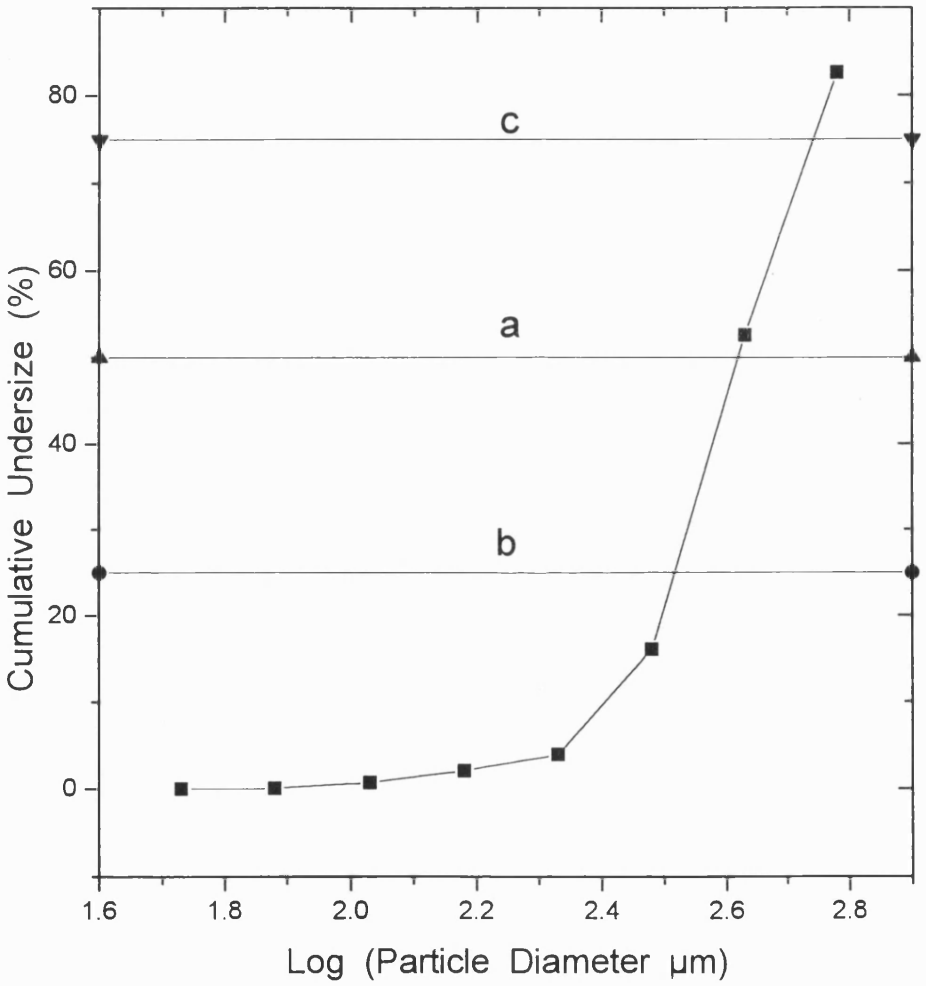

NB:- for Composite Excipient 3 (CE3) see table 2.1 (a)

Figure 3.3:- Percent Frequency Sieve Analysis Curve of Composite Excipient 3 Particles

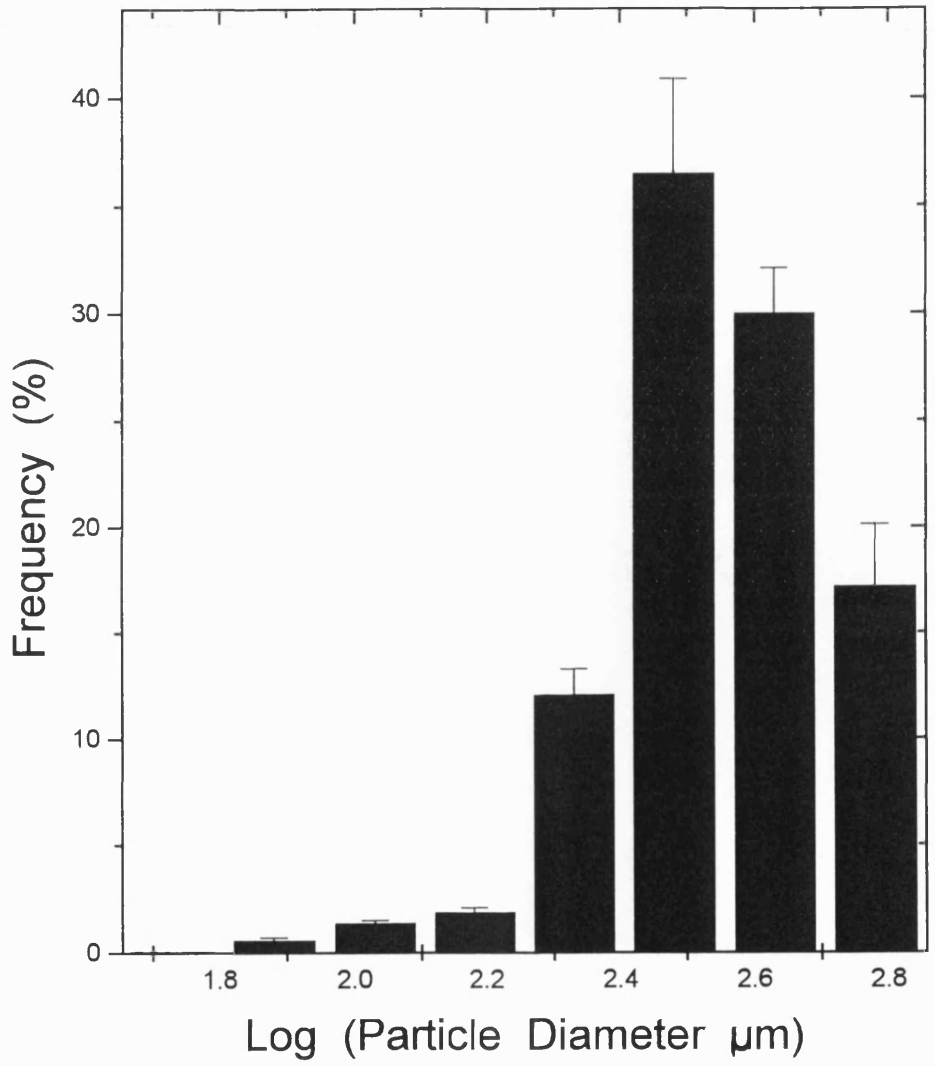

NB:- for Composite Excipient 3 (CE3) see table 2.1 (a)

ease of compaction and flowability. However, the three above diameters are approximately within the same range.

From figure 3.2:-

Median diameter (a) = antilog 2.62 = $10^{2.62}$ = 417 μm

Lower quartile diameter (b) = antilog 2.52 = $10^{2.52}$ = 331 μm

Upper quartile diameter (c) = antilog 2.74 = $10^{2.74}$ = 550 μm

The inter-quartile coefficient of skewness (IQCS), which indicates the degree of skewness, can be calculated from the equation below. IQCS can have a value range of -1 to +1 (0 value indicates curve symmetry between the quartile points).

$\therefore$ IQCS = {(c-a)-(a-b) / (c-a)+(a-b)}

$\Rightarrow$ IQCS = (133-86) / (133+86) = 47 / 219 = 0.21

From the IQCS and figure 3.3, the distribution of CE3 particles is positively skewed (skewed to the right). This is typical of powders produced by granulation and indicates that the majority of CE3 particles are large with minimal fines. This is desirable in a formulation since an excess of fines impede flowability and promote destructive capping.

3.4 Drug Release Mechanism of Processed HVO Matrices

Previous studies on controlling drug release from hydrophobic matrices for direct compression, have been carried out using Emvelop. [96] Emvelop is mainly hydrogenated cotton seed oil. In the present study, using composite excipients (CEs) based on hydrogenated castor oil/soybean oil (Sterotex K), tablets were prepared at approximately 12 kN from CE5/B1/Prop, CE5/B1/Theo (see tables 2.1 (a) and 2.2) and ACE/B1 (see section 2.3.2 and table 2.2) and subjected to dissolution testing. CE5 was prepared as described in section 2.3.1.1. A compaction force of 12 kN was selected because it produced compacts with constant reproducible drug release profiles and it is within the range of compaction forces used in industry to produce tablets. The tablet thickness before and after dissolution was measured using a digital micrometer.

The release data up to approximately 60 % from CE5/B1/Prop, CE5/B1/Theo and ACE/B1 tablets was evaluated according to the Higuchi and first order release mechanisms. For the Higuchi model, drug release was plotted against square root of time. For first order release, $\log_{10}$ {***amount of drug*** (*either propranolol hydrochloride or theophylline*) ***remaining***} was plotted against time. Linear regression analysis on the resulting plots for each individual tablet was carried out with the aid of a microcomputer software programme, ***Microcal Origin***. The summary of the linear regression analysis data for each tablet of the above three formulations is shown in appendix 1, tables A9 and A10.

The drug release profiles from CE5/B1/Prop, CE5/B1/Theo and ACE/B1 tablets are shown in figure 3.4. The summary of the *in vitro* release kinetics from the tablets according to the above mechanisms is shown in table 3.3. The values ± sd quoted are for the mean of the six individual tablet dissolution profiles.

As can be seen from figure 3.4, drug release from processed HVO does not follow zero order kinetics. The Higuchi model appeared to describe drug release from CE5/B1/Prop, CE5/B1/Theo and ACE/B1 matrices better than the first order mechanism (r = 99958, 0.99942 and 0.99497 respectively) (table 3.3). The Higuchi mechanism assumes that the matrix device is completely wetted at time zero and that there is complete removal of air. Ideally, the intercepts ought to be zero.

The release kinetics data (table 3.3), coupled with the fact that the tablet dimensions failed to alter significantly after dissolution, confirmed diffusion controlled release of drug from HVO matrices. Therefore drug release from HVO matrices probably involved leaching by the dissolution fluid that contacted the embedded drug. This formed pore - channels and cracks through which further fluid entered and leached out more drug. Due to the increase in the diffusional distance with time, release rate gradually decreased with time.

CE5/B1/Prop and ACE/B1 matrices had higher release rates than CE5/B1/Theo matrices (figure 3.4). Theophylline has a lower aqueous solubility (0.833 % w/v) [115] than propranolol hydrochloride (5 % w/v), [114] hence lower release rates in

Figure 3.4:- Propranolol Hydrochloride and Theophylline Release from CE5/B1/Prop, CE5/B1/Theo and ACE/B1 Matrices made at approximately 12 kN

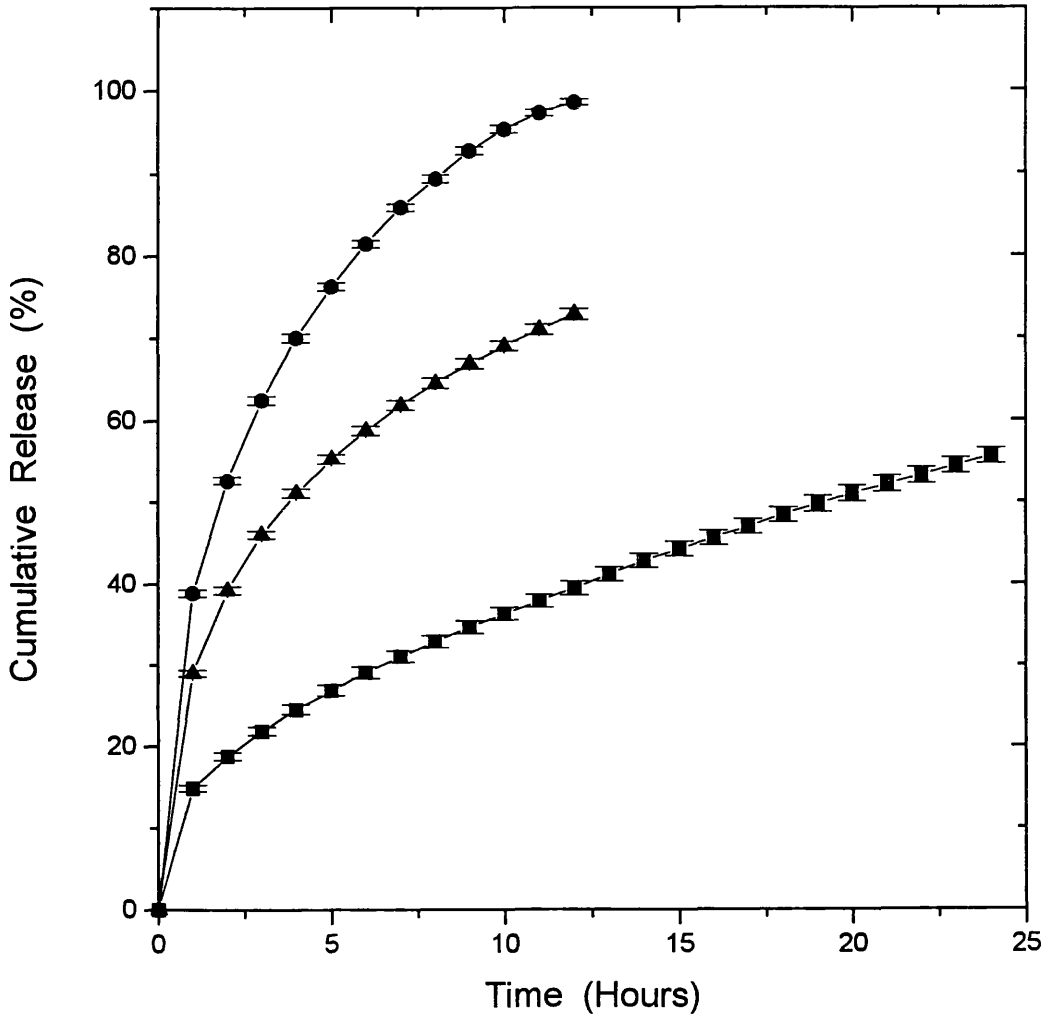

Key:-

—●— CE5/B1/Prop

—▲— ACE/B1

—■— CE5/B1/Theo

NB:- for details of CE5/B1/Prop, CE5/B1/Theo and ACE/B1 formulations see tables 2.1 (a) and 2.2 and section 2.3.2.

Table 3.3:- *In Vitro* Release Kinetics Data of Propranolol Hydrochloride and Theophylline from CE5/B1/Prop, CE5/B1/Theo and ACE/B1 Matrices Made at approximately 12 kN (n = 6)

	CE5/B1/Prop	CE5/B1/Theo	ACE/B1
	First Order:- $\log_{10}(100\ \% - Q) = kt$		
Slope (hr^{-1})	-0.11078 ± 0.00400	-0.01160 ± 0.00088	-0.04763 ± 0.00207
Intercept	1.9009 ± 0.0051	1.9262 ± 0.0060	1.8902 ± 0.0045
r	0.99838 ± 0.00064	0.99835 ± 0.00040	0.98778 ± 0.00088
	Higuchi Mechanism:- $Q = kt^{1/2}$		
Slope ($\%hr^{-1/2}$)	33.10 ± 0.67	10.58 ± 0.49	21.03 ± 0.52
Intercept (%)	5.57 ± 0.96	3.33 ± 1.10	8.33 ± 0.80
r	0.99958 ± 0.00030	0.99942 ± 0.00033	0.99497 ± 0.00056

NB:- for details of CE5/B1/Prop, CE5/B1/Theo and ACE/B1 formulations see tables 2.1 (a), 2.2 and section 2.3.2.

tablets containing the former than in those containing the latter. As drug solubility in dissolution medium decreases, release becomes more and more dependent on drug ***dissolution*** rather than ***diffusion*** in hydrophobic matrices such as those made from processed HVO. ACE/B1 matrices had lower propranolol hydrochloride release rates than CE5/B1/Prop matrices (figure 3.4). In the preparation of ACE by melt - granulation (section 2.3.2), some of the drug was probably completely encapsulated by the hydrophobic HVO. This, probably, is the main reason why drug release was retarded in ACE/B1 matrices.

3.5 Enhancement of Tensile Strength of Processed HVO Compacts

As indicated at the beginning of this chapter, process changes were studied in relation to the release - sustaining characteristics of the processed HVO tablets. The release - sustaining characteristics of processed HVO matrices could be inferred from the time for 50 % drug release (T50) or from the Higuchi release constant. Release - sustaining characteristics were directly related to T50 and inversely related to the Higuchi release constant. T50 was used as the preferred method of summarising release data and release - sustaining characteristics, due to the directness of comparison with previously published data and because it enabled simple qualitative interpretation of a given controlled release efficiency.

3.5.1 Effect of Binder Concentration on Tensile Strength and Release-Sustaining Characteristics

In this section, CE1/B1/Prop - CE10/B1/Prop (see tables 2.1 (a) and 2.2) tablets made at approximately 12 kN were used. A compaction force of 12 kN was selected for the same reasons given in section 3.4. CE1 - CE10 were prepared as described in section 2.3.1.1. Effects of binder concentration on tensile strength and release-sustaining characteristics of the compacts are summarised in figures 3.5 and 3.6. Each point on the curve in figure 3.5 is a mean of 15 tablets, while each point on the curve in figure 3.6 is a mean of 6 tablets. Tensile strength and release-sustaining characteristics values for each individual tablet are shown in appendix 1, tables A3 and A4.

Student t - tests and one way analysis of variance (ANOVAR) at 5 % significant level were carried out on the data. The calculated t value, t_{cal}, and calculated F value, F_{cal}, as in the case of one way ANOVAR, were compared with values in the statistical tables (t_{tab}, F_{tab}) at the appropriate degrees of freedom and probability, p, of 0.05.

Increase in binder concentration resulted in increase in tensile strength of the compacts (figure 3.5). Reports in the literature show that increasing amount of binder produce granules of greater strength than those of low binder concentrations, [16, 17] hence strong tablets. This is probably due to the formation of more and stronger inter-particulate bonds within the granules at high binder concentrations than at low ones.

Figure 3.5:- Effect of PVP K-30 (Binder) Concentration on Tensile Strength of CE1/B1/Prop - CE10/B1/Prop Compacts made at approximately 12 kN

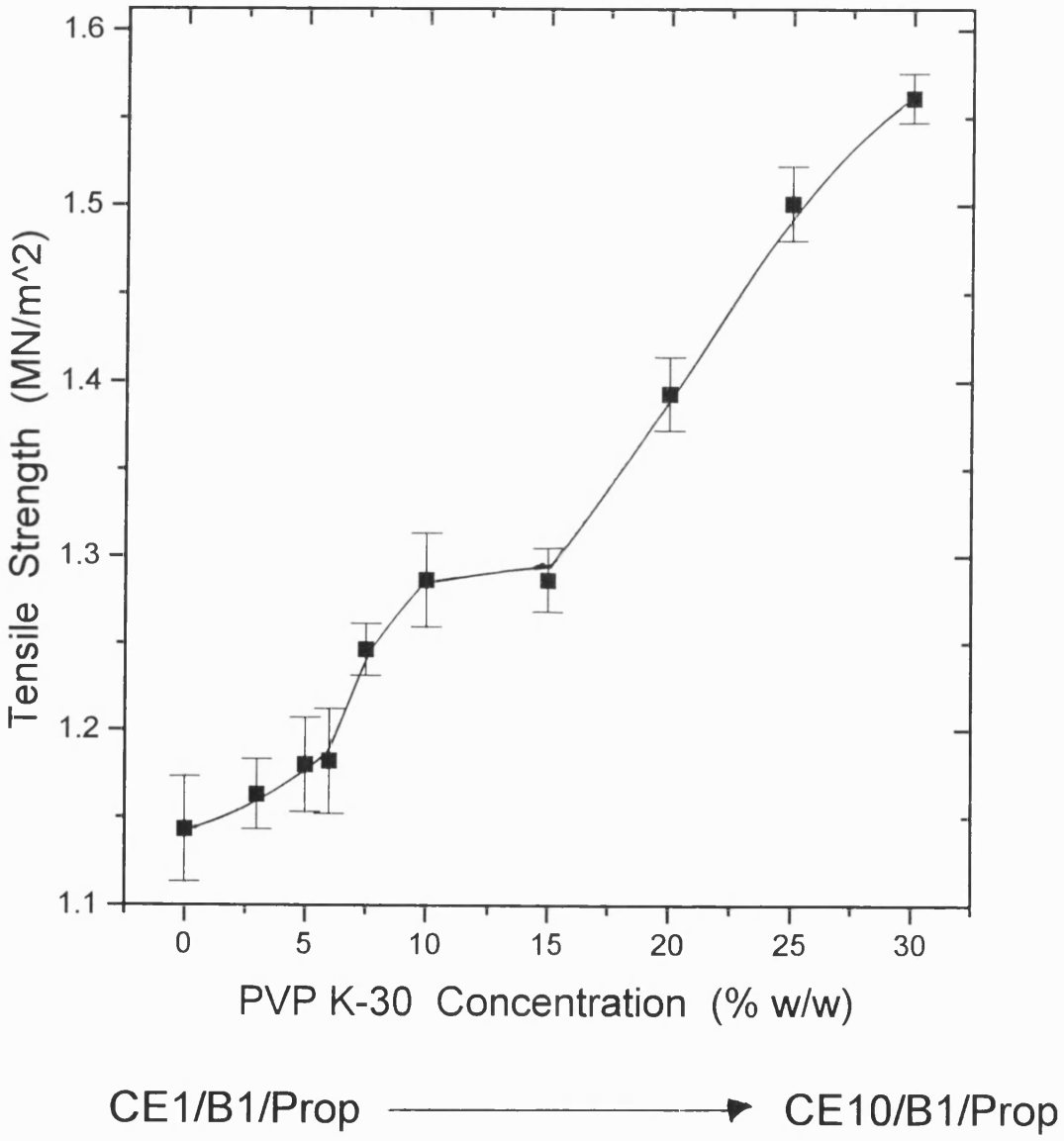

NB:- for details of CE1/B1/Prop - CE10/B1/Prop formulations, see tables 2.1 (a) and 2.2

Figure 3.6:- Effect of PVP K-30 (Binder) Concentration on Release - Sustaining Characteristics of CE1/B1/Prop - CE10/B1/Prop Matrices made at approximately 12 kN

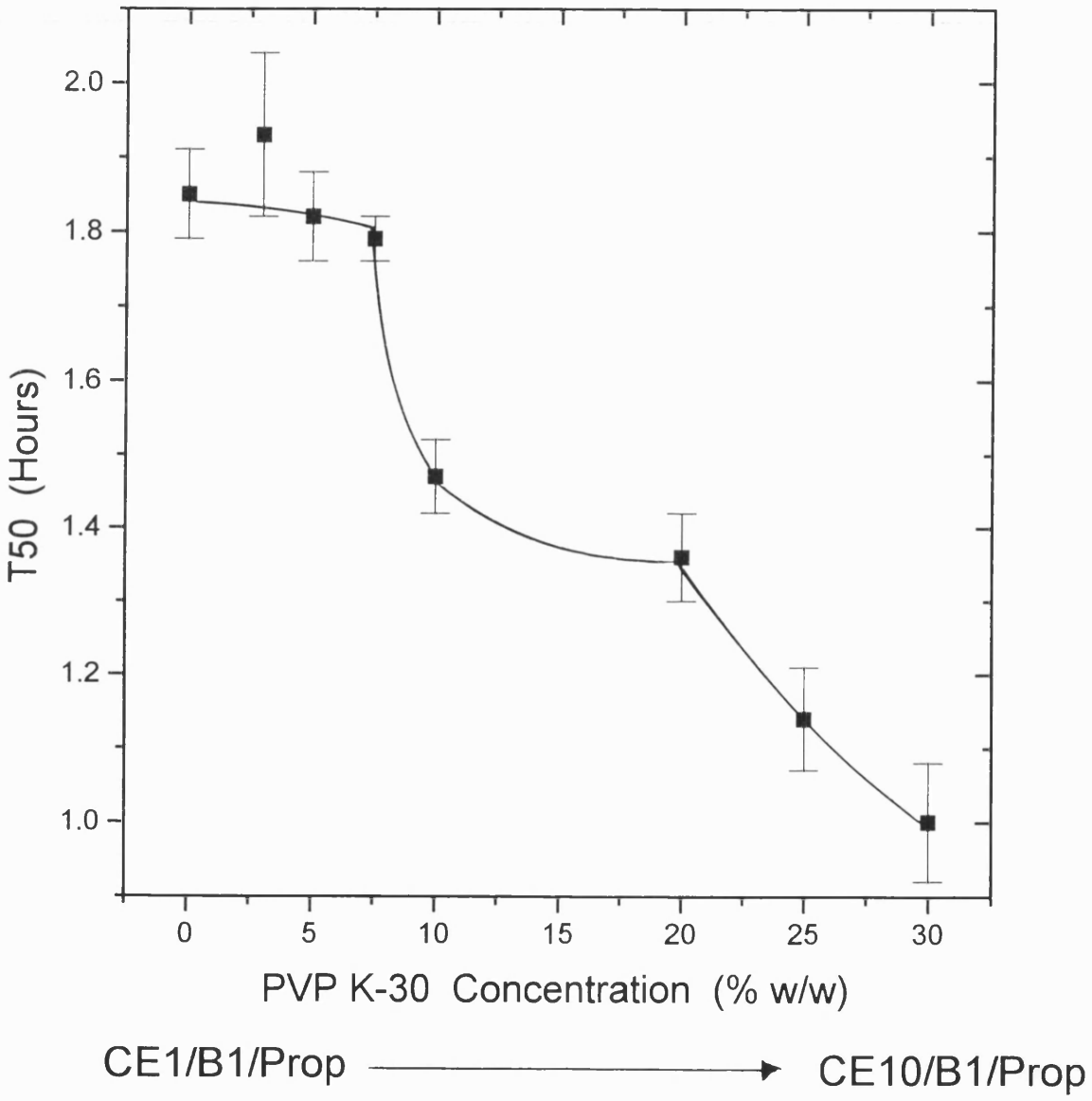

NB:- for details of CE1/B1/Prop - CE10/B1/Prop formulations, see tables 2.1 (a) and 2.2

One way ANOVAR on the tensile strengths of tablets made from CE1/B1/Prop - CE4/B1/Prop (0 - 6 % w/w binder concentrations respectively) revealed that these tensile strengths were not significantly different ($F_{cal} = 0.51$, $F_{tab} \approx 2.76$, $p = 0.05$). Therefore the minimum binder concentration that imparted appreciable improved tensile strength to the HVO compacts was approximately 7 % w/w (figure 3.5). The maximum tensile strength was obtained with tablets made from CE10/B1/Prop (30 % binder concentration). As tensile strength improved, the release - sustaining characteristics gradually depreciated as shown in figure 3.6. This was attributed to the hydrophilicity of the binder, PVP K-30, which probably enhanced drug leaching by acting as a channelling agent. Matrices containing 0 - 7.5 % binder concentration (CE1/B1/Prop - CE5/B1/Prop tablets) had the same release - sustaining characteristics ($F_{cal} = 0.73$, $F_{tab} = 2.76$). This was probably due to the fact that up to approximately 7 % binder concentration, the hydrophilicity nature of PVP K-30 had minimal effect on the release - sustaining characteristics of the matrix. Above 7.5 % binder concentration, release - sustaining characteristics depreciated significantly ($T50 = 1.79 \pm 0.08$ hr at 7.5 % (CE5/B1/Prop) and $T50 = 1.47 \pm 0.13$ hr at 10 % (CE6/B1/Prop); $t_{cal} \geq 5.13$, $t_{tab} = 2.23$, $p = 0.05$). Since PVP K-30 at approximately 7 % improved tensile strength but had negligible effect on release - sustaining characteristics, processed HVO containing 7.5 % w/w PVP K-30 (CE5/B1/Prop) was investigated further.

Apparently the PVP K-30 did not alter the release mechanism of the processed HVO matrices. The binder probably gradually increased the porosity factor, ϵ,

in the Higuchi equation which increased release. This is depicted by the shift to the left of the release profiles with increase in PVP K-30 concentration as shown in figure 3.7 and the increase in the Higuchi release constant with increase in binder concentration as shown in figure 3.8.

The characteristics of compacts made from the formulations containing varying concentrations of PVP K-30 (CE1/B1/Prop - CE10/B1/Prop) are shown in table 3.4. As binder concentration increased the tablet relative density increased, being most marked from 15 % w/w to 30 % w/w binder concentration (CE7/B1/Prop - CE10/B1/Prop respectively). This increase in compact relative density with increase in binder concentration was matched by a decrease in tablet thickness. This was possibly due to the formation of stronger and possibly more bonds within the compacts at higher binder concentration than at lower ones. Total compaction time and tablet weight were relatively constant at all binder concentrations. However, dense strong tablets had poor release - sustaining characteristics due to the hydrophilic nature of PVP K-30.

Figure 3.7:- Effect of PVP K-30 (Binder) Concentration on Propranolol Hydrochloride Release from CE1/B1/Prop, CE5/B1/Prop, CE8/B1/Prop and CE10/B1/Prop Matrices made at approximately 12 kN

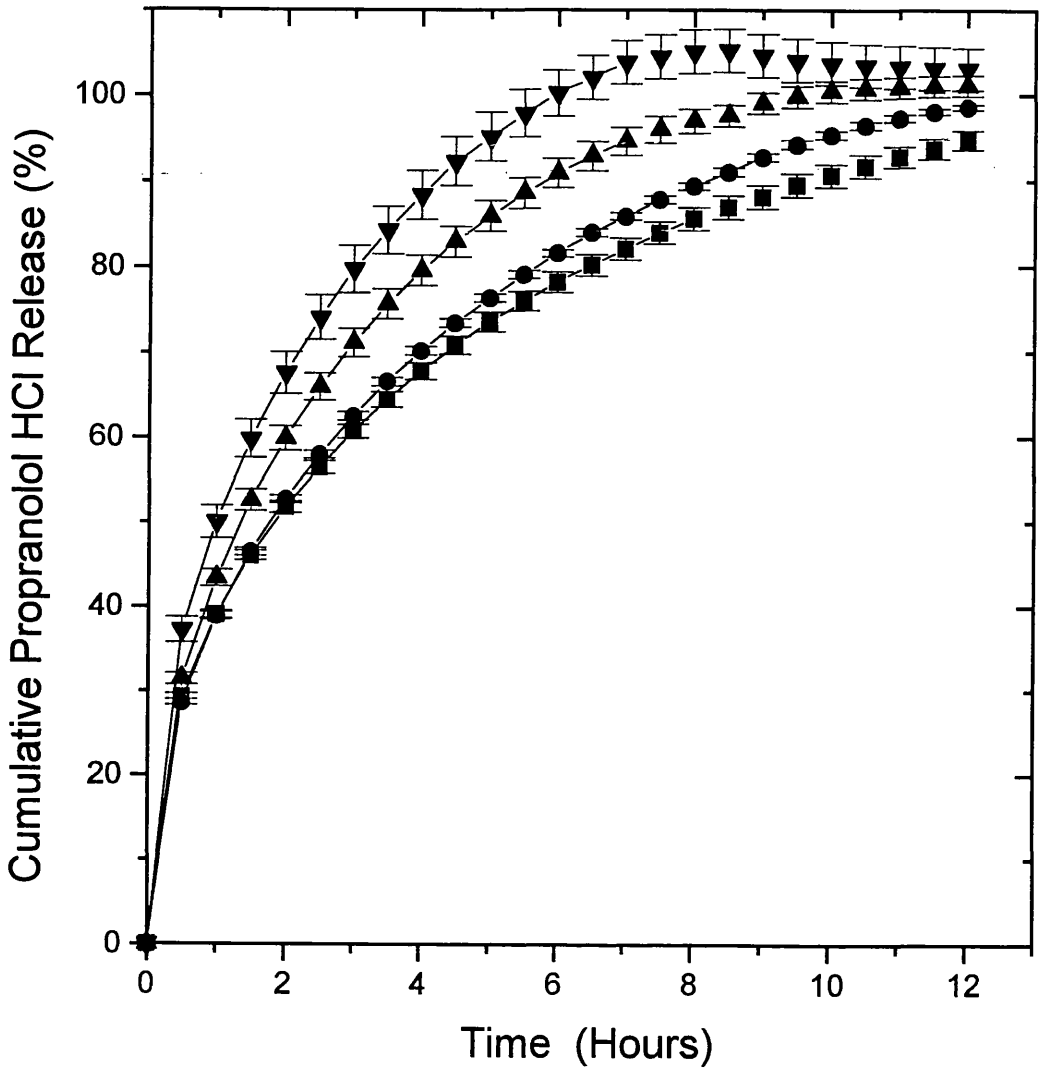

		Formulation	PVP K-30 Concentration
Key:-	—■—	CE1/B1/Prop	0 % w/w
	—●—	CE5/B1/Prop	7.5 % w/w
	—▲—	CE8/B1/Prop	20 % w/w
	—▼—	CE10/B1/Prop	30 % w/w

NB:- for details of CE1/B1/Prop - CE10/B1/Prop formulations, see tables 2.1 (a) and 2.2

Figure 3.8:- Propranolol Hydrochloride Release According to the Higuchi Mechanism, from CE1/B1/Prop, CE5/B1/Prop and CE10/B1/Prop Matrices made at approximately 12 kN

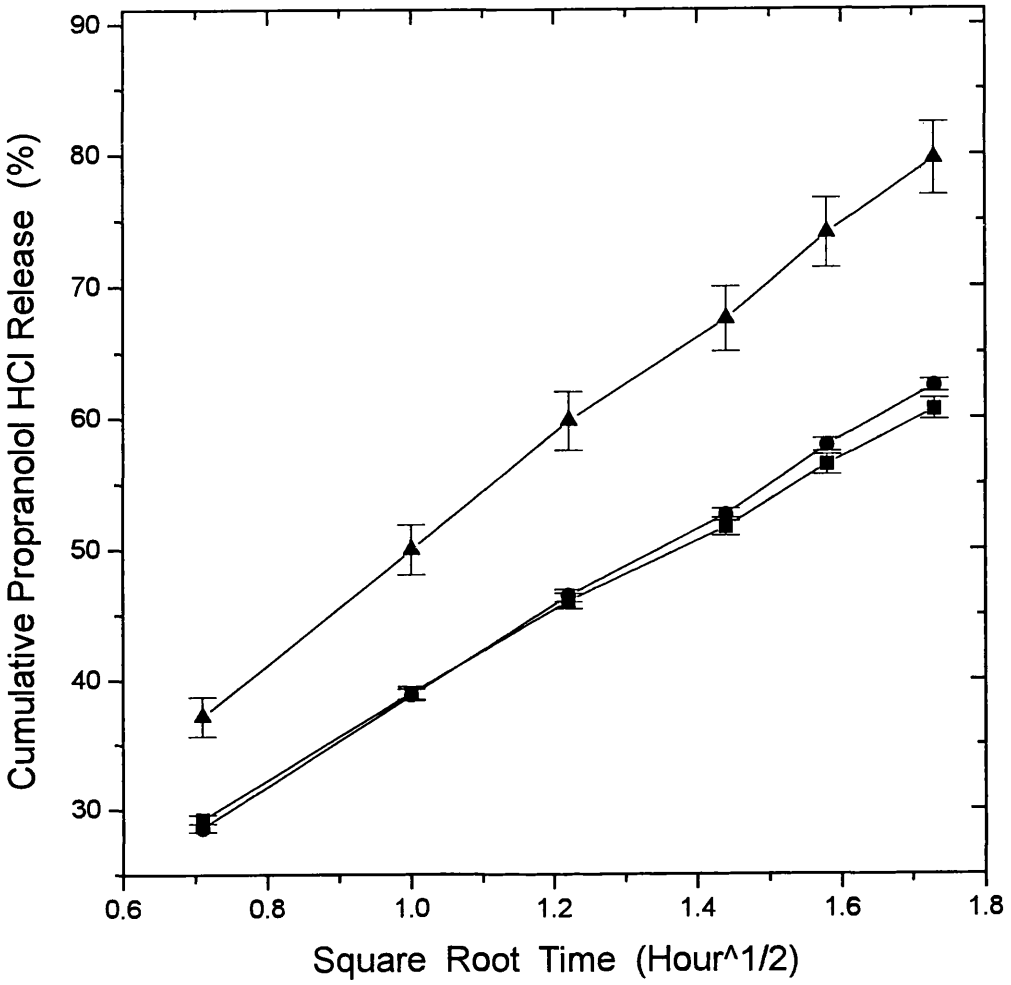

	PVP K-30 conc.	Slope (%hr$^{-1/2}$)	Intercept (%)	r
Key:- —■—	0 % w/w	30.59 ± 1.38	8.14 ± 1.04	0.99931
—●—	7.5 % w/w	33.10 ± 0.67	5.57 ± 0.96	0.99958
—▲—	30 % w/w	41.59 ± 3.43	8.27 ± 2.46	0.99947

where:- CE1/B1/Prop contains 0 % binder, CE5/B1/Prop contains 7.5 % binder and CE10/B1/Prop contains 30 % binder.

NB:- for details of CE1/B1/Prop, CE5/B1/Prop and CE10/B1/Prop formulations see tables 2.1 (a) and 2.2. conc. = concentration

Table 3.4:- The effect of PVP K-30 Concentration on Properties of CE1/B1/Prop - CE10/B1/Prop Tablets made at approximately 12 kN (n = 15)

[PVP] % w/w	Tab. Rel. Dens. (gcm^{-3})		Tot. Comp. Tim. (s)		Tab. Weight (mg)		Tab. Thickness (mm)	
	mean	sd	mean	sd	mean	sd	mean	sd
0	1.037	0.002	0.48	0.02	152.1	0.4	2.919	0.008
3	1.030	0.002	0.47	0.02	151.7	0.4	2.931	0.008
5	1.035	0.001	0.48	0.06	151.5	0.3	2.914	0.005
6	1.037	0.002	0.46	0.02	151.9	0.3	2.914	0.007
7.5	1.038	0.002	0.47	0.03	151.5	0.3	2.904	0.003
10	1.036	0.001	0.49	0.02	151.7	0.2	2.913	0.007
15	1.045	0.002	0.47	0.03	152.2	0.2	2.897	0.007
20	1.049	0.002	0.48	0.02	152.2	0.3	2.886	0.006
25	1.052	0.002	0.49	0.03	152.0	0.4	2.874	0.006
30	1.056	0.002	0.48	0.02	152.4	0.2	2.871	0.008

NB:- Tab. Rel. Dens. = Tablet Relative Density

Tot. Comp. Tim. = Total Compression Time (contact time)

Tab. Thickness = Tablet Thickness

[PVP] = PVP K-30 Concentration

NB:- for details of CE1/B1/Prop - CE10/B1/Prop formulations see tables 2.1 (a) and 2.2

3.5.2 Effect of Type of Binder on Tensile Strength and Release - Sustaining Characteristics

In this section, tablets were made at approximately 12 kN from CE1/B1/Prop, CE5/B1/Prop, CE12/B1/Prop, CE13/B1/Prop and CE14/B1/Prop (see tables 2.1 (a), 2.1 (b) and 2.2). CE1, CE5, CE12, CE13 and CE14 were prepared as described in section 2.3.1.1. Subsequent tablets had their tensile strength (15 tablets per batch) and dissolution properties (6 tablets per batch) evaluated. The effect of the type of binder on tensile strength and release-sustaining characteristics of processed HVO tablets is summarised in figure 3.9. Student t - tests were done on the data obtained with results evaluated at the 5 % significance level.

Besides retaining the basic release-sustaining characteristics, CE12/B1/Prop, which contained PVP K-90 as binder, (T50 = 1.90 ± 0.19 hr for CE12/B1/Prop tablets and T50 = 1.85 ± 0.14 hr for CE1/B1/Prop tablets; $t_{cal} = 0.52$, $t_{tab} = 2.23$, $p = 0.05$) produced tablets with significantly superior strength to those made from CE5/B1/Prop, which contained PVP K-30 as binder, (tensile strength = 1.362 ± 0.066 MN/m^2 for CE12/B1/Prop tablets and 1.246 ± 0.060 MN/m^2 for CE5/B1/Prop tablets; $t_{cal} = 5.22$, $t_{tab} = 2.05$). Since the former has a higher relative molecular mass (RMM = 360 kDa) than the latter (RMM = 40 kDa), this probably is the main reason why it is a better binder. PVP K-90 is also less hydrophilic than PVP K-30, therefore it has negligible effect on the release-sustaining characteristics of processed HVO tablets.

Figure 3.9:- Effect of the Type of Binder in CE1/B1/Prop, CE5/B1/Prop and CE12/B1/Prop - CE14/B1/Prop tablets on Tensile Strength and Release - Sustaining Characteristics (Force ≈ 12 kN)

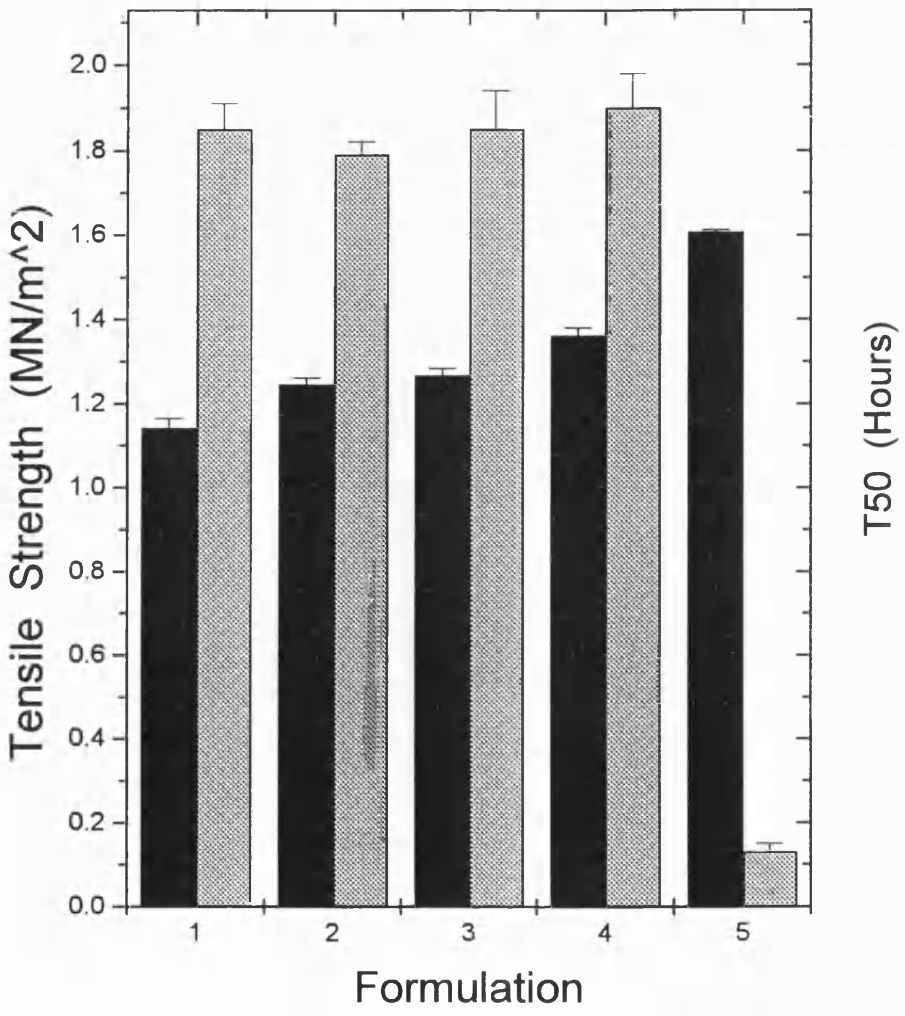

Key:- 1 = CE1/B1/Prop, **no binder**

2 = CE5/B1/Prop, **binder = PVP K-30**

3 = CE13/B1/Prop, **binder = Luviskol**

4 = CE12/B1/Prop, **binder = PVP K-90**

5 = CE14/B1/Prop, **binder = Polyplasdone**

Tensile strength

T50

NB:- for details of CE1/B1/Prop, CE5/B1/Prop and CE12/B1/Prop-CE14/B1/Prop formulations see tables 2.1 (a), 2.1 (b) and 2.2

Polyplasdone which has sometimes been termed a "super-disintegrant", produced tablets (CE14/B1/Prop tablets) with the best tensile strength compared to the other three binders (PVP K-30, PVP K-90 and Luviskol). However, it totally destroyed the release-sustaining characteristics of processed HVO matrix, as dissolution was complete within 15 minutes. Although Polyplasdone is insoluble in water, it is highly hydrophilic. Upon absorption of water, the lattice structure of Polyplasdone expands, [15] rupturing the processed HVO matrix. Unlike PVP which forms soft granules, Polyplasdone forms hard granules, hence stronger tablets than the former.

Luviskol imparted the same tensile strength properties to the processed HVO matrix (CE13/B1/Prop) as PVP K-30 (CE5/B1/Prop) although compacts made with the former had a slightly numerical higher value for strength than the latter (tensile strength = 1.267 ± 0.062 MN/m^2 for CE13/B1/Prop tablets and 1.246 ± 0.060 MN/m^2 for CE5/B1/Prop tablets; $t_{cal} = 0.80$). Furthermore, there is no significant difference between the release - sustaining characteristics of the tablets containing Luviskol and PVP K-30 as binders ($t_{cal} = 0.61$). However, Luviskol unlike PVP, is a copolymer of PVP and polyvinylacetate. Further, this copolymer is not very stable because it is labile in hot solutions, or when subjected to vigorous stirring. Consequently, PVP K-30 was selected over Luviskol as binder.

PVP K-90 was selected over the other three binders for use in the final optimum composite excipient. It imparted significantly better tensile strength to

processed HVO compacts than either Luviskol or PVP K-30 (t_{cal} = 4.07 and 5.22 respectively). Unlike Polyplasdone which destroyed the release-sustaining characteristics of processed HVO, PVP K-90 had negligible effect on the release - sustaining characteristics of the matrix (t_{cal} = 0.52).

The binders in order of increasing tensile strength of the tablets they produced were as follows:- PVP K-30 ≤ Luviskol < PVP K-90 << Polyplasdone. The order of the binders in reducing release - sustaining characteristics of processed HVO tablets followed the order:- Polyplasdone >> PVP K30 ≥ Luviskol ≥ PVP K-90.

3.5.3 Effect of Type of Matrix on Tensile Strength and Controlled Release Efficiency

In this section, the basic release sustaining matrix material was either Sterotex K (CE5/B1/Prop) or Compritol (CE15/B1/Prop) (see tables 2.1 (a), 2.1 (b) and 2.2). CE5 and CE15 were prepared as described in section 2.3.1.1. Tablets made at approximately 12 kN from the two formulations were subjected to dissolution tests and tensile strength measurement. The results are summarised in figure 3.10. The data was subjected to Student t - tests with results evaluated at the 5 % significance level.

CE5/B1/Prop matrices, which contained Sterotex K (HVO) as the basic release - sustaining characteristics matrix material, had significantly superior release-sustaining characteristics to CE15/B1/Prop matrices, which contained Compritol

Figure 3.10:- Effect of Type of Basic Release - Sustaining Matrix Material on Tensile Strength and Release - Sustaining Characteristics

(Compaction Force ≈ 12 kN)

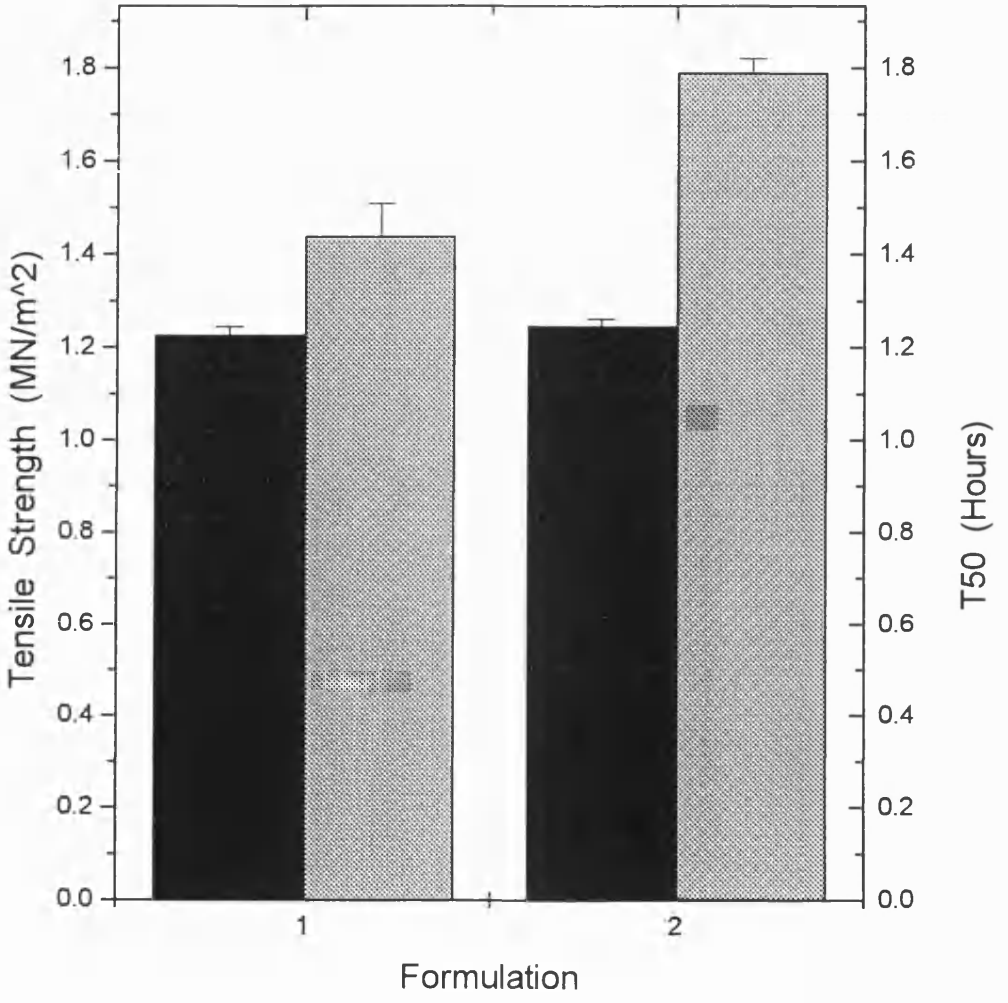

Matrix Material

Key:- 1 = CE15/B1/Prop Compritol — Tensile strength

2 = CE5/B1/Prop Sterotex K — T50

NB:- for details of CE5/B1/Prop and CE15/B1/Prop formulations, see tables 2.1 (a), 2.1 (b) and 2.2

($t_{cal} = 4.66$, $t_{tab} = 2.23$, $p = 0.05$). However, there was no significant difference in tensile strength of the tablets made from the two formulations ($t_{cal} = 0.8$, $t_{tab} = 2.05$). HVO was thus selected over Compritol for use in further studies as the basic release - sustaining characteristics matrix material due to its superior controlled release efficiency.

3.5.4 Optimisation of Tensile Strength and Release Sustaining Characteristics of Processed HVO Compacts

In this section, release - sustaining characteristics were inferred from T50 values rather than from the Higuchi release constants for the same reasons mentioned in section 3.5.

3.5.4.1 Effect of Particle Size on Tablet Tensile Strength and Release - Sustaining Characteristics

The general consensus is that one of the most important factors determining the strength of tablets is the particle size of the granulation or powder from which the compacts have been made. [18, 23, 25, 99, 135] Due to this fact, there is now more interest in particle engineering with a perspective of optimising compaction behaviour. [1] Therefore in order to utilise this property, in an attempt to optimise the tensile strength and release-sustaining characteristics of processed HVO, tablets were prepared at approximately 12 kN from different size fractions of CE5 (500-710 μm, 355-500 μm, 250-355 μm, 180-250 μm and <180 μm exclusively), plus propranolol hydrochloride (ratio = 110 : 40 respectively). CE5 was prepared as described in section 2.3.1.1, while

fractionation was done as described in section 2.3.3. The tablets made from these various size fractions plus drug, were subjected to tensile strength evaluation (15 tablets per batch) and dissolution testing (6 tablets per batch). Tensile strength and release-sustaining characteristics values for each individual tablet are shown in appendix 1, tables A2 and A5 respectively.

The effect of particle diameter on compact tensile strength is summarised in figure 3.11, while the effect of particle diameter on release - sustaining characteristics is summarised in figure 3.12. The properties of the resulting compacts are shown in table 3.5. The data was subjected to Student t - tests and one way ANOVAR, with evaluations done at the 5 % significance level.

Tablet tensile strength was found to increase with an increase in particle size, at small particle diameters and at large particle diameters (figure 3.11). The three medium particle diameters (180-250 μm, 250-355 μm, 355-500 μm) produced tablets with the same tensile strength ($F_{cal} = 0.7$, $F_{tab} \approx 3.23$, $p = 0.05$). There was a significant difference in tensile strength between tablets made from the smallest particles (< 180 μm) and tablets from the three medium particle size ranges ($t_{cal} \geq 3.49$, $t_{tab} = 2.05$). Further, significant difference in tensile strength exists, between compacts made from the three medium particle size ranges and compacts made from the largest particles (500-710 μm) ($t_{cal} \geq 3.14$).

This trend was ***almost mirrored*** by the effect of particle size on release - sustaining characteristics as shown in figure 3.12. The main difference is that

Figure 3.11:- The Effect of Particle Diameter on Tensile Strength of Tablets Made from CE5/Prop at approximately 12 kN

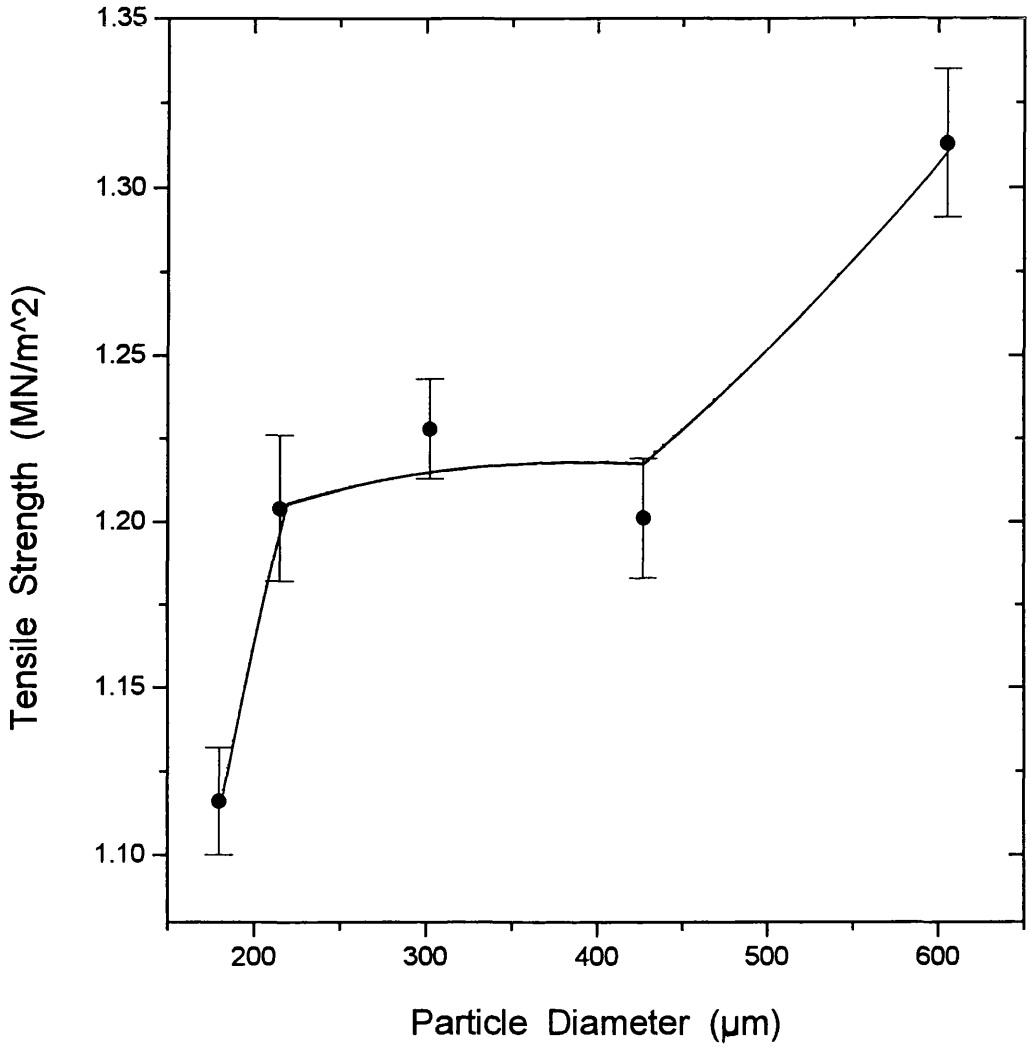

NB:- for details of CE5/Prop formulation, see table 2.1 (a)

Figure 3.12:- The effect of Particle Diameter on Release - Sustaining Characteristics of Matrices Made from CE5/Prop at approximately 12 kN

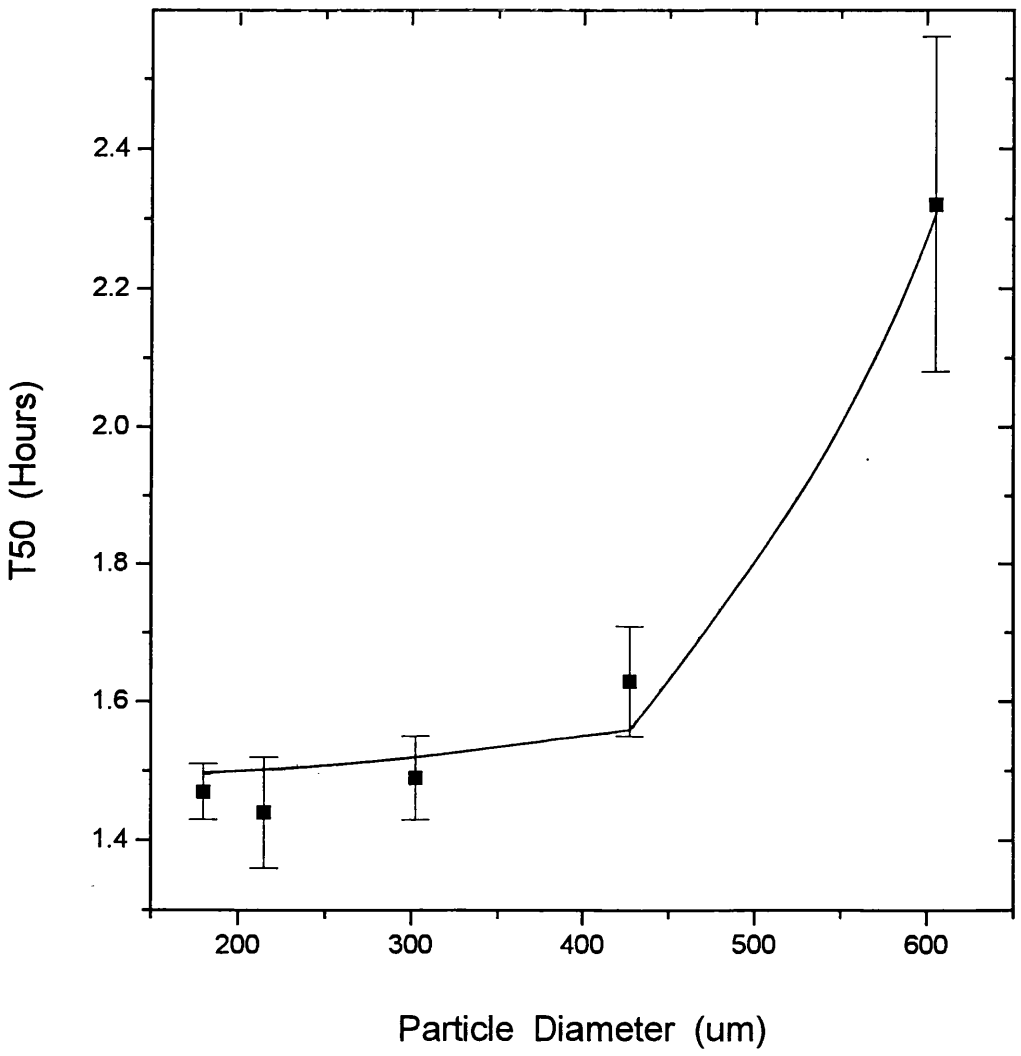

NB:- for details of CE5/Prop formulation see table 2.1 (a)

Table 3.5:- The Effect of Particle Diameter on Properties of Compacts Made from CE5/Prop at approximately 12 kN (n = 15)

Particle Size (μm)	R - value		Tab. Rel. Dens. (gcm^{-3})		Tab. Weight (mg)		Tab. Thickness (mm)	
	mean	sd	mean	sd	mean	sd	mean	sd
500-710	0.893	0.004	1.039	0.002	151.3	0.3	2.896	0.008
355-500	0.891	0.004	1.036	0.002	150.9	0.3	2.898	0.008
250-355	0.888	0.008	1.034	0.002	150.8	0.5	2.902	0.009
180-250	0.890	0.004	1.030	0.002	149.9	0.6	2.895	0.013
< 180	0.888	0.004	1.027	0.002	149.6	0.5	2.899	0.009

NB:- mean total compaction time = 0.48 ± 0.02 seconds

Key:- Tab. Rel. Dens. = Tablet Relative Density

Tab. Weight = Tablet Weight

Tab. Thick. = Tablet Thickness

NB:- for details of CE5/Prop formulation see tables 2.1 (a) and 2.2

matrices made from the smallest particles (< 180 μm) had the same release - sustaining characteristics as matrices made from the three medium particle size ranges (180-250 μm, 250-355 μm, 355-500 μm) (F_{cal} = 1.5, F_{tab} = 3.10). However, compacts made from the largest particles (500-710 μm) had significantly superior release - sustaining characteristics to those made from the rest particle size ranges ($t_{cal} \geq 5.68$).

Generally, for particles that mainly undergo plastic deformation, an increase in particle size result in weak compacts. High drug release rates are also expected with large particles due to increased inter-particulate porosity. However, in some systems, [94] drug release has been shown to decrease with an increase in particle size due to a reduction in surface area exposed to the dissolution medium. Literature generally suggest that the compaction of smaller particles of ductile materials such as HVOs, result in stronger compacts than larger particles. Smaller particles yield larger areas of true contact than larger particles after the rearrangement phase of consolidation, which promote the formation of more and/or stronger bonds than the latter do. [5, 25, 136, 137] However, in some studies involving sodium chloride the reverse has been found. [8, 25, 137] Generally, with ductile materials such as HVO, the difference in packing density is usually retained throughout the compaction process, with tablet strength and porosity dependent on initial particle size distribution. [5]

The larger particles of CE5/Prop had initial high die fill volumes compared to the smaller particles, prior compaction. This implied different initial packing

densities for the various particle size fractions. [5] Therefore the larger particles had a higher deformation potential than the smaller particles, [18] which resulted in significantly stronger compacts with the former than with the latter.

The fraction of the upper punch force transmitted to the stationary lower punch (R-value) significantly decreased with decrease in particle size (t_{cal} = 2.16), between the 500-710 μm and 250-355 μm particles. Tablets made from the two smallest particle size ranges (< 180 μm and 180-250 μm) had significantly smaller tablet weights than tablets made from the rest of the particle size ranges ($t_{cal} \geq 4.10$). This reason is probably sufficient to explain the anomaly in the R - values post 250-355 μm (table 3.5).

Generally, there is a decrease in particle die wall friction as particle size increases due to a decrease in the true area of contact between the die wall and particles. A decrease in the ejection force as particle size increased has been reported. [25, 30] This has been attributed to an decrease in the force lost to the die wall due to two factors namely:- (a) a decrease in the total contact area and (b) a decrease in the effective shear strength. Therefore all these factors will cause larger particles to have:- (i) lower die wall contact areas, (ii) lower force lost to the die wall and (iii) more upper punch force transmitted to the lower punch; than smaller particles, on compaction. All this results in the production of stronger and less porous compacts with larger particles than with smaller particles, as obtained in this study.

Generally, there is an increase in the force per unit area (pressure) on compaction of larger particles than smaller particles [137] due to the smaller total surface area of the former than the latter. This probably results in more partial melt-fusion (cold welding phenomenon) of the HVO and stearic acid in the formulation containing larger particles than that containing smaller particles. This promotes the formation of more solid bridge tablet bonds within the former than within the latter. In addition, large particles generally possess more strength than small ones, hence the formation of stronger compacts from the former than from the latter.

Nystrom and co-workers [8] found that for plastically deforming materials that probably partially melted during compaction (such as HVO), bonding with solid bridges occurred only for the coarser particles. The compacts produced were quite strong even though the surface area involved in the solid bridge formation, as measured by gas adsorption, was small in relation to the total surface area of the compact.

The constant compact strength with the three medium particle size ranges (180-250 μm, 250-355 μm, 355-500 μm) in figure 3.11, corresponding to the constant release - sustaining characteristics in figure 3.12, was attributed to the compensation between partial melting/fusion effects and ductile effects of these particles during compaction. It was concluded that large particles of CE5 (500-710 μm) containing propranolol hydrochloride, produced tablets with significantly superior tensile strength and release - sustaining characteristics than particles

smaller than 500 μm. Therefore the final optimum formulation, CE29/B2/Prop (see tables 2.1 (e) and 2.2), contained a large proportion of large particles.

3.5.4.2 Effect of Compaction Force on Tablet Tensile Strength and Release-Sustaining Characteristics

The magnitude of the compacting load is one of the major determinants of the tensile strength of compacts. This is because it increases:- (i) the area of true contact between particles and (ii) the strength and/or number of bonds formed. [3, 99] In the case of HVOs and other low melting substances, compaction force influences the extent of the partial melt - fusion phenomenon thereby affecting the number of solid bridges produced.

In order to determine the effect of compaction force on tensile strength and release - sustaining characteristics of processed HVO matrices, CE5/B1/Prop (table 2.1 (a) and 2.2), was compacted at 3 - 18 kN. The resulting tablets were evaluated for tensile strength and release - sustaining characteristics. The results are summarised in figures 3.13 and 3.14. The tablet properties are shown in table 3.6. For the tensile strength results (figure 3.13), each point on the curve is a mean of 15 tablets (except at approximately 6 kN, where n = 12), while for release - sustaining characteristics (figure 3.14), each point on the curve is a mean of 6 tablets. Tensile strength and release-sustaining characteristics values for each individual tablet are shown in appendix 1, tables A1 and A6 respectively. Statistical analysis done on the data include Student t - tests and one way ANOVAR with results evaluated at the 5 % significance level.

Figure 3.13:- The Effect of Compaction Force on Tensile Strength of Tablets Made from CE5/B1/Prop

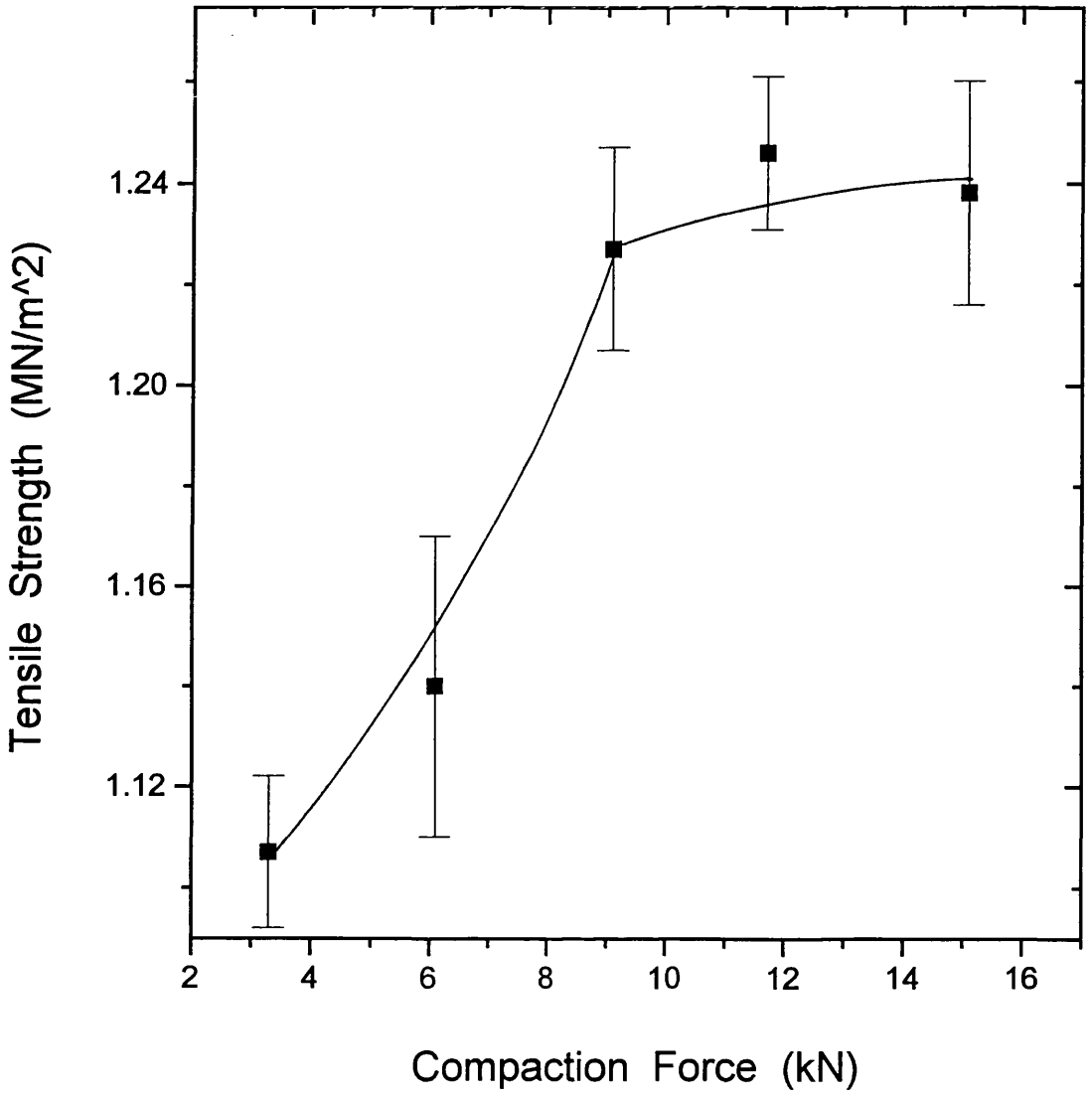

NB:- for details of CE5/B1/Prop formulation, see tables 2.1 (a) and 2.2

Figure 3.14:- Effect of Compaction Force on Release - Sustaining Characteristics of Matrices Made from CE5/B1/Prop

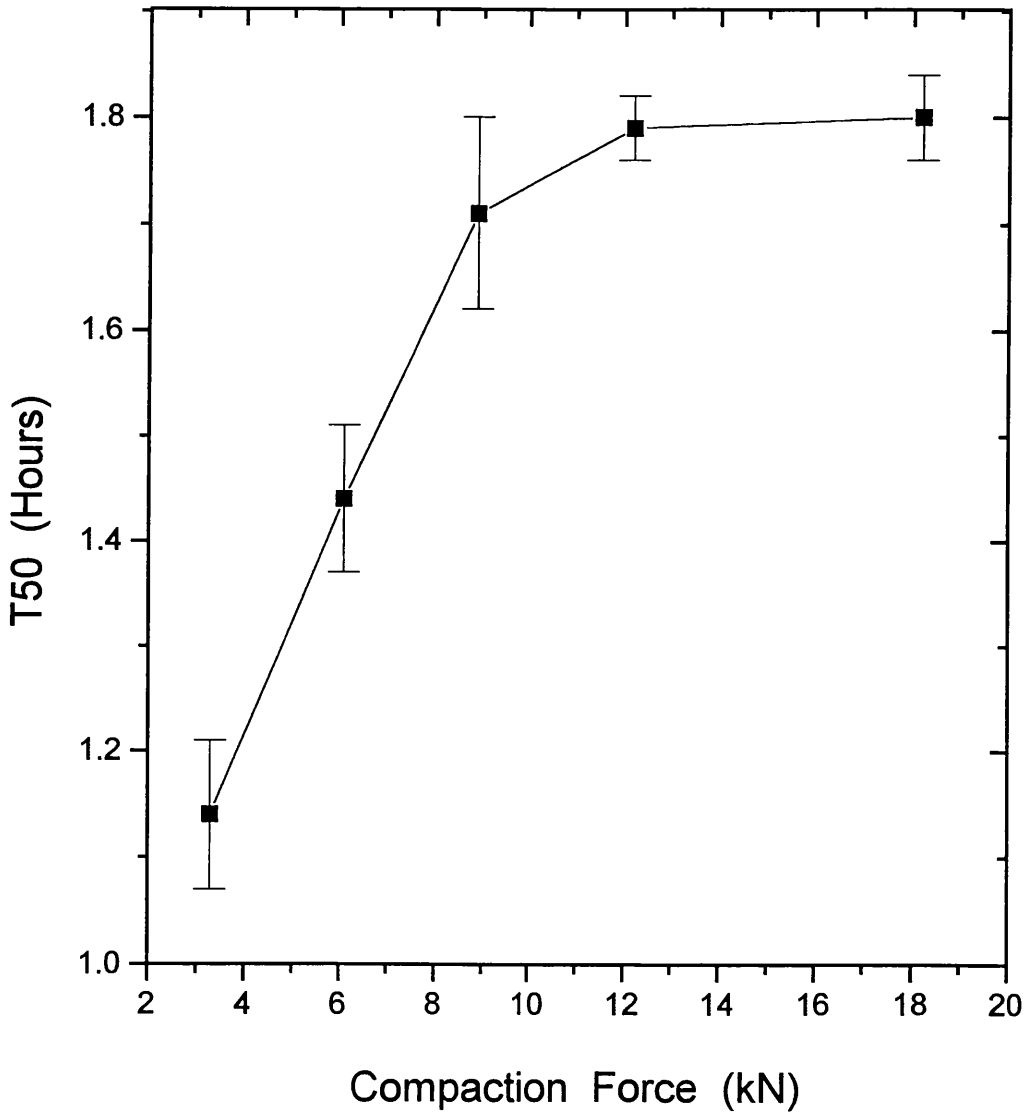

NB:- for details of CE5/B1/Prop formulation, see tables 2.1 (a) and 2.2

Table 3.6:- The Effect of Compaction Force on Properties of Compacts Made from CE5/B1/Prop at approximately 12 kN (n =15)

Com. For. (kN)		Time (s)		R-value		Tab. Mass (mg)		Tab. Thick. (mm)		Density (gcm^{-3})	
mean	sd	mean	sd	mean	sd	mean	sd	mean	sd	mean	sd
3.3	0.1	0.37	0.02	0.597	0.019	151.9	0.3	2.962	0.006	1.020	0.002
6.1	0.1	0.41	0.02	0.720	0.006	151.7	0.4	2.920	0.009	1.034	0.002
9.1	0.1	0.43	0.02	0.802	0.007	151.6	0.3	2.906	0.005	1.038	0.002
11.7	0.1	0.47	0.03	0.861	0.006	151.5	0.3	2.904	0.003	1.038	0.003
15.1	0.1	0.52	0.02	0.850	0.004	151.4	0.3	2.900	0.006	1.039	0.002
18.3	0.1	0.59	0.03	0.866	0.003	151.1	0.3	2.890	0.006	1.040	0.001

Where:-

Com. For. = Compaction Force

Time = Total Compression Time

Tab. Thick. = Tablet Thickness

Density = Tablet Relative Density

sd = standard deviation

NB:- for details CE5/B1/Prop formulation see tables 2.1 (a) and 2.2

Compact tensile strength was found to increase with the compacting load to a limiting value/plateau (figure 3.13). Compacts made at approximately 9 kN - 15 kN had constant maximum tensile strength ($F_{cal} = 1.05$, $F_{tab} \approx 3.23$, $p = 0.05$) plus constant maximum relative density (table 3.6). This probably implied constant tablet porosity at these forces. Therefore the minimum force required to achieve maximum tensile strength was approximately 9 kN. Compacts made at approximately 6 kN and below had significantly lower tensile strength values than those made at approximately 9 kN and above ($t_{cal} \geq 2.60$, $t_{tab} = 2.05$, $p = 0.05$).

The above results were ***mirrored*** by the effect of compaction force on release-sustaining characteristics of CE5/B1/Prop matrices, summarised in figure 3.14. Tablets made at approximately 9 kN to 18 kN had the same maximum release - sustaining characteristics ($F_{cal} = 0.6$, $F_{tab} \approx 2.76$), confirming constant minimum matrix porosity at these compaction forces, thus the minimum force required to produce the maximum release - sustaining characteristics was also approximately 9 kN. Tablets made at approximately 6 kN and below had significantly inferior release - sustaining characteristics to those made at approximately 9 kN and above ($t_{cal} \geq 2.36$).

Besides the magnitude of the compacting load, the duration and rate of application of a compacting load are also important in the final strength of a compact. [3] The application of force to a material imparts work to that material. The amount of work is a function of the distance the upper punch penetrates

into the die and power is a function of time over which the load is applied. The greater the area under the force versus distance curve the greater the work done. The work done is also a function of the magnitude of the compacting load. Due to manual operation of the tablet machine it was impossible to obtain constant compaction times at the different compaction forces (see table 3.6).

The rate of application of the load influences the material's reaction to the load while being compacted. During a compaction cycle, when the particles are confined and exhibiting their characteristic flow properties, the rate of application of the load is a major factor in determining compact strength. [3] Generally, for ductile materials such as HVOs, slowing the press speed and increasing dwell/contact time favours more time-dependent deformation, producing stronger tablets than high press speed. [5]

However, as compaction force increased, it was noted that there was an increase in CE5/B1/Prop adhesion to tablet tooling. This was so, even though the tablet-die wall contact area decreased (tablet thickness = 2.962 mm at approximately 3.3 kN and tablet thickness = 2.890 mm at approximately 18.3 kN, t_{cal} = 32.86). This was attributed to an increased reaction at the lower punch. [30] Also the fraction of the upper punch force transmitted to the lower punch increased with an increase in compaction force (R - value = 0.597 at approximately 3.3 kN and R - value = 0.866 at approximately 18.3 kN), thereby enhancing formulation adherence to tablet tooling surface.

3.5.5 Scanning Electron Photomicrography of Tablet Surfaces

In this section, scanning electron photomicrography was carried out (as described in section 2.3.13) on CE5 (table 2.1 (a)) fractionated plus propranolol hydrochloride (ratio 110:40 respectively) tablet surfaces and on CE5/B1/Prop (table 2.1 (a) and 2.2) tablet surfaces before and after dissolution. Tablets made from the fractionated formulations (i.e. various particle sizes of CE5), were made at approximately 12 kN, while those from CE5/B1/Prop were made at approximately 3 - 12 kN. The study was more of qualitative analysis rather than quantitative analysis. The aim was to visualise the surfaces of the compacts pre and post - dissolution so as to ***qualitatively*** assess the differences in terms of release - sustaining characteristics versus particle diameter and compaction force. Lockwood [96] used mercury porosimetry and helium diffusion through leached HVO matrices, to quantitatively determine the nature of the pore structure within the matrices. He found out that a wide pore size distribution existed within the HVO matrices.

In this study, single surfaces of tablets from different batches were examined at x15 and x35 magnification. Four different fields from each tablet surface were examined for regularity and reproducibility. If these were all considered regular and representative of each other qualitatively, then one field was photographed twice to provide the record. The scanning electron photomicrography results are shown in figures 3.15 - 3.17. Figure 3.15 depicts photographs of CE5/Prop matrices made from:- (a) < 180 μm, (b) 250-355 μm and (c) 500-710 μm size

Figure 3.15:- Scanning Electron Photomicrography of Tablets Made from Different Fractions of CE5/Prop, at approximately 12 kN, Imaged *Before* Dissolution

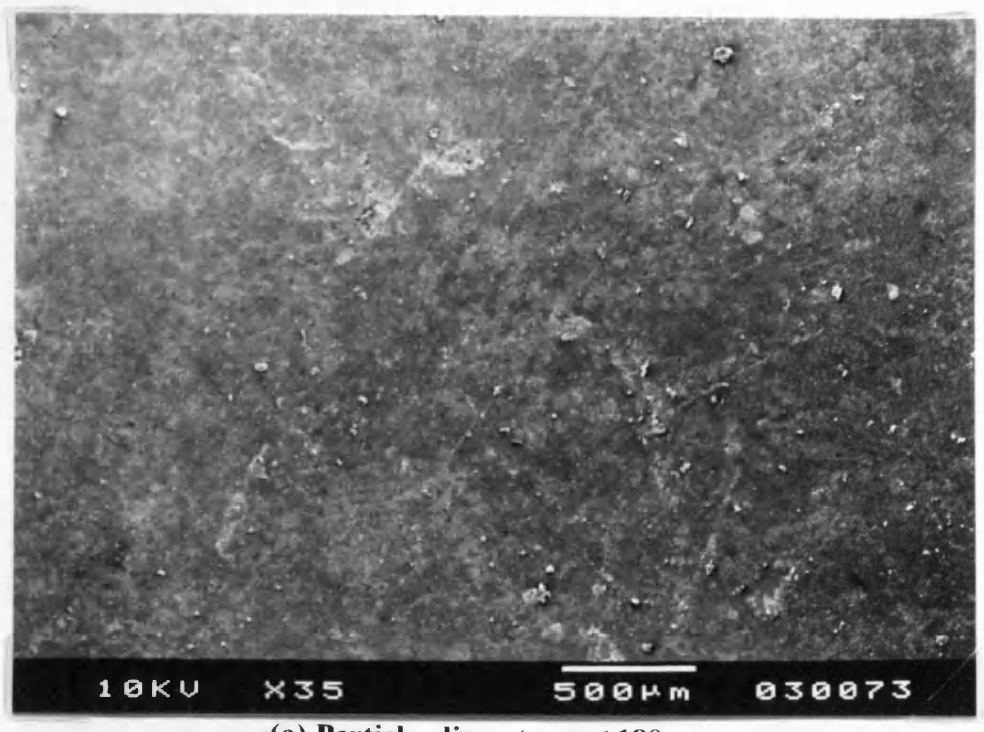

(a) Particle diameter = < 180 µm

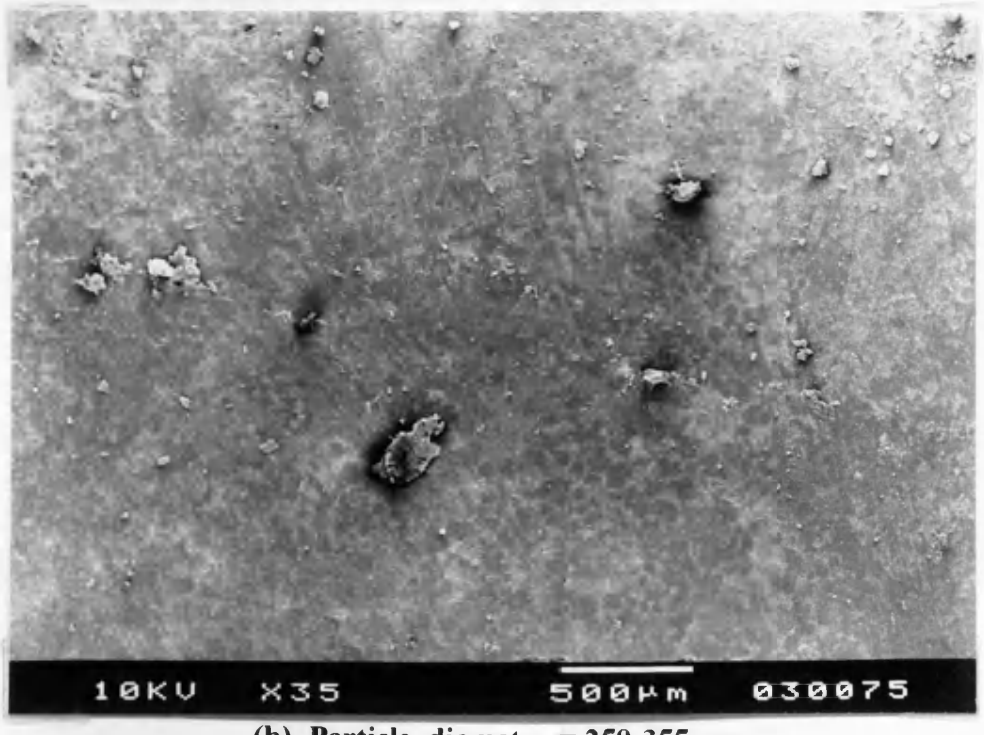

(b) Particle diameter = 250-355 µm

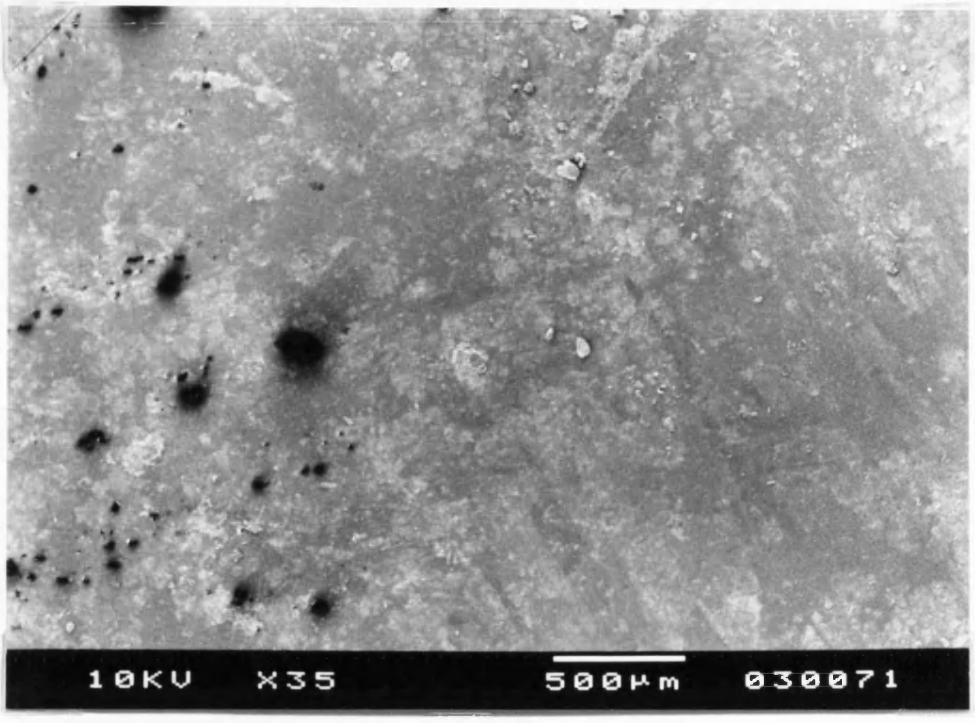

(c) Particle diameter = 500-710 µm

NB:- Compaction force ≈ 12 kN

Figure 3.16:- Scanning Electron Photomicrography of Tablets Made from Different Fractions of CE5/Prop, at approximately 12 kN, Imaged *After* Dissolution

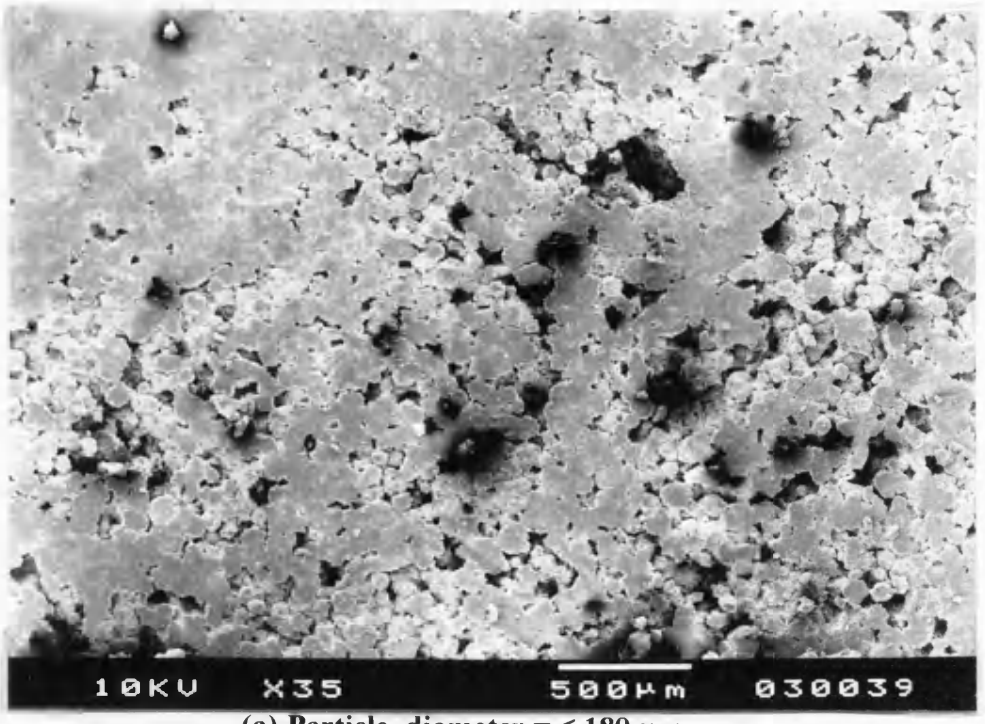

(a) Particle diameter = < 180 µm

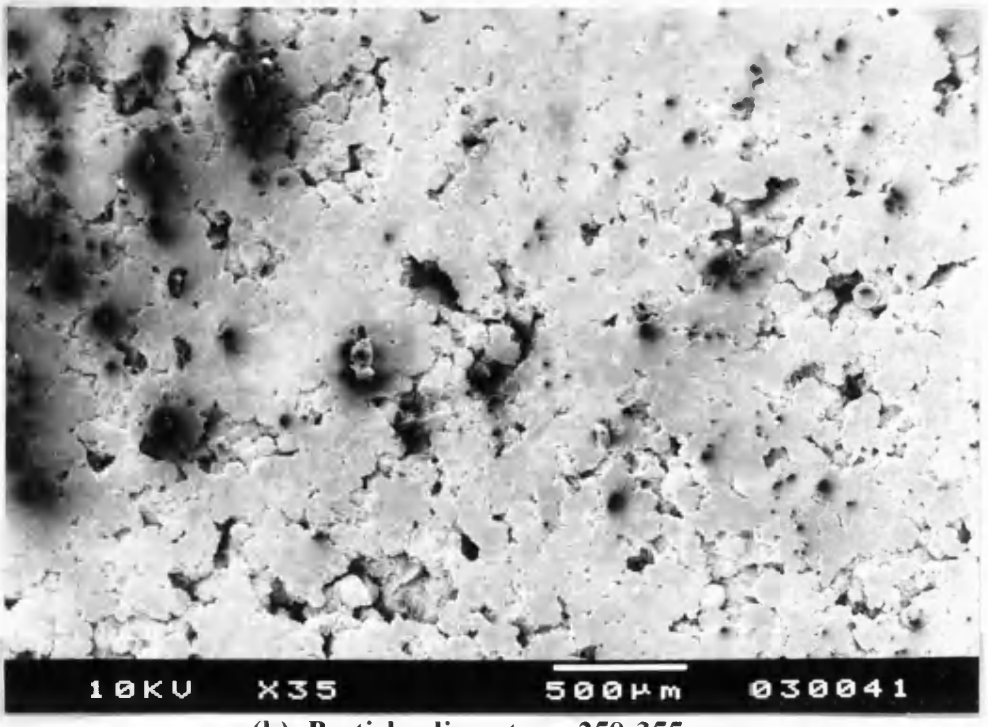

(b) Particle diameter = 250-355 µm

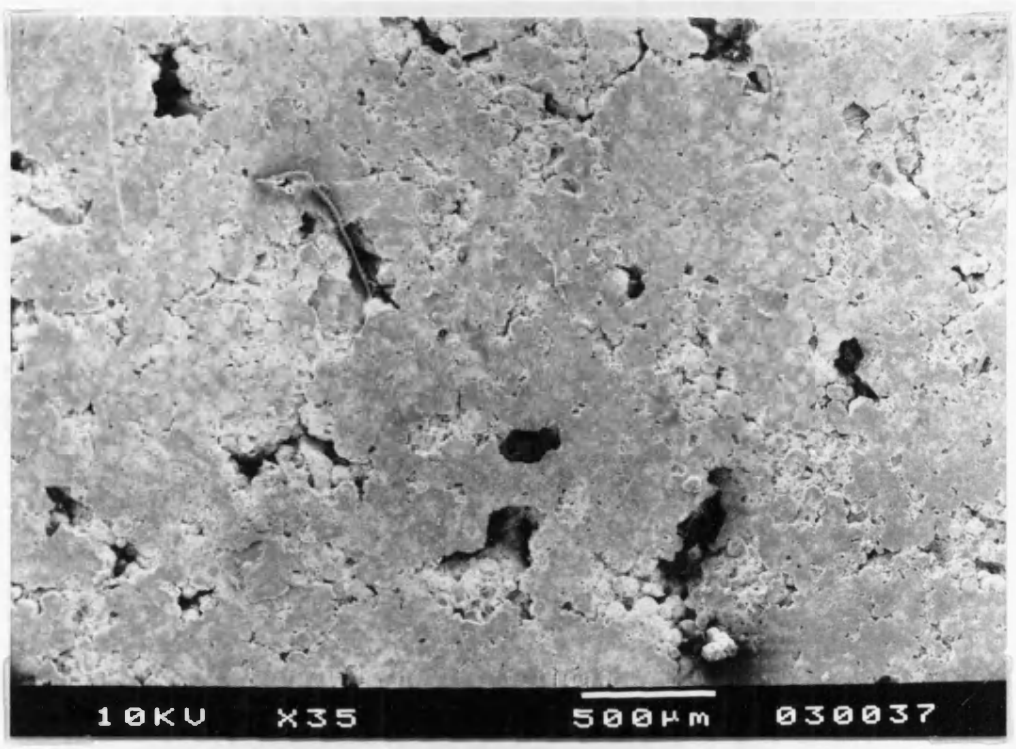

(c) Particle diameter = 500-710 µm

NB:- Compaction force ≈ 12 kN

Figure 3.17:- Scanning Electron Photomicrography of Tablets Made from CE5/B1/Prop at 3 Different Compaction Forces, Imaged *After* Dissolution

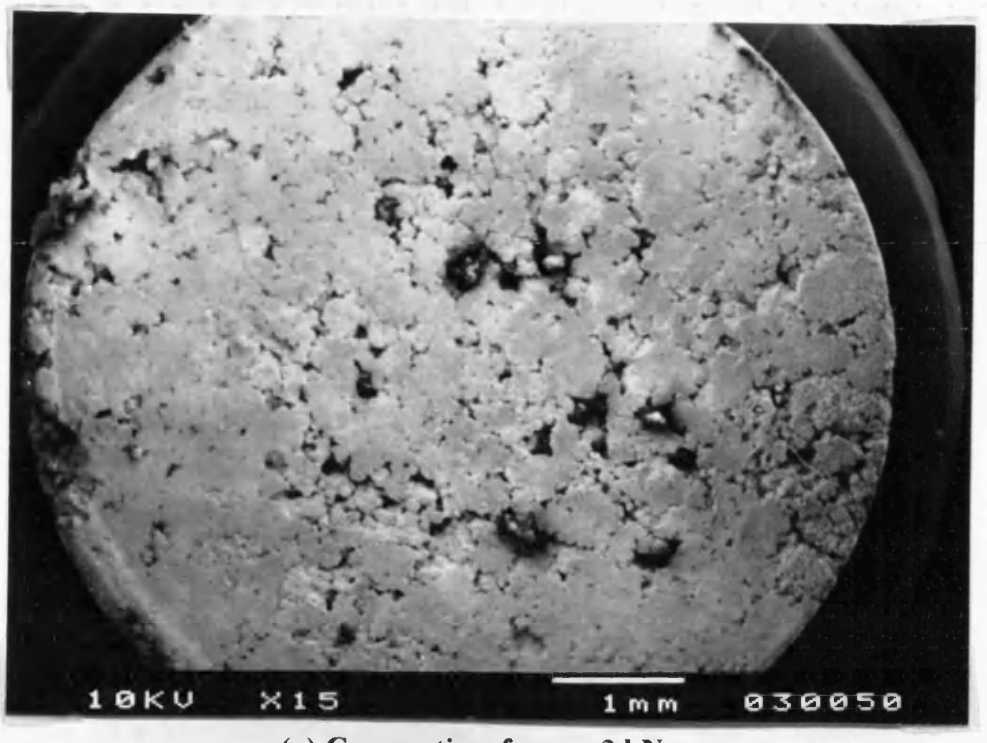

(a) Compaction force ≈ 3 kN

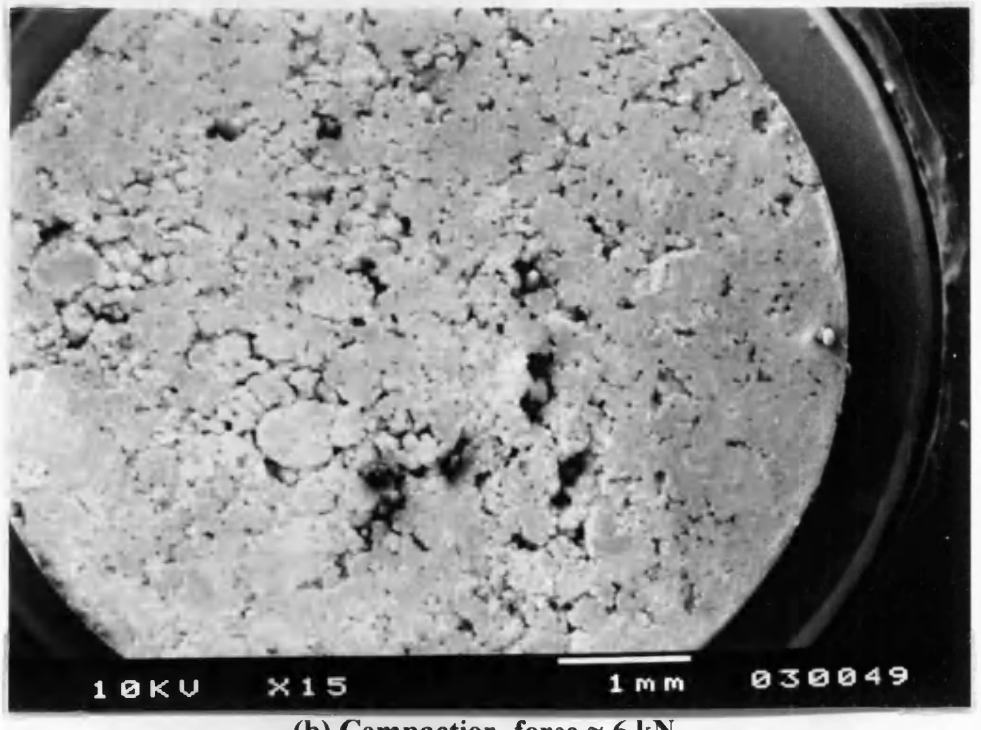

(b) Compaction force ≈ 6 kN

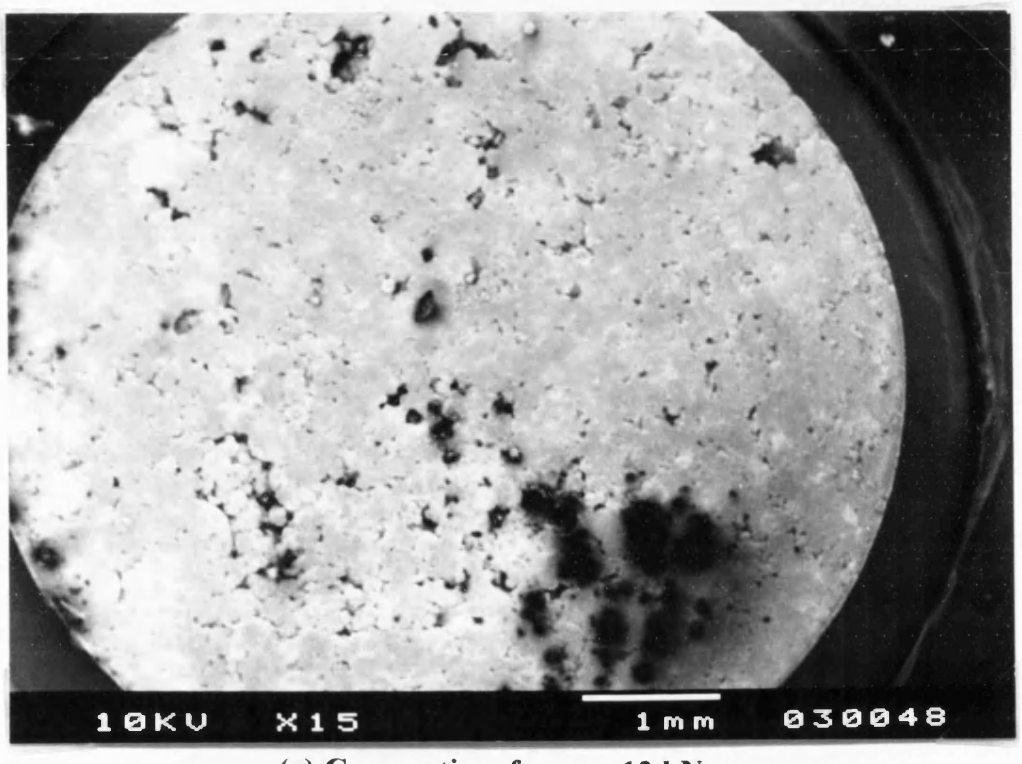

(c) Compaction force ≈ 12 kN

fractions, plus drug (propranolol hydrochloride), before dissolution. Figure 3.16 shows photographs of CE5/Prop matrices made from the above size fractions plus drug, after dissolution. Figure 3.17 depicts photographs of CE5/B1/Prop matrices made at:- (a) ≈ 3 kN, (b) ≈ 6 kN and (c) ≈ 12 kN, after dissolution.

The scanning electron photomicrography results in figure 3.15 seemed to confirm the fact that processed HVO partially softened and/or melted on compaction and fused on decompaction to form solid compacts. The tablet surfaces made from the three different particle diameters ranges:- (a) < 180 μm, (b) 250-355 μm and (c) 500-710 μm; plus drug (ratio = 110 : 40 respectively), before dissolution hardly show any particle structure.

As particle size increased the number of pores seemed to decrease in figure 3.16 (compare (a) <180 μm and (c) 500-710 μm). This partly confirmed the theory that large particles partially melted and fused to a greater extent than small ones. These results seem to tie in with those in figure 3.12, which show better release - sustaining properties with tablets containing large particles (500-710 μm) than with those containing particles less than 500 μm in diameter ($t_{cal} \geq 5.68$).

Compacts of CE5/B1/Prop made at the two lower compaction forces (approximately 3 and 6 kN) did not seem to look different from each other (figure 3.17). However, the tablet made at approximately 12 kN appeared to

have less pores than those made at the two lower forces. These results seem to tie in with those shown in figure 3.14, which depict significantly better release - sustaining characteristics at approximately 9 - 18 kN than at approximately 3 - 6 kN ($t_{cal} \geq 2.36$).

3.6 Reduction of Adhesion of Processed HVO to Tablet Tooling

In this section, adhesion of lubricated and unlubricated CE11/B1/Theo (tables 2.1 (a) and 2.2) to the upper punch face was evaluated. CE11 was prepared as described in section 2.3.1.1. The anti-adherents used were magnesium stearate, stearic acid, leucine and Compritol. Anti-adherent addition to CE11/B1/Theo was done as described in section 2.3.6. Evaluation of formulation adhesion to the upper punch face was done as described in section 2.3.7.4.

The effect of the different anti-adherents at two different concentrations (1 % and 5 %) on CE11/B1/Theo's adhesion to the upper punch face is summarised in figure 3.18, while the effect of the anti-adherents on the tensile strength of compacts made from CE11/B1/Theo at approximately 12 kN is summarised in table 3.7. The tensile strengths of tablets made from CE11/B1 and CE11/B1/Prop at approximately 12 kN are also shown in table 3.7. The data on tensile strength was subjected to Student t - tests and results analysed at the 5 % significance level.

With all the anti-adherents used except magnesium stearate, adhesion was found to gradually increase with time (figure 3.18). Magnesium stearate was an

Figure 3.18:- Effect of Type and Concentration of Anti-adherent on Adhesion of CE11/B1/Theo to the Upper Punch Face

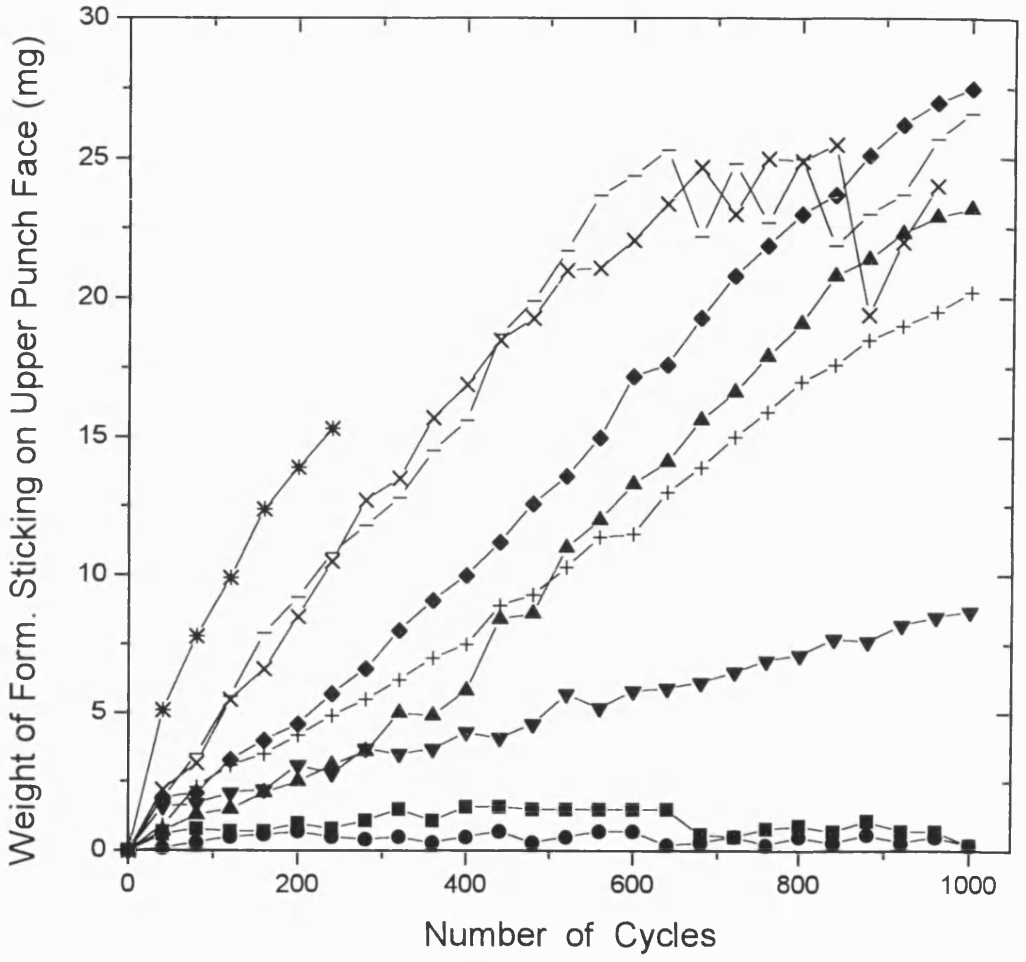

Key:-

- Mg Stearate 1%
- Mg Stearate 5%
- Leucine 1%
- Leucine 5%
- Compitrol 1%
- Compitrol 5%
- Stearic acid 1%
- Stearic acid 5%
- No antiadherent

NB:- for details of CE11/B1/Theo formulation, see tables 2.1 (a) and 2.2

Form. = Formulation

Table 3.7:- The Effect of Type and Concentration of Anti-adherent on the Tensile Strength of Tablets Made from CE11/B1/Theo at approximately 12 kN

Anti-adherent added	Formulation	Tensile Strength (MNm^{-2}) mean	sd
None	CE11/B1	0.964	0.066
None	CE11/B1/Prop	1.267	0.073
None	CE11/B1/Theo	1.370	0.084
Mg Stearate 1 %	CE11/B1/Theo	1.277	0.053
Leucine 1 %	CE11/B1/Theo	1.330	0.050
Leucine 5 %	CE11/B1/Theo	1.310	0.057
Compritol 1 %	CE11/B1/Theo	1.353	0.063
Compritol 5 %	CE11/B1/Theo	1.455	0.070
Stearic acid 1 %	CE11/B1/Theo	1.378	0.078
Stearic acid 5 %	CE11/B1/Theo	1.543	0.070

NB:- for details of CE11/B1, CE11/B1/Prop and CE11/B1/Theo formulations, see tables 2.1 (a) and 2.2

(n = 15)

effective anti-adherent for CE11/B1/Theo at both concentrations (1 % and 5 %). After 700 cycles there was negligible difference in anti-adherent activity between 1 % magnesium stearate and 5 % magnesium stearate. There was, however, marked capping in tablets containing 5 % magnesium stearate such that no tensile strength measurements were performed on these tablets. The 1 % magnesium stearate tablets' adhesion to tablet tooling was negligible but their loss in tensile strength was significant (t_{cal} = 3.64, t_{tab} = 2.05, p = 0.05) (compared to CE11/B1/Theo tablets without anti-adherent). Magnesium stearate and stearic acid have the same basic carbon chain, C_{18}, with the former having a higher melting point (approximately 88.5° C) [116] than the latter (51- 69°). [109, 111] This probably accounts for the different anti-adherent properties of the two materials.

Compritol at both concentrations reduced adhesion to tablet tooling. However, tablets containing 5 % Compritol showed minor capping during the cycle run. 1 % Compritol and 1 % stearic acid did not significantly alter the tensile strength of CE11/B1/Theo compacts (t_{cal} = 0.63 and 0.27 respectively) (compared to CE11/B1/Theo without anti-adherent). However, both lubricants at 5 % concentration, significantly improved tensile strength (t_{cal} = 6.12 for stearic acid and t_{cal} = 3.02 for Compritol), with stearic acid having a significantly more marked effect than Compritol (t_{cal} = 3.44). This was attributed to the lower melting point of stearic acid (51-69°) [109, 111] than that of Compritol (67-72° C). [109] Due to their relatively low melting points, Compritol and stearic acid probably partially melt upon compression just as the HVO does, and on

decompression they fuse (cold welding effect). This, possibly, helps in the formation of strong and/or more bonds/solid bridges. Even though 5 % stearic acid had deleterious effects by enhancing CE11/B1/Theo adhesion to tablet tooling, due to the fact that it had a more significant positive effect on tensile strength than 5 % Compritol, it was included in future CE formulations, so as to function as an "auxiliary" binder to the PVP.

There was hardly any difference between the adhesion of CE11/B1/Theo containing 1 % stearic acid and CE11/B1/Theo without anti-adherent (figure 3.18). CE11/B1/Theo containing 5 % stearic acid had very poor flowability properties and this is the reason why only 240 cycles were run with this formulation. Generally, as glidant concentration increases in a formulation, flowability improves up to a certain point, thereafter it is impeded. [17] Therefore this could be responsible for the poor flowability properties of this formulation.

Up to approximately 500 cycles, 1 % leucine had better anti-adherent effect than 5 % Compritol (figure 3.18). The former at 1 % concentration had no negative effect on the tensile strength of CE11/B1/Theo compacts (t_{cal} = 1.59), (compared to CE11/B1/Theo without anti-adherent), but, 5 % leucine had a significant negative effect on tensile strength (t_{cal} = 2.28). Despite this, 5 % leucine had superior anti-adherent properties than all the other anti-adherents, except magnesium stearate. However, 1 % magnesium stearate had a greater negative effect on the tensile strength of CE11/B1/Theo compacts (t_{cal} = 3.64) than 5 % leucine (t_{cal} = 2.28), therefore leucine was selected over magnesium

stearate for use in the final optimum formulation to function as an anti-adherent.

Theophylline (CE11/B1/Theo tablets without anti-adherent) imparted significantly better tensile strength properties to the HVO matrix than propranolol hydrochloride (CE11/B1/Prop tablets without anti-adherent) (t_{cal} = 3.57). However, both formulations produced tablets with higher tensile strength values than those produced from CE11/B1.

Lubricants generally interfere with particle bonding by forming a lubricant film around the particle during blending. [15] Fragmenting particles like lactose, are less sensitive or even insensitive to lubricants as compared to plastically deforming solids such as HVO, sodium chloride and starch. This is due to the creation of clean surfaces free of lubricant during fragmentation of the former. [5] The anti-adherents used in order of increasing anti-adherent activity are as follows:-

stearic acid < Compritol < leucine < magnesium stearate.

Therefore the beneficial effects of processed HVO include:- (i) significantly improved tablet tensile strength, (ii) improved release - sustaining characteristics, (iii) improved anti-adhesion properties, (iv) compaction force independent drug release and release - sustaining characteristics after approximately 9 kN and (v) compaction force independent tablet tensile strength after approximately 9 kN.

CHAPTER 4

MODIFICATION OF THE MECHANISM OF DRUG RELEASE FROM PROCESSED HVO MATRICES

4.1 OBJECTIVES

In this part of the study, the main objective was to alter the release profile of processed HVO tablets from the predominantly Higuchi type drug release (square root of time depended drug release) to zero order or still more desirably, to an increase in drug release rate with time. Drug release was evaluated in terms of the data fit to the above mechanisms, as well as first order and diffusion-relaxation models. The overall objective was to formulate a per-oral controlled release tablet system capable of releasing all the drug within 12 hours in the proximal colon.

All the dissolution tests were carried out as described in section 2.3.12. As in chapter 3, the error bars on all the figures in this chapter are standard errors of mean, while the ± values quoted in the text and the tables are standard deviations.

4.2 Enhancement of Drug Release from Processed HVO Matrices

Although processed HVO matrices fulfil the "protracted" drug release aspect of controlled release, the release rate is probably not high enough for the maintenance of therapeutic blood levels. This is especially important where the target site is the proximal colon where drug absorption is reduced due to consolidation of faecal matter and poor absorption capability by colonic epithelium. [66] Therefore this section was aimed at increasing the release rate of processed HVO tablets with time as a means of compensating for the factors mentioned above.

Three hydrophilic materials, Junlon, Avicel and Starch 1500; were each incorporated into composite excipient formulations at 5 % concentration as described in section 2.3.1.2.1 to produce CE16 - CE18 (see table 2.1 (c)). Tablets made from CE16/B1/Prop - CE18/B1/Prop (see also table 2.2) at approximately 12 kN were subjected to dissolution testing. The resulting release data up to approximately 60 % was analysed according to the Higuchi model and first order mechanism. For the Higuchi mechanism, cumulative drug release was plotted against the square root of time. For first order release, $\log_{10}$ (*amount of propranolol hydrochloride remaining in the matrix*), was plotted against time. Linear regression analysis (with the aid of a microcomputer software programme, ***Microcal Origin***) was carried out on the resulting plots for each individual tablet.

Linear regression analysis data for each tablet is shown in appendix 1, tables A9 and A10. The *in vitro* propranolol hydrochloride release kinetics from tablets of the above formulations is summarised in table 4.1, while their release profiles are shown in figure 4.1.

The hydrophilic materials tested can be arranged with respect to their effect on enhancing propranolol hydrochloride release in the following order:- Avicel < Starch < Junlon (figure 4.1). The *in vitro* release kinetics revealed that drug release fitted square-root of time kinetics better than first order mechanism especially with CE18/B1/Prop tablets which contained Junlon. However, with CE17/B1/Prop and CE16/B1/Prop tablets, which contained Starch 1500 and Avicel respectively, first order mechanism seemed to fit the drug release data equally well. All the matrices made from the three formulations (CE16/B1/Prop-CE18/B1/Prop) gradually disintegrated with time.

With CE18/B1/Prop, which contained Junlon, propranolol hydrochloride release was complete within 3 hours (figure 4.1), indicating that these tablets had the minimum release-sustaining characteristics. The superior effect of Junlon in accelerating drug release was probably due to its marked contribution to create pores in the matrix. Junlon has a high affinity for water and is soluble in water. [129] It is a polymer of acrylic acid and therefore has got free carboxylic groups (-COOH) with the majority probably in the ionised state ($-COO^- + H^+$) in the de-aerated distilled water ($pH = 5.5 \pm 0.1$) used in the dissolution tests.

Table 4.1:- *In Vitro* Release Kinetics of Propranolol Hydrochloride from CE16/B1/Prop - CE18/B1/Prop Tablets made at approximately 12 kN (n = 6)

	CE18/B1/Prop	CE17/B1/Prop	CE16/B1/Prop
First Order:- $\log_{10}(100\ \% - Q) = kt$			
Slope (hr^{-1})	-0.51959 ± 0.12989	-0.18927 ± 0.02482	-0.15935 ± 0.02245
Intercept	2.0834 ± 0.0576	1.9089 ± 0.0090	1.8992 ± 0.0087
r	0.99370 ± 0.00377	0.99968 ± 0.00026	0.99960 ± 0.00041
Higuchi Mechanism:- $Q = kt^{1/2}$			
Slope ($\%hr^{-1/2}$)	84.52 ± 9.30	44.45 ± 3.22	39.79 ± 3.13
Intercept (%)	-24.05 ± 4.63	3.17 ± 1.84	5.46 ± 1.70
r	0.99936 ± 0.00078	0.99975 ± 0.00015	0.99960 ± 0.00041

NB:- for details of CE16/B1/Prop - CE18/B1/Prop formulations, see tables 2.1 (c) and 2.2

Figure 4.1:- The Effect of the Type of Hydrophilic Material on Propranolol Hydrochloride Release from CE16/B1/Prop-CE18/B1/Prop Tablets made at approximately 12 kN

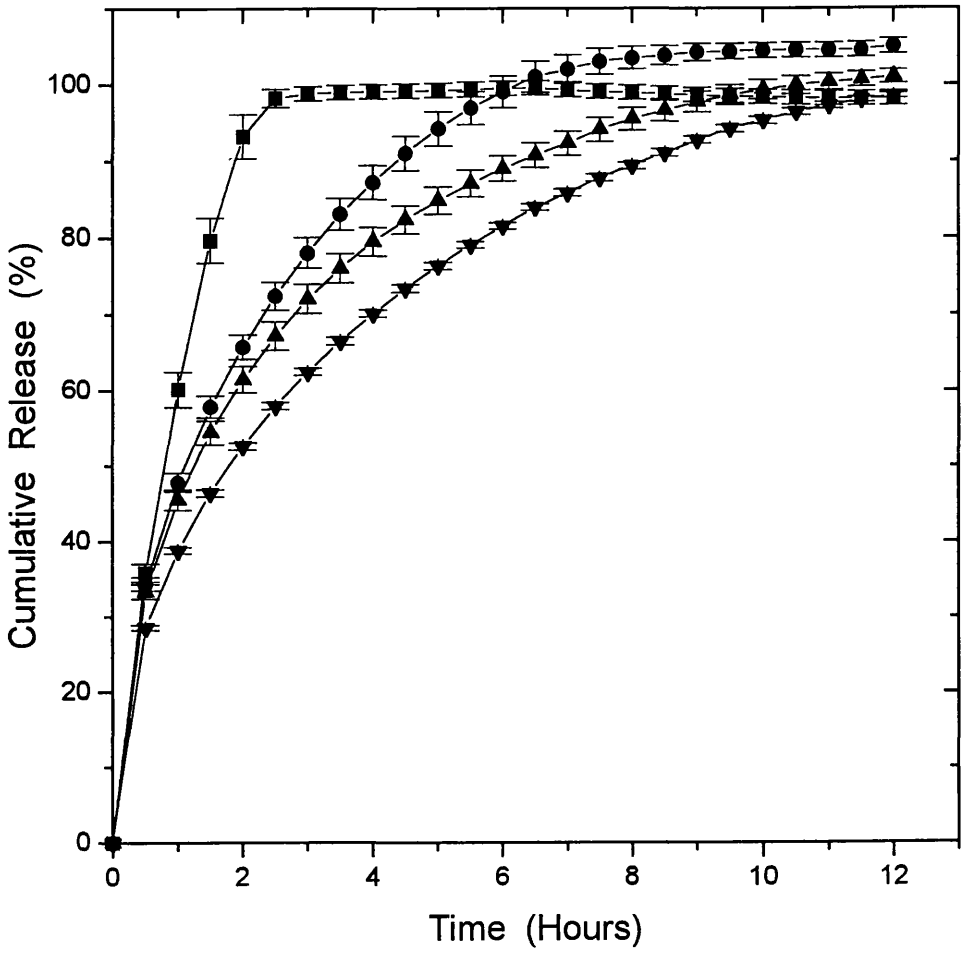

		Hydrophilic Material	Formulation
Key:-	—■—	Junlon	CE18/B1/Prop
	—●—	Starch	CE17/B1/Prop
	—▲—	Avicel	CE16/B1/Prop
	—▼—	None	CE5/B1/Prop

NB:- for details of CE5/B1/Prop, CE16/B1/Prop-CE18/B1/Prop formulations, see tables 2.1(a), 2.1 (c) and 2.2

These highly hydrophilic groups probably increased the wettability and rapid solvent penetration into the tablets, to dissolve the propranolol hydrochloride rapidly so that it would diffuse out. Therefore Junlon might have increased the porosity, ϵ, of the tablets and reduced the diffusional distance of the drug, propranolol hydrochloride, by rupturing the tablets.

Starch is a well known binder and disintegrant. Like Junlon, it is also hydrophilic and dissolves slowly in hot water. It can form a paste with cold water. It probably exerted its effect on the HVO matrix (CE17/B1/Prop) by swelling and wicking. [15] Starch is a mixture of naturally occurring high molecular weight polysaccharides, amylose and amylopectin. Amylose (straight chains) make up 20-30 % of starch grains while amylopectin (branched chains) make up 70-80 % of the grains. The starch used in this study, Starch 1500, is partially hydrolysed and probably contains more amylose than natural starch does. It is only the amylose component, which although insoluble in cold water, absorbs a large amount of water and swells. It is therefore most likely responsible for the rupture of the HVO matrix. However, the extent of swelling in starch grains and the nature of the force created is not fully accepted and understood. [15] Starch is also known to increase porosity of tablets due to its non-compressibility and low cohesiveness. Therefore water can wick into the tablet as a result of pore capillarity or sorption and dissolve the drug before allowing it to elute out. Further, the general opinion is that at high compaction forces, starch grains deform plastically, although at low compaction forces, starch grains are generally thought to deform elastically. [15] These

deformed starch grains are energy rich and swell rapidly in water, rupturing the matrix. In addition, these 3 factors (swelling, wicking, deformation) of starch grains, probably reduced tortuosity, τ, increased porosity, ϵ, of the matrices and reduced the diffusional distance for propranolol hydrochloride.

Although Avicel (MCC) is insoluble in water, it has hydroxyl groups (-OH) which render it hydrophilic. These groups probably help in wicking water into the CE16/B1/Prop tablets which dissolves and elutes out the propranolol hydrochloride. The matrix gradually disintegrated with time due to the hydrophilicity of the Avicel. The Avicel probably enhanced matrix wettability and reduced the diffusional distance which improved propranolol hydrochloride release.

4.3 Alteration of Mechanism of Drug Release from Processed HVO Matrices

As indicated in chapter 2, oral controlled release formulations targeted to the proximal colon, preferably, ought to have an increasing release rate with time so as to counteract the consolidation of faecal matter as the drug delivery system moves up the colon. [66] Therefore this section was aimed at altering the predominately Higuchi model release mechanism of processed HVO matrices to at least zero order or more preferably to an increasing release rate with time. Total drug release was targeted to be complete within 12 hours as this is approximately the total proximal colon transit time. [66]

4.3.1 Effect of Biological Enzymes on Propranolol Hydrochloride Release from Processed HVO Matrices

Lipase and esterase were used at pH 7.00 to try and degrade the processed HVO within 12 hours. Tablets were made from CE5/B1/Prop (tables 2.1 (a) and 2.2) at approximately 12 kN. CE5 was prepared as described in section 2.3.1.1. An excess of enzyme was added to each dissolution vessel (lipase = 75 units; esterase = 171 units; per dissolution vessel). The results are shown in figure 4.2.

There was no significant difference between the release profile without enzyme and the ones with enzymes. Since the vegetable oil is hydrogenated it probably ceased to be a natural enzyme substrate. This, coupled with the fact that enzymatic activity is at molecular level with effects hardly recognisable after 12 hours, is probably sufficient to account for the insignificant alteration in drug release. Most enzymatic activities on bioerodible polymers and materials become manifest after a couple of weeks or even months. [42]

Figure 4.2:- The Effect of Biological Enzymes on Propranolol Hydrochloride Release from CE5/B1/Prop Matrices made at approximately 12 kN

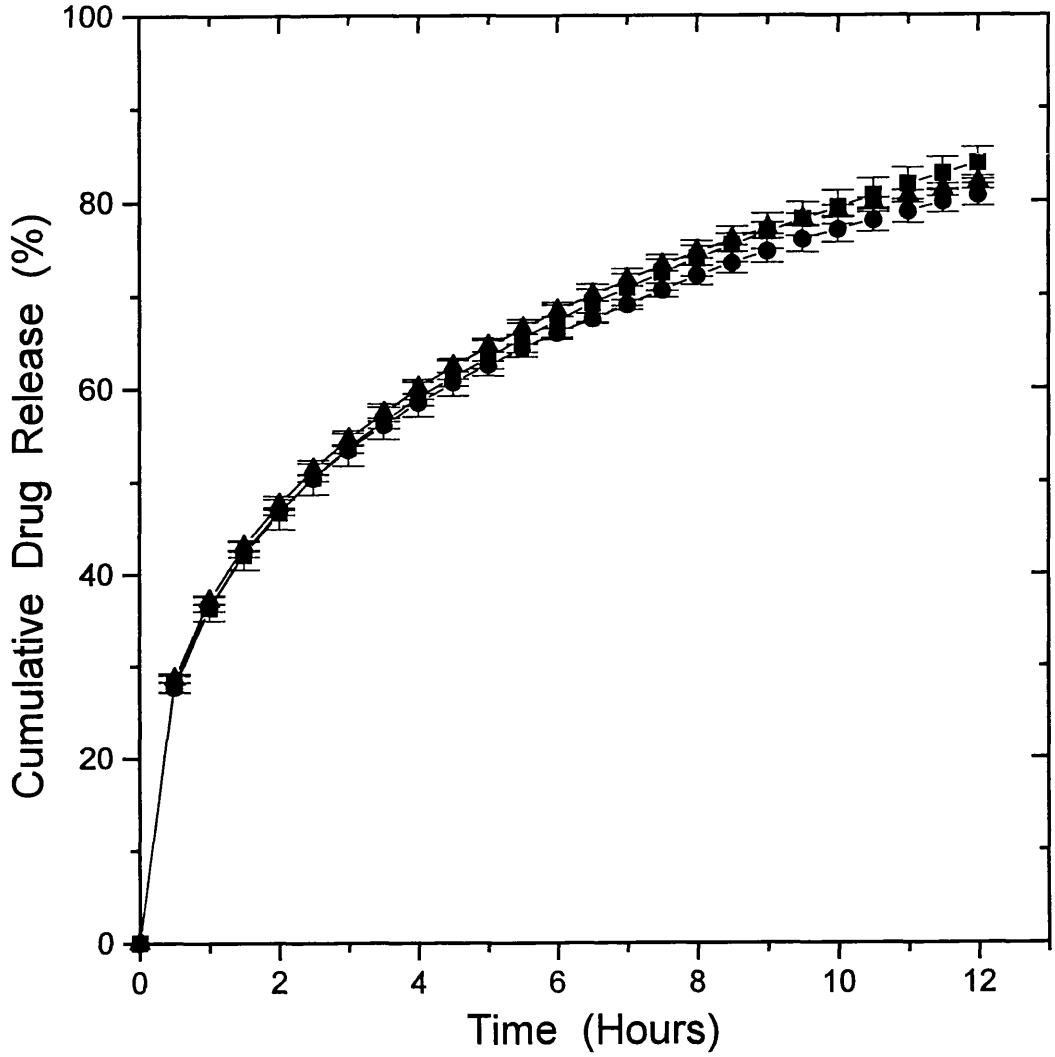

Key:-

—■— No enzyme

—●— Lipase

—▲— Esterase

NB:- for details of CE5/B1/Prop formulation, see tables 2.1 (a) and 2.2

4.3.2 Propranolol Hydrochloride Release from Tablets made from Myverol-Based Water-Free Composite Excipient Formulations

In order to assess alteration of propranolol hydrochloride release from processed HVO matrices containing Myverol, propranolol hydrochloride release from Myverol compacts without the HVO was investigated first. Since the Myverol was too soft to be processed into tablets on its own, it was adsorbed on carriers, silicas (Aerosil® 200, Sipernat® D17, Sipernat® 22 and Aerosil® R 974), as described in section 2.3.1.3, to form the following composite excipients:- CE19, CE20, CE21 and CE22 (table 2.1 (d)). Tablets were then made from the resulting formulations:- CE19/B3/Prop, CE20/B3/Prop CE21/B3/Prop and CE22/B3/Prop (see also table 2.2) at approximately 3 - 12 kN. It was difficult to make tablets at compaction forces greater than 12 kN due to excess tablet tooling adhesion and compact lamination and picking.

The formulations had very high die fill volumes, especially CE19/B3/Prop and CE22/B3/Prop which contained Aerosil 200 and Aerosil R 974 respectively, as carriers. Therefore each sample had to be manually packed into the die using a long thin spatula. Besides this, due to the low melting point of the Myverol there was an excess of tablet tooling adhesion by the formulations. Hence before and after each tablet compaction, a mixture of MCC and magnesium stearate (1:1) was compressed in order to lubricate the die and punches so as to reduce adhesion. With all precautions taken, tablets made from CE19/B3/Prop - CE22/B3/Prop formulations still were somewhat flaky especially at high compaction forces and with Aerosil 200 and Aerosil R 974 as carriers.

When Aerosil 200, Sipernat D17 and Aerosil R 974 were used as carriers (CE19/B3/Prop, CE20/B3/Prop and CE22/B3/Prop respectively), drug release was faster at high compaction forces than at low ones. This was possibly due to minute tablet lamination and picking at these high forces. Aerosil R 974 and Sipernat D17 which have been termed "hydrophobic silicas" produced formulations (CE22/B3/Prop and CE20/B3/Prop respectively), with higher release rates than those of Aerosil 200 (CE19/B3/Prop) and Sipernat 22 (CE21/B3/Prop), at all compaction forces. When Sipernat 22 was used as carrier, tablets produced were more compact and less flaky than those made from the other three carriers (Aerosil 200, Aerosil R 974 and Sipernat D17), with release from the former tablets gradually decreasing with increase in compaction force. From this study, the order of increasing hydrophilicity of the three carriers was as follows:-

Sipernat D17 < Aerosil R 974 < Sipernat 22 < Aerosil 200

Propranolol hydrochloride release rates from CE19/B3/Prop and CE21/B3/Prop tablets made at approximately 9 kN and calculated as illustrated below are shown in figure 4.3. Propranolol hydrochloride release profile of CE22/B3/Prop tablets made at approximately 9 kN is in figure 4.4, while the corresponding release rates calculated in the same manner illustrated below are shown in figure 4.5.

Figure 4.3:- Propranolol Hydrochloride Release Rate from CE19/B3/Prop and CE21/B3/Prop Tablets Made at approximately 9 kN

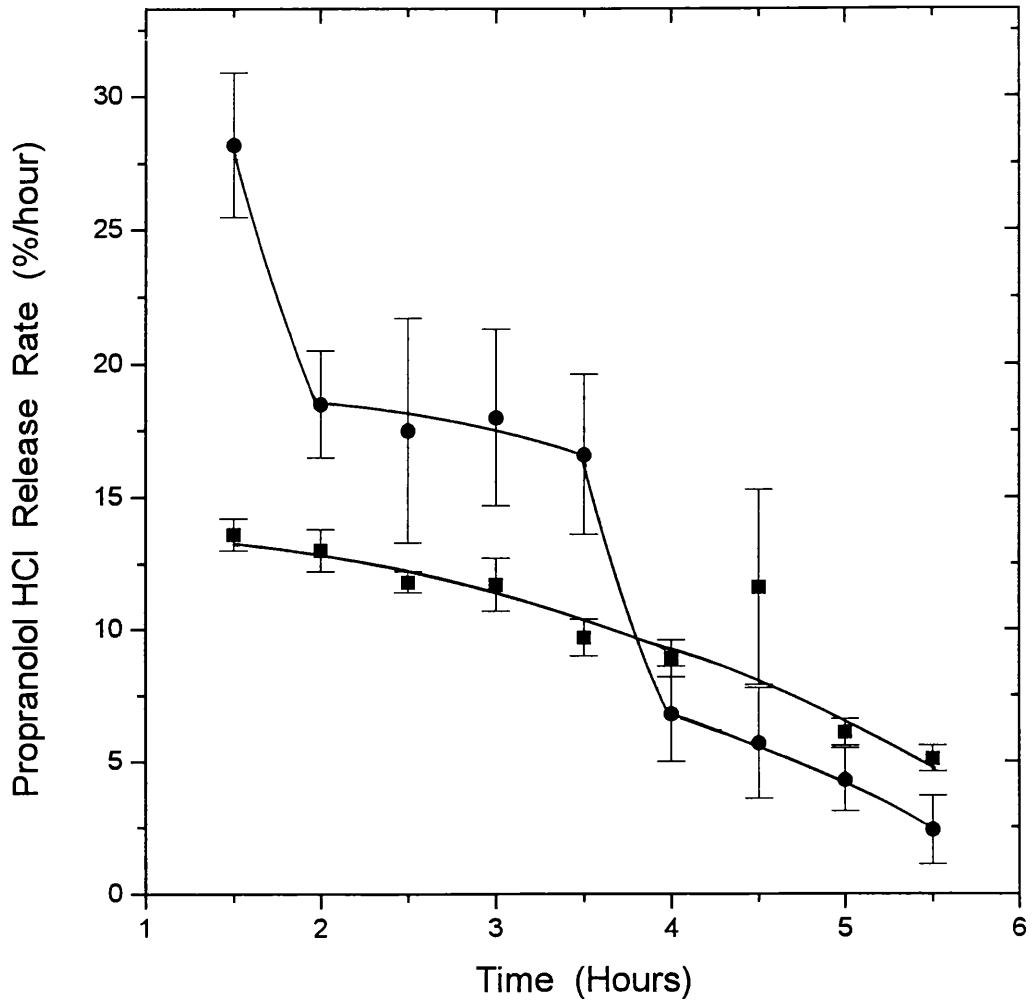

Key:- —■— CE19/B3/Prop tablets

—●— CE21/B3/Prop tablets

NB:- for details of CE19/B3/Prop and CE21/B3/Prop formulations, see tables 2.1 (d) and 2.2

Figure 4.4:- Propranolol Hydrochloride Release from CE22/B3/Prop Tablets made at approximately 9 kN

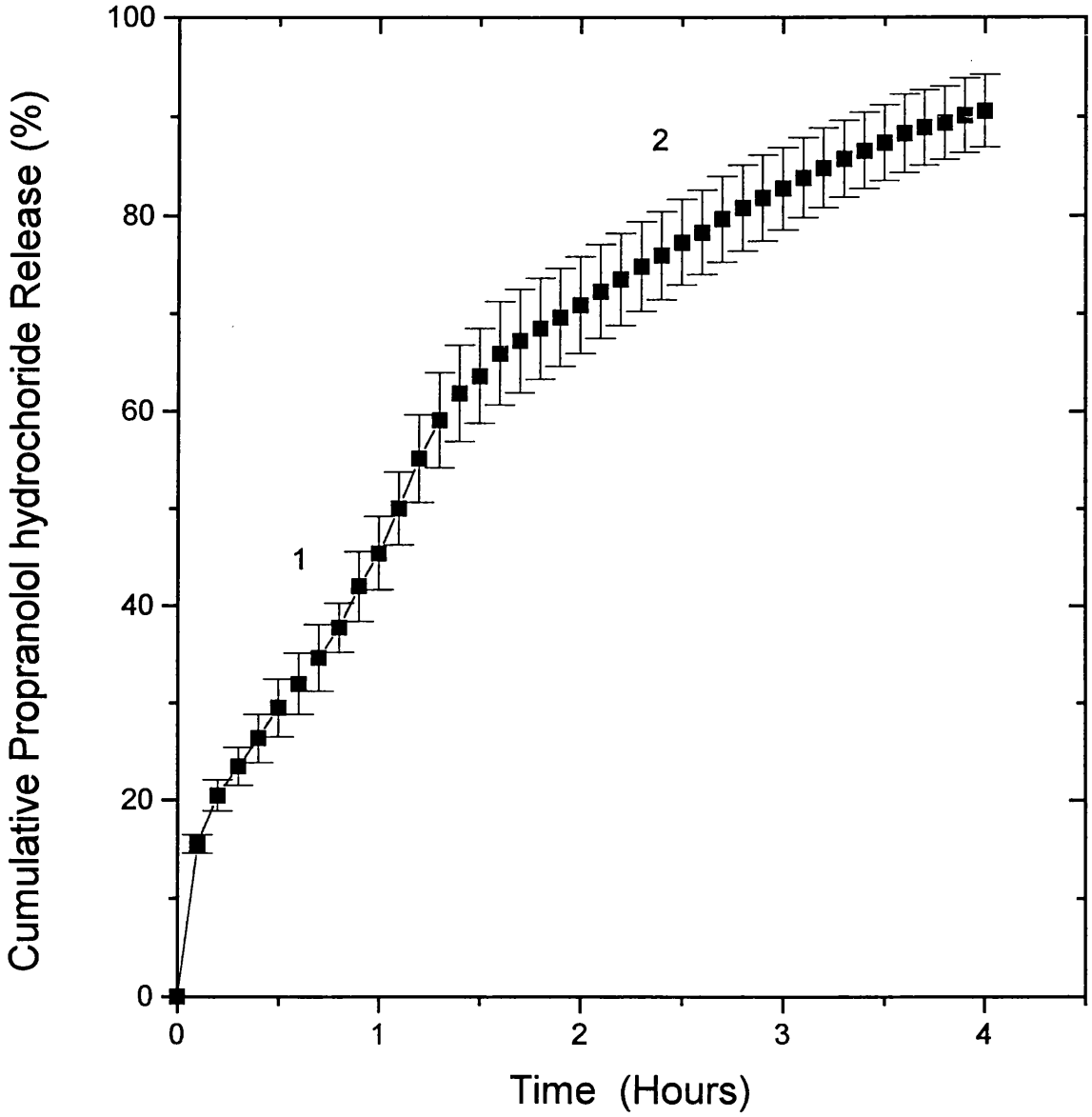

NB:- for details of CE22/B3/Prop formulation, see tables 2.1 (d) and 2.2

Figure 4.5:- Propranolol Hydrochloride Release Rate from CE22/B3/Prop Tablets made at approximately 9 kN

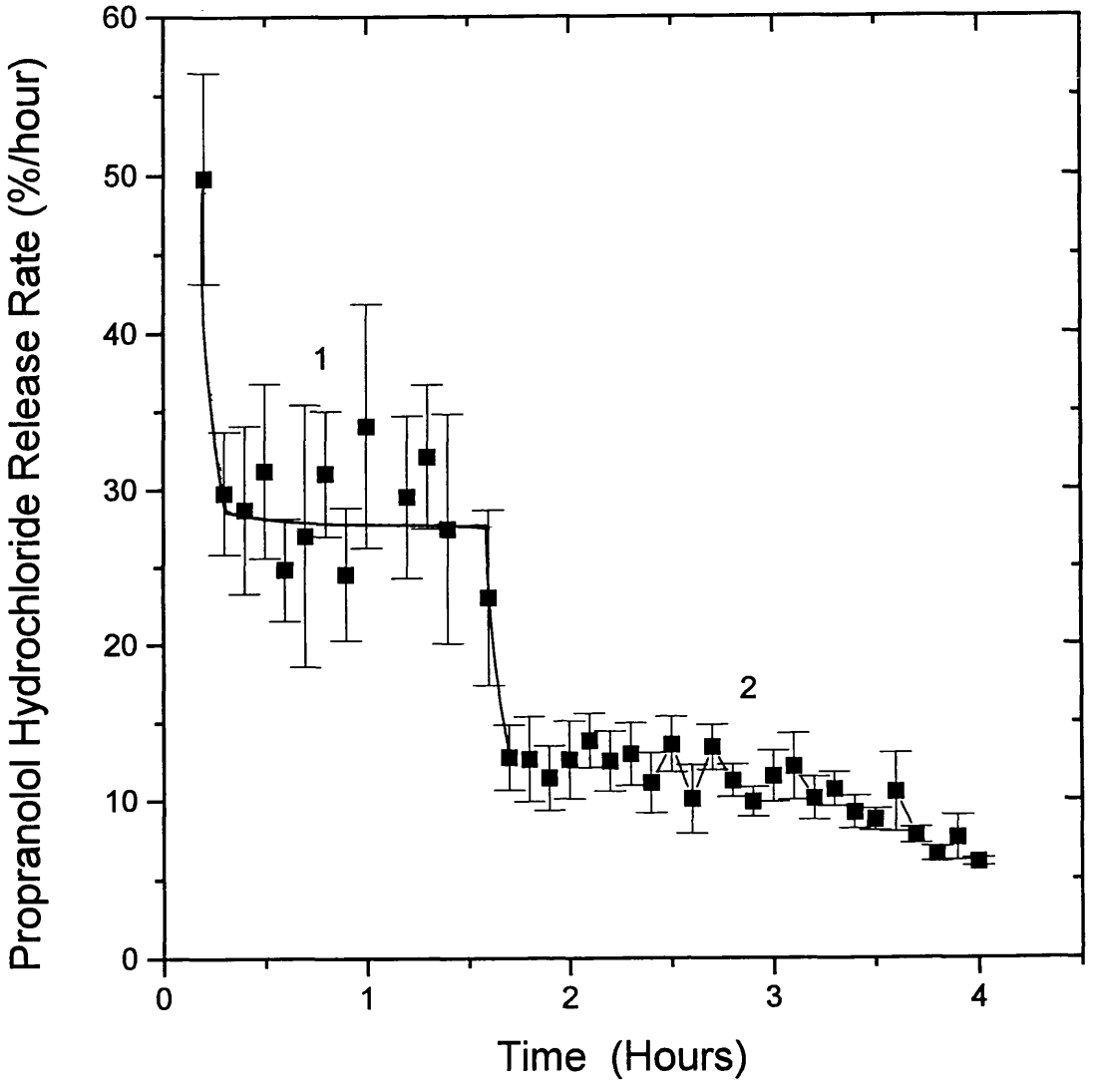

NB:- for details of CE22/B3/Prop formulation, see tables 2.1 (d) and 2.2

As an example, drug release rates from CE19/B3/Prop tablets were calculated as follows:-

Cumulative drug release (%) 0.00 25.83 34.90 41.68 48.20 54.12 ····· 98.57

Time (hours) 0.00 0.50 1.00 1.50 2.00 2.50 ····· 12.00

$\therefore$ drug release rate at $t_{0.5}$ = {(25.83-0.00)/(0.50-0.00)} %/hour = <u>51.66 %/hour</u>

What is of important significance is that CE21/B3/Prop tablets were capable of releasing propranolol hydrochloride at a constant release rate from 2.0 to 3.5 hours (1.5 hours) ($F_{cal} = 0.2$, $F_{tab} = 3.10$, $p = 0.05$). CE22/B3/Prop tablets' release profile (figure 4.4) had two distinct regions (regions 1 & 2) with different release rates. Region 1 (0.3-1.6 hours) had a higher ***constant*** ($F_{cal} = 0.30$, $F_{tab} \approx 1.98$, $p = 0.05$), release rate than region 2 (1.7-4.0 hours) ($F_{cal} = 1.58$, $F_{tab} \approx 1.63$, $p = 0.05$), as shown in figure 4.5. The initial constant release rate was possibly due to drug release from the deaggregating tablets. The second constant release rate was attributed to drug release from the deaggregated tablet particles. In this stage the Myverol was probably in the cubic phase form, hence a lower sustained release fashion. [119]

Therefore Myverol was incorporated into HVO composite excipients during processing in order to attempt to alter the drug release mechanism of processed HVO tablets (square root of time dependency) so as to achieve at least zero order drug release.

4.3.3 Determination of Optimum Myverol Concentration

Various Myverol concentrations (10 - 40 % w/w) were incorporated into HVO formulations as described in section 2.3.1.2.2, to produce CE23 - CE26 (table 2.1 (e)). Tablets were then made at approximately 12 kN from the resulting formulations:- CE23/B1/Prop, CE24/B1/Prop, CE25/B1/Prop and CE26/B1/Prop (see also table 2.2). The resulting tablets were subjected to dissolution testing. Propranolol hydrochloride release rates from the tablets are summarised in figure 4.6. These release rates were calculated in the same manner as in section 4.3.2.

As Myverol concentration increased there was a corresponding increase in tablet tooling adhesion of the formulations, hence there was need to compress MCC and magnesium stearate mixture (1:1) before and after each tablet compaction. Concentrations of Myverol greater than 40 % w/w produced composite excipients impossible to process due to stickiness.

Tablets made from CE23/B1/Prop - CE26/B1/Prop formulations gradually disintegrated with time during dissolution testing. This was probably due to the Myverol acting as a surfactant and plasticizer, weakening the matrix structure. This effectively decreased the drug diffusional distance. Figure 4.6 shows Myverol formulations' release rates relative to baseline (no Myverol) release rates. These values increased with Myverol concentration from 10-30 % (CE23/B1/Prop - CE25/B1/Prop tablets respectively). At 40 % Myverol concentration (CE26/B1/Prop tablets), release rates were lower than those of

Figure 4.6:- The Effect of Myverol Concentration on Propranolol Hydrochloride Release Rate from CE23/B1/Prop - CE26/B1/Prop Tablets Made at approximately 12 kN

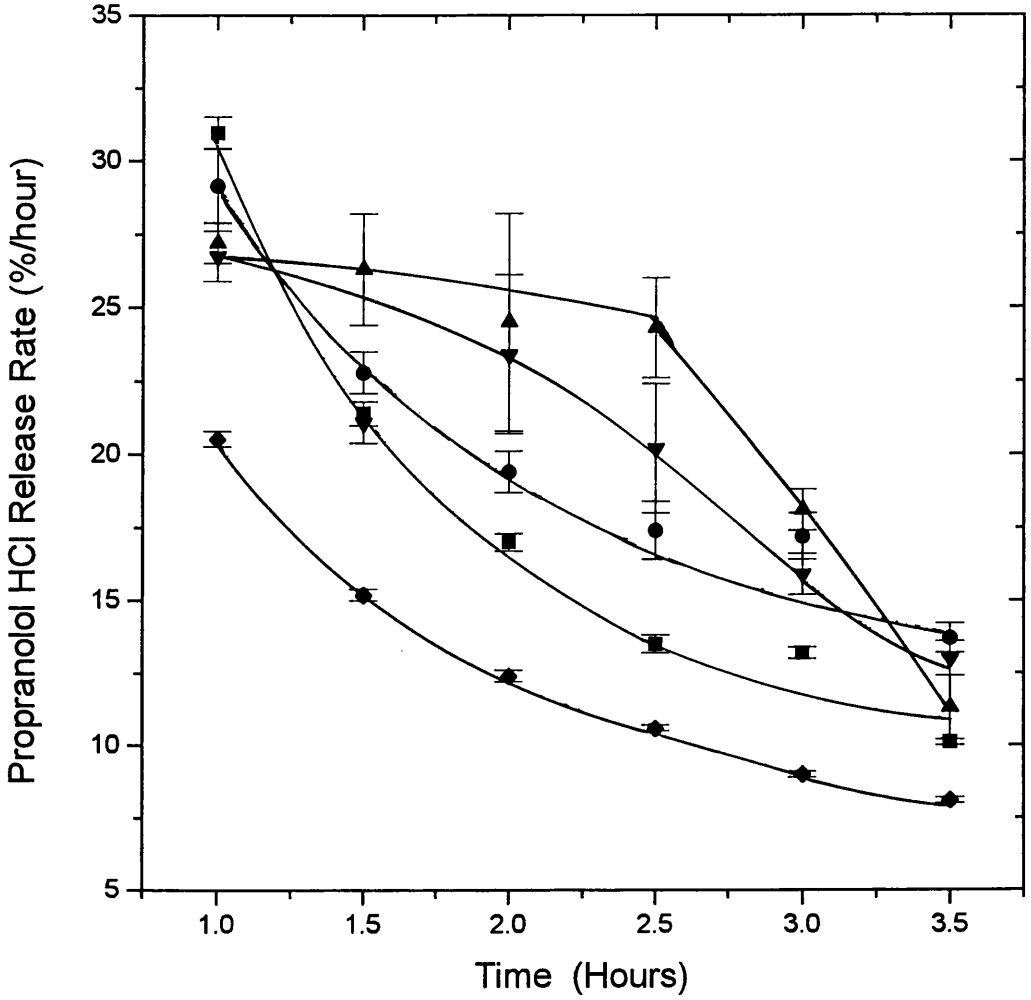

	Myverol Concentration	Formulation
Key:-	10 % w/w	CE23/B1/Prop
	20 % w/w	CE24/B1/Prop
	30 % w/w	CE25/B1/Prop
	40 % w/w	CE26/B1/Prop
	0 % w/w	CE5/B1/Prop

NB:- for details of CE5/B1/Prop, CE23/B1/Prop - CE26/B1/Prop formulations, see tables 2.1 (a) 2.1 (e) and 2.2

tablets made from CE25/B1/Prop (30 % Myverol concentration). CE25/B1/Prop tablets were found to have enhanced release rates that were constant for 1.5 hour (1.0-2.5 hours) ($F_{cal} = 0.33$, $F_{tab} = 3.10$, $p = 0.05$). Therefore CE25/B1/Prop was further investigated.

CE30/B1/Prop (tables 2.1 (e) and 2.2) tablets which contained hydrogenated rapeseed oil at an equivalent Myverol concentration (i.e. 30 % w/w) in CE25/B1/Prop, still released drug via the Higuchi mechanism, although the release rates were higher than those of CE5/B1/Prop (tables 2.1 (a) and 2.2) matrices made at the same compaction force.

4.3.4 Drug Release Properties of Tablets made from Composite Excipient 25 Formulation (30 % Myverol)

Propranolol hydrochloride release from CE25/B1/Prop (tables 2.1 (e) and 2.2) tablets (up to approximately 90 % release) made at approximately 3, 6 and 15 kN was analysed according to zero order, Higuchi mechanism and diffusion-relaxation models. Release greater than 60 % was selected because ***constant release rates*** were obtained after approximately 50-60 % release. For zero order and Higuchi plots for each individual tablet, linear regression analysis was applied. The linear regression analysis data for each tablet according to the above mechanisms is in appendix 1, tables A11 and A10 respectively. For the diffusion - relaxation model, multiple regression analysis was done on the data, with amount of drug released, Q, as the dependent variable, and time, $t^{0.46}$ and $t,^{0.92}$ (see equation 1.37 in section 1.5.1.6.2), as the independent variables.

Multiple regression analysis data on each individual tablet according to this model is in appendix 1, table A12. All linear regression analysis and multiple regression analysis were carried out with the aid of a microcomputer software, ***Microcal Origin.*** The *in vitro* release kinetics of propranolol hydrochloride from CE25/B1/Prop tablets made at approximately 3, 6 and 15 kN are shown in table 4.2.

Propranolol hydrochloride release from CE25/B1/Prop tablets made at approximately 3, 6 and 15 kN was poorly explained by the zero order model (table 4.2). The diffusion - relaxation model was a superior fit to the Higuchi mechanism in explaining drug release from CE25/B1/Prop tablets especially at 3 and 6 kN ($r = 0.99975$ and 0.99977 respectively). However, the relaxation contribution (denoted by k_2), at low compaction forces ($\approx$ 3 kN) was significantly higher than that at high compaction forces ($\approx$ 15 kN) ($t_{cal} = 3.01$, $t_{tab} = 2.26$, $p = 0.05$). Therefore low compaction forces were selected over high ones, since they enhanced the relaxation and ultimate erosion of the matrix.

Therefore, by incorporating Myverol at 30 % w/w into the HVO formulation, the predominantly diffusion controlled square root of time dependent release mechanism of the tablets was altered to a diffusion coupled with relaxation mechanism, especially at low compaction forces. All the tablets gradually disintegrated with time, possibly due to effects of Myverol. Even though Myverol is a non - dispersible non - ionic water insoluble material, it is still a

Table 4.2:- *In Vitro* Release Kinetics of Propranolol Hydrochloride from CE25/B1/Prop Matrices made at approximately 3, 6 and 15 kN (n = 6)

	≈ 3 kN	≈ 6 kN	≈ 15 kN
Zero Order:- Q = kt			
Slope (%hr^{-1})	23.30 ± 1.68	22.46 ± 1.26	22.09 ± 2.27
Intercept (%)	22.28 ± 1.73	21.59 ± 0.95	22.98 ± 2.01
r	0.99288 ± 0.00323	0.99311 ± 0.00237	0.98883 ± 0.00244
Higuchi model:- Q = kt$^{1/2}$			
Slope (%hr$^{-1/2}$)	54.09 ± 3.73	53.34 ± 5.42	54.19 ± 2.94
Intercept (%)	-5.77 ± 3.16	-5.77 ± 3.64	-7.41 ± 1.71
r	0.99852 ± 0.00088	0.99865 ± 0.00117	0.99931 ± 0.00084
Diffusion Relaxation Model:- Q = $k_1t^{0.46} + k_2t^{0.92}$			
k_1 (%hr$^{-0.46}$)	*36.57 ± 2.50	36.59 ± 7.94	48.40 ± 7.30
k_2 (%hr$^{-0.92}$)	*10.42 ± 2.90	9.91 ± 4.11	4.40 ± 3.65
Intercept (%)	*0.15 ± 0.12	-0.53 ± 3.91	-5.42 ± 2.75
r	*0.99975 ± 0.00007	0.99977 ± 0.00026	0.99951 ± 0.00063

NB:- for details of CE25/B1/Prop formulation see tables 2.1 (e) and 2.2

*** n = 5**

"surface active" substance. Its two free hydroxyl groups (-OH) on the glyceryl moiety are hydrophilic and probably helped in rapid tablet surface wetting followed by gradually relaxation and ultimate erosion of the matrix.

Release - sustaining characteristics of CE25/B1/Prop tablets could be inferred from the Higuchi constant (even though drug release from CE25/B1/Prop was best explained by the diffusion-relaxation model), or T50 (time for 50 % drug release). Release - sustaining characteristics were inversely related to the Higuchi constant and directly related to T50. T50 was the preferred method for evaluating the above properties for the same reasons mentioned in chapter 3, section 3.5.

The T50 values used in release - sustaining characteristics evaluation are shown in table 4.3. Release - sustaining characteristics of CE25/B1/Prop tablets were constant over approximately 3 - 15 kN compaction force range ($F_{cal} = 0.64$, $F_{tab} = 2.76$, $p = 0.05$). Compacts made at approximately 18 kN had significantly inferior release - sustaining characteristics in comparison to the rest of the compacts ($t_{cal} \geq 3.76$, $t_{tab} = 2.23$, $p = 0.05$). This was possibly due to tablet lamination at these high compaction forces. Therefore, CE25/B1/Prop tablets had compaction force independent release - sustaining characteristics from approximately 3 to 15 kN. In contrast, CE5/B1/Prop matrices had compaction force independent release - sustaining characteristics from approximately 9 to 18 kN (see section 3.5.4.2).

Table 4.3:- Release - Sustaining Characteristics of CE25/B1/Prop Matrices made at Different Compaction Forces

Tab.	≈ 3 kN	≈ 6 kN	≈9 kN	≈ 12 kN	≈ 15 kN	≈ 18 kN
			T50 VALUES (Hours)			
1	1.13	1.08	1.16	0.94	1.01	0.95
2	0.99	1.17	1.02	1.14	1.26	0.92
3	1.01	1.06	1.18	1.19	1.11	1.09
4	1.10	1.16	1.11	1.17	1.25	0.96
5	1.11	1.17	1.27	1.07	1.08	0.92
6	1.13	1.25	1.14	1.17	0.97	0.94
mean	1.08	1.15	1.15	1.11	1.11	0.96
sd	0.06	0.07	0.08	0.09	0.12	0.05

NB:- for details of CE25/B1/Prop formulation see tables 2.1 (e) and 2.2

Tab. = Tablet

Propranolol hydrochloride release rates from CE25/B1/Prop and CE5/B1/Prop tablets made at approximately 3 kN, from 1.0 to 3.5 hours, are shown in figure 4.7. Release rates were calculated in the same manner as in section 4.3.2. Drug release rate from CE25/B1/Prop tablets was constant from 1.50 - 3.25 hours (F_{cal} = 0.49, F_{tab} = 2.25, p = 0.05). These compacts released propranolol hydrochloride via zero order mechanism for 1.75 hours within the release profile (figure 4.7). In contrast, CE5/B1/Prop tablets' release rate decreased with time within the same time period (figure 4.7). CE25/B1/Prop tablets made at approximately 6 and 9 kN had release rate profiles ***similar*** to those of tablets made at approximately 3 kN, although the actual release rates were lower and the duration for ***constant*** release rate were smaller as well. Compacts made at compaction forces greater than 9 kN did not have constant release rates within their release profiles. Their release rates gradually decreased with time just as CE5/B1/Prop tablets' did. Therefore low compaction forces were selected since they enhanced constant release rates within the release profiles.

The effect of particle size on release - sustaining characteristics of CE25/Prop compacts made at approximately 3 kN is summarised in figure 4.8. Maximum release - sustaining characteristics were achieved at approximately 428 μm (355-500 μm) particle diameter (t_{cal} = 0.21). Probably at this particular particle diameter, CE25/Prop compacts achieved the minimum porosity. However, below 355-500 μm particle diameter, release - sustaining characteristics steadily increased with increase in particle diameter.

Figure 4.7:- Propranolol Hydrochloride Release Rate from CE25/B1/Prop and CE5/B1/Prop Tablets made at approximately 3kN

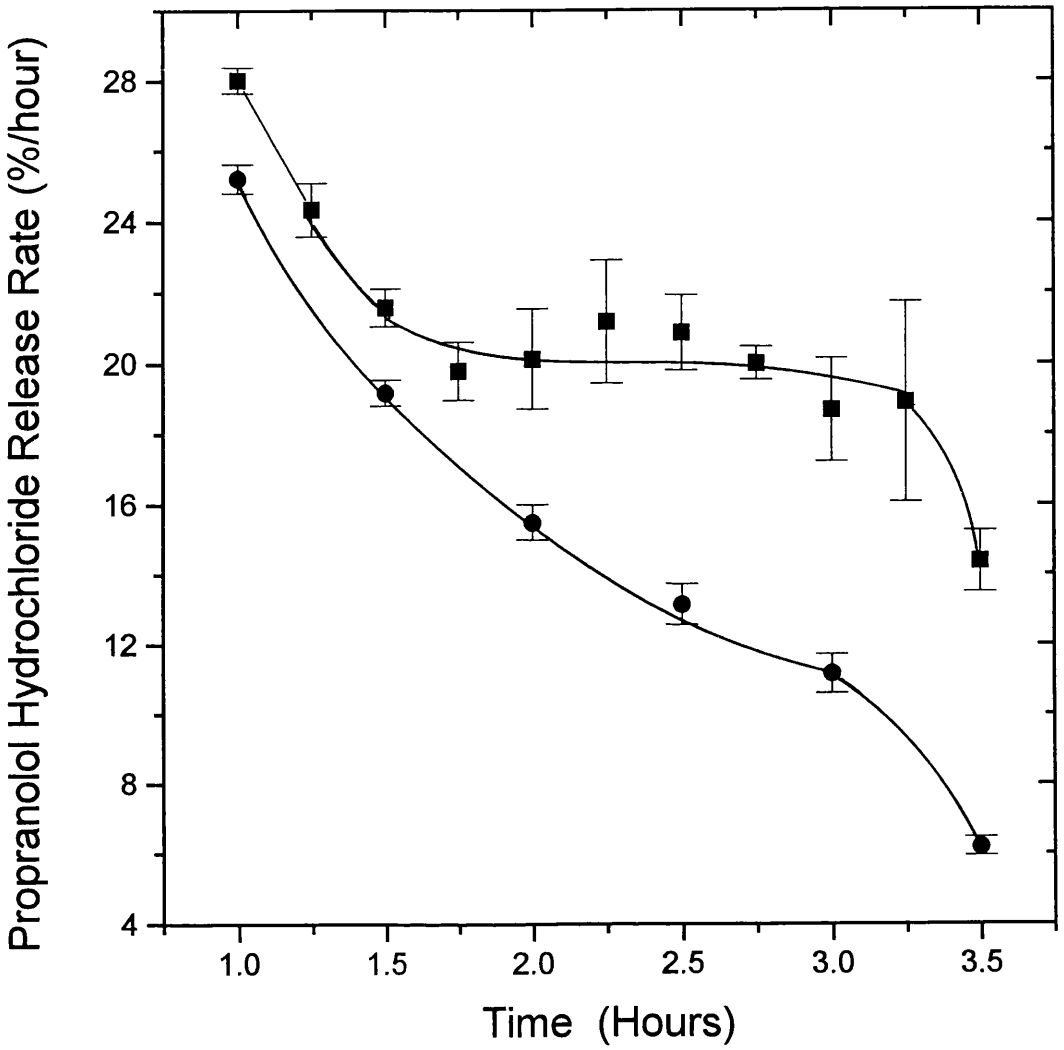

Key:- —■— CE25/B1/Prop tablets

—●— CE5/B1/Prop tablets

NB:- for details of CE5/B1/Prop and CE25/B1/Prop formulations, see tables 2.1 (a), 2.1 (e) and 2.2

Figure 4.8:- The Effect of Particle Diameter on Release - Sustaining Characteristics of CE25/Prop Compacts Made at approximately 3 kN

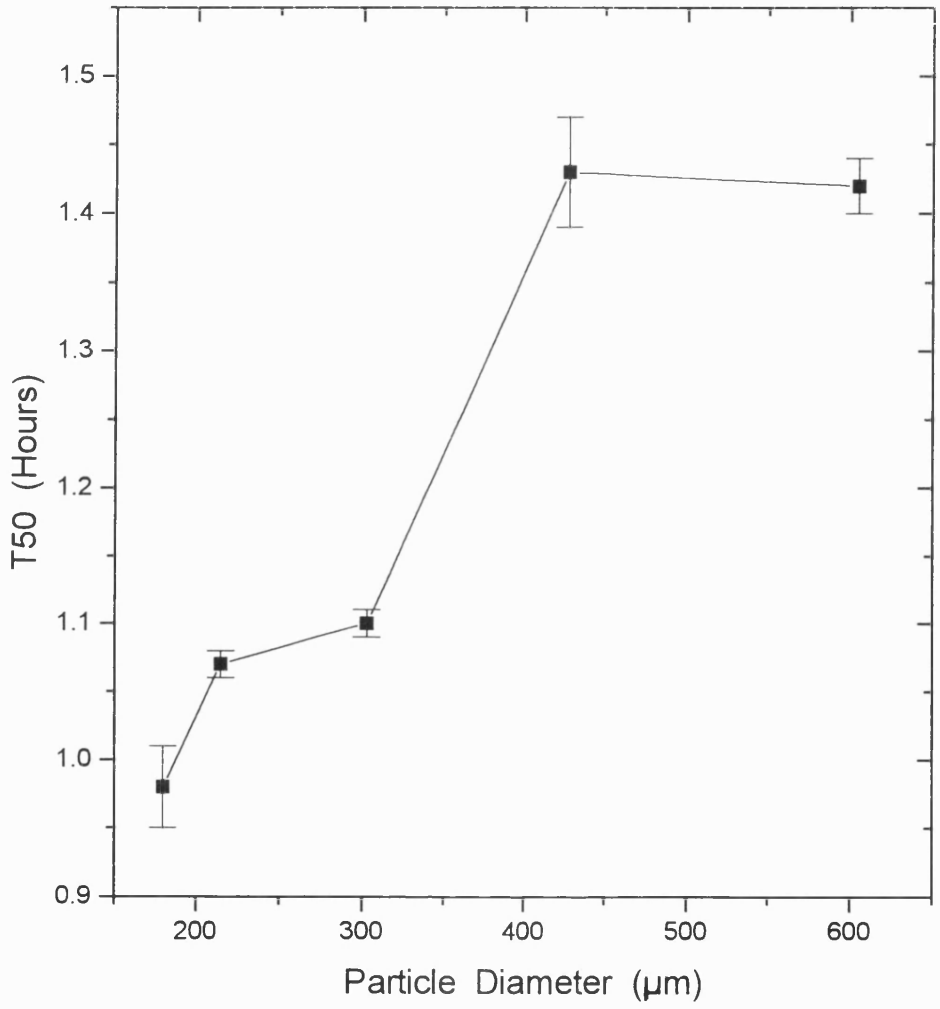

NB:- for details of CE25/Prop formulation, see table 2.1 (e)

CE25 tablets made at approximately 3 kN from four particle size fractions (500-710 μm, 355-500 μm, 250-355 μm, and 180-250 μm) plus propranolol hydrochloride (ratio = 110 : 40 respectively) did not have constant release rate within their release profiles such as that observed with CE25/B1/Prop tablets where a multi-blend particle size composite excipient was used. These tablets from size fractionated CE25 plus drug had release rates that mainly decreased with time. However, tablets made at approximately 3 kN from the smallest particles of CE25 (< 180 μm), plus propranolol hydrochloride (ratio = 110 : 40 respectively), had a constant drug release rate within the release profile, but this was not as pronounced and prolonged as that obtained with CE25/B1/Prop tablets made at the same compaction force. It seems as if a blend of the particle size fractions of CE25, such as B1, B2 or B3 (table 2.2), was necessary for the constant release rate within the release profile to be obtained.

To investigate whether the constant release rate within the release profile of CE25/B1/Prop compacts was either a matrix property or a drug property, an alternative drug, theophylline was used in place of propranolol hydrochloride. Tablets made at approximately 3 kN from CE25/B1/Theo (tables 2.1 (e) and 2.2) were subjected to dissolution testing. The results are summarised in figures 4.9 and 4.10.

With theophylline, release rate became constant from approximately 7 hours but after approximately 13 hours, there was a "second burst" release followed by constant release rate again (figure 4.10). Therefore the constant release rate or

Figure 4.9:- Theophylline Release from CE25/B1/Theo Tablets made at approximately 3 kN

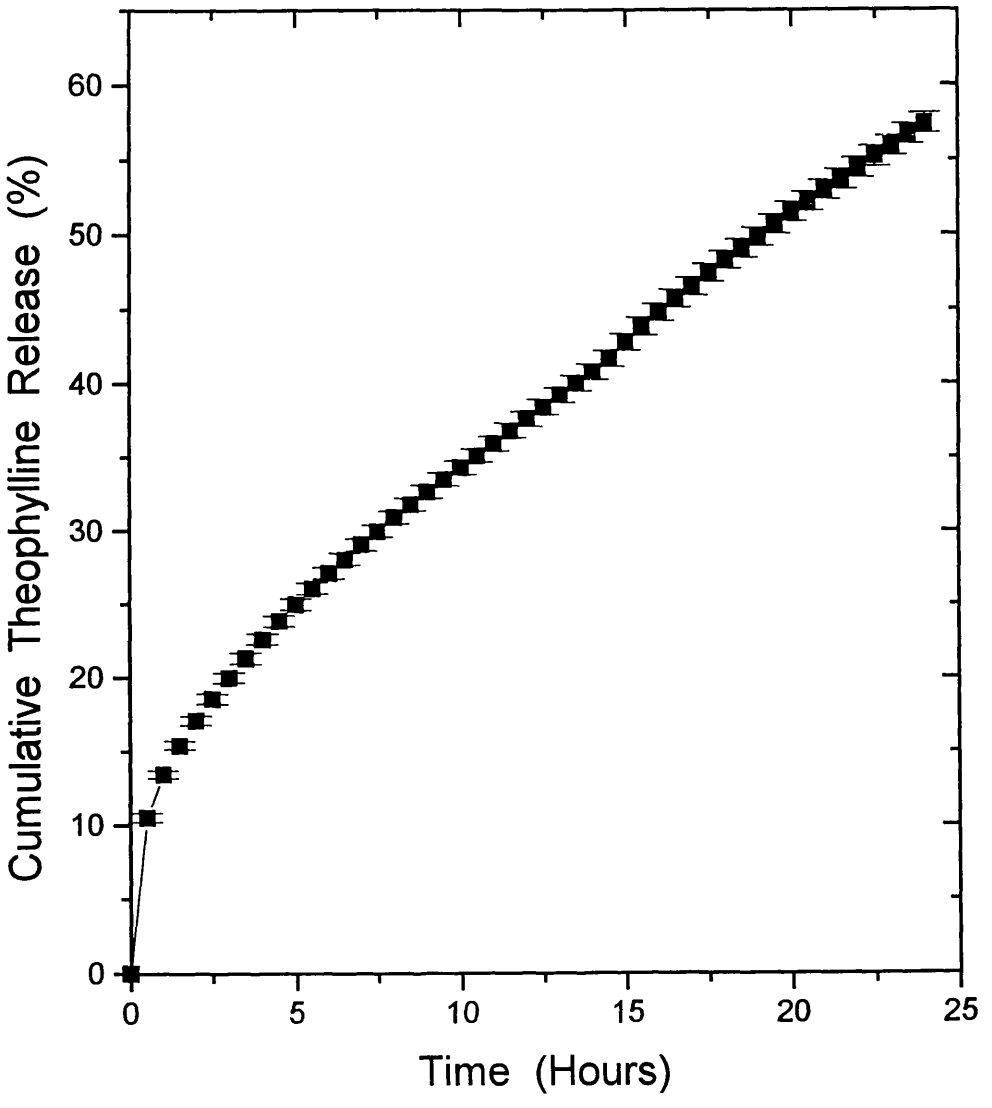

NB:- for details of CE25/B1/Theo formulation see tables 2.1 (e) and 2.2

Figure 4.10:- Theophylline Release Rate from CE25/B1/Theo Tablets made at approximately 3 kN

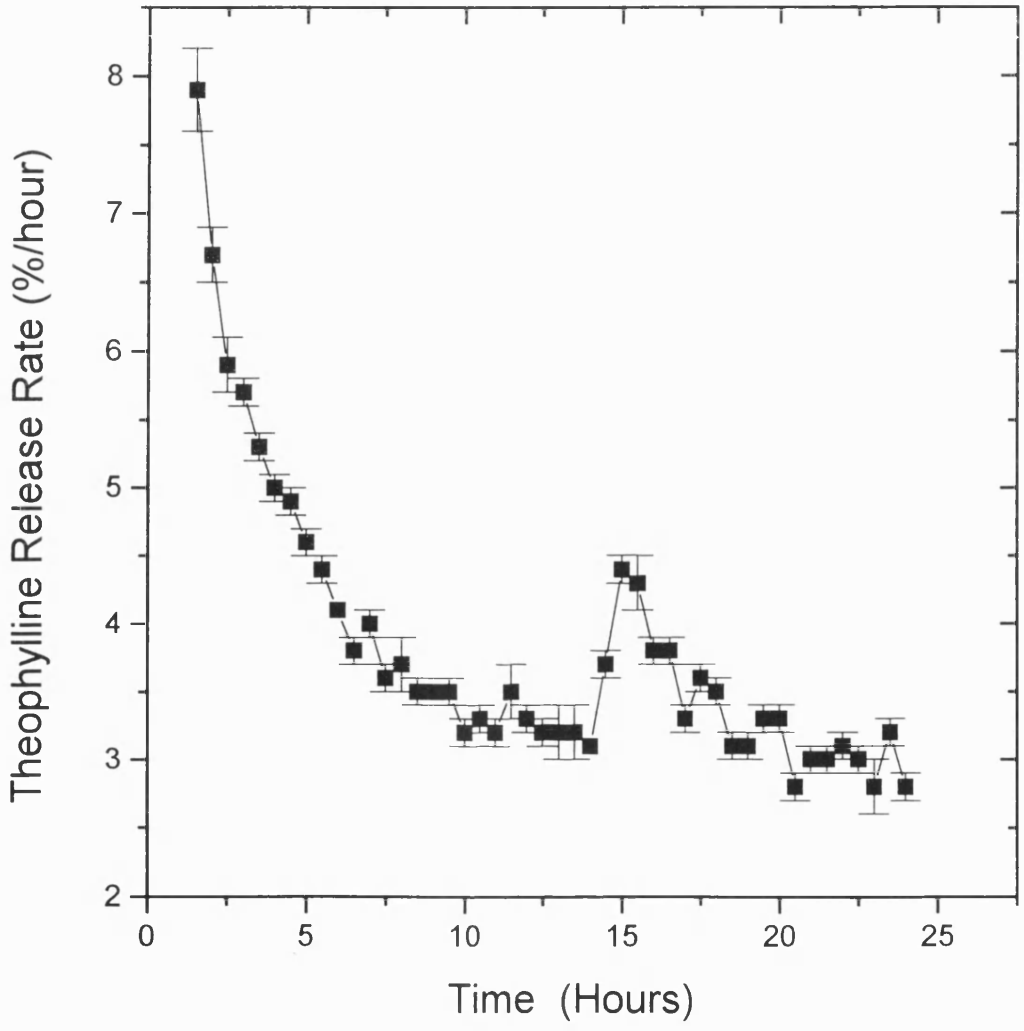

NB:- for details of CE25/B1/Theo formulation see tables 2.1 (e) and 2.2

second burst release was a matrix property. Due to the fact that theophylline has a lower solubility than propranolol hydrochloride, the potential of the HVO/Myverol matrix was more apparent with the former than with the latter. These results also seem to suggest that the relaxation and erosion of the HVO/Myverol matrix is time dependent.

4.3.5 Optimisation of the Constant Release Rate or "Second Burst" Release

Even though a constant release rate and a second burst release was obtained by incorporating Myverol into HVO formulation and processing to produce a composite excipient, CE25 (table 2.1 (e)), it was not as pronounced and prolonged as desired. Consequently, a fifth ingredient, Eudragit S100, at two different concentrations (20 % w/w and 30 % w/w) was incorporated into the HVO formulations and processed to respective composite excipients, CE27 and CE28 (see table 2.1 (e)), as described in section 2.3.1.2.2. Tablets were prepared at 3 - 18 kN from CE27/B3/Prop and CE28/B3/Prop (see also table 2.2) and then subjected to dissolution testing. Drug release profiles from CE27/B3/Prop and CE28/B3/Prop tablets made at approximately 6 kN are shown in figure 4.11.

CE28/B3/Prop compacts were found to have a more enhanced second burst release than CE27/B3/Prop compacts (figure 4.11). All the six tablets of each formulation had this characteristic second burst release starting after approximately 2 hours. This second burst release was found to be more pronounced at low compaction forces than at high ones. Since CE28/B3/Prop

Figure 4.11:- Propranolol Hydrochloride Release from Tablets made from CE27/B3/Prop and CE28/B3/Prop at approximately 6 kN

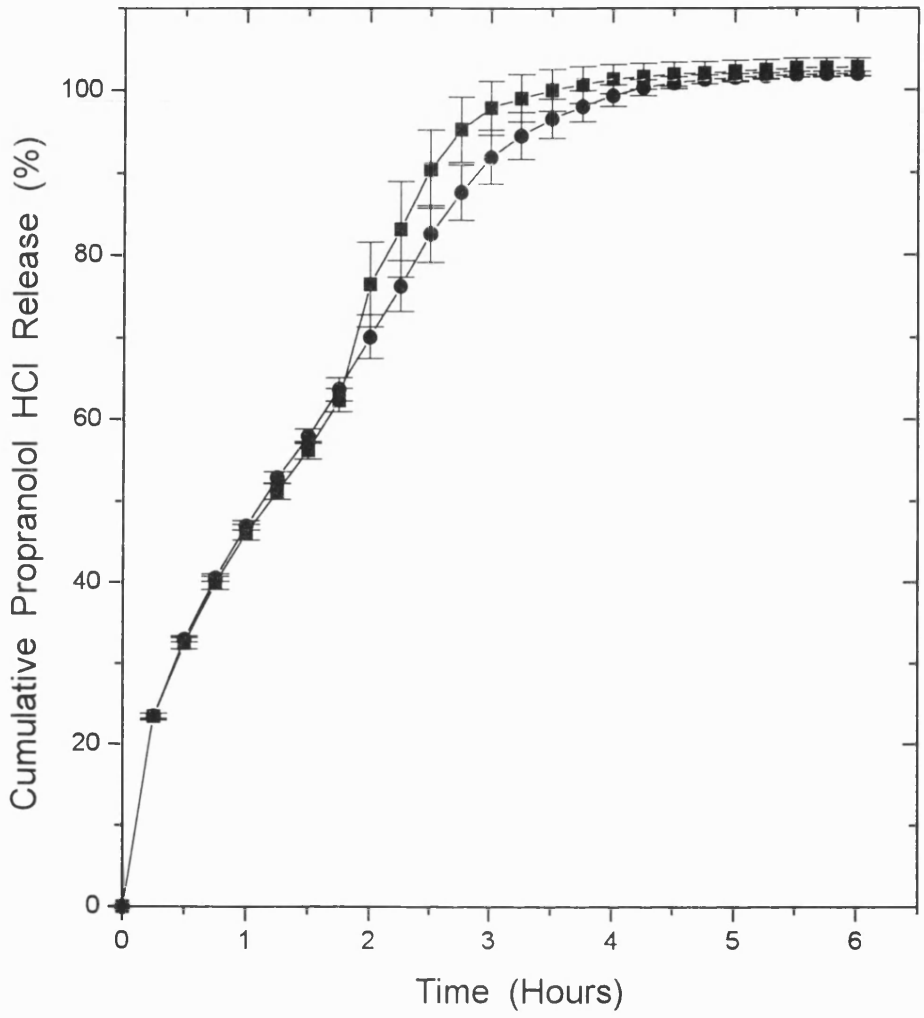

Key:- —■— CE28/B3/Prop

—●— CE27/B3/Prop

NB:- for details of CE27/B3/Prop and CE28/B3/Prop formulations, see tables 2.1 (e) and 2.2

tablets had a more enhanced second burst release than CE27/B3/Prop tablets, CE28 was selected over CE27.

An optimum formulation, CE29/B2/Prop (tables 2.1 (e) and 2.2), based on the results obtained in the various sections of the study was prepared. CE29 was prepared as described in section 2.3.1.2.2. CE29/B2/Prop contained a high percentage of large particles as these enhanced release - sustaining characteristics and compact tensile strength (sections 3.5.4.1). Myverol and Eudragit S100 were incorporated so as to alter and enhance the drug release mechanism respectively (sections 4.3.2 - 4.3.5). PVP K-90 was used as the binder (section 3.5.2), while leucine functioned as the anti-adherent (section 3.6). Tablets were made at relatively low compaction forces (approximately 6 kN) since these enhanced matrix relaxation and erosion (section 4.3.4). Dissolution was carried out in distilled water and in buffer solutions. The results are summarised in figures 4.12 - 4.15.

CE29/B2/Prop's adherence to tablet tooling was much less than that of CE25/B1/Prop. This was partly due to the effects of leucine, the anti-adherent, and Eudragit S100. However, CE29/B2/Prop adhered more to tablet tooling than CE5/B1/Prop, with the former's compact tensile strength (0.693 ± 0.052 MN/m^2) being approximately half that of the latter (1.253 ± 0.120 MN/m^2), (**n = 15**), (as measured by Schleuniger, type 2E, Germany).

Figure 4.12:- Propranolol Hydrochloride Release from CE29/B2/Prop Tablets made at approximately 6 kN, in Distilled Water

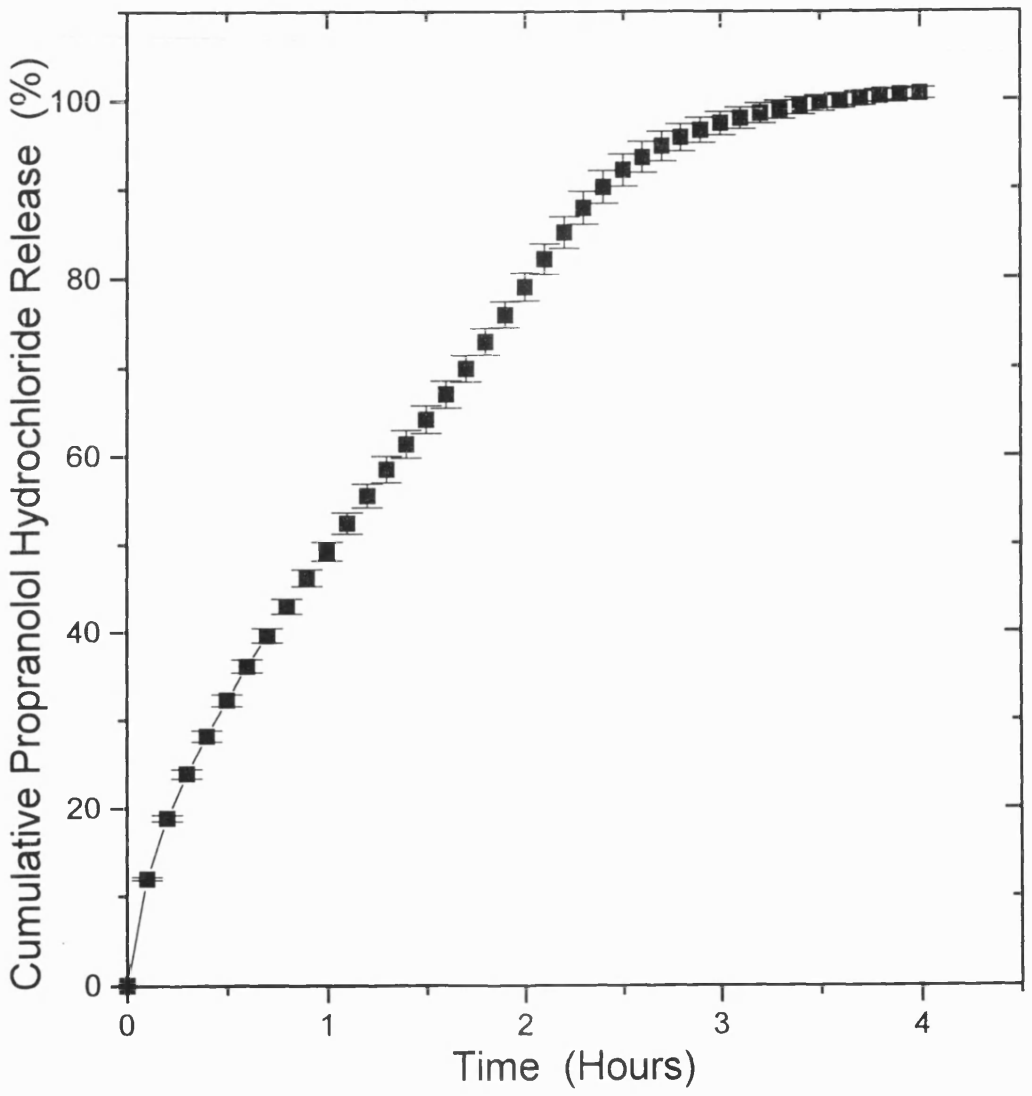

NB:- for details of CE29/B2/Prop formulation, see tables 2.1 (e) and 2.2

Figure 4.13:- Propranolol Hydrochloride Release Rate from CE29/B2/Prop Tablets made at approximately 6 kN, in Distilled Water

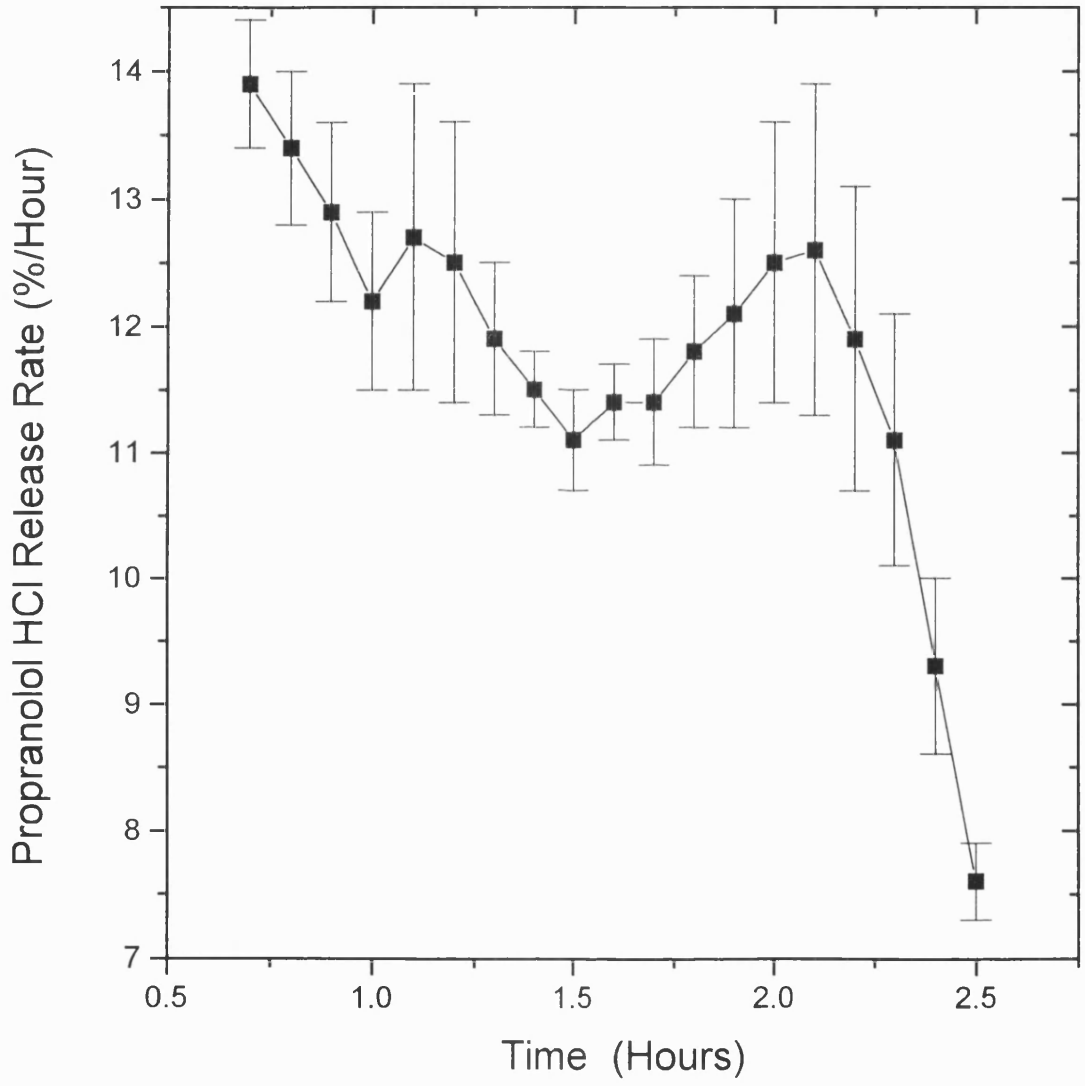

NB:- for details of CE29/B2/Prop formulation, see tables 2.1 (e) and 2.2

Figure 4.14:- Propranolol Hydrochloride Release from CE29/B2/Prop Tablets made at approximately 6 kN, in Buffer Solutions

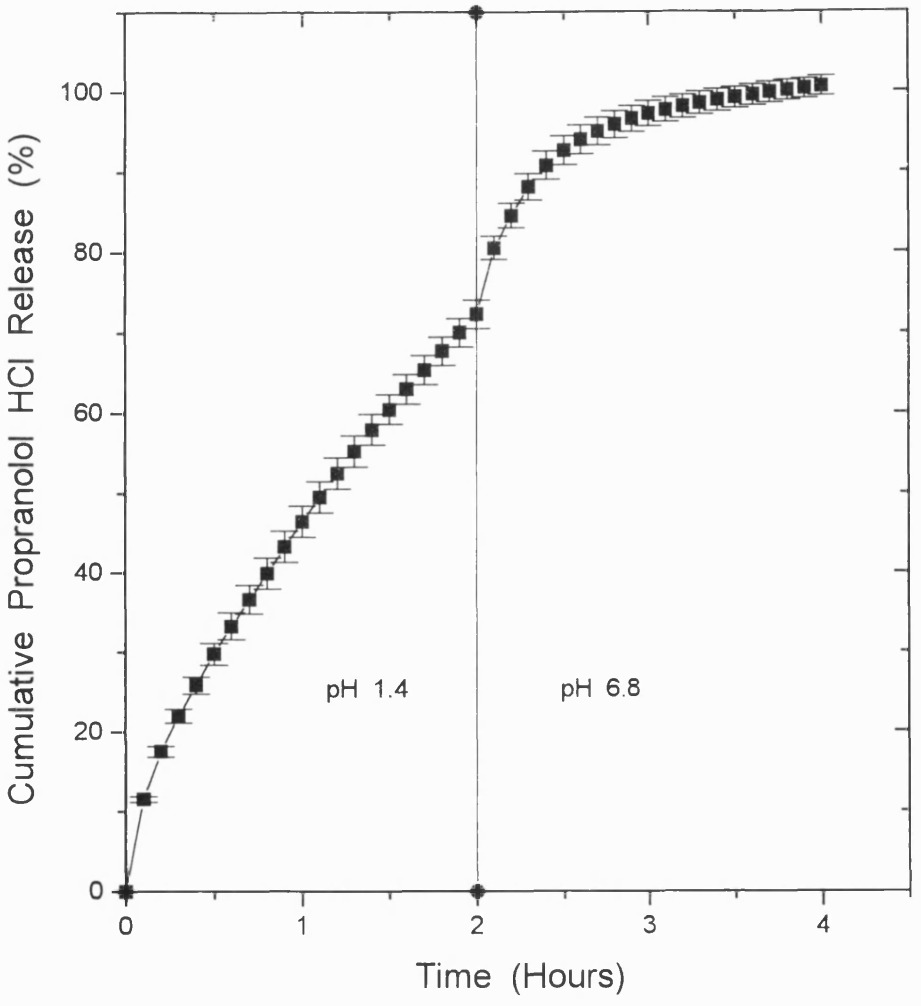

NB:- for details of CE29/B2/Prop formulation, see tables 2.1 (e) and 2.2

Figure 4.15:- Propranolol Hydrochloride Release Rate from CE29/B2/Prop Tablets made at approximately 6 kN, in Buffer Solutions

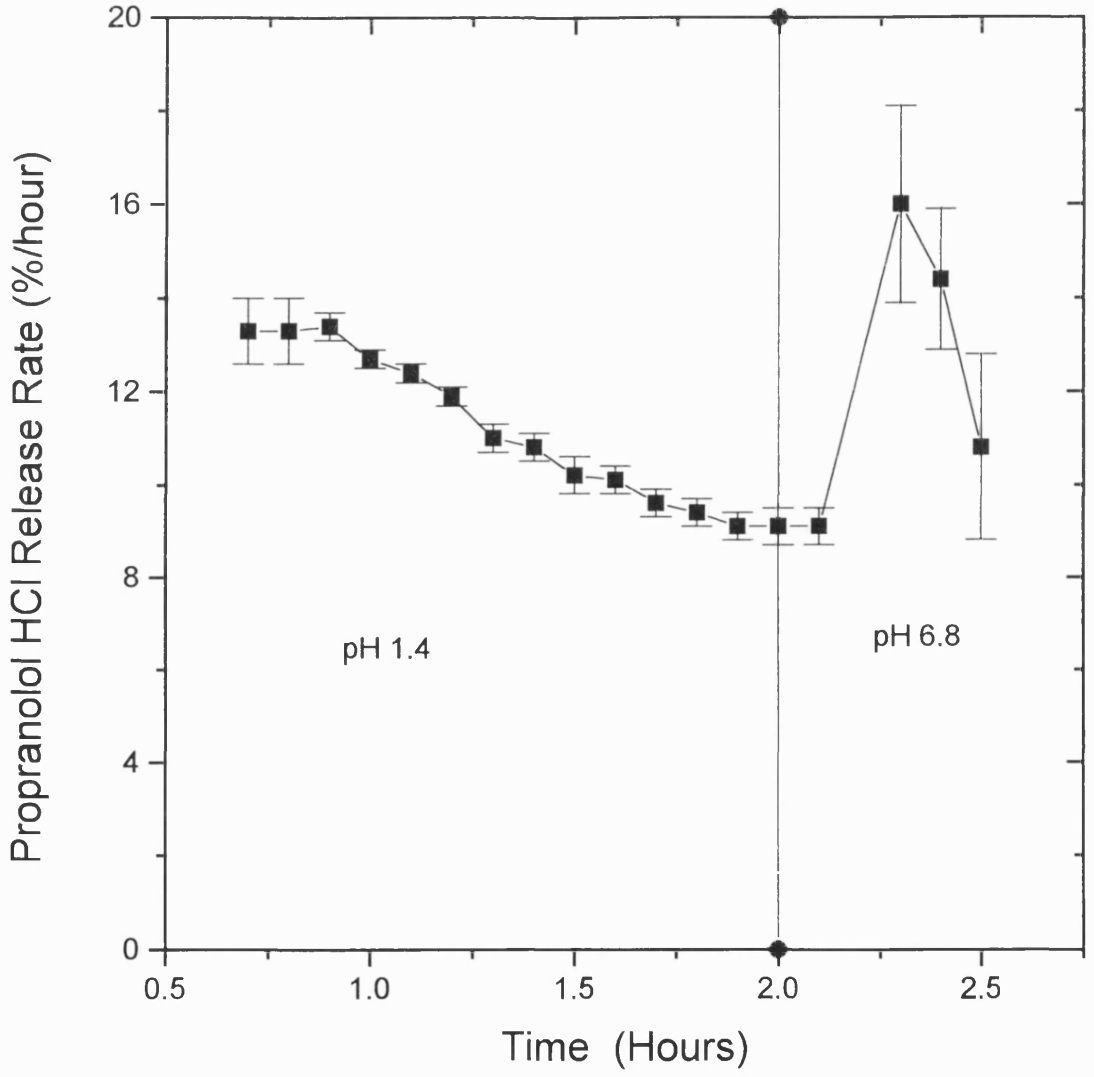

NB:- for details of CE29/B2/Prop formulation, see tables 2.1 (e) and 2.2

CE29/B2/Prop tablets gradually eroded with time, both in distilled water and in the buffer solutions. Propranolol hydrochloride release from these tablets in distilled water ***appeared*** to follow zero order release mechanism as shown in figure 4.12. However, on consideration of figure 4.13, which is the summary of the corresponding drug release rate from 0.7 - 2.5 hours, after approximately 1.5 hours there was a gradual increase in release rate with time for approximately half an hour.

Propranolol hydrochloride was initially released into pH 1.4 (simulated gastric pH) buffer solution for 2 hours which approximates the mean gastric residence time. The tablets were then transferred into pH 6.8 (simulated small intestine pH) buffer solution (figure 4.14). There was a significant increase in drug release and drug release rate in pH 6.8 ($t_{cal} = 3.22$).

According to the **Henderson-Hasselbalch** equation:-

$$pH = pK_a + \log_{10} \{[base]/[salt]\},$$

the percent fraction of the salt form of the drug (propranolol hydrochloride), which is soluble in water, at pH 1.4 is 99.99 % while at pH 6.8 this is 99.8 % ($pKa \approx 9.5$). [114] Since there were no propranolol hydrochloride solubility problems with the buffer solutions used, the increase in release rate with time in the buffer solutions was solely a time factor rather than a pH factor.

Approximately 70 % of the propranolol hydrochloride was released in the gastric simulated pH while the remainder was released in the small intestine

simulated pH. For a per-oral controlled release system intended for the proximal colon, it is preferable that no drug is released in the stomach, followed by minimal release along the small intestine and maximum release as the system enters the proximal colon.

Therefore drug release from processed HVO tablets can be altered from the predominantly Higuchi mechanism of release to a constant release rate and/or increase in release rate with time, within the release profile, by the incorporation of a non - dispersible non - ionic surfactant, Myverol, into the formulation and controlling the particle size distribution and the compaction force.

4.3.6 Analysis of Mechanism of Propranolol Hydrochloride Release from Tablets Made from Composite Excipient 29 Formulation, in Distilled Water

As previously stated in section 4.3.5, tablets made from CE29/B2/Prop (tables 2.1 (e) and 2.2) gradually eroded with time in the dissolution medium and this effectively reduced the drug diffusional distance, altering the predominately square root of time dependent release kinetics. The release data up to approximately 90 % (so as to include analysis of the second burst release which started after approximately 60 % release), from CE29/B2/Prop tablets made at approximately 6 kN, was analysed according to zero order, Higuchi mechanism, first order and diffusion - relaxation models. The regression analysis data on each individual tablet according to the above mechanisms is shown in appendix 1, tables A11, A10, A9 and A12 respectively. The *in vitro* release

kinetics of propranolol hydrochloride from CE29/B2/Prop matrices according to the above mechanisms is shown in table 4.4. The Fickian diffusion and case II relaxation fractions at each time, t, are shown in figure 4.16.

Clearly, propranolol hydrochloride release from CE29/B2/Prop tablets did not follow first order release kinetics (table 4.4). Although zero order and Higuchi mechanisms had approximately the same fit (r = 0.99503 and 0.99450 respectively), the Higuchi mechanism suggested a relatively long lag time before drug release (intercept = -12.48 ± 1.84). Since the Myverol, a surfactant, is supposed to enhance tablet wetting, the Higuchi intercept was expected to be zero or at least close to zero. Zero order mechanism gave a relatively high intercept (intercept = 15.23 ± 1.19). Drug release from CE29/B2/Prop matrices was best described by the diffusion - relaxation model (r = 0.99960). The Fickian release constant (k_1 = 28.38 ± 3.03) was significantly higher than the relaxation constant (k_2 = 21.06 ± 2.52) (t_{cal} = 4.54, t_{tab} = 2.23, p = 0.05).

Figure 4.16 shows that the Fickian diffusion contribution was initially predominant over the relaxation contribution. The relaxation contribution became predominant after approximately 1.9 hours. The Fickian diffusion fraction, F, was calculated according to equation 1.39 in section 1.5.1.6.2:-

$$F = 1/\{1 + (k_2/k_1)t^{0.46}\}$$

The relaxation (Case II) fraction, F_r, was calculated according to the following equation:-

$$F_r = 1 - F$$

Table 4.4:- *In Vitro* Release Kinetics of Propranolol Hydrochloride from CE29/B2/Prop Tablets made at approximately 6 kN, in Distilled Water (n = 6)

First Order:- $\log_{10}(100\ \% - Q) = kt$	
Slope (hr^{-1})	-0.37803 ± 0.06098
Intercept	2.0482 ± 0.0327
r	0.96792 ± 0.01990
Zero Order:- $Q = kt$	
Slope ($\%hr^{-1}$)	32.17 ± 1.80
Intercept (%)	15.23 ± 1.19
r	0.99503 ± 0.00215
Higuchi Mechanism:- $Q = kt^{1/2}$	
Slope ($\%hr^{-1/2}$)	63.93 ± 3.61
Intercept (%)	-12.48 ± 1.84
r	0.99450 ± 0.00354
Diffusion - Relaxation Mechanism:- $Q = k_1t^{0.46} + k_2t^{0.92}$	
k_1 ($\%hr^{-0.46}$)	28.38 ± 3.03
k_2 ($\%hr^{-0.92}$)	21.06 ± 2.52
Intercept (%)	0.03 ± 0.09
r	0.99960 ± 0.00034

Figure 4.16:- Fickian Diffusion Release Fractions and Case-II Relaxation Release Fractions from CE29/B2/Prop Tablets made at approximately 6 kN, in Distilled Water

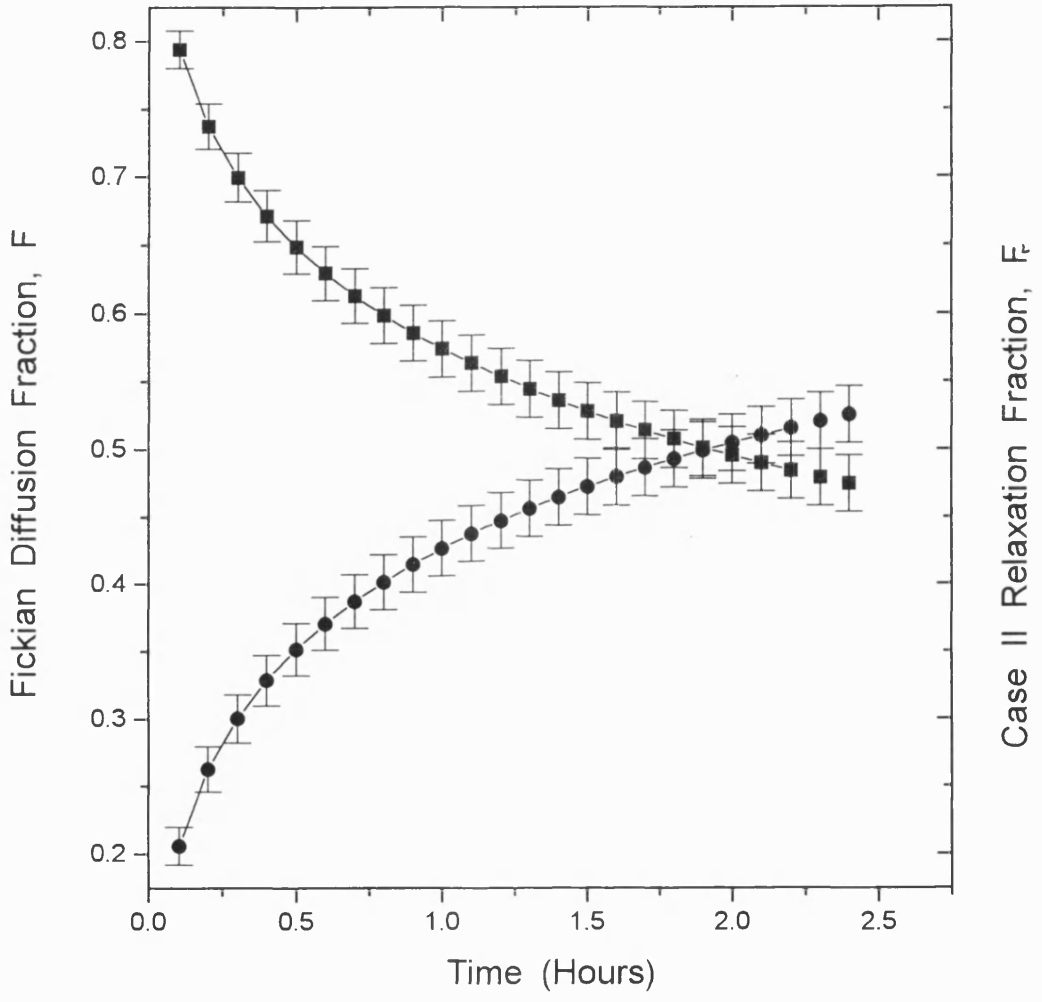

Key:- —■— Diffusion fraction, F

—●— Relaxation fraction, F_r

NB:- for details of CE29/B2/Prop formulation, see tables 2.1 (e) and 2.2

Therefore drug release from CE29/B2/Prop tablets probably involved rapid wetting due to Myverol, followed by a predominantly Fickian diffusion coupled with gradual relaxation and ultimate erosion of the matrix. The gradual relaxation and erosion of the matrix were primarily due to Myverol and possibly Eudragit S100, giving rise to a second burst release.

CHAPTER 5

CONCLUSIONS

The physico-mechanical properties of hydrogenated vegetable oil (HVO), Sterotex K, tablets were significantly improved by processing the HVO with binders. Incorporation of an additional meltable binder such as stearic acid during processing, reinforced compact strength. Tablet tensile strength was found to be dependent on type and concentration of binder. Highly hydrophilic binders such as Polyplasdone reduced release-sustaining characteristics of the matrix.

Large particles of processed HVO composite excipient (500-710 μm exclusively), were found to produce compacts of significantly superior tensile strength to the remainder of the particle sizes (355-500 μm, 250-355 μm, 180-250 μm, < 180 μm exclusively). This was attributed to the greater extent in partial melt-fusion in the former than the latter due to:- (a) increased pressure per unit surface area, (b) increased fragmentation potential and (c) reduced inter-particle and die-tablet wall contact. The medium particle sizes (355-500 μm, 250-355 μm, 180-250 μm exclusively), produced tablets with the same tensile strength. It was hypothesised that there was compensation between partial melt-fusion effects and ductile effects in these particles. The smallest particles (< 180 μm) produced tablets with significantly inferior tensile strengths in comparison to the rest of the particle sizes. The above trend almost mirrored the effect of particle size on release - sustaining characteristics of processed HVO tablets. The only

difference was that 355-500 μm, 250-355 μm, 180-250 μm and < 180 μm particles produced compacts with the same release sustaining characteristics.

Compact strength and release-sustaining characteristics of processed HVO formulations were found to be dependent on compaction force up to approximately 9 kN. Thereafter compact strength and release-sustaining characteristics were independent of compaction force. However, processed HVO formulation containing 30 % Myverol had compaction force independent release-sustaining characteristics from 3 to 15 kN.

Addition of lubricants to processed HVO formulations significantly reduced tablet tooling adhesion. Anti-adherent activity was dependent on the type and concentration of lubricant. However, lubricants significantly reduced the tensile strength of the matrix by effectively reducing the total area of clean surfaces capable of forming bonds. Due to the fact that tensile strength of processed HVO tablets was dependent on particle size and tablet lubricants concentration, it was concluded that the main mechanism of consolidation in this material is plastic deformation.

The beneficial effects of processing a HVO include:-

- significantly improved tablet strength,
- significantly improved anti-adhesion properties,
- improved release-controlling efficiency and
- compaction force independent drug release and tablet strength.

However, incorporation of a hydrophobic binder with strength imparting properties of Polyplasdone would be desirable. A HVO with a higher melting point than Sterotex K/soybean oil would help in reducing tablet tooling adhesion.

Drug release from processed HVO matrices was explained by a diffusion/dissolution model corresponding to the Higuchi mechanism. Addition of hydrophilic materials such as Avicel, Starch 1500 and Junlon improved drug release without altering the release mechanism. Enzymes such as lipase and esterase failed to degrade the ester-linkages of the HVO within 12 hours. This was attributed to the relatively short time period and the fact that Sterotex K probably ceases to be a natural enzymatic substrate due to hydrogenation.

Incorporation of a mainly monoglyceride material, Myverol, (30 %), into HVO formulations and processing to composite excipients altered the drug release mechanism of the resulting tablets. This form of processed HVO released drug via a diffusion - relaxation model. Tablets altered from a monolithic formulation to disintegrating tablets. An increase in release rate with time was obtained for at least half an hour within the dissolution profile. Such a release profile would be desirable in drug targeting to the proximal colon. However, in order to target such a system to the proximal colon, there ought to be a lag time corresponding to gastric residence time plus small intestine transit time. Delay of onset of drug delivery could be achieved by coating the system with pH or time dependent polymers.

REFERENCES

1. Johansson, B., Wikberg, M., Ek, R. and Alderborn, G. (1995). Compression behaviour and compactability of microcrystalline cellulose pellets in relationship to their pore structure and mechanical properties. *Int. J. Pharm.*, **117** 57-73.

2. Parrot, E. L. (1990). Compression. In: Pharmaceutical Dosage Forms: Tablets, Vol. 2. H. A. Lieberman, L. Lachman and J. B. Schwartz, (Eds.), pp. 201-243, Marcel Dekker, Inc., New York & Basel.

3. Wray, P. E. (1992). The physics of tablet compaction revisited. *Drug Dev. Ind. Pharm.*, **18** 627-658.

4. Otsuka, M. and Matsuda, Y. (1993). Effects of environmental temperature and compression energy on polymorphic transformation during tableting. *Ibid,* **19** 2241-2269.

5. Katikaneni, P. R., Upadrashta, S. M., Rowlings, C. E., Neau, S. H. and Hileman, G. A. (1995). Consolidation of ethylcellulose: Effect of particle size, press speed and lubricants. *Int. J. Pharm.*, **117** 13-21.

6. Sheik-Salem, M. and Fell, J. T. (1982). The tensile strength of tablets of lactose, sodium chloride and their mixtures. *Acta Pharm. Suec.*, **19** 391-396.

7. Garr, J. S. M. and Rubinstein, M. H. (1992). Consolidation and compaction characteristics of a three-component particulate system. *Int. J. Pharm.*, **82** 71-77.

8. Nyström, C., Alderborn, G., Durberg, M. and Karehill, P-G. (1993). Bonding surface area and bonding mechanism - two important factors for the understanding of powder compactibility. *Drug Dev. Ind. Pharm.*, **19** 2143-2196.

9. Roberts, R. J. and Rowe, R. C. (1985). The effect of punch velocity on the compaction of a variety of materials. *J. Pharm. Pharmacol.*, **37** 377-384.

10. Roberts, R. J. and Rowe, R. C. (1986). The effect of the relationship between punch velocity and particle size on the compaction behaviour of materials with varying deformation mechanisms. *Ibid,* **38** 567-571.

11. Wells, J. I. and Langridge, J. R. (1981). Dicalcium phosphate dihydrate - microcrystalline cellulose systems in direct compression tableting. *Int. J. Pharm. Tech. & Prod. Mfr.*, **2** 1-8.

12. Rankell, A. S. and Higuchi, T. (1968). The physics of tablet compression XV: Thermodynamic and kinetic aspects of adhesion under pressure. *J. Pharm. Sci.*, **57** 574-577.

13. Jarosz, P. J. and Parrot, E. L. (1982). Factors influencing axial and radial tensile strength of tablets. *Ibid,* **71** 607-614.

14. Shangraw, R. F. (1991). Evaluation of tablets and capsules. Proceeds for Modern Granulation, Tableting and Capsule Technology, pp. 1-72, The Center for Professional Advancement, Amsterdam, Netherlands.

15. Shangraw, R. F. (1991). Formulation of tablets - role of excipients. Proceeds for Modern Granulation, Tableting and Capsule Technology, pp. 1-86, The Center for Professional Advancement, Amsterdam, Netherlands.

16. Symecko, C. W. and Rhodes, C. T. (1995). Binder functionality in tableted systems. *Drug Dev. Ind. Pharm.*, **21** 1091-1114.

17. Gordon, R. E., Rosanke, T. W. and Fonner, D. E. (1990). Granulation technology and tablet characterization. In: Pharmaceutical Dosage Forms:

Tablets, Vol. 2. H. A. Lieberman, L. Lachman and J. B. Schwartz, (Eds.), pp. 245-348, Marcel Dekker, Inc., New York & Basel.

18. Zuurman, K., Riepma, K. A., Bolhuis, G. K., Vromans, H. and Lerk, C. F. (1994). The relationship between bulk density and compactibility of lactose granulations. *Int. J. Pharm.*, **102** 1-9.

19. Wikberg, M. and Alderborn, G. (1993). Compression characteristics of granulated materials. VII. The effect of intragranular binder distribution on the compactability of some lactose granulations. *Pharm. Res.*, **10** 88-94.

20. Nyström, C. and Glazer, M. (1985). Studies on direct compression of tablets. XIII. The effect of some dry binders on the tablet strength of compounds with different fragmentation propensity. *Int. J. Pharm.*, **23** 255-263.

21. Monedero Perales, M. C., Muñoz - Ruiz, A., Velasco Antequera, M. V. and Jiménez - Castellanos Ballesteros, M. R. (1994). Study of the compaction mechanism of lactose based direct compression excipients using identation hardness. *J. Pharm. Pharmacol.*, **46** 177-181.

22. Monedero Perales M. C., Muñoz Ruiz, A., Velasco Antequera, M. V., Muñoz Muñoz, N. and Jiménez - Castellanos, M. R. (1994). Analysis comparative of methods to evaluate consolidation mechanisms in plastic and viscoelastic materials used as direct compression excipients. *Drug Dev. Ind. Pharm.*, **20** 327-342.

23. Çelik, M. and Driscoll, C. E. (1993). An overview of the effects of some physico-chemical and mechanical characteristics of particulates on the compaction and post-compaction properties of compacts. *Ibid,* **19** 2119-2141.

24. Alderborn, G., and Nyström, C. (1984). Radial and axial tensile strength and strength variability of paracetamol tablets. *Acta Pharm. Suec.*, **21** 1-8.

25. Alderborn, G., and Nyström, C. (1982). Studies on direct compression of tablets IV. The effect of particle size on the mechanical strength of tablets. *Ibid,* **19** 381-390.

26. Duberg, M. and Nyström, C. (1982). Studies on direct compression of tablets VI. Evaluation of methods for the estimation of particle fragmentation during compaction. *Ibid,* **19** 421-436.

27. Duncan - Hewitt, W. C. (1993). Uniaxial compaction modelled using the properties of single crystals. *Drug Dev. Ind. Pharm.*, **19** 2197-2240.

28. Rees, J. E. and Rue, P. J. (1978). Work required to cause failure of tablets in diametral compression. *Ibid,* **4** 131-156.

29. Bhushan, B., Israelachvili, J. N. and Landman, U. (1995). Nanotribology: Friction, wear and lubrication at the atomic scale. *Nature,* **374** 607-616.

30. Mitrevej, A. and Augsburger, L. L. (1980). Adhesion of tablets in a rotary tablet press I. Instrumentation and preliminary study of variables affecting adhesion. *Drug Dev. Ind. Pharm.*, **6** 331-377.

31. Staniforth, J. N., Cryer, S., Ahmed, H. A. and Davies, S. P. (1989). Aspects of pharmaceutical tribology. *Ibid,* **15** 2265-2294.

32. Staniforth, J. N. (1987). Use of hydrogenated vegetable oil as a tablet lubricant. *Ibid,* **13** 1141-1158.

33. Schumann, S. and Searle G. D. (1992). The effect of chromium nitride ion bombardment treatment of tableting tooling on tablet adherence. *Ibid,* **18** 1037-1061.

34. Mitreveji, K. T. and Augsburger, L. L. (1982). Adhesion of tablets in a rotary tablet press II. Effects of blending time, running time and lubricant concentration. *Drug Dev. Ind. Pharm.,* **8** 237-282.

35. Shah, N. H., Stiel, D., Weiss, M., Infeld, M. H. and Malick, A. W. (1986). Evaluation of two new tablet lubricants - sodium stearyl fumarate and glyceryl behenate. Measurement of physical parameters (compaction, ejection, and residual forces) in the tableting process and effect on the dissolution rate. *Ibid,* **12** 1329-1346.

36. Müller, B. W., Steffens, K. -J. and List, P. H. (1982). Tribological laws and Experimental results in tablet technology. *Drugs Made Ger.,* **25** 53-60.

37. Waring, M. J., Sen, H., Forrester, J. W. and Salmon, J. R. (1987). Instrumented and computer-interfaced single-punch tablet press for the rapid evaluation of compression and lubrication behaviour. In: Pharmaceutical Technology - tableting technology, Vol. I. M. H. Rubinstein, (Ed.), pp. 113-126, Ellis Horwood Ltd., Chichester, England.

38. Nelson, E., Naqvi, S. M., Busse, L. W. and Higuchi, T. (1954). The physics of tablet compression IV. Relationship of ejection and upper and lower punch forces during compressional process: Application of measurement to comparison of tablet lubricants. *J. Am. Pharm. Ass.,* **43** 596-602.

39. Leinonen, U. I., Jaionen, H. U., Vihervaara, P. A. and Laine, E. S. U. (1992). Physical and lubrication properties of magnesium stearate. *J. Pharm. Sci.,* **8** 1194-1198.

40. McKenna, A. and McCafferty, D. F. (1982). Effect of particle size on the compaction mechanism and tensile strength of tablets. *J. Pharm. Pharmacol.*, **34** 347-351.

41. Eriksson, M. and Alderborn, G. (1995). The effect of original particle size and tablet porosity on the increase in tensile strength during storage of sodium chloride tablets in a dry atmosphere. *Int. J. Pharm.*, **113** 199-207.

42. Merkus, F. W. H. M. (1986). Controlled and rate-controlled drug delivery, principal characteristics, possibilities and limitations. In: Rate Controlled Drug Administration and Action, H. A. J. Struyker - Boudier, (Ed.), pp. 15-47, CRC Press, Inc., Boca Raton, Florida.

43. Heller, J. (1993). Modulated release from drug delivery devices. *Crit. Rev. Ther. Drug Carr. Syst.*, **10** 253-305.

44. Pozzi, F., Furlani, P., Gazzaniga, A., Davis S. S. and Wilding, I. R. (1994). The TIME CLOCK* system: a new oral dosage form for fast and complete release of drug after a predetermined lag time. *J. Contrl. Rel.*, **31** 99-108.

45. Wilding, I. R., Davis, S. S., Hardy, J. G., Robertson, C. S., John, V. A., Powell, M. L., Leal, M., Lloyd, P. and Walker, S. M. (1991). Relationship between systemic drug absorption and GI transit after simultaneous oral administration of carbamazepine as a controlled-release system and as a suspension of ^{15}N-labelled drug to healthy volunteers. *Br. J. Clin. Pharmacol.*, **32** 573-579.

46. Channer, K. S. and Virjee, J. P. (1985). The effect of formulation on oesophageal transit. *J. Pharm. Pharmacol.*, **37** 126-129.

47. Channer, K. S. and Roberts, C. J. C. (1985). Effect of delayed oesophageal transit on acetaminophen absorption. *J. Clin. Pharmacol. Ther.*, **37** 72-76.

48. Channer, K. S. and Virjee, J. P. (1982). Effect of posture and drink volume on the swallowing of capsules. *Br. Med. J.*, **285** 1702.

49. Heller, S. R., Fellows, I. W., Ogilvie, A. L. and Atkinson, M. (1982). Non-steroidal anti-inflammatory drugs and benign oesophageal stricture. *Ibid,* **285** 167-168.

50. Fell, J. T. (1983). Oesophageal transit of tablets and capsules. *Am. J. Hosp. Pharm.*, **40** 946-948.

51. Swisher, D. A., Sendelbeck, S. L. and Fara, J. W. (1984). Adherence of various oral dosage forms to the oesophagus. *Int. J. Pharm.*, **22** 219-228.

52. Wilson, C. G. and Washington, N. (1989). The stomach: its role in oral drug delivery. In: Physiological Pharmaceutics, biological barriers to drug absorption, M. H. Rubinstein, (Ed.), pp. 47-70, Ellis Horwood Ltd., Chichester, England.

53. Jenkins, J. R. F., Hardy, J. G. and Wilson, C. G. (1983). Monitoring antiacid preparations in the stomach using gamma scintigraphy. *Int. J. Pharm.*, **14** 143-148.

54. Kaus, L. C., Fell, J. T., Sharma, H. and Taylor, D. C. (1984). On the intestinal transit of a single non-disintegrating object. *Ibid,* **20** 315-323.

55. Wilson, C. G., Parr, G. D., Kennerly, J. W., Taylor, M. J., Davis, S. S., Hardy, J. G. and Rees, J. A. (1984). Pharmacokinetics and *in vivo* scintigraphic monitoring of a sustained release acetylsalicylic acid formulation. *Ibid,* **18** 1-8.

56. Moës, A. J. (1993), Gastroretentive Dosage forms. *Crit. Rev. Ther. Drug Carr. Sys.*, **10** 143-195.

57. Abrahamsson, B., Svenheden, A. and Tölli, J. (1993). Absorption, gastrointestinal transit and tablet erosion of felodipine extended-release (ER) tablets. *Pharm. Res.*, **10** 709-714.

58. Aoyagi, N., Ogata, H., Kaniwa, N., Uchiyama, M., Yasudu, Y. and Tanioka, Y. (1992). Gastric emptying of tablets and granules in humans, dogs, pigs and stomach-emptying-controlled rabbits. *J. Pharm. Sci.*, **81** 1170-1174.

59. Wilson, C. G., Washington, N., Greaves, J. L., Kamali, F., Rees, J. A., Sempik, A. K. and Lampard, J. F. (1989). Bimodal release of ibuprofen in a sustained-release formulation: A scintigraphic and pharmacokinetic open study in healthy volunteers under different conditions of food intake. *Int. J. Pharm.*, **50** 155-161.

60. Christensen, F. N., Davis, S. S., Hardy, J. G., Taylor, M. J., Whalley, D. R. and Wilson, C. G. (1985). The use of gamma scintigraphy to follow the GI transit of pharmaceutical formulations. *J. Pharm. Pharmacol.*, **37** 91-95.

61. Hardy, J. G., Evans, D. F., Zaki, I., Clark, A. G., Tonnesen, H. H. and Gamst, O. N. (1987). Evaluation of an enteric coated naproxen tablet using gamma scintigraphy and pH monitoring. *Int. J. Pharm.*, **37** 245-250.

62. Ch'ng, H. S., Park, H., Kelly, P. and Robinson, J. R. (1985). Bioadhesive polymers as platforms for oral controlled drug delivery II: Synthesis and evaluation of some swelling, water-insoluble bioadhesive polymers. *J. Pharm. Sci.*, **74** 399-405.

63. Hardy, J. G., Wilson, C. G. and Wood, E. (1985). Drug delivery to the proximal colon. *J. Pharm. Pharmacol.*, **37** 874-877.

64. Coupe, A. J., Davis, S. S. and Wilding, I. R. (1991). Variation in GI transit of pharmaceutical dosage forms in healthy subjects. *Pharm. Res.*, **8** 360-364.

65. Steed, K. P., Wilson, C. G. and Washington, N. (1989). Drug delivery to the large intestine. In: Physiological Pharmaceutics, biological barriers to drug absorption, M. H. Rubinstein, (Ed.), pp. 91-108, Ellis Horwood Ltd., Chichester, England.

66. Mrsny, R. J. (1992). The colon as a site for drug delivery. *J. Contrl. Rel.*, **22** 15-34.

67. Wood, J. F. (1994). Enzymatic barriers for GI peptide and protein delivery. *Crit. Rev. Ther. Drug Carr. Syst.*, **11** 61-95.

68. Van den Mooter, G., Samyn, C. and Kinget, R. (1994). The relation between swelling properties and enzymatic degradation of azo polymers designed for colon-specific drug delivery. *Pharm. Res.*, **11** 1737-1741.

69. Ashford, M., Fell, J., Attwood, D., Sharma, H. and Woodhead, P. (1994). Studies on pectin formulation for colonic drug delivery. *J. Contrl. Rel.*, **30** 225-232.

70. Kim, J. S., Oberle, R. L., Krummel, D. A., Dressman, J. B. and Fleisher, D. (1994). Absorption of ACE inhibitors from small intestines and colon. *J. Pharm. Sci.*, **83** 1350-1356.

71. Ashford, M., Fell, J. T., Attwood, D., Sharma, H. L. and Woodhead, P. J. (1992). *In vitro* and *in vivo* evaluation of pectin for colonic drug delivery.

Proceed. Int. Symp. Control. Rel. Bioact. Mater., Controlled Release Society, Inc., **19** 351-352.

72. Yeh, P-Y., Kopecková, P. and Kopecek, J. (1992). Hydrogels for colon-specific oral delivery of proteins: *In vitro* and *in vivo* degradation studies. Proceed. Int. Symp. Contrl. Rel. Bioact. Mater., Controlled Release Society, Inc., **19** 323-324.

73. Lundgren, B., Carlsson, E. and Ek, L. (1982). Pafenolol, I. β-blocking potency and selectivity in *in vivo* and *in vitro* experiments. *Acta Phys. Scand., Suppl.,* **508** 44.

74. Price, J. M. C., Davis, S. S., Sparrow, R. A. and Wilding, I. R. (1993). The effect of meal composition on the gastrocolonic response: Implications for drug delivery to the colon. *Pharm. Res.,* **10** 722-726.

75. Wood, E., Wilson, C. G. and Hardy, J. G. (1985). The spreading of foam and solution enemas. *Int. J. Pharm.,* **25** 191-197.

76. Brondsted, H. and Kopecek, J. (1992). Hydrogels for site-specific drug delivery to the colon: *In vitro* and *in vivo* degradation. *Pharm. Res.,* **9** 1540-1545.

77. Rao S. S. and Ritschel, W. A. (1992). Development and *in vitro/in vivo* evaluation of a colonic release capsule of vasopressin. *Int. J. Pharm.,* **86** 35-41.

78. Kopecek, J. (1990). The potential of water-soluble polymeric carriers in targeted and site-specific drug delivery. *J. Contrl. Rel.,* **11** 279-290.

79. Bogentoft, C., Eskilsson, C., Jansson, U. E., Lagerström, P. O., Lövgren, K. and Rosén, L. (1983). Delivery of drugs to the colon by means of a new microencapsulated oral dosage form. *Acta Pharm. Suec.*, **20** 311-314.

80. Van den Mooter, G., Samyn, C. and Kinget, R. (1992). Azo polymers for colon-specific drug delivery. *Int. J. Pharm.*, **87** 37-46.

81. Van den Mooter, G., Samyn, C. and Kinget, R. (1993). Azo polymers for colon-specific drug delivery. II: Influence of the type of azo polymer on the degradation by intestinal microflora. *Ibid,* **97** 133-139.

82. Rubinstein, A., Nakar, D. and Sintov, A. (1992). Chondroitin Sulphate: A potential biodegradable carrier for colon-specific drug delivery. *Ibid,* **84** 141-150.

83. Rajabi-Siahboomi, A. R., Bowtell, R. W., Mansfield, P., Henderson, A., Davies, M. C. and Melia, C. D. (1994). Structure and behaviour in hydrophilic matrix sustained release dosage forms. 2. NMR-imaging studies of dimensional changes in the gel layer and core of HPMC tablets undergoing hydration. *J. Contrl. Rel.*, **31** 121-128.

84. Fernández Degiorgi, C., Mallo, R. A., Smolko, E. E. and Lambardo, J. H. (1995). Ampicillin release from swellable controlled system. *Ibid,* **33** 343-348.

85. Pham, A. T. and Lee, P. I. (1994). Probing the mechanism of drug release from hydroxypropylmethyl cellulose matrices. *Pharm. Res.*, **11** 1379-1384.

86. Wan, L. S. C., Heng, P. W. S. and Wong, L. F. (1995). Matrix swelling: A simple model describing extent of swelling of HPMC matrices. *Int. J. Pharm.*, **116** 159-168.

87. Conte, U., Maggi, L., Colombo, P. and La Manna, A. (1993). Multi-layered hydrophilic matrices as constant release devices (Geomatrix™ systems*). *J. Contrl. Rel.*, **26** 39-47.

88. Staniforth, J. N. and Baichwal, A. R. (1993). Synergistically interacting heterodisperse polysaccharides-function in achieving controllable drug delivery. In: Polymeric Delivery Systems: Properties and applications, M. A. El-Nokaly, D. M. Piatt, B. A. Charpentier, (Eds.), pp. 327-350, Am. Chem. Soc., Washington, DC. Reprinted from ACS Symp. Series, No. 520.

89. Bonferoni, M. C., Rossi, S., Tamayo, M., Pedraz, J. L., Dominguez-Gil, A. and Caramella, C. (1993). On the employment of λ-carrageenan in a matrix system. I. Sensitivity to dissolution medium and comparison with Na carboxymethylcellulose and xanthan gum. *J. Contrl. Rel.*, **26** 119-127.

90. Wan, L. S. C., Heng, P. W. S. and Wang, L. F. (1993). Relationship between swelling and drug release in a hydrophilic matrix. *Drug Dev. Ind. Pharm.*, **19** 1201-1210.

91. Peppas, N. A. and Sahlin, J. J. (1989). A simple equation for the description of solution release: III. Coupling of diffusion and relaxation. *Int. J. Pharm.*, **57** 169-172.

92. Fan, L. T. and Singh, S. K. (1989). In: Controlled Release: A quantitative treatment, polymers/properties and applications 13, H-J. Cantow, H. J. Harwood, J. P. Kennedy, A. Ledwith, J. Meißner, S. Okamura, G. Henrici-Olivé, S. Olivé, (Eds.), pp. 1-83, Springer-Verlag, Berlin, Heidelberg.

93. Zahirul, M. and Ichan, I. (1995). Recent trends and progress in sustained or controlled oral delivery of some water soluble drugs: Morphine salts, diltiazem and captopril. *Drug Dev. Ind. Pharm.*, **21** 1037-1070.

94. El-Shanawany, S. (1993). Sustained release of nitrofurantoin from inert wax matrices. *J. Contrl. Rel.*, **26** 11-19.

95. Bansal, P., Patil, J. and Plakogiannis, F. M. (1993). Release of low dose water soluble medicinal agent from inert wax matrix tablets. *Drug Dev. Ind. Pharm.*, **19** 2103-2108.

96. Lockwood, P. J. (1990). The development & characterization of directly-compressible oral controlled drug delivery systems. *Ph. D. Thesis,* Univ. Bath, UK.

97. Ramzan, B. (1992). A study of modified matrix forming systems for achieving controlled drug delivery. Final Year Honours Project Report for Bachelor of Pharmacy Degree, Univ. Bath, UK.

98. Juul Thomsen, L., Schæfer, T., -Sonnergaard, J. M. and Kristensen, H. G. (1993). Prolonged release matrix pellets prepared by melt pelletization I. Process variables. *Drug Dev. Ind. Pharm.*, **19** 1867-1887.

99. Kaewvichit, S. and Tucker, I. G. (1994). The release of macromolecules from fatty acid matrices: Complete factorial study of factors affecting release. *J. Pharm. Pharmacol.*, **46** 708-713.

100. Otsuka, M. and Matsuda, Y. (1994). Effect of co-grinding on the release of pentoxifylline from waxy matrix. *J. Pharm. Sci.*, **83** 956-961.

101. Yao Su, X., Al-Kassas, R. and Li Wan Po, A. (1994). Statistically modelling of ibuprofen release from spherical lipophilic matrices. *Eur. J. Pharm. Biopharm.*, **40** 73-76.

102. Higuchi, T. (1961). Rate of release of medicaments from ointment bases containing drugs in suspension. *J. Pharm. Sci.*, **50** 874-875.

103. Desai, S. J., Singh, P., Simonelli, A. P. and Higuchi, W. I. (1966), Investigation of factors influencing release of solid drug dispersed in inert matrices, II-IV. *Ibid,* **55** 1224-1244.

104. Hsieh, D. S. T., Rhine, W. D. and Langer, R. S. (1983). Zero-order controlled-release polymer matrices for micro- and macromolecules. *J. Pharm. Sci.*, **72** 17-22.

105. Hansson, A. G., Giardino, A., Cardinal, J. R. and Curatolo, W. (1988). Perforated coated tablets for controlled release of drugs at constant rate. *Ibid,* **77** 322-324.

106. Bechard, S. and McMullen, J. N. (1988). Solute release from a porous polymeric matrix: Inwardly tapered disk with a central releasing hole. *Ibid,* **77** 222-228.

107. Staniforth, J. N. (1993). Controlled release device with an impermeable coating having an orifice for release of drug. UK Patent, Publication No. GB 2 222 948 B.

108. Handbook of Pharmaceutical Excipients, (1987). Hydrogenated castor oil, pp. 45-50, The Pharmaceutical Press, London, UK.

109. Juul Thomsen, L., Schæfer, T. and Kristensen, H. G. (1994). Prolonged release matrix pellets prepared by melt pelletization II. Hydrophobic substances as meltable binders. *Drug Dev. Ind. Pharm.*, **20** 1179-1197.

110. Handbook of Pharmaceutical Excipients, (1987). Povidone, pp. 234-239, The Pharmaceutical Press, London, UK.

111. Handbook of Pharmaceutical Excipients, (1987). Stearic acid, pp. 298-300, The Pharmaceutical Press, London, UK.

112. Musikabhumma, P., Rubinstein, M. H. and Khan, K. A. (1982). Evaluation of stearic acid and polyethylene glycol as binders for tableting potassium phenethicillin. *Drug Dev. Ind. Pharm.*, **8** 169-188.

113. Albin, P., Markus, A., Ben - Zvi, Z. and Pelah, Z. (1993). A new slow release formulation of metoprolol: *in vitro* and *in vivo* evaluation in dogs. *J. Contrl. Rel.*, **23** 1-12.

114. British Pharmacopoeia, Vol. I (1993). Propranolol hydrochloride, pp. 554-555, Her Majesty's Stationery Office, London, UK.

115. British Pharmacopoeia, Vol. I (1993). Theophylline, pp. 663, Her Majesty's Stationery Office, London, UK.

116. Handbook of Pharmaceutical Excipients, (1987). Magnesium stearate, pp. 173-175, The Pharmaceutical Press, London, UK.

117. The Merck Index (1989). Leucine, pp. 857, S. Budavari, M. J. O'Neil, A. Smith, P. E. Heckelman, (Eds.), Merck & Co., Inc., Rahway, New Jersey, USA.

118. Handbook of Pharmaceutical Excipients, (1987). Glyceryl monostearate, pp. 125-126, The Pharmaceutical Press, London, UK.

119. Wyatt, D. M. and Dorschel, D. (1992). A cubic-phase delivery system composed of glyceryl monooleate and water for sustained release of water soluble drugs. *Pharm. Technol.*, **16** 116-130.

120. Fontell, K. (1990). Cubic phases in surfactant and surfactant-like lipid systems. *Colloid Poly. Sci.*, **268** 264-285.

121. Ohlson, J. S. R. (1983). Rapeseed oil. *J. Am. Oil Chem. Soc.*, **60** 385-386.

122. Krishna Murthy, M. N., Rajalakshmi, S., Mallika, T., Vibhakar, S., Ankaiah Nasirullah, K. N., Nagaraja, K. V. and Kapur, O. P. (1983). Physico-chemical characteristics and fatty acid composition of some imported and indigenous varieties of rapeseed oil. *J. Food Sci. & Technol.*, **20** 32-34.

123. Handbook of Pharmaceutical Excipients, (1987). Colloidal silicon dioxide, pp. 253-256, The Pharmaceutical Press, London, UK.

124. Technical Bulletin Pigments, (1977). Aerosil® in pharmaceuticals and cosmetics, No. 49, pp. 3-18, Degussa, Germany.

125. Aerosil, fumed silica. Surface chemistry, pp. 4; Characteristic properties of individual Aerosil types, pp. 12; Technical data for Aerosil types, pp. 30, Degussa, Germany.

126. Precipitated Silicas and Silicates. Production, characteristics and applications, pp. 2-5, Degussa, Germany.

127. Doelker, E., Massuelle, D., Veuillez, F. and Humbert - Droz, P. (1995). Morphological, packing, flow and tableting properties of new avicel types. *Drug Dev. Ind. Pharm.*, **21** 643-661.

128. Eudragit® Data Sheets (1978). Eudragit L and S: Application in the production of pharmaceutical preparations, pp. 2-3, Röhm Pharm, GMBH, Germany.

129. Handbook of Pharmaceutical Excipients, (1987). Carbomer, pp. 41-42, The Pharmaceutical Press, London, UK.

130. Pharmaceutical Handbook, (1985). Constant humidity solutions, pp. 592, The Pharmaceutical Press, London, UK.

131. Geigy scientific tables, (1975). Buffer solutions, K. Diem, C. Lentner (Eds.), pp. 280-282, Geigy Pharmaceuticals, Macclesfield, Ciba - Geigy Ltd., Basle, Switzerland.

132. The Merck Index (1989). Propranolol hydrochloride, S. Budavari, M. J. O'Neil, A. Smith, P. E. Heckelman, (Eds.), pp. 1246, Merck & Co., Inc., Rahway, New Jersey, USA.

133. Venkataram, S., Khohlokwame, M. and Wallis, S. H. (1995). Differential scanning calorimetry as a quick technique for solid state stability studies. *Drug Dev. Ind. Pharm.*, **21** 847-855.

134. The Merck Index (1989). Palmitic acid and Stearic acid, pp. 1107 and 1386 respectively, S. Budavari, M. J. O'Neil, A. Smith, P. E. Heckelman, (Eds.), Merck & Co., Inc., Rahway, New Jersey, USA.

135. Alderborn, G. and Nyström, C. (1982). Studies on direct compression of tablets III. The effect on tablet strength of changes in particle shape and texture obtained by milling. *Acta Pharm. Suec.*, **19** 147-156.

136. Otsuka, M., Matsumoto, T., Higuchi, S., Otsuka, K. and Kaneniwa, N. (1995). Effect of compression temperature on the consolidation mechanism of chlorpropamide polymorphs. *J. Pharm. Sci.*, **84** 614-618.

137. Alderborn, G., Börjesson, E., Glazer, M. and Nyström, C. (1988). Studies on direct compression of tablets, XIX. The effect of particle size, shape on the mechanical strength of sodium bicarbonate tablets. *Acta Pharm. Suec.*, **25** 31-40.

APPENDIX 1

Table A1

CE5/B1/Prop Tablets: Effect of Compaction Force on Tensile Strength

UP force (kN)	R - value	Tot. Time (s)	Tab. Weight (mg)	Tab. Thick. (mm)	Tens. Str. (MN/m^2)
3.4	0.622	0.35	152.5	2.970	0.994
3.3	0.581	0.35	152.3	2.965	1.112
3.2	0.558	0.35	151.8	2.958	1.168
3.2	0.575	0.37	151.7	2.949	1.134
3.3	0.574	0.37	152.0	2.963	1.099
3.4	0.610	0.39	152.2	2.968	1.034
3.4	0.617	0.35	152.2	2.963	0.998
3.3	0.597	0.41	151.7	2.962	1.064
3.3	0.587	0.38	151.8	2.957	1.160
3.3	0.592	0.41	151.8	2.957	1.134
3.4	0.604	0.35	151.8	2.968	1.119
3.3	0.622	0.36	151.8	2.963	1.141
3.4	0.607	0.35	151.7	2.959	1.100
3.3	0.591	0.36	151.6	2.970	1.172
3.4	0.612	0.38	152.0	2.963	1.180

Table A1 continued

UP Force (kN)	R - value	Tot. Time (s)	Tab. Weight (mg)	Tab. Thick. (mm)	Tens. Str. (MN/m^2)
6.0	0.725	0.43	151.1	2.905	1.248
6.2	0.731	0.41	152.1	2.920	1.154
6.2	0.716	0.43	152.0	2.919	1.233
6.0	0.720	0.44	151.1	2.918	1.128
6.1	0.726	0.42	151.3	2.919	1.235
6.0	0.725	0.42	151.6	2.915	0.925
6.3	0.722	0.44	152.3	2.932	1.211
6.2	0.717	0.40	152.1	2.925	1.129
6.2	0.727	0.41	152.1	2.934	1.187
6.0	0.718	0.40	151.9	2.927	1.079
5.9	0.716	0.41	152.2	2.927	1.185
5.8	0.718	0.40	152.0	2.923	0.965
9.1	0.802	0.42	151.8	2.902	1.234
9.1	0.795	0.39	151.3	2.906	1.198
9.0	0.790	0.44	151.3	2.902	1.232
9.1	0.805	0.41	151.6	2.903	1.237
9.2	0.803	0.44	152.5	2.912	1.142
9.3	0.791	0.44	151.6	2.906	1.254

Table A1 continued

UP Force (kN)	R - value	Tot. Time (s)	Tab. Weight (mg)	Tab. Thick. (mm)	Tens. Str. (MN/m^2)
9.1	0.808	0.44	151.5	2.908	1.280
9.3	0.793	0.43	151.4	2.904	1.303
9.2	0.810	0.39	151.7	2.907	1.359
9.1	0.810	0.42	151.8	2.906	1.285
9.0	0.809	0.42	151.2	2.901	1.231
9.2	0.809	0.42	151.6	2.909	1.137
9.1	0.801	0.45	151.4	2.900	1.262
9.0	0.802	0.46	151.5	2.900	1.213
9.3	0.802	0.45	152.1	2.917	1.038
11.9	0.869	0.54	151.3	2.904	1.248
11.9	0.860	0.44	151.5	2.905	1.093
11.7	0.865	0.42	151.5	2.905	1.241
12.0	0.866	0.48	152.2	2.908	1.343
11.6	0.863	0.44	151.3	2.904	1.330
11.9	0.862	0.46	151.8	2.906	1.205
11.6	0.868	0.45	151.4	2.904	1.188
11.6	0.860	0.50	151.4	2.904	1.263
11.8	0.872	0.48	151.3	2.903	1.290

Table A1 continued

UP Force (kN)	R - value	Tot. Time (s)	Tab. Weight (mg)	Tab. Thick. (mm)	Tens. Str. (MN/m^2)
11.7	0.857	0.47	151.5	2.905	1.257
11.7	0.858	0.52	151.8	2.906	1.258
11.7	0.859	0.50	151.7	2.905	1.235
11.6	0.851	0.46	151.2	2.900	1.201
11.5	0.859	0.44	151.0	2.896	1.256
11.8	0.851	0.51	151.3	2.903	1.255
15.1	0.855	0.48	151.1	2.897	1.388
15.1	0.855	0.52	151.4	2.897	1.239
15.0	0.852	0.49	151.0	2.898	1.256
15.3	0.853	0.51	151.7	2.906	1.270
15.1	0.852	0.50	151.5	2.903	1.351
15.2	0.848	0.52	151.3	2.898	1.264
15.2	0.852	0.51	151.7	2.904	1.263
15.0	0.855	0.50	151.2	2.889	1.112
15.1	0.848	0.52	151.6	2.908	1.272
15.4	0.847	0.52	151.8	2.903	1.174
15.1	0.848	0.52	151.5	2.907	1.208
15.0	0.852	0.53	150.8	2.897	1.219

Table A1 continued

UP Force (kN)	R - value	Tot. Time (s)	Tab. Weight (mg)	Tab. Thick. (mm)	Tens. Str. (MN/m^2)
15.1	0.845	0.53	151.3	2.893	1.336
15.3	0.843	0.55	151.8	2.904	1.107
15.0	0.844	0.54	150.8	2.889	1.112
18.4	0.864	0.57	151.3	2.898	1.228
18.2	0.866	0.57	151.3	2.886	1.256
18.2	0.866	0.67	151.0	2.891	1.062
18.2	0.866	0.57	150.9	2.891	1.047
18.2	0.868	0.62	151.0	2.886	1.231
18.4	0.862	0.60	151.6	2.896	1.251
18.4	0.863	0.57	151.3	2.891	1.251
18.4	0.863	0.52	151.4	2.897	1.199
18.2	0.862	0.58	150.9	2.888	1.301
18.2	0.870	0.59	151.3	2.891	1.154
18.2	0.868	0.59	151.4	2.891	1.199
18.4	0.872	0.61	151.4	2.899	1.209
18.3	0.870	0.59	151.0	2.883	1.278
18.3	0.870	0.59	150.9	2.886	1.171
18.1	0.868	0.60	150.5	2.880	1.171

Table A2

CE5/Prop Tablets: Effect of Particle Size on Tensile Strength

UP Force (kN)	R - value	Tot. Time (s)	Tab. Weight (mg)	Tab. Thick. (mm)	Tens. Str. (MN/m^2)
		500 - 710 µm			
12.2	0.897	0.56	151.3	2.896	1.332
12.1	0.894	0.50	151.5	2.909	1.294
11.9	0.898	0.49	151.0	2.893	1.360
12.0	0.897	0.52	151.7	2.903	1.396
11.9	0.894	0.51	151.1	2.885	1.473
11.9	0.896	0.51	150.9	2.890	1.436
11.9	0.885	0.53	151.4	2.902	1.205
11.8	0.890	0.52	150.7	2.886	1.278
11.8	0.884	0.48	151.4	2.901	1.276
12.0	0.898	0.54	151.4	2.895	1.173
11.9	0.892	0.51	151.2	2.902	1.242
12.1	0.893	0.54	151.4	2.900	1.263
12.1	0.889	0.49	151.6	2.908	1.427
11.8	0.894	0.51	151.3	2.891	1.283
11.7	0.893	0.51	151.1	2.885	1.255

Table A2 continued

UP Force (kN)	R - value	Tot. Time (s)	Tab. Weight (mg)	Tab. Thick. (mm)	Tens. Str. (MN/m^2)
		355 - 500 µm			
12.4	0.890	0.49	151.1	2.906	1.211
12.0	0.881	0.47	150.4	2.886	1.196
11.9	0.892	0.46	150.6	2.892	1.235
12.2	0.898	0.47	151.0	2.901	1.054
11.9	0.890	0.45	150.6	2.896	1.140
12.0	0.887	0.47	150.7	2.889	1.094
12.2	0.891	0.47	151.0	2.899	1.197
12.1	0.899	0.46	151.2	2.894	1.340
11.9	0.892	0.47	151.1	2.897	1.270
11.9	0.892	0.49	150.4	2.888	1.263
12.3	0.899	0.48	151.2	2.909	1.173
12.2	0.887	0.45	151.3	2.908	1.211
12.3	0.895	0.46	151.1	2.909	1.234
12.2	0.888	0.48	151.0	2.896	1.232
12.1	0.892	0.46	151.3	2.903	1.162

Table A2 continued

UP Force (kN)	R - value	Tot. Time (s)	Tab. Weight (mg)	Tab. Thick. (mm)	Tens. Str. (MN/m^2)
		250 - 355 µm			
11.9	0.893	0.50	150.4	2.892	1.284
11.8	0.890	0.53	150.7	2.900	1.257
11.8	0.886	0.52	150.9	2.906	1.189
11.6	0.877	0.54	149.7	2.880	1.189
12.7	0.903	0.54	150.4	2.895	1.303
12.6	0.896	0.50	150.2	2.895	1.158
12.8	0.903	0.55	150.9	2.904	1.223
12.9	0.891	0.53	151.0	2.906	1.317
11.6	0.883	0.48	150.7	2.897	1.202
11.6	0.885	0.47	151.0	2.904	1.238
11.5	0.881	0.46	150.3	2.901	1.263
11.6	0.879	0.47	150.8	2.900	1.199
12.0	0.881	0.45	151.9	2.914	1.195
11.8	0.880	0.49	151.3	2.916	1.287
11.8	0.891	0.45	151.2	2.915	1.117

Table A2 continued

UP Force (kN)	R - value	Tot. Time (s)	Tab. Weight (mg)	Tab. Thick. (mm)	Tens. Str. (MN/m^2)
		180 - 250 µm			
12.4	0.887	0.45	150.3	2.902	1.080
11.8	0.893	0.45	149.0	2.879	1.196
12.5	0.897	0.47	150.7	2.902	1.184
12.3	0.895	0.47	150.1	2.898	1.082
12.0	0.895	0.47	149.7	2.891	1.278
12.2	0.890	0.45	150.0	2.897	1.219
11.7	0.890	0.45	149.2	2.879	1.166
11.9	0.882	0.45	149.7	2.887	1.221
11.7	0.887	0.47	149.0	2.878	1.214
12.3	0.894	0.47	150.2	2.907	1.369
11.8	0.884	0.49	149.6	2.880	1.257
11.9	0.890	0.50	149.8	2.898	1.133
12.2	0.892	0.52	150.5	2.909	1.346
12.5	0.889	0.47	151.3	2.920	1.156
12.0	0.887	0.47	149.8	2.896	1.157

Table A2 continued

UP Force (kN)	R - value	Tot. Time (s)	Tab. Weight (mg)	Tab. Thick. (mm)	Tens. Str. (MN/m^2)
		< 180 µm			
12.1	0.889	0.46	149.4	2.885	1.178
12.1	0.891	0.45	149.0	2.886	1.151
12.4	0.892	0.47	149.9	2.904	1.147
12.4	0.887	0.44	150.0	2.903	1.024
12.0	0.890	0.46	149.2	2.896	1.131
12.0	0.882	0.46	149.2	2.896	1.069
11.7	0.884	0.44	149.0	2.890	1.108
12.4	0.893	0.44	149.7	2.911	1.140
12.0	0.888	0.46	149.7	2.901	1.173
11.9	0.886	0.44	149.4	2.890	1.123
11.8	0.882	0.47	149.7	2.903	1.044
11.8	0.894	0.47	149.5	2.898	1.159
12.0	0.885	0.44	150.5	2.902	1.006
11.7	0.890	0.44	149.0	2.895	1.060
12.4	0.893	0.44	150.3	2.919	1.223

Table A3

Effect of Binder Concentration on Tensile Strength

UP Force (kN)	R - value	Tot. Time (s)	Tab. Weight (mg)	Tab. Thick. (mm)	Tens. Str. (MN/m^2)
		0% w/w (CE1/B1/Prop)			
12.0	0.823	0.46	152.1	2.910	1.242
12.1	0.822	0.52	151.8	2.925	1.116
12.3	0.825	0.47	152.6	2.920	1.139
11.9	0.825	0.47	152.0	2.914	1.145
12.1	0.825	0.48	151.5	2.915	1.017
12.3	0.825	0.50	151.9	2.913	1.254
12.2	0.823	0.49	151.5	2.910	1.210
12.4	0.832	0.49	152.2	2.919	1.177
12.1	0.822	0.47	152.0	2.918	1.151
12.4	0.830	0.54	151.7	2.912	1.174
12.3	0.826	0.48	152.2	2.930	0.935
12.6	0.823	0.48	152.5	2.931	1.230
12.4	0.824	0.46	152.6	2.934	1.074
12.4	0.830	0.46	152.5	2.922	1.138
12.2	0.825	0.47	152.0	2.909	1.146

Table A3 continued

UP Force (kN)	R - value	Tot. Time (s)	Tab. Weight (mg)	Tab. Thick. (mm)	Tens. Str. (MN/m^2)
		3% w/w (CE2/B1/Prop)			
12.0	0.844	0.49	151.8	2.939	1.220
11.8	0.847	0.48	151.6	2.925	1.165
11.8	0.844	0.47	151.6	2.934	1.054
11.8	0.842	0.46	151.5	2.931	1.099
11.7	0.841	0.45	151.4	2.917	1.120
11.7	0.842	0.46	151.2	2.919	1.262
11.9	0.846	0.47	151.7	2.937	1.217
11.7	0.852	0.46	151.7	2.930	1.155
11.9	0.846	0.49	151.7	2.927	1.159
11.9	0.850	0.47	151.4	2.922	1.249
11.9	0.885	0.46	151.6	2.939	1.048
11.9	0.847	0.44	152.3	2.938	1.144
11.8	0.844	0.47	152.4	2.937	1.327
11.9	0.847	0.51	152.3	2.940	1.090
11.9	0.847	0.51	151.6	2.930	1.140

Table A3 continued

UP Force (kN)	R - value	Tot. Time (s)	Tab. Weight (mg)	Tab. Thick. (mm)	Tens. Str. (MN/m^2)
		5 % w/w (CE3/B1/Prop)			
12.1	0.841	0.48	151.4	2.915	1.232
12.3	0.839	0.45	151.5	2.918	1.306
12.1	0.855	0.47	151.4	2.910	1.269
12.3	0.853	0.52	152.0	2.918	1.188
12.4	0.849	0.46	151.7	2.918	1.056
12.2	0.856	0.51	151.4	2.912	1.064
12.5	0.852	0.50	152.0	2.923	1.085
12.3	0.847	0.46	151.5	2.914	1.044
12.3	0.845	0.47	151.5	2.908	1.319
12.2	0.844	0.47	151.2	2.905	1.201
12.5	0.840	0.49	151.5	2.908	1.211
12.5	0.842	0.47	151.5	2.912	1.297
12.5	0.845	0.47	151.6	2.911	1.282
12.5	0.849	0.47	151.1	2.915	1.056
12.3	0.845	0.49	151.9	2.919	1.097

Table A3 continued

UP Force (kN)	R - value	Tot. Time (s)	Tab. Weight (mg)	Tab. Thick. (mm)	Tens. Str. (MN/m^2)
		6 % w/w (CE4/B1/Prop)			
12.0	0.857	0.46	151.8	2.915	1.284
12.4	0.856	0.44	152.5	2.929	1.113
11.8	0.850	0.45	151.8	2.912	1.273
11.8	0.847	0.49	151.9	2.908	1.233
11.9	0.853	0.46	151.8	2.916	1.339
12.0	0.847	0.47	152.2	2.919	1.191
11.9	0.851	0.46	151.9	2.920	0.909
11.9	0.856	0.48	152.2	2.914	1.328
11.9	0.841	0.48	152.1	2.910	1.170
11.9	0.848	0.45	151.7	2.916	1.214
11.8	0.842	0.48	151.3	2.906	1.027
12.1	0.851	0.44	152.0	2.914	1.076
11.9	0.849	0.44	151.7	2.910	1.222
12.0	0.850	0.44	152.0	2.916	1.191
11.9	0.847	0.46	151.3	2.898	1.166

Table A3 continued

UP Force (kN)	R - value	Tot. Time (s)	Tab. Weight (mg)	Tab. Thick. (mm)	Tens. Str. (MN/m^2)
		7.5 % w/w (CE5/B1/Prop)			
11.9	0.869	0.54	151.3	2.904	1.248
11.9	0.860	0.44	151.5	2.905	1.093
11.7	0.865	0.42	151.5	2.905	1.241
12.0	0.866	0.48	152.2	2.908	1.343
11.6	0.863	0.44	151.3	2.904	1.330
11.9	0.862	0.46	151.8	2.906	1.205
11.6	0.868	0.45	151.4	2.904	1.188
11.6	0.860	0.50	151.4	2.904	1.263
11.8	0.872	0.48	151.3	2.903	1.290
11.7	0.857	0.47	151.5	2.905	1.257
11.7	0.858	0.52	151.8	2.906	1.258
11.7	0.859	0.50	151.7	2.905	1.235
11.6	0.851	0.46	151.2	2.900	1.201
11.5	0.859	0.44	151.0	2.896	1.256
11.8	0.851	0.51	151.3	2.903	1.255

Table A3 continued

UP Force (kN)	R - value	Tot. Time (s)	Tab. Weight (mg)	Tab. Thick. (mm)	Tens. Str. (MN/m^2)
		10 % w/w (CE6/B1/Prop)			
12.0	0.826	0.47	151.6	2.906	1.455
12.1	0.825	0.45	151.6	2.912	1.216
12.3	0.828	0.48	151.8	2.919	1.290
12.1	0.824	0.47	151.2	2.902	1.414
12.1	0.823	0.48	151.6	2.907	1.370
12.1	0.823	0.48	151.9	2.919	1.336
11.9	0.819	0.45	151.7	2.908	1.388
12.3	0.820	0.51	152.0	2.917	1.299
12.1	0.824	0.48	151.5	2.904	1.061
12.0	0.822	0.48	151.9	2.916	1.214
12.4	0.831	0.47	151.5	2.914	1.314
12.4	0.826	0.50	152.2	2.925	1.158
12.3	0.823	0.53	151.7	2.914	1.329
12.4	0.826	0.53	151.8	2.919	1.238
12.0	0.818	0.50	151.6	2.912	1.203

Table A3 continued

UP Force (kN)	R - value	Tot. Time (s)	Tab. Weight (mg)	Tab. Thick. (mm)	Tens. Str. (MN/m^2)
		15 % w/w (CE7/B1/Prop)			
11.8	0.844	0.48	152.3	2.897	1.250
11.5	0.839	0.44	152.2	2.890	1.390
11.7	0.839	0.51	152.2	2.897	1.364
11.5	0.836	0.46	152.1	2.893	1.221
11.6	0.836	0.46	152.3	2.892	1.298
11.7	0.836	0.47	152.2	2.897	1.305
11.7	0.832	0.48	152.2	2.893	1.199
11.8	0.836	0.56	152.2	2.907	1.335
11.7	0.838	0.46	152.1	2.897	1.151
11.6	0.835	0.49	151.9	2.890	1.279
11.7	0.837	0.46	152.2	2.901	1.323
11.7	0.827	0.46	152.5	2.898	1.264
11.6	0.832	0.45	151.9	2.894	1.251
12.0	0.843	0.45	152.5	2.917	1.170
11.6	0.839	0.46	151.8	2.899	1.237

Table A3 continued

UP Force (kN)	R - value	Tot. Time (s)	Tab. Weight (mg)	Tab. Thick. (mm)	Tens. Str. (MN/m^2)
		20 % w/w (CE8/B1/Prop)			
11.9	0.836	0.48	152.3	2.889	1.297
11.9	0.833	0.46	152.4	2.884	1.340
11.8	0.836	0.47	152.0	2.880	1.467
11.7	0.839	0.43	152.3	2.879	1.463
11.7	0.839	0.47	152.0	2.885	1.401
11.6	0.843	0.48	152.1	2.887	1.529
11.8	0.842	0.48	152.1	2.886	1.406
11.7	0.843	0.48	152.4	2.892	1.270
11.6	0.840	0.46	151.8	2.883	1.403
11.9	0.844	0.50	152.2	2.889	1.443
12.2	0.845	0.50	152.8	2.900	1.214
11.7	0.839	0.46	152.0	2.881	1.376
11.9	0.849	0.52	152.0	2.886	1.389
12.1	0.844	0.48	152.5	2.894	1.454
11.7	0.842	0.48	152.0	2.876	1.442

Table A3 continued

UP Force (kN)	R - value	Tot. Time (s)	Tab. Weight (mg)	Tab. Thick. (mm)	Tens. Str. (MN/m^2)
		25 % w/w (CE9/B1/Prop)			
12.1	0.840	0.53	152.2	2.876	1.506
12.0	0.837	0.49	152.0	2.876	1.502
12.4	0.837	0.55	152.6	2.884	1.412
12.1	0.834	0.47	151.8	2.875	1.307
12.2	0.838	0.48	152.2	2.879	1.560
12.3	0.829	0.51	152.0	2.879	1.594
12.1	0.833	0.49	152.0	2.874	1.597
12.1	0.839	0.50	151.8	2.866	1.598
12.3	0.841	0.46	152.1	2.878	1.595
12.2	0.831	0.52	151.8	2.874	1.444
11.9	0.836	0.45	151.1	2.867	1.475
12.4	0.848	0.49	152.1	2.873	1.482
12.0	0.847	0.48	151.6	2.861	1.468
12.3	0.841	0.48	152.2	2.877	1.464
12.4	0.843	0.51	152.6	2.878	1.508

Table A3 continued

UP Force (kN)	R - value	Tot. Time (s)	Tab. Weight (mg)	Tab. Thick. (mm)	Tens. Str. (MN/m^2)
		30 % w/w (CE10/B1/Prop)			
12.0	0.826	0.51	152.4	2.866	1.548
11.8	0.825	0.46	152.2	2.861	1.605
11.8	0.820	0.44	151.9	2.860	1.443
12.0	0.832	0.46	152.3	2.880	1.426
12.1	0.828	0.47	152.4	2.867	1.567
12.2	0.821	0.50	152.2	2.870	1.550
12.2	0.826	0.50	152.6	2.869	1.600
12.1	0.831	0.48	152.3	2.870	1.600
12.3	0.839	0.50	152.7	2.877	1.595
12.0	0.834	0.46	152.5	2.888	1.559
12.2	0.835	0.50	152.7	2.866	1.601
12.2	0.830	0.47	152.3	2.880	1.591
12.1	0.835	0.51	152.5	2.863	1.581
11.9	0.832	0.46	152.3	2.868	1.551
12.3	0.835	0.47	152.9	2.880	1.592

Table A4

Effect of Binder (PVP K-30) concentration on Release Sustaining Characteristics

T50 (Hours)

0 %	2.01	1.63	1.82	1.99	1.81	1.85
3 %	2.03	1.95	1.90	1.64	2.38	1.70
5 %	2.03	1.82	1.81	1.71	1.92	1.61
7.5 %	1.86	1.73	1.89	1.84	1.70	1.73
9 %	1.65	1.76	1.34	1.76	1.38	1.90
10 %	1.58	1.31	1.50	1.57	1.58	1.28
15 %	1.25	1.01	1.52	1.37	0.93	1.06
25 %	1.38	1.00	0.90	1.14	1.30	1.13
30 %	0.84	1.03	1.09	1.34	0.92	0.79

Table A5

CE5/Prop Tablets : Effect of Particle Size on Release Sustaining Characteristics

μm	T50 (Hours)					
500-710	1.39	2.15	2.35	3.18	2.45	2.39
355-500	1.86	1.57	1.44	1.46	1.56	1.90
250-355	1.54	1.62	1.55	1.44	1.22	1.57
180-250	1.31	1.12	1.41	1.58	1.55	1.68
< 180	1.37	1.49	1.39	1.65	1.45	1.46

Table A6

CE5/B1/Prop Tablets : Effect of Compaction Force on Release Sustaining Characteristics

kN	T50 (Hours)					
3.3	1.17	0.93	1.36	1.23	1.17	1.00
6.1	1.21	1.43	1.55	1.47	1.66	1.33
8.9	1.78	1.68	1.34	2.01	1.63	1.84
12.2	1.86	1.73	1.89	1.84	1.70	1.73
18.2	1.68	1.97	1.85	1.82	1.71	1.78

Table A7

CE25/Prop Tablets : Effect of Particle Size on Release Sustaining Characteristics

μm	T50 (Hours)					
500-710	1.42	1.33	1.42	1.49	1.44	1.41
355-500	1.27	1.48	1.37	1.41	1.55	1.51
250-355	1.13	1.08	1.11	1.10	1.05	1.14
180-250	1.01	1.08	1.06	1.07	1.11	1.08
< 180	0.98	1.01	1.06	1.02	0.98	0.82

Table A8

CE25/B1/Prop Tablets : Compaction Force Effect on Release Sustaining Characteristics

kN	T50 (Hours)					
2.5	1.13	0.99	1.01	1.10	1.11	1.13
5.7	1.08	1.17	1.06	1.16	1.17	1.25
9.3	1.16	1.02	1.18	1.11	1.27	1.14
11.9	0.94	1.14	1.19	1.17	1.07	1.17
15.2	1.01	1.26	1.11	1.25	1.08	0.97
17.6	0.95	0.92	1.09	0.96	0.92	0.94

Table A9

First Order Kinetics:- $\log_{10}(100\ \% - Q) = kt$

Tablet No.	Slope (hr^{-1})	Intercept	r
	CE5/B1/Theo		
1	-0.01083	1.9228	0.99779
2	-0.01299	1.9194	0.99815
3	-0.01284	1.9215	0.99823
4	-0.01120	1.9276	0.99839
5	-0.01164	1.9337	0.99861
6	-0.01160	1.9325	0.99895
Mean	-0.01185	1.9262	0.99835
sd	0.00088	0.0060	0.00040
	ACE/B1		
1	-0.04764	1.8878	0.98700
2	-0.04716	1.8930	0.98829
3	-0.04740	1.8940	0.98768
4	-0.04774	1.8944	0.98903
5	-0.04468	1.8890	0.98662
6	-0.05116	1.8827	0.98804
Mean	-0.04763	1.8902	0.98778
sd	0.00207	0.0045	0.00088

Table A9 Continued

First Order Kinetics:- $\log_{10}(100\ \% - Q) = kt$

Tablet No.	Slope (hr^{-1})	Intercept	r
	CE5/B1/Prop		
1	-0.10832	1.9043	0.99865
2	-0.11121	1.8950	0.99779
3	-0.10703	1.9050	0.99896
4	-0.10808	1.9029	0.99790
5	-0.11212	1.8936	0.99776
6	-0.11790	1.9043	0.99919
Mean	-0.11078	1.9009	0.99838
sd	0.00400	0.0051	0.00064
	CE16/B1/Prop		
1	-0.13665	1.9035	0.99848
2	-0.15236	1.9006	0.99891
3	-0.17894	1.9118	0.99986
4	-0.13071	1.9007	0.99904
5	-0.17988	1.8901	0.99845
6	-0.17756	1.8885	0.99930
Mean	-0.15935	1.8992	0.99901
sd	0.02245	0.0087	0.00053

Table A9 Continued

First Order Kinetics:- $\log_{10}(100\ \% - Q) = kt$

Tablet No.	Slope (hr^{-1})	Intercept	r
	CE17/B1/Prop		
1	-0.17900	1.8964	0.99924
2	-0.22503	1.9161	0.99996
3	-0.14967	1.9141	0.99952
4	-0.19669	1.9193	0.99978
5	-0.19768	1.9052	0.99976
6	-0.18754	1.9023	0.99982
Mean	-0.18927	1.9089	0.99968
sd	0.02482	0.0090	0.00026
	CE18/B1/Prop		
1	-0.41768	2.0343	0.99747
2	-0.66716	2.1529	0.98890
3	-0.64783	2.1455	0.99252
4	-0.54360	2.0925	0.99740
5	-0.50891	2.0621	0.98998
6	-0.33234	2.0129	0.99595
Mean	-0.51959	2.0834	0.99370
sd	0.12989	0.0576	0.00377

Table A9 Continued

First Order Kinetics:- $\log_{10}(100\ \% - Q) = kt$

Tablet No.	Slope (hr^{-1})	Intercept	r
	CE29/B2/Prop		
1	-0.43306	2.0777	0.94298
2	-0.44289	2.0757	0.95590
3	-0.30497	2.0182	0.96622
4	-0.40035	2.0712	0.95956
5	-0.38299	2.0461	0.98716
6	-0.30389	2.0003	0.99568
Mean	-0.37803	2.0482	0.96792
sd	0.06098	0.0327	0.01990

Table A10

Higuchi Mechanism Kinetics:- $Q = kt^{1/2}$

Tablet No.	Slope (%$hr^{-1/2}$)	Intercept (%)	r
	CE5/B1/Theo		
1	9.89	4.56	0.99955
2	11.13	4.20	0.99981
3	11.10	3.81	0.99969
4	10.21	3.38	0.99933
5	10.63	1.81	0.99922
6	10.53	2.24	0.99890
Mean	10.58	3.33	0.99942
sd	0.49	1.10	0.00033
	ACE/B1		
1	20.97	8.75	0.99450
2	21.01	7.83	0.99543
3	21.17	7.53	0.99496
4	21.22	7.52	0.99575
5	20.12	8.94	0.99491
6	21.70	9.38	0.99426
Mean	21.03	8.33	0.99497
sd	0.52	0.80	0.00056

Table A10 Continued

Higuchi Mechanism Kinetics:- $Q = kt^{1/2}$

Tablet No.	Slope (%$hr^{-1/2}$)	Intercept (%)	r
	CE5/B1/Prop		
1	32.88	4.98	0.99978
2	32.85	6.67	0.99927
3	32.62	4.98	0.99991
4	32.87	5.11	0.99943
5	32.92	6.92	0.99924
6	34.45	4.78	0.99984
Mean	33.10	5.57	0.99958
sd	0.67	0.96	0.00030
	CE1/B1/Prop		
1	29.83	7.42	0.99966
2	32.62	7.87	0.99926
3	29.45	9.76	0.99859
4	29.55	8.05	0.99914
5	32.05	6.85	0.99985
6	30.04	8.86	0.99937
Mean	30.49	8.14	0.99931
sd	1.38	1.04	0.00044

Table A10 Continued

Higuchi Mechanism Kinetics:- $Q = kt^{1/2}$

Tablet No.	Slope (%$hr^{-1/2}$)	Intercept (%)	r
	CE10/B1/Prop		
1	42.81	10.97	0.99909
2	41.24	7.52	0.99964
3	39.58	7.96	0.99944
4	36.27	6.04	0.99976
5	46.22	5.65	0.99932
6	43.43	11.50	0.99957
Mean	41.59	8.27	0.99947
sd	3.43	2.46	0.00024
	CE16/B1/Prop		
1	36.93	4.99	0.99966
2	39.15	5.15	0.99967
3	43.61	2.54	0.99996
4	35.56	5.97	0.99993
5	42.08	6.75	0.99883
6	41.42	7.37	0.99957
Mean	39.79	5.46	0.99960
sd	3.13	1.70	0.00041

Table A10 Continued

Higuchi Mechanism Kinetics:- $Q = kt^{1/2}$

Tablet No.	Slope (%$hr^{-1/2}$)	Intercept (%)	r
	CE17/B1/Prop		
1	42.37	5.63	0.99950
2	48.95	1.85	0.99970
3	39.80	2.42	0.99995
4	46.60	0.69	0.99974
5	45.22	3.87	0.99973
6	43.75	4.55	0.99987
Mean	44.45	3.17	0.99975
sd	3.22	1.84	0.00015
	CE18/B1/Prop		
1	78.22	-21.01	0.99995
2	93.46	-27.98	0.99988
3	94.22	-29.42	0.99997
4	89.12	-27.16	0.99960
5	81.26	-19.25	0.99840
6	70.84	-19.49	0.99834
Mean	84.52	-24.05	0.99936
sd	9.30	4.63	0.00078

Table A10 Continued

Higuchi Mechanism Kinetics:- $Q = kt^{1/2}$

Tablet No.	Slope ($\%hr^{-1/2}$)	Intercept (%)	r
	CE25/B1/Prop at ≈ 3 kN		
1	50.79	-3.96	0.99884
2	51.59	-1.75	0.99965
3	58.97	-8.54	0.99815
4	57.42	-9.42	0.99753
5	55.88	-7.63	0.99765
6	50.19	-3.32	0.99931
Mean	54.09	-5.77	0.99852
sd	3.73	3.16	0.00088
	CE25/B1/Prop at ≈ 6 kN		
1	55.03	-7.10	0.99933
2	53.06	-6.69	0.99687
3	57.80	-8.25	0.99853
4	56.59	-10.19	0.99770
5	53.04	-7.19	0.99973
6	49.60	-5.05	0.99974
Mean	54.19	-7.41	0.99865
sd	2.94	1.71	0.00117

Table A10 Continued

Higuchi Mechanism Kinetics:- $Q = kt^{1/2}$

Tablet No.	Slope (%$hr^{-1/2}$)	Intercept (%)	r
	CE25/B1/Prop at ≈ 15 kN		
1	56.50	-6.17	0.99904
2	47.37	-3.72	0.99989
3	49.50	-2.30	0.99977
4	50.26	-5.91	0.99950
5	62.04	-12.58	0.99772
6	54.38	-3.95	0.99993
Mean	53.34	-5.77	0.99931
sd	5.42	3.64	0.00084
	CE29/B2/Prop		
1	65.41	-11.90	0.99342
2	66.87	-12.45	0.99710
3	58.43	-10.52	0.98936
4	65.95	-14.73	0.99187
5	66.57	-14.51	0.99663
6	60.36	-10.78	0.99860
Mean	63.93	-12.48	0.99450
sd	3.61	1.84	0.00354

Table A11

Zero Order Kinetics:- Q = kt

Tablet No.	Slope ($\%hr^{-1}$)	Intercept (%)	r
	CE25/B1/Prop at ≈ 3 kN		
1	21.87	22.41	0.99274
2	22.07	25.26	0.98709
3	25.46	21.95	0.99492
4	24.82	20.22	0.99536
5	24.03	21.07	0.99551
6	21.57	22.79	0.99167
Mean	23.30	22.28	0.99288
sd	1.68	1.73	0.00323
	CE25/B1/Prop at ≈ 6 kN		
1	22.28	22.45	0.99146
2	22.17	21.55	0.99554
3	24.09	22.63	0.99449
4	23.63	19.96	0.99563
5	22.00	21.34	0.99082
6	20.57	21.63	0.99069
Mean	22.46	21.59	0.99311
sd	1.26	0.95	0.00237

Table A11 Continued

Zero Order Kinetics:- Q = kt

Tablet No.	Slope ($\%hr^{-1}$)	Intercept (%)	r
	CE25/B1/Prop at ≈ 15 kN		
1	23.33	24.39	0.98597
2	19.58	21.89	0.98743
3	20.49	24.39	0.98913
4	20.87	21.08	0.99183
5	25.80	20.67	0.99154
6	22.46	25.46	0.98706
Mean	22.09	22.98	0.98883
sd	2.27	2.01	0.00244
	CE29/B2/Prop		
1	32.98	16.37	0.99589
2	33.56	16.65	0.99477
3	29.60	14.56	0.99637
4	33.37	13.63	0.99770
5	33.39	14.48	0.99389
6	30.14	15.67	0.99155
Mean	32.17	15.23	0.99503
sd	1.80	1.19	0.00215

Table A12

Diffusion - Relaxation Kinetics:- $Q = k_1 t^{0.46} + k_2 t^{0.92}$

Tablet No.	k_1 ($\%hr^{-0.46}$)	k_2 ($\%hr^{-0.92}$)	Intercept (%)	r
	CE25/B1/Prop at ≈ 3 kN			
1	38.40	7.73	0.11	0.99972
2	36.69	12.51	0.15	0.99981
3	33.40	13.23	0.19	0.99967
4	34.83	11.74	0.33	0.99971
5	39.51	6.89	-0.01	0.99982
Mean	36.57	10.42	0.15	0.99975
sd	2.50	2.90	0.12	0.00007
	CE25/B1/Prop at ≈ 6 kN			
1	43.38	7.37	-3.34	0.99972
2	25.63	14.12	5.35	0.99928
3	35.06	12.28	1.15	0.99991
4	29.12	14.27	1.72	0.99981
5	44.52	5.94	-4.97	0.99996
6	41.85	5.45	-3.09	0.99994
Mean	36.59	9.91	-0.53	0.99977
sd	7.94	4.11	3.91	0.00026

Table A12 continued

Diffusion - Relaxation Kinetics:- $Q = k_1t^{0.46} + k_2t^{0.92}$

Tablet No.	k_1 ($\%hr^{-0.46}$)	k_2 ($\%hr^{-0.92}$)	Intercept (%)	r
	CE25/B1/Prop at ≈ 15 kN			
1	58.23	1.64	-9.42	0.99901
2	47.73	1.85	-5.87	0.99989
3	45.72	3.73	-2.40	0.99984
4	39.20	6.92	-2.26	0.99992
5	43.66	10.58	-5.61	0.99846
6	55.83	1.67	-6.96	0.99994
Mean	48.40	4.40	-5.42	0.99951
sd	7.30	3.65	2.75	0.00063
	CE29/B2/Prop			
1	30.35	21.05	0.08	0.99951
2	31.73	20.82	-0.01	0.99993
3	26.25	19.54	0.14	0.99898
4	23.98	24.71	0.09	0.99962
5	27.24	22.81	-0.06	0.99972
6	30.73	17.45	-0.08	0.99982
Mean	28.38	21.06	0.03	0.99960
sd	3.03	2.52	0.09	0.00034

Table A13

Linear Regression Calibration Data

Vessel No.	Slope	Intercept	r
Propranolol Hydrochloride in Distilled Water			
1	0.01884	0.00300	0.99989
2	0.01902	0.00260	0.99990
3	0.01898	-0.00440	0.99972
4	0.01887	0.00010	0.99987
5	0.01912	-0.00060	0.99995
6	0.01878	0.01140	0.99988
Mean	0.01894	0.00202	0.99987
sd	0.00013	0.00531	0.00008
Theophylline in Distilled Water			
1	0.01737	0.00015	0.99997
2	0.01737	0.00196	0.99994
3	0.01736	0.00104	0.99997
4	0.01737	0.00032	0.99996
5	0.01733	0.00118	0.99990
6	0.01737	0.00078	0.99995
Mean	0.01736	0.00091	0.99995
sd	0.00002	0.00065	0.00003

Table A13 Continued

Linear Regression Calibration Data

Repeat No.	Slope	Intercept	r
Propranolol Hydrochloride in Buffer Solution:- pH ≈ 6.8			
1	0.01881	-0.00034	0.99996
2	0.01862	0.00031	0.99993
Mean	0.01872	-0.00002	0.99995
sd	0.00013	0.00044	0.00002
Propranolol Hydrochloride in Buffer Solution:- pH ≈ 1.4			
1	0.01928	0.00260	0.99988
2	0.01908	0.00096	0.99984
Mean	0.01918	0.00178	0.99986
sd	0.00014	0.00116	0.00003

APPENDIX 2

BASIC PROGRAMME FOR TABLETING

```
10  REM **HAND TABLETING
20  MODE128
30  DIM U% (500), D% (500), L% (500), T% (500)
40  PRINT "CALIB ? Y/N"
50  PRINT "X TO EXIT CALIB ROUTINE"
60  Z%=GET
70  IF Z%<>78 AND Z%<> 89 THEN 60
80  IF Z%=89 THEN PROCCAL
90  PRINT "MONITOR FORCE ? Y/N"
100 PRINT "X TO EXIT MONITOR ROUTINE"
110 Z%=GET
120 IF Z%<>78 AND Z%<> 89 THEN 110
130 IF Z%=89 THEN PROCMONIT
140 PRINT "TABLET MAKING"
150 PRINT "PRESS SPACE WHEN READY"
160 PRINT "X TO EXIT ROUTINE"
170 IF INKEY (-67) = -1 GOTO 40
180 IF GET <> 32 THEN 170
190 CLS
200 PROCCOLL
210 GOTO 150
220 END
230 DEF PROCCOLL
240 ?&FC02=2
250 ?&FC00=0
260 IF (?&FC00*256+?&FC01) <300 THEN 250
270 ?&FC00=0
280 IF (?&FC00*256+?&FC01) >300 THEN 250
290 PRINT "COLLECTING"
300 TIME=0
310 FOR N%=1 TO 500
320 ?&FC02=1
330 ?&FC00=0
340 U%(N%) = ?&FC00*256+?&FC01
350 ?&FC02=2
360 ?&FC00=0
370 L%(N%) = ?&FC00*256+?&FC01
380 ?&FC02=3
390 GOTO420
400 ?&FC00=0
410 D%(N%) = ?&FC00*256+?&FC01
420 NEXT N%
430 ET%=TIME
440 PRINT "TIME = "ET%
```

```
450 UMX%=U%(1) : STI=ET%/500
460 FOR N%=1 TO 500
470 IF U%(N%) < UMX% GOTO 490
480 UMX%=U%(N%) : PK%=N%
490 NEXT
500 UMN%=UMX% : MN%=PK%
510 FOR N%=PK% TO 500
520 IF U%(N%) >= UMN% GOTO 540
530 UMN%=U%(N%) : MN%=N%
540 NEXT
550 LMX%=L%(1)
560 FOR N%=1 TO 500
570 IF L%(N%) < LMX% GOTO 590
580 LMX%=L%(N%) : PL%=N%
590 NEXT
600 FL%=0
610 FOR I%=PK% TO 500
620 IF U%(I%) < 1000 FL%=1
630 IF FL%=1 THEN 650
640 FI%=I%
650 NEXT
670 DMX%=D%(1)
680 FOR N%=1 TO 500
690 IF D%(N%) < DMX% GOTO 710
700 DMX%=D%(N%)
710 NEXT
730 PRINT "DIGITAL VALUE, TOP PUNCH = "UMX%
740 PRINT "DIGITAL VALUE, LOWER PUNCH = "LMX%
750 REM PRINT "DIGITAL VALUE, DISP = "DMX%
760 PRINT "N TOP PUNCH = "UMX%/2.34
770 PRINT "N LOWER PUNCH = "(LMX% - 3375)/1.292
780 PRINT "PUNCH RATIO UP/LP
790 PRINT "PUNCH RATIO
800 PRINT "UPPER PF - LOWER PF = "(UMX%/2.34)-((LMX%-3375)/1.292)
810 PRINT RESID F LOWER PUNCH = "(L%(MN%+10)-3375/1.292)
820 @%=10
830 PRINT "TIME TO PF = "STI*PK%/100
840 PRINT "TOT. COMP. TIME = "STI*FI%/100
850 IF GET <> 32 THEN 850
860 CLS
870 FOR N%=1 TO 500
880 PLOT69, N%*2, U%(N%)/2.34/20
890 NEXT
900 FOR N%=1 TO 500
910 PLOT69, (N%*2)+400, (L%(N%)-3375)/1.292/20
920 NEXT
930 ENDPROC
940 DEF PROCDV
```

```
950 J%=1
960 REPEAT
970 FOR N%=J% TO J%+19
980 PRINT U%(N%), L%(N%)
990 NEXT
1000 PRINT "NEXT 20" "N%=" N%
1010 J%=J%+20
1020 REPEAT : UNTIL GET$<>""
1030 UNTIL J%=500
1040 ENDPROC
1050 DEF PROCSTAT
1060 PRINT "STATUS = "~S%
1070 PRINT "IF STATUS IS F8 ERROR IN SWITCH SETTING ELSE CONV.
INCOMPLETE"
1080 ENDPROC
1090 DEF PROCCAL
1100 ?&FC02=1
1110 ?&FC00=0
1120 FOR I%=1 TO 5
1130 NEXT I%
1140 S%=?&FC03
1150 IF S% <> &F9 AND S% <> &FA AND S% <> &FC THEN PROCSTAT
1160 CH=(?&FC00*256+?&FC01)
1170 ?&FC02=2
1180 ?&FC00=0
1190 FOR I%=1 TO 5
1200 NEXT I%
1210 S%=?&FC03
1220 IF S% <> &F9 AND S% <> &FA AND S% <> &FC THEN PROCSTAT
1230 CH2=(?&FC00*256+?&FC01)
1240 ?&FC02=3
1250 ?&FC00=0
1260 FOR I%=1 TO 5
1270 NEXT I%
1280 S%=?&FC03
1290 IF S% <> &F9 AND S% <> &FA AND S% <> &FC THEN PROCSTAT
1300 PRINT  CH" "CH2" "(?&FC00*256+?&FC01)
1310 IF INKEY (-67) = -1 GOTO 1320 ELSE 1100
1320 ENDPROC
1330 DEF PROCMONIT
1340 PRINT "PRESS SPACE BAR WHEN READY"
1350 IF GET <> 32 THEN 1350
1360 ?&FC02=2
1370 ?&FC00=1
1380 TT%=TIME
1390 REPEAT : UNTIL TIME=TT%+20
1400 F%="(?&FC00*256+?&FC01)/2.34
1410 PRINT F%
```

```
1420 IF INKEY (-67) = -1 GOTO 1430 ELSE 1360
1430 ENDPROC
```

BASIC PROGRAMME FOR DISSOLUTION

```
 10  FACTOR 1
 20  ON ERROR GOTO 130
 30  REM AUTO DISSOL
 40  REM  SAB(0,X)=TIME,  SAB(1-6,X)=REPS  1-6,  SAB(7,X)=MEAN,
SAB(8,X)=STD DEV, SAB(9,X)=SE, SAB(10,X)=TEMPSTORE FOR REP, X,
SAB(1-6,0)=TAMTAB
 50  DIM SAB (10, 25), Z (6)
 60  PROCINIT
 70  PROCCLEAR
 80  PROCDESC
 90  PROCMENU
100  FL%=1
110  PROCKEY
120  ON FL5 GOTO 110, 90, 60, 150
130  PROCEND
140  PRINT ERR, ERL
150  PROCEND
160  STOP
170  DEF PROCMENU
180  CLS
190  PRINT "F0  -  CALIBRATE/ZERO" '
200  PRINT "F1  -  CONTINUE WITH RUN" '
210  PRINT "F2  -  PRINTOUT RESULTS" '
220  PRINT "F3  -  SAVE DATA ON DISC" '
230  PRINT "F4  -  START ANOTHER RUN" '
240  PRINT "F5  -  FINISHED" '
250  ENDPROC
260  DEF PROCKEY
270  IF INKEY (-33) = -1  PROCCALIB
280  IF INKEY (-114) = -1  PROCRUN
290  IF INKEY (-115) = -1  PROCPRINT
300  IF INKEY (-116) = -1  PROCSAVE
310  IF INKEY (-21) = -1  FL%=3
320  IF INKEY (-117) = -1  PROCEND
330  ENDPROC
340  FL%=1
350  DEF PROCRUN
360  CLS
370  INPUT "ENTER NUMBER OF REPS "K%
380  INPUT "ENTER RUN TIME h "TM
390  INPUT "ENTER SAMPLE FREQUENCY (NO. OF SAMPLES PER HOUR
"JJ%
```

```
400 PRINT "ENTER TOTAL AMOUNT IN TABLET
410 FOR I%=1 TO K%
420 PRINT I%
430 INPUT SAB (I%, 0)
440 NEXT
450 J%=(JJ%*TM) + 1
460 PRINT "TO START DATA COLLECTION RUN PRESS"
470 @%=&20306
480 IF GET <> 32 THEN 480
490 FOR N%=1 TO J%
500 SAB (0, N%) = (TM/(J%-1)*(N%-1))
510 I%=0
520 PROCWAIT
530 FOR I%=1 TO K%
540 IF I%=1 THEN 560
550 PROCWAIT
560 PRINT "SAMPLE "N%
570 PRINT "REP. "I%
580 PROCAV
590 SAB (I%, N%) = ((AV%*2.82E-5) + 0.019) *A1
600 IF N%=1 THEN Z(I%) = SAB (I%, N%)
610 SAB (I%, N%) = SAB (I%, N%) - Z(I%)
620 IF SAB (I%, N%) < 0.0189 THEN SAB (I%, N%) = 0.0001
630 IF PR1%=1 THEN 650
640 VDU2
650 PRINT SAB (I%, N%)
660 VDU3
670 NEXT
680 NEXT
690 @%=10
700 IF PR1%=1 THEN 720
710 VDU2
720 FOR N%=1 TO J%
730 FOR I%=1 TO K%
740 PRINT SAB (I%, N%) " ";
750 NEXT
760 PRINT
770 NEXT
780 VDU3
790 FOR I%=1 TO K%
800 FOR N%=1 TO J%
810 SAB (I%, N%) = SAB (I%, N%) - 0.0001
820 SAB (I%, N%) = SAB (I%, N%) / 0.01893
830 SAB (I%, N%) = SAB (I%, N%) / SAB (I%, 0)*100
840 NEXT
850 NEXT
860 PROCMSD
870 PROCT
```

```
880 FL%=2
890 ENDPROC
900 DEF PROCPRINT
910 IF PR%=1 THEN 930
920 VDU2
930 TI%=2
940 FL%=2
950 IF SAB (0, J%) > 12 THEN TI%=1
960 PRINT "SAMPLE "SC$
970 PRINT DESC$ ' '
980 PRINT "TIME";
990 FOR I%=1 TO 6
1000 PRINT "REP"; I%;
1010 NEXT
1020 PRINT "MEAN  SD  SE"
1030 PRINT "AM. TAB";
1040 @%=&20206
1050 FOR I%=1 TO 9
1060 PRINT SAB (I%, 0) "  ";
1070 NEXT
1080 PRINT
1090 FOR N%=1 TO J%
1100 PRINT "  ";
1110 FOR I%=0 TO 9
1120 PRINT SAB (I%, N%) "   ";
1130 NEXT
1140 TT%=TIME
1150 PRINT
1160 NEXT
1170 IF SK%=1 THEN 1200
1180 PRINT   "T50 = "T50
1190 PRINT "T90 = "T90
1200 @%=10
1210 VDU3
1220 ENDPROC
1230 DEF PROCCLEAR
1240 FOR I%=0 TO 10
1250 FOR N%=0 TO 25
1260 SAB (I%, N%) = 0
1270 NEXT
1280 NEXT
1290 ENDPROC
1300 DEF PROCINIT
1310 CLS
1320 SK%=0
1330 VDU15
1340 PRINT "WILL YOU HAVE A PRINTER AT THE END ?  Y/N"
1350 Z%=GET
1360 IF Z% > 90 THEN Z%=Z%-32
```

```
1370 IF Z% <>78 AND Z% <> 89 THEN 1350
1380 IF Z%=78  PR%=1
1390 IF Z%=89  PR%=0
1400 PRINT "DO YOU HAVE A PRINTER DURING THE RUN ?  Y/N"
1410 Z%=GET
1420 IF Z% > 90 THEN Z%=Z%-32
1430 IF Z% <>78 AND Z% <> 89 THEN 1410
1440 IF Z%=78  PR1%=1
1450 IF Z%=89  PR1%=0
1460 *FX15, 1
1470 INPUT "SET REQUIRED ABSORBANCE  .5  OR  1  OR  2  "A1
1480 FG%=0
1490 *FX229, 1
1500 *FX16, 2
1510 ENDPROC
1520 DEF PROCMSD
1530 FOR N%=0 TO J%
1540 FOR I%=1 TO K%
1550 SAB (7, N%) = SAB (7, N%) = SAB (I%, N%)
1560 NEXT
1570 SAB (7, N%) = SAB (7, N%)/K%
1580 NEXT
1590 FOR N%=1 TO J%
1600 FOR I% TO K%
1610 SAB (8, N%) = SAB (8, N%) + ((SAB (I%, N%) - SAB (7, N%)) ^2)
1620 NEXT
1630 SAB (8, N%) = SQR (SAB (8, N%)/(K%-1))
1640 SAB (9, N%) = SAB (8, N%)/(SQR(K%))
1650 NEXT
1660 ENDPROC
1670 DEF PROCDESC
1680 INPUT "ENTER SAMPLE CODE "SC$
1690 INPUT "ENTER DESCRIPTION  (MAX 80 CHRS)  "DESC$
1700 ENDPROC
1710 DEF PROCT
1720 C50%=0:C90%=0
1730 T50 = -1 : T90 = -1
1740 FOR N%=1 TO J% -1
1750 IF SAB (7, N%)>=50 THEN 1780
1760 C50%=N%+1
1770 GOTO  1800
1780 IF SAB (7, N%)>=90 THEN 1800
1790 C90%=N%+1
1800 NEXT
1810 IF C50%=0 THEN T50=0
1820 IF T50=0 THEN 1870
1830 P50D=SAB (7, C50%) - SAB (7, (C50%-1))
1840 P50=(SAB (7, C50%) -50)/P50D
```

```
1850 TI50=SAB (0, C50%) -SAB (0, (C50%-1))
1860 T50=SAB (0, C50%) - (P50*TI50)
1870 IF C90=0 THEN T90=0
1880 IF T90=0 THEN 1930
1890 P90D=SAB (7, C90%) - SAB (7, (C90%-1))
1900 P90=(SAB (7, C90%) -90) /P90D
1910 TI90=SAB (0, C90%) -SAB (0, (C90%-1))
1920 T90=SAB (0, C90%) - (P90*TI90)
1930 ENDPROC
1940 DEF PROCSAVE
1950 FL%=2
1960 INPUT "ENTER FILENAME "FLNM$
1970 FLNM$=LEFT$ (FLNM$, 7)
1980 X%=OPENIN (FLNM$)
1990 IF X%=0 THEN 2120
2000 CLOSE# X%
2010 PRINT "FILENAME ALREADY IN USE"
2020 PRINT "RENAME FILE ? Y/N"
2030 Z%=GET
2040 IF Z%>90 THEN Z%=Z%-32
2050 IF Z%=89 THEN 1960
2060 IF Z%< >78 THEN 2030
2070 PRINT "THIS OPTION OVERWRITES THE FILE OK ? Y/N"
2080 Z%=GET
2090 IF Z%>90 THEN Z%=Z%-32
2100 IF Z%=78 THEN 1960
2110 IF Z%< >89 THEN 2080
2120 X%=OPENOUT (FLNML$)
2130 PRINT "CODE "SC$
2140 PRINT "DESCRIPTION "DESC$
2150 PRINT# X%, SC$, DESC$, K%, J%, T50, T90
2160 FOR I%=0 TO 10
2170 FOR N%=0 TO J%
2180 PRINT# X%, SAB (I%, N%)
2190 NEXT
2200 NEXT
2210 CLOSE# X%
2220 ENDPROC
2230 DEF PROCWAIT
2240 IF I%=0 AND N%=1 THEN 2260
2250 IF ?&FC00=254 THEN 2250
2260 IF INKEY (-113) = -1 THEN FG%=1
2270 IF FG%=1 THEN 2290
2280 IF ?&FC00=255 THEN 2260
2290 ENDPROC
2300 ENDPROC
2310 DEF PROCAV
2320 AV%=0
```

```
2330 TT%=TIME
2340 FOR M%=1 TO 100
2350 AV%=AV%+ADVAL (2)
2360 IF TIME<TT%+5 THEN 2360
2370 TT%=TIME
2380 NEXT
2390 AV%=AV%/100
2400 ENDPROC
2410 DEF PROCCALIB
2420 CLS
2430 PRINT "ABSORBANCE ON SPEC SHOULD BE "A1
2440 PRINT "DWELL TIME MUST BE AT LEAST 10 SECONDS"
2450 PRINT "PRESS SPACE TO CONTINUE"
2460 IF GET< >32 THEN 2460
2470 FOR L%=1 TO 6
2480 PROCWAIT
2490 IF FG%=1 THEN 2550
2500 PROCAV
2510 IF FG%=1 THEN 2550
2520 @%=&20306
2530 CAL=((AV%*2.82E -5) + 0.019)*A1
2540 PRINT CAL;
2550 NEXT
2560 PRINT
2570 IF FG%=1 THEN 2590
2580 GOTO 2470
2590 @%=10
2600 FL%=2
2610 FG%=0
2620 ENDPROC
2630 DEF PROCEND
2640 CLOSE #X%
2650 *FX229, 0
2660 FL%=4
2670 ENDPROC
```